

ANALYSIS AND INTERPRETATION OF ECG SIGNAL USING WAVELET TRANSFORM

A THESIS

*Submitted in fulfilment of the
requirements for the award of the degree*

of

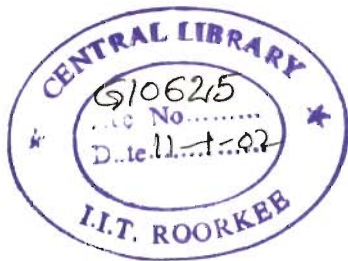
DOCTOR OF PHILOSOPHY

in

ELECTRICAL ENGINEERING

By

SATISH TUKARAM HAMDE



**DEPARTMENT OF ELECTRICAL ENGINEERING
UNIVERSITY OF ROORKEE
ROORKEE-247 667 (INDIA)**

DECEMBER, 2000

CANDIDATE'S DECLARATION

I hereby certify that the work which is being presented in the thesis entitled "ANALYSIS AND INTERPRETATION OF ECG SIGNAL USING WAVELET TRANSFORM" in fulfillment of the requirement for the award of the Degree of Doctor of Philosophy and submitted in the Department of Electrical Engineering of the University is an authentic record of my own work carried out during a period from ~~Aug~~ 1997 to December 2000 under the supervision of Dr. S. C. Saxena, Professor & Head and Dr. Vinod Kumar, Professor, Department of Electrical Engineering.

The matter presented in this thesis has not been submitted by me for the award of any other degree of this or any other University.



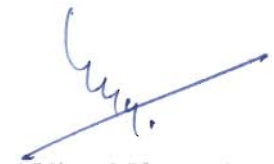
(SATISH TUKARAM HAMDE)

This is to certify that the above statement made by the candidate is correct to the best of our knowledge.

Date: 30.12.2000

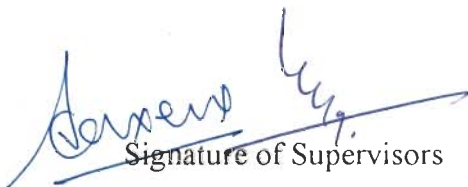


(S.C. Saxena)

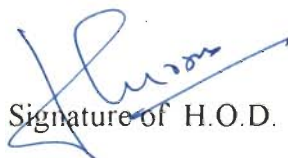


(Vinod Kumar)

The Ph.D. Viva-Voce examination of Shri Satish Tukaram Hamde, Research Scholar, has been held on 20-06-2001



Signature of Supervisors



Signature of H.O.D.



Signature of External Examiner

ACKNOWLEDGEMENT

I express my deepest sense of gratitude towards my supervisors Dr. S.C.Saxena, Professor and Head, and Dr. Vinod Kumar, Professor, Department of Electrical Engineering for their inspiring guidance, constant encouragement, moral support, and keen interest in minute details of the work.

I am thankful to Dr. H. K. Verma, Professor in the Department of Electrical Engineering for his invaluable encouragement and support, and above all the noblest treatment extended by him.

I am grateful to the Principal, Shri Guru Gobind Singhji College of Engineering and Technology, Nanded, for sponsoring me to the Doctoral Programme. In addition, I am also grateful to the Ministry of Human Resources and Development, Government of India and AICTE, New Delhi, for providing opportunity under Quality Improvement Programme.

I extend my sincere thanks to Dr. R.P. Maheshwari, Dr. R.S. Anand, Prof. C.B. Deshpande, Prof. S.G. Kahalekar and Madam Ambalika Shrama for sharing their experiences. I am thankful to my colleagues Dr. R.H. Chile, Mr. L.M. Waghmare, Dr. G. Vijaya, Dr. P.K. Kulkarni, Mr. A.S. Arora and Mr. Saad for having spent their valuable time in constructive discussions. I am thankful to my friends Dr. M.L. Waikar, R.G. Jamkar, P. G. Solankar, M.P. Rajurkar, S.B. Sharma, Dr. R.S. Holambe, Dr. B.M. Patre, , N.P. Kaushik, P. D. Dahe, Govind Pandey, A. K. Wadhawani, P. Bodkhe and Shri. N. G. Megde who helped me in every respect, during my difficult periods. I also extend special thanks to V. K. Giri and Dr. R.N. Kagne for their encouragement.

I express my sense of gratitude to J. Prasad and other non-teaching staff of I. & S. P. Laboratory and Electrical Engineering Department for their cooperation and assistance.

The use of CSE and MIT/BIH database library, papers and books referred for my work and the help tendered by the medical experts is greatly acknowledged.

I owe a debt of gratitude to my mother for her consistent support and encouragement. Words can hardly explain the co-operation and patience of my children Gaurav and Gayatri. I have no words to express the appreciation for my wife Mrs. Sunita who stood by me at every moment & keeping myself free from almost all the liabilities of home issues during my work.

Last but not the least, I am thankful to the Almighty who gave me the strength and health, particularly in the period of sickness and sudden demise of my beloved father.

(Satish Tukaram Hamde)

LIST OF ABBREVIATIONS

AHA	: American Heart Association
AMI	: Anterior Myocardial Infarction
ANS	: Autonomic Nerves System
AZTEC	: Amplitude Zone Time Epoch Coding
BBB	: Bundle Branch Block
BPM	: Beats Per Minute
CICU	: Cardiac Intensive Care Unit
CMRR	: Common Mode Rejection Ratio
CORTES	: Coordinate Reduction Time Encoding System
CR	: Compression Ratio
CSE	: Common Standards for quantitative Electrocardiography
CWT	: Continuous Wavelet Transform
D-00001	: Diagnostic data record no. 1
DDC	: Distribution Density Curve
DPCM	: Delta Pulse Code Modulation
DS -3	: Data Set - 3
DU-6	: Daubechies six coefficient wavelet
DWT	: Discrete Wavelet Transform
DyWT	: Dyadic Wavelet Transform
EMG	: ElectroMyoGram
FPA	: Frontal Plane Axis
FT	: Fourier Transform
HFP	: High Frequency Power
HR	: Heart Rate
HRV	: Heart Rate Variability
IBI	: Inter Beat Interval
KLT	: Karhunen Loeve Transform
LAD	: Left Axis Deviation
LBBB	: Left Bundle Branch Block
LFP	: Low Frequency Power
LMI	: Lateral Myocardial Infarction
LVH	: Left Ventricular Hypertrophy

MA-001	: Multi-lead Artificial record no. 1
MEANS	: Modular ECG Analysis System
MI	: Myocardial Infarction
MIT/BIH	: Massachusetts Institute of Technology/Beth Israel Hospital
MO-001	: Multi-lead Original record no. 1
MOD	: Modified
MREF	: Median of Referee's Results
MRI	: Magnetic Resonance Imaging
NL	: Normal
NRT-DDC	: Non-Redundant Template Direct Data Compression
PET	: Positron Emission Tomography
PGM	: Median of Program Results
PRD	: Percent RMS Difference
PVC	: Premature Ventricular Contraction
QSWT	: Quadratic Spline Wavelet
RAD	: Right Axis Deviation
RBBB	: Right Bundle Branch Block
RMSE	: Root Mean Square Error
RRC	: Respiration Response Curve
RVH	: Right Ventricular Hypertrophy
SD	: Standard Deviation
SDNN	: SD of Normal to Normal R-R Interval
SE	: Standard Error
SL	: Standard Lead
STFT	: Short Time Fourier Transform
SV	: Standard Variance
T-limit	: Tolerance limit
TP	: Turning Point
VQ	: Vector Quantization
WT	: Wavelet Transform

LIST OF FIGURES

Figure No.	Caption	Page No.
Fig. 1.1	Block diagram of a 12-lead ECG system	3
Fig. 1.2	Cross section of the heart	4
Fig. 1.3	Conduction system of the heart	5
Fig. 1.4	Characteristic action potentials at different locations of the heart	7
Fig. 1.5	Action potentials of (a) Ventricular and (b) Pacemaker	8
Fig. 1.6	Important ECG segments and intervals	10
Fig. 1.7	Cardiac vectors in frontal plane and their normal ranges	13
Fig. 1.8	ECG waveforms in various recording situations: (a) motion artifact, (b) baseline wander, (c) EMG noise and (d) electrical interference	16
Fig. 1.9	ECG electrodes	17
Fig. 2.1	Mother wavelet and effect of time dilation and contraction on the amplitude	44
Fig. 2.2	Implementation of wavelet transform	45
Fig. 3.1	Extraction of detail signals at different scales	59
Fig. 3.2	Wavelet transform based QRS detection steps	61
Fig. 3.3	Normal ECG and accurate detection of QRS segments by six WT's (Record No. MA-001.DCD, Lead I)	69
Fig. 3.4	Small amplitude ECG with QRS segment present at extreme of data (Record No. MA-015.DCD, Lead aVL)	70
Fig. 3.5	Typical ECG with high P and T waves (Record No. MA-009.DCD, Lead II)	73
Fig. 3.6	ECG with like QRS segments having same frequency (Record No. MA-012.DCD, Lead VI)	74
Fig. 3.7	ECG with high frequency noise (Record No. MA-120.DCD, Lead II)	75
Fig. 3.8	QRS detection in high amplitude P and T waves ECG using QSWT	77

Figure No.	Caption	Page No.
Fig.3.9	QRS detection in inverted T wave ECG using QSWT	78
Fig.3.10	Sample record of MIT/BIH database	79
Fig. 3.11	Sample record of MIT/BIH database	80
Fig. 3.12	Detection of QRS complexes using the MIT/BIH database	82
Fig. 3.13	False positive detection of QRS complexes using the CSE database	83
Fig. 4.1	Flowchart for WT based ECG feature extraction	97
Fig. 4.2	Detection of ECG waves	98
Fig. 4.3(a)	Analysis of 5 beats in a ECG signal (CSE DS-3 record MA-001.DCD, Lead I)	100
Fig. 4.3(b)	Analysis of 5 beats in a ECG signal (CSE DS-3 record MA-001.DCD, Lead II)	101
Fig.4.3 (c)	Analysis of 5 beats in a ECG signal (CSE DS-3 record MA-001.DCD, Lead III)	102
Fig. 4.4	Flowchart to identify uniphasic or biphasic P and T waves	106
Fig. 4.5	Identification of biphasic P and T waves	107
Fig. 4.6	Flow chart for determination of FPA and QTc	108
Fig. 4.7	Determination of FPA from the QRS complex in leads I, II, and III	109
Fig. 4.8(a)	Comparison of P onset program measurements with referee results	113
Fig 4.8 (b)	Comparison of P offset program measurements with referee results	114
Fig. 4.8(c)	Comparison of QRS onset program measurements with referee results	115
Fig. 4.8(d)	Comparison of QRS offset program measurements with referee results	116
Fig. 4.8(e)	Comparison of T end program measurements with referee results	117
Fig. 4.8(f)	Comparison of five fiducial program measurements with referee results	118

Figure No.	Caption	Page No.
Fig. 4.8(g)	Comparison of ECG wave fiducial measurements of CSE DS-3 records	119
Fig. 4.9(a)	Analysis of a ECG signal recorded in the laboratory	121
Fig. 4.9(b)	Analysis of a ECG signal recorded in the laboratory	122
Fig. 4.9(c)	Analysis of a ECG signal recorded in the laboratory	123
Fig. 4.9(d)	Analysis of a ECG signal recorded in the laboratory	124
Fig. 4.9(e)	Analysis of a ECG signal recorded in the laboratory	125
Fig. 4.10(a)	Analysis of 5 beats in a ECG signal. (CSE DS-5 record D-00001.DCD, Lead I)	127
Fig. 4.10(b)	Analysis of 5 beats in a ECG signal (CSE DS-5 record D-00001.DCD, Lead II)	128
Fig. 4.10(c)	Analysis of 5 beats in a ECG signal (CSE DS-5 record D-00001.DCD, Lead III)	129
Fig. 5.1	Precordial leads in LVH	146
Fig. 5.2	Precordial leads in RVH	148
Fig. 5.3	Right and Left precordial leads in RBBB	150
Fig. 5.4	Decision tree classifier using modified scoring criteria for LVH, RVH and MI	154
Fig. 6.1	HRV power spectrum. (T- thermoregulation fluctuations, B -blood pressure fluctuations, R -respiratory fluctuations)	192
Fig. 6.2(a)	Flow chart for HRV analysis	195
Fig. 6.2(b)	WT subroutine	196
Fig. 6.2(c)	PSD subroutine	197
Fig. 6.3	Detection of R peaks using WT in long recording	198
Fig. 6.4	Comparison of HRV signals in different respiration phases	201
Fig. 7.1	Steps of ECG compression and decompression using NRT-DDC	205
Fig. 7.2	Signal reconstruction by interpolating template samples (NRT-DDC)	210
Fig. 7.3	Three stages of analysis and synthesis of a wavelet transform	212
Fig. 7.4	Difference signal extracted from original and reconstructed signals (NRT-DDC) (Record No. MA-001.DCD, Lead I)	217
Fig. 7.5	Performance evaluation of the algorithm using standard signals	218

Figure No.	Caption	Page No.
Fig. 7.6	Compression and decompression using a ECG signal with base line wander (NRT) (Record No. D-00001.DCD, Lead II)	219
Fig. 7.7	Compression and decompression using a typical ECG signal (NRT-DDC) (Record No. MA-120.DCD, Lead II)	222
Fig. 7.8	WT based ECG data compression (CR 8:1) (Record No. MA-001.DCD, Lead I)	229
Fig. 7.9	WT based ECG data compression (CR 16:1) (Record No. MA-001.DCD, Lead I)	230
Fig. 7.10	WT based ECG data compression using a signal containing noise (CR 8:1) (Record No. MA-120.DCD, Lead III)	231
Fig. 7.11	WT based ECG data compression using a signal containing noise (CR 16:1) (Record No. MA-120.DCD, Lead III)	232
Fig. 7.12	WT based ECG data compression using a signal with baseline wander (CR 8:1) (Record No. D-00001.DCD, Lead II)	233
Fig. 7.13	WT based ECG data compression using a signal with baseline wander (CR 16:1) (Record No. D-00001.DCD, Lead II)	234

LIST OF TABLES

Table No.	Caption	Page No.
Table 1.1	Definition of ECG leads	14
Table 2.1	Wavelets and their application areas	50
Table 3.1	Details of wavelet filters analysed for QRS detection	63
Table 3.2	QRS detection performance of six wavelets (using first 25 records of CSE DS-3 database)	64
Table 3.3	Detection of QRS peak amplitude and location in d^4 signal by six wavelets (using CES DS-3 Record No. MA-001.DCD)	67
Table 3.4	Detection of QRS peak amplitude and location by mapping the detected location in d^4 with original ECG signal (MA-001.DCD)	68
Table 3.5	WT based QRS detection (Record MA-032.DCD, Lead aVF)	77
Table 3.6	WT based QRS detection (Record MA-108.DCD, Lead V3)	78
Table 3.7	WT based QRS detection (Record MIT/BIH 100)	79
Table 3.8	WT based QRS detection (Record MIT/BIH 200)	80
Table 3.9	WT based QRS detection of Record No. MA-010.DCD	84
Table 3.10	Results of QRS detection by using quadratic spline wavelet (Records of the CSE DS-3, use of 12 Leads)	85
Table 3.11	Results of QRS detection for the MIT/BIH database	86
Table 3.12	Comparison of ECG analysis results	87
Table 4.1	Measurement of ECG parameters by using wavelet transform of Record No. MA-001..DCD	103
Table 4.2	ECG parameters of CSE DS-3 Record No. MA-001..DCD	104
Table 4.3	Summary of ECG analysis results of 25 cases of CSE DS-3 database	112
Table 4.4 (a)	Fundamental and diagnostically important ECG parameters of Record CSE DS-5 D-00001.DCD, beat-1	131

Table No.	Caption	Page No.
Table 4.4 (b)	Fundamental and diagnostically important ECG parameters of Record CSE DS-5 D-00001.DCD, beat-2	132
Table 4.4 (c)	Fundamental and diagnostically important ECG parameters of Record CSE DS-5 D-00001.DCD, beat-3	133
Table 4.4 (d)	Fundamental and diagnostically important ECG parameters of Record CSE DS-5 D-00001.DCD, beat-4	134
Table 4.4 (e)	Fundamental and diagnostically important ECG parameters of Record CSE DS-5 D-00001.DCD, beat-5	135
Table 5.1	Scoring criteria for RBBB and LBBB	140
Table 5.2	Existing and modified LVH scoring criteria	141
Table 5.3	Existing and modified RVH scoring criteria	142
Table 5.4	Existing and modified MI scoring criteria	151
Table 5.5	Heart disease diagnostic results using CSE DS-3 database	157
Table 5.6	Disease diagnosis using existing scoring schemes (first 10 records of CSE DS-5)	158
Table 5.7	Complete procedure to interpret the ECG by decision tree classifier Using five beats of record CSE D-00008.DCD	165
Table 5.8	Disease diagnosis using modified scoring criteria (on CSE DS-5)	173
Table 5.9	Comparison of results	175
Table 5.10	Comparison of program results with experts' opinion	176
Table 5.11	Disease diagnostic results from the best of 5 interpretations using a decision tree classifier (25 Records of CSE DS-5)	177
Table 5.12	Disease diagnosis using the ECGs recorded in the laboratory	182
Table 6.1	Extraction of spectral and non-spectral indices	199
Table 6.2	Effect of abnormal beat on HRV indices	199
Table 6.3	Effect of slow, normal and fast respiration rates on HRV indices studied over consecutive four days	200
Table 7.1	Performance indices for NRT-DDC technique	220

Table No.	Caption	Page No.
Table 7.2	Amplitudes measured in original and reconstructed signals for NRT-DDC (for CR 8:1)	223
Table 7.3	ECG wave onset and offset measured in original and reconstructed Signals for NRT-DDC technique (for CR 8:1)	223
Table 7.4	Diagnostically important parameters measured in original and reconstructed signals for NRT-DDC technique	224
Table 7.5	Comparison of data compression techniques	225
Table 7.6	Performance indices for WT based data compression technique	227
Table 7.7	Diagnostically important parameters measured in original and reconstructed signals for WT based compression technique	228

ABSTRACT

Electrocardiogram (ECG) is a graphical representation of the electromechanical activity of the cardiac system. It provides a fast and reliable information to the expert cardiologist with respect to the functional aspects of the heart. The ECG is recorded in many situations, viz., to know the state of a patient under medical diagnosis and treatment, to keep a watch on the state of patients in the intensive cardiac care units, to know the response of the patient under medical treatment, to know the condition of cardiac system under stressed conditions, and to monitor the state of the ambulatory patients. The number of cardiac patients are increasing at an alarming rate and it is not possible for the existing number of cardiologists to take care of all the cardiac patients under all the conditions. This problem was realized about four decades back and a large number of individuals and groups started work on the computer aided analysis and interpretation of ECG signal throughout the world. One of the first attempts to automate the ECG analysis was made in 1957 by Pipberger and his group in USA.

The ECG data acquisition and preprocessing; detection of waves, peaks, and interwave segments; feature extraction of all waves, peaks and segments; and usage of these in disease classification and diagnostics are the important stages in computer aided ECG analysis and interpretation. After carrying out the detailed survey about four years back by the author, it was found that there is a gap between what is ideally required and what has been achieved so far in the area of computer aided ECG analysis and interpretation. The gaps were identified and the work has been carried out in this thesis to bridge the gaps in the automated analysis and interpretation of the ECG signal by making effective use of the wavelet transform. The work covers the ECG feature detection & extraction, and cardiac disease diagnostics using multilead ECGs, disease diagnostics using rhythm analysis and data compression using non-redundant template and wavelet transform.

After dealing with the general introduction and the brief outline of the work, the first stage of the work deals with the QRS detection using wavelet transform. In this study, the detection of QRS complexes by different wavelets, using standard CSE and MIT/BIH data bases has been carried out. Looking at the potentials of various approaches, it is very difficult to claim that a particular method (syntactic, non-syntactic, hybrid or transformative type) is always suitable for QRS detection. Due to the physiological variability of the QRS wave and the presence of noise and artifacts in the ECG signal, none of the technique has claimed an

accuracy of 100% in QRS detection. In recent times, the use of wavelet transform in QRS detection has shown upper edge in terms of no-need of preprocessing, accuracy of detection, and simplicity in calculations. And it has been found that even with the wide variations in ECG morphologies, QRS detection is more accurate by wavelet. In the present work, five existing wavelets (WT1, WT2, WT3, WT4, WT5) and a new wavelet (WT6) developed by the author have been used for the QRS detection. Their performance is checked using the first 25 records of the CSE database. The WT1, having high and low magnitude filter coefficients, gives QRS detection rate of 99.11%. The performance of WT2 is similar to WT1 and gives QRS detection rate of 99.16%. These long filter length wavelets usually fail to detect QRS complex, if it present at the start or end of data. The compact wavelet WT3 is computationally simple, faces less difficulty in detecting the end point QRS complexes, and gives high detection rate of 99.91%. The WT4 faces difficulty in detecting QRS complex when the signal amplitude is low, and gives QRS detection rate of 88.18%. The WT5 is computationally suitable for detection of end point QRS complexes, and gives detection rate of 99.70%. After the performance evaluation of WT1-WT5 and also by keeping in view the selection guidelines for wavelets, a new wavelet (WT6) has been constructed. The WT6 gives QRS detection rate of 99.89%. The quadratic spline wavelet (QSWT i.e., WT3) and WT6 are found to be the most suitable for QRS detection as they detect QRS complexes even with the wide variety of ECG morphologies, noise and/ or artifacts. The developed software gives the QRS detection rate of 99.866%. The QSWT, when tested on all 48 records of the MIT/BIH, gives the QRS detection rate of 99.806%. This performance of the developed software proves the utility of the wavelets for the detection of QRS complexes.

In the second stage of the work, all the fundamental ECG parameters have been detected and measured by using the QRS location as a time reference. From these parameters, diagnostically important features namely, heart rate, P amplitude, P duration, PR interval, QRS interval, QRS peak-to-peak amplitude, QT interval, VAT and T amplitude are obtained. The comparison of five wave fiducial points shows that most of the values are well within the tolerance limits suggested by the CSE working party and the overall accuracy in the measurement is about 91.00%. Out of a total of 125 fiducial location estimates in 25 records, 11 estimates deviate from the tolerance. The software has also been tested using the ECGs recorded in the laboratory, and 5 beats have been selected for feature extraction and the resulting diagnostic parameters have been extracted. After confirmation of the reliability of software using CSE DS-3 and the ECG records of this lab, diagnostic dataset DS-5 has been used for the analysis and disease diagnosis. As there are no measurement results published by

the CSE for dataset DS-5, statistical analysis has been used to see the distribution of program estimates around a mean value. From a record, five regular beats per lead are selected and 29 parameters per beat per lead are extracted. Therefore, the software extracts the parameters from five such beats in 12 standard leads and stores the feature extraction data. Statistical parameters are used to see measurement performance of the developed software. With respect to interval and amplitude measurements of various components of the QRS complex as well as of the P wave and ST-T complex, a median value of the results from 12 standard leads (SL) has been used as a reference. The median value derived from 12 SL measurements proved to correlate in the best way with the results of the visual analysis. The statistical parameters namely, variance and standard deviation (SD) derived from 12 SL measurements show the best performance in the ECG analysis.

As the ultimate aim of the ECG analysis is disease diagnosis, therefore, in the third stage of the work, the diseases namely, Left Ventricular Hypertrophy (LVH), Right Ventricular Hypertrophy (RVH), Myocardial Infarction (MI) (anterior, lateral, and inferior), Right Bundle Branch Block (RBBB), Left Bundle Branch Block (LBBB), Tachycardia and Bradycardia are considered for disease classification. The disease classification is based on the main features of the ECG.

The testing of disease diagnostic has been carried out on all 125 cases of CSE DS-3 database. For this data two diagnostic criteria have been used to enable the validation of the disease classification. It is observed that the final diagnostic results obtained according to the score and the thresholds by both the criteria are the same. After the testing of software on CSE DS-3, the disease diagnosis of CSE DS-5 records and the ECGs recorded from different subjects in the laboratory have been carried out. The combined results of existing scoring schemes for LVH, RVH and MI diseases are used to give an overall diagnostic statement, which is a resultant statement based on the results obtained by the existing three LVH, three RVH and two MI scoring criteria.

A typical record D-00008.DCD from the CSE DS-5 has been used and the five data files of ECG parameters and the corresponding disease interpretation by existing as well as modified scoring schemes have been carried out. The ultimate result is obtained from the net results of five interpretations given by modified scoring schemes. Using the strategy of disease diagnostics from the features of five ECG beats, the validation of the software has been carried out using the CSE database. The results of this evaluation are compared with the results obtained by the existing scoring schemes and also with the diagnostic truth given by the CSE Committee. The CSE Working Party has considered the case as normal even if the

record shows minor abnormalities such as non-specific ST-T changes, incomplete right or left BBB, left anterior fascicular block, minor intraventricular conduction defects (QRS <120ms) or even myocardial ischemia, as a single statement without making reference to any of the seven primary categories, namely, Normal, LVH, RVH, BVH AMI, IMI, and MIX MI. To compare the results of existing and modified scoring schemes with the CSE results, the diseases Bradycardia, Tachycardia, RBBB, and LBBB are not considered. From the comparison with the CSE diagnostic results of first 10 records of DS-5, the diagnostic interpretation performed by existing scoring criteria matches up to 60% with the truth and by the modified criteria up to 80% , thereby resulting a gain of 20% . The gain is due to three factors: i) use of combined wavelets for feature extraction, ii) use of five beats in place of one beat for analysis, and iii) the use of modified scoring scheme.

In addition to the disease diagnosis using multilead ECGs, rhythm analysis using single lead recording has been carried out to study heart rate variability (HRV) in the next stage of work. This includes the use of the WT for QRS detection and removal of ectopic beats and artifacts, determination of spectral and non-spectral indices and displaying of HRV related plots, namely R-R interval and PSD curves. The system performance has been evaluated by using the standard MIT/BIH database, because this database has long records and the database created by on-line recording from different subjects in the laboratory itself. The WT has been used to detect the R-R normal intervals from the ectopic beats and artifacts. This is due to splitting the ECG signal in different band of frequencies and the use of frequency band containing the QRS complexes. On the basis of these results, it can be stated that the HRV spectral and non-spectral indices are less prone to fluctuations in heart rate due to autonomic imbalance than the fluctuations due to improper and incorrect detection of a single heart beat. This false detection gives substantial rise to the values of heart rate (HR), standard deviation of normal to normal R-R intervals (SDNN), low frequency power (LFP) and high frequency power (HFP) parameters. Thus, HRV analysis needs accurate detection of normal R-R intervals. The second set of database obtained from the subjects in the laboratory characterises the dynamic response of the heart to the vagus nerve i.e. during slow, comfortable and fast paced respiration. Three different rates, 12, 19, and 24 breaths/min, were chosen to represent slow, comfortable, and fast pacing rates, respectively. Quantization of the data in terms of their relative spectral and non-spectral indices for different respiration phases illustrates the influence on the vagal activity, HRV and corresponding PSD curves. For slow respiration, the HR gradually changes and this change is in the range of 80 to 100 BPM. So far as normal breathing is concern, the HR change is fast

and varies from 80 to 120 BPM. For fast respiration, the HR variations are less, the change is in the range from 90 to 110 BPM. There is a negative relationship between the respiratory rate and the spectrum measures of parasympathetic activity (vagal power). For slow respiration, high power peak emerges around the frequency of 0.3 Hz. A low power peak emerges in case of fast respiration. This indicates the influence of vagal control on the heart activity. The test results are consistent and reliable and show high promise for the effective use of WT based R-R detection technique for the HRV study and analysis.

To handle the large volume of ECG data without losing the diagnostic information, it is necessary to use faithful data compression techniques. Thus, there is a need to develop such techniques which have better performance in comparison to existing techniques. In the present work a simple technique has been introduced named as non-redundant-template direct data compression (NRT-DDC) technique. It performs the compression by downsampling the ECG signal in steps. The removed data samples in the process of downsampling are stored in a data array as non-redundant template. The signal is compressed by a factor of 8 for the ECG signal sampled at 500 Hz or 16 for the signals sampled at 1000 Hz. The performance evaluation of the non-redundant template NRT-DDC has been carried out using the CSE data sets-3 and -5. The reconstruction accuracy even in the low frequency and low amplitude (baseline) region is within the tolerance limits, which helps in accurate detection of onsets and offsets of the ECG waves. Aspect of holding the information of the ECG locations is being carried out by storing the compressed signal. Hence, this helps to retain 100% accurate diagnostic information. To compare the performance of this method with the existing techniques, we have selected the reported data as well as the techniques reported with the performance evaluation based on compression ratio (CR) and percent root mean square difference (PRD) for data sampled with 500Hz. The CR by the existing techniques ranges from 7 to 10 in most of the cases (except in two, having high CR of about 16) and PRD from 3 to 28. It means that only CR or PRD does not give proper scale for comparison. Therefore, the only way is to see whether the clinical information is being retained or can be retrieved or not from the reconstructed signal. This aspect has been considered to evaluate the performance of the developed methods in this work and the comparison of the diagnostically important parameters measured in original and reconstructed signal is carried out with the CSE results. In addition to this data compression technique, an algorithm for WT based data compression has also been developed. Cardiologists suggest that the clinically useful information present in original ECG signals is preserved by 8:1 compression, and in most

cases 16:1 compressed ECGs are clinically useful. Considering this, the data compression has been carried out using the WT technique to provide the CR of 8:1 and 16:1.

Finally it can be stated that the work contributes significantly to the area of computer aided analysis and interpretation of ECG signal. It also raises number of questions for carrying out further work. The overall work done in this thesis may be considered a positive and significant contribution in this field.

CONTENTS

	Page
Candidate's Declaration	i
Acknowledgement	ii
List of Abbreviations	iii
List of Figures	v
List of Tables	ix
Abstract	xii
Contents	xviii

CHAPTER I: INTRODUCTION

1.1 General	1
1.2 Electrocardiogram	1
1.2.1 The heart	2
1.2.2 Cardiac electrophysiology	6
1.2.3 Genesis of ECG	9
1.2.4 ECG nomenclature	9
1.2.5 ECG wave intervals and segments	11
1.3 Cardiac vectors	12
1.4 Lead systems	14
1.5 Sources of interference in ECG recording	15
1.6 Clinical aspects of ECG	18
1.7 Standard ECG databases	19
1.7.1 CSE database	19
1.7.2 MIT/BIH database	21
1.8 Literature review	22
1.8.1 Methods of ECG analysis and interpretation	22
1.8.2 Feature extraction of ECG signal	25
1.8.3 Disease diagnosis	31
1.8.4 ECG data compression	36
1.9 Scope of present work	38
1.10 Organization of the thesis	39

CHAPTER II: WAVELET TRANSFORM

2.1 Introduction	40
2.2 Wavelet transform Vs. Fourier transform	41
2.3 Types of wavelets	42
2.4 Wavelet transform	43
2.5 Properties of Wavelet Functions	47
2.6 Wavelets and their applications	48
2.7 Conclusion	52

CHAPTER III: DETECTION OF QRS COMPLEX

3.1 Introduction	53
3.2 Methods of QRS detection	53
3.3 Wavelet transform	57
3.3.1 Implementation of wavelet transform	58
3.3.2 Identification of ECG waves	58
3.4 Selection of wavelets for QRS detection	60
3.5 QRS detection using existing wavelets	65
3.5.1 Test Results with existing wavelets	66
3.6 Construction of new wavelet	66
3.6.1 Construction	71
3.6.2 Test results	71
3.7 Discussions	72
3.8 Conclusions	88

CHAPTER IV: FEATURE EXTRACTION OF ECG SIGNAL

4.1 Introduction	89
4.2 Feature Extraction Techniques	89
4.2.1 Feature extraction	90
4.2.2 Interpretation	91
4.3 Selection of beats	91
4.4 Amplitude measurement procedure	92
4.5 Interval measurement procedure	93
4.6 P, Q-R-S and T waves detection	94
4.6.1 Method	94
4.7 Diagnostic parameters	99
4.7.1 Heart rate	99
4.7.2 Ventricular activation time	99
4.7.3 Uniphasic/ Biphasic P and T waves	105
4.7.4 Frontal plane axis	105
4.7.5 QT-interval	110
4.8 Test results using CSE DS-3 and discussions	110
4.9 Test results using CSE DS-5 and discussions	126
4.10 Statistical analysis of ECG parameters	130
4.11 Conclusions	136

CHAPTER V: DISEASE DIAGNOSIS USING MULTILEAD ECG

5.1 Introduction	138
5.2 Cardiac diseases	139
5.2.1 Electrical axis of QRS	139
5.2.2 Significance of the QRS axis	143
5.2.3 Left ventricular hypertrophy	144
5.2.4 Right ventricular hypertrophy	147
5.2.5 Intraventricular conduction delay	149
5.2.6 Myocardial infarction	149
5.3 Existing and modified disease diagnostic criteria	152
5.4 Software development	155
5.5 Test results and discussions	156
5.5.1 Disease diagnosis using CSE dataset-3	156
5.5.2 Disease diagnosis using CSE dataset-5	161
5.6 Conclusions	183

CHAPTER VI: DISEASE DIAGNOSTICS USING RHYTHM ANALYSIS

6.1 Introduction	184
6.2 Importance of HRV analysis	186
6.3 Autonomic nervous system	188
6.4 SA node and respiration entrainment	188
6.5 Methodology	189
6.6 Detection of R-R event series	191
6.7 Test Results and Discussions	194
6.8 Conclusions	202

CHAPTER VII: ECG DATA COMPRESSION USING NON-REDUNDANT TEMPLATE AND WAVELET TRANSFORM

7.1 Introduction	203
7.2 A New non-redundant template -direct data compression technique	206
7.2.1 Compression	206
7.2.2 Decompression	208
7.3 Wavelet transform based ECG data compression	211
7.3.1 Method	211
7.4 Performance evaluation of data compression techniques	214
7.5 Results and discussions	216
7.6 Conclusions	235

CHAPTER VIII: CONCLUSIONS AND SCOPE FOR FUTURE WORK	
8.1 Conclusions	237
8.2 Scope for future work	240
APPENDIX – I Panel of Medical Experts	241
APPENDIX – II Author’s Research Contribution	242
REFERENCES	243

INTRODUCTION

1.1 GENERAL

Electrocardiograph (ECG) enables a rapid observation of the behavior of the heart activity in terms of heart rhythm, conduction intervals, morphological aspects of the waves (P,Q,R,S,T) associated to depolarization and repolarization of the auricles and ventricles. The late potentials (LP) are a particular case of delayed inhomogeneous depolarization, which may occur elsewhere, for example, under the QRS or after and under the P wave. The presence of late potentials and more particularly ventricular late potentials (VLP) increase the probability of sudden death [119]. It is also important to observe the His signal, which occurs between the P and Q waves and reflects the conduction from the auricles to the ventricles. Also there is increased importance of study and analysis of heart rate variability (HRV) in clinical practice because time and frequency domain analysis of HRV allows to predict mortality risk after cardiac infarction and congestive heart failure [83,121]. A proper technique allowing the detection and analysis of ECG features is of precious help to the physicians. A typical way to analyze cardiac signals, which are of non-stationary nature, is through a time-frequency analysis and more particularly using wavelet transforms (WT). Considering the increased number of cardiac patients and need of sophistication due to want of information on pressing a tip of finger, there is no better alternative than the automated ECG analysis and disease diagnosis system to assist an expert cardiologist.

1.2 ELECTROCARDIOGRAM

The electrical activity of the human heart can be detected on the body surface. Though it is quite low in amplitude (about 1 mV), it is recorded as an ECG signal. The ECG has considerable diagnostic significance and applications of ECG monitoring are quite diverse and are widely used [49,134]. For example, a diagnostic ECG recording is usually made in a doctor's chamber in a routine checkup and a full 12-lead ECG is recorded from a resting patient on a chart paper to diagnose the cardiovascular diseases. In cardiac intensive care units (CICUs), a patient's one-lead ECG is continuously displayed on a cathode ray tube and monitored for signs of cardiac distresses. ECG monitoring capability is incorporated into various devices, the cardio-tachometer, which measures the heart rate [143]. Some other devices like the automated defibrillator, acquire ECG signals to determine the absence of normal sinus rhythm and the correct instant in the cardiac cycle at which a high-voltage

defibrillation shock is to be delivered. Modern pacemakers and implantable defibrillators also require ECG acquisition capability [145].

The primary function of the acquisition system is to amplify the ECG signal and reject environmental and biological noise and artifacts. Diagnostic ECGs are obtained in routine checkups as well as for specific interpretation of cardiac diseases such as left ventricular hypertrophy (LVH), right ventricular hypertrophy (RVH), myocardial infarction (MI) or electrical conduction defects. Modern diagnostic ECG machines also have built-in microcomputers that analyze the signal and give preliminary interpretation.

Figure 1.1 is a block diagram of a 12-lead diagnostic ECG system. The electrodes are attached to the patient's body on the four limbs and the chest. The typical 12-lead system uses 3 limb leads, 3 augmented leads, and 6 precordial leads [145]. A driven-right-leg circuit may be used to reduce electrical interference. The signals from limb electrodes RA, LA, and LL are connected to a resistor network called Wilson's central terminal which is driven from the limb leads I, II, and III, and augmented leads aVL, aVR, and aVF. Generally, three leads are acquired at a time (I-II-III, aVL-aVR-aVF, V1-V2-V3, and V4-V5-V6).

1.2.1 The Heart

The heart contains four chambers; two thin-walled atria separated from each other by an inter-atrial septum and two thicker-walled ventricles possessing common wall in the inter-ventricular septum. Atria and ventricles are connected by a fibrous A-V ring. This ring is penetrated on the right side by the tricuspid valve and on the left side by the mitral valve as shown in Fig.1.2. The two valves consist of flaps or cusps, which are attached at the periphery of the valve ring. On the right side, the pulmonary orifice is guarded by the pulmonary or semilunar valve, which consists of three flaps. A similarly constructed valve (aortic) is situated at the aortic orifice. These valves open at the onset of ventricular ejection and close when the relevant arterial pressure exceeds that of the corresponding ventricle and it begins to relax. The closure of atrioventricular valve produces the first heart sound and closure of the semilunar valve causes the second heart sound [58,74]. The mechanical activity of the heart is under the control of electrical conduction.

The heart wall, which is composed of a cardiac muscle tissue, is referred as the myocardium. The components involved in the conduction system of the heart are shown in the Fig.1.3. The muscle cells of myocardium are classified into five functionally and anatomically separate parts namely, sinoatrial (SA) node, atrioventricular (AV) node, His-purkinje system, atrial muscle and ventricular muscle each having different characteristic

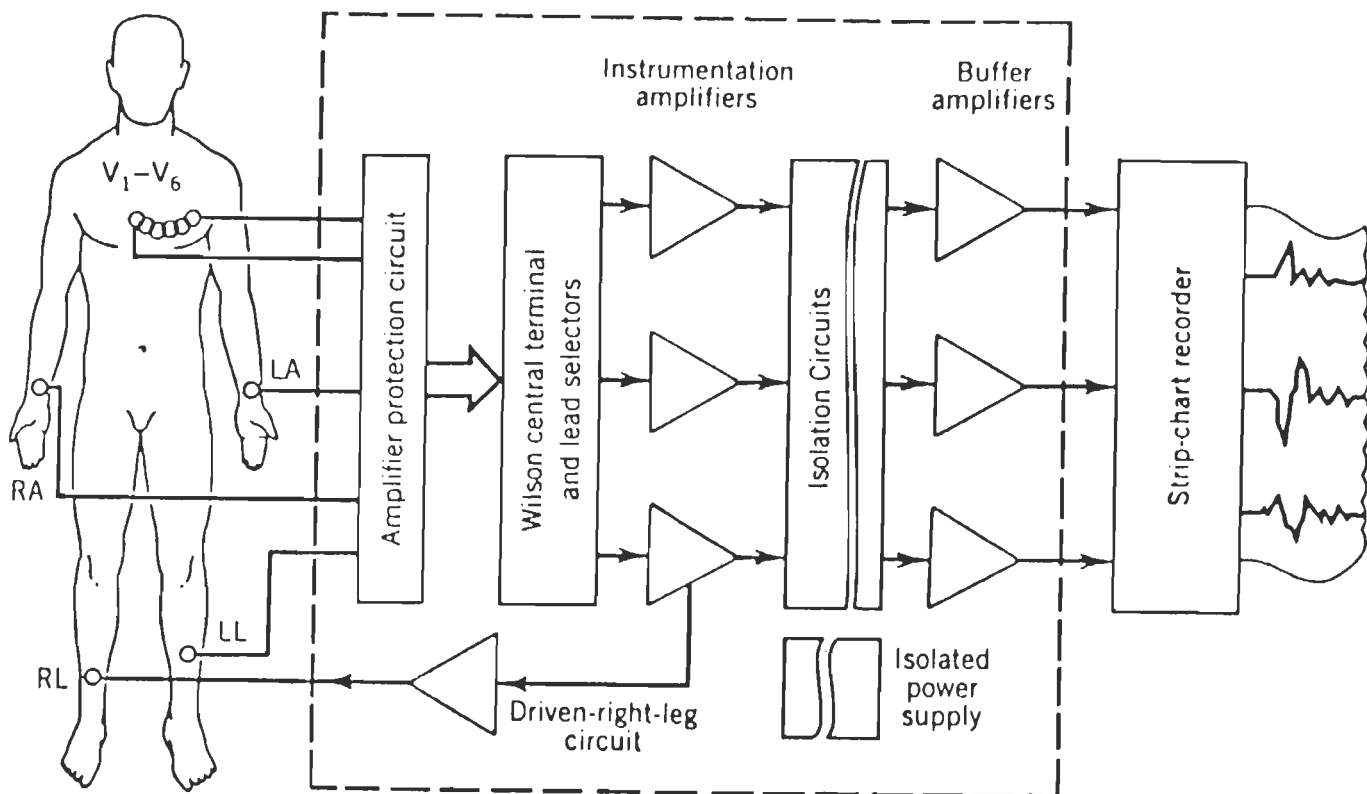


Fig.1.1 Block diagram of a 12-lead ECG system
 [Webster J. G., 1988, (145)]

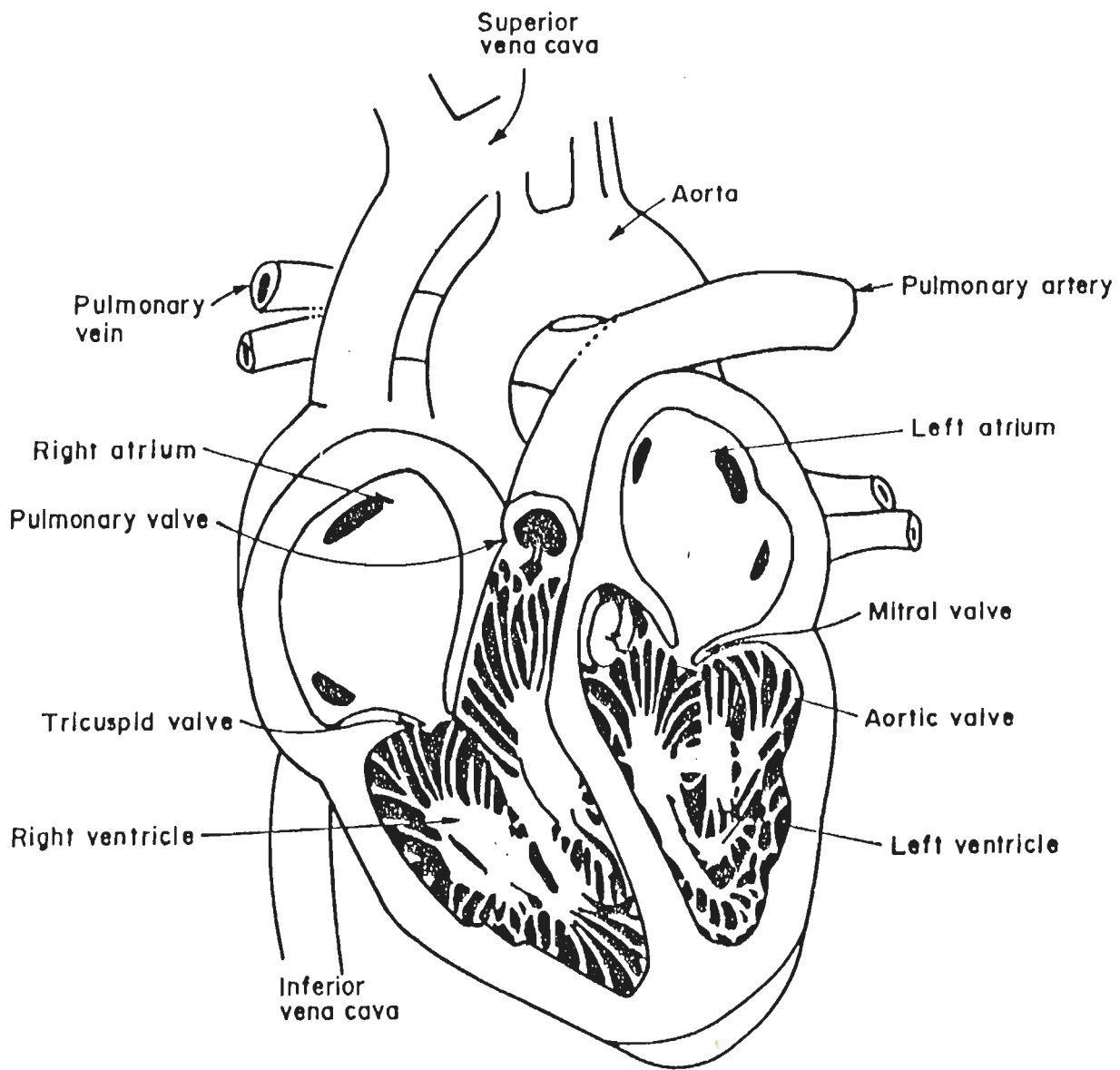


Fig.1.2 Cross section of the heart

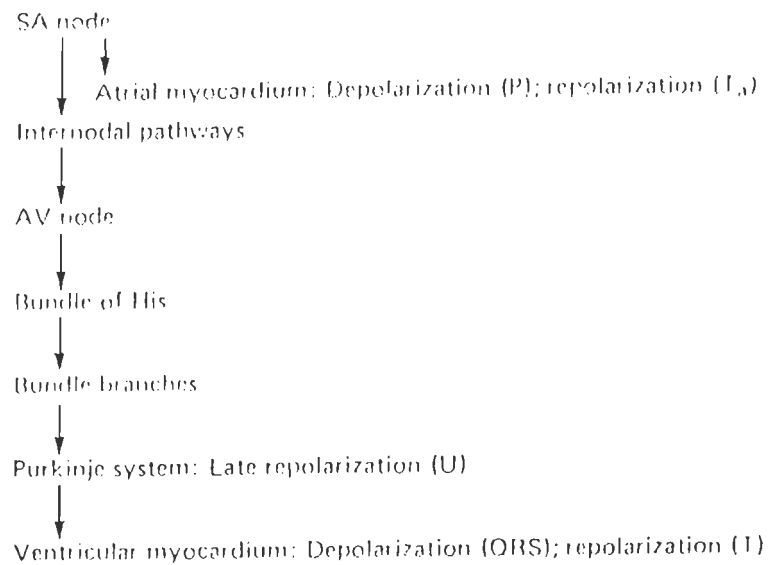
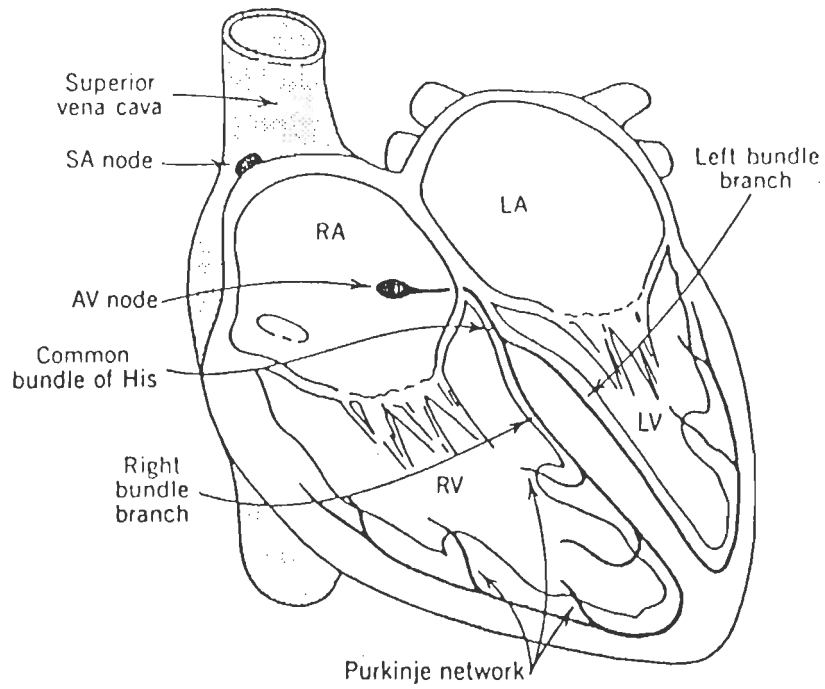


Fig.1.3 Conduction system of the heart
 [Macfarlane P. W., and Lamarie T.D.V., 1989 (78)]

action potentials as shown in Fig.1.4 [78]. They are mainly involved in the maintenance of two primary and well synchronized physiological events, namely, the heart's mechanical activity (pumping of the blood) and the heart's electrical activity (the transmission of electrochemical impulses for the coordination of the heart's effort). These two activities give rise to an orderly heartbeat.

1.2.2 Cardiac Electrophysiology

Cardiac electrophysiology recognizes the presence of several cell types in the heart. These include the ventricular cells, the atrial cells and cells that constitute the conduction system (Purkinje fibers), and the pacemaker cells. The pacemaker cell is self-excitatory and undergoes repetitive cyclic activation. This cyclic activation initiates a contraction and the result of the cyclic electrical activity is the periodic heartbeat. Fig.1.5 shows the ventricular and pacemaker action potentials, phase 0 –activation, phase 1 -initial recovery, phase 2 -a period of fairly steady depolarization, phase 3 -recovery and phase 4 -the resting potential.

The conduction system of the heart is shown in Fig.1.3. The pacemaker cells are located in the region of the sinoatrial (SA) node and is of the size of a pencil tip located at the site of entry of the descending vena cava. The repetitive activity is initiated at this point and propagates to adjoining atrial tissue by means of the local-circuit (action) currents. The flow of this current from active to inactive neighboring cells is facilitated by the presence of low-resistance intercellular structure. The activation proceeds from cell to cell until the entire right and then left atria are activated. Because the atria and ventricles are separated by fibrous tissue, direct propagation from the atria to ventricles cannot occur. Instead, the activation follows a path that starts in the atria at the atrioventricular (AV) node and proceed through the common and then right and left bundles of His to the terminal Purkinje fibers which arborize and invaginate the endocardial ventricular tissue. The initial part of this path involves slow conduction in the AV junction. Since electrical activation of cardiac muscle initiates the successive mechanical contraction, this results in a delay in ventricular activation and contraction. It is beneficial as it allows the completion of atrial contraction. Once the electrical impulse reaches the bundles of His, the conduction becomes very rapid, resulting in the initiation of ventricular activation over a wide region. The subsequent cell-to-cell propagation is consequently sequenced and coordinated, resulting in a mechanical contraction that is similarly synchronized and efficient.

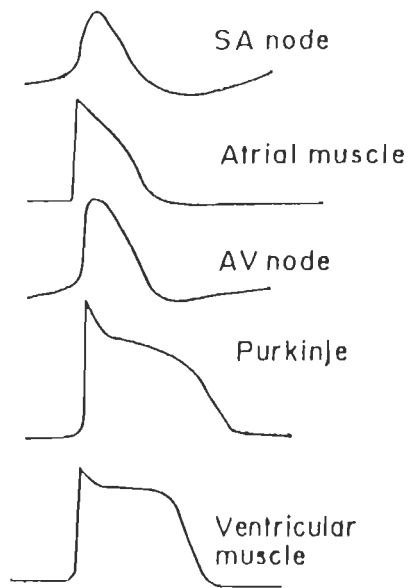


Fig.1.4 Characteristic action potentials at different locations of the heart

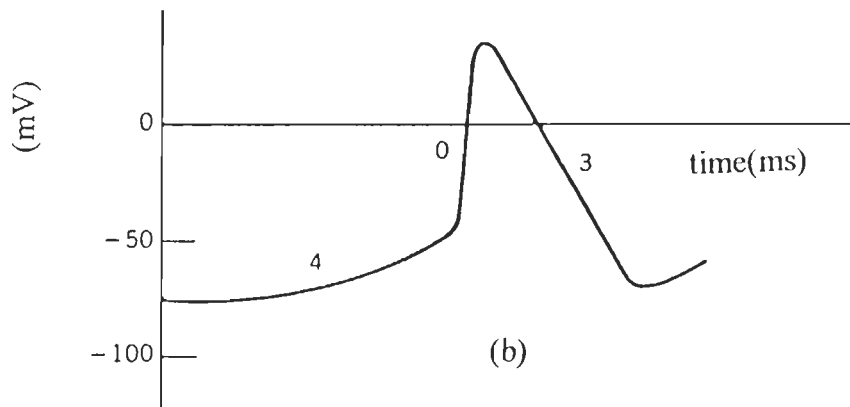
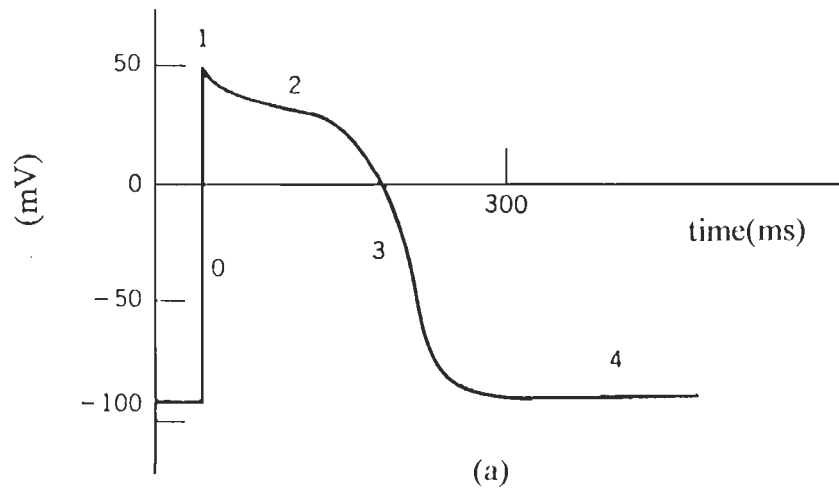


Fig. 1.5 Action potential of (a) Ventricular and (b) Pacemaker cell

1.2.3 Genesis of ECG

In the beginning, about 100 years ago, Waller measured voltages between two electrodes on the body surface and found change in it with rhythm of the heart beat [78]. It is now known that the ECGs arise because active tissues within the heart generate electrical currents, which flow most intensively within the heart muscle itself, and with lesser intensity throughout the body. The flow of current creates voltages between the sites on the body surface where the electrodes are placed. These voltages, measured as a function of time, are called ECG.

Macfarlane et al. [78] reported that the capillary electrometer used by Waller gave tracings of poor quality. Electrocardiography greatly advanced when Einthoven invented the string galvanometer around the year 1900. The string galvanometer produced ECG waveforms that had a quality comparable with the modern recordings. An ECG waveform as a whole was seen to consist of a series of deflections. For the purpose of identification, Einthoven marked the peaks of the successive major deflections by the labels P, Q, R, S, and T. There were substantial differences of opinions about the origin of the deflections, or even whether they had clinical significance. Einthoven demonstrated their clinical significance by showing the differences between waveforms recorded from normal subjects and patients suffering from dysrhythmias. Lewis recognized that the temporal sequence of the deflections of the ECG occurred because there was a temporal sequence in which different cardiac structures became electrically active. To prove this, Lewis measured the sequence of electrical excitation from the atria and ventricles of dogs, and simultaneously measured the ECGs from the body surface [78].

In 1949, Ling and Gerald introduced the glass microelectrode [78], a tool suitable for measuring potential differences across the membranes of individual cells, thereby greatly advancing the study of transmembrane potentials. The active tissues within the heart generate electrical currents, which flow most intensely within the heart muscle itself, but with lesser intensity throughout the entire body. As a consequence of the voltages created by the flow of electrical currents through out the body volume, the electrodes placed at the sites on the body surface pick-up these voltages as ECG signal.

1.2.4 ECG Nomenclature

A normal ECG lead II signal is shown in Fig.1.6, and its salient features are labeled as per the standard procedure. The first deflection, labeled P, corresponds to atrial depolarization. The following series of deflections, labeled QRS, arise from ventricular

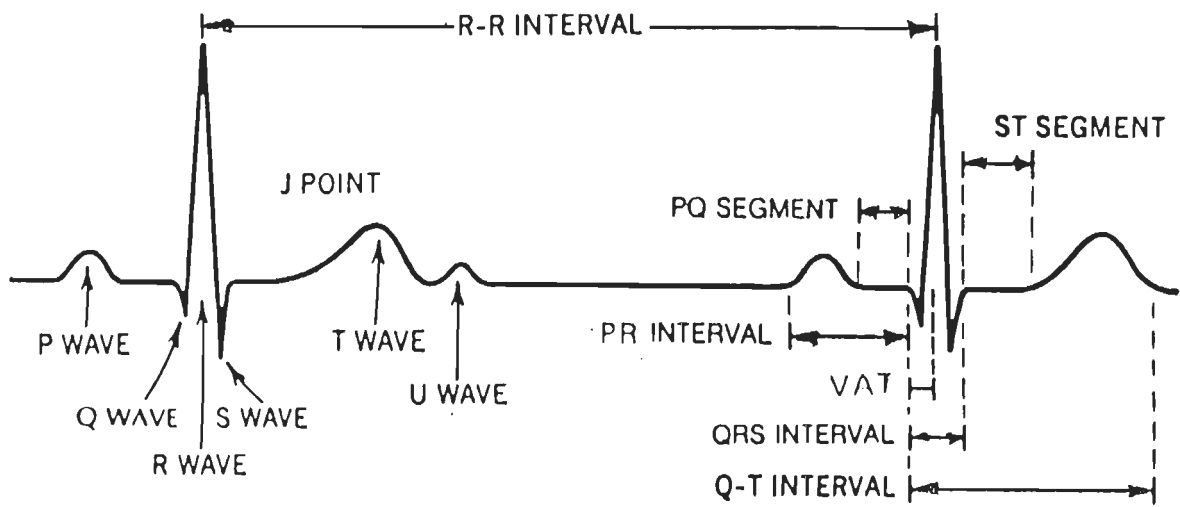


Fig.1.6 Important ECG segments and intervals

activation. According to the convention, the Q wave is the first downward deflection before any upward deflection, the R wave is the first upward deflection, and the S wave is the first downward deflection after an upward deflection. Some additional features like R', S may occur. The qRSR' designates a QRS contour where the Q wave is less than 0.5 mV and R' with greater than 0.5 mV is followed by S. The wave generated by ventricular repolarization is designated as T wave. The U wave is a low-amplitude which sometimes follow the T wave.

The time intervals are very important in ECG diagnosis and are indicated in Fig.1.6. The intervals and durations generally reflect electrophysiological processes and carry clinical implication when they lie outside the normal range of variation. The QRS interval, for example, is a measure of the total duration of ventricular tissue depolarization. The normal QRS interval is 0.06-0.10 sec in the adult. The PR interval is measured from the beginning of the P wave to the beginning of the QRS complex and reflects in part the AV conduction time. The normal adult range of which is 0.12-0.20 sec. The QT interval is measured from the onset of the QRS to the termination of the T wave and reflects the total period of ventricular depolarization and repolarization. The normal values of QT are dependent on the sex and heart rate (HR). The HR is usually determined from the RR interval.

1. 2.5 ECG Wave Intervals and Segments

RR interval: The RR interval is the distance between two successive R peaks. If the ventricular rhythm is regular, the interval (in seconds or fractions of a second) between the peaks of two successive R waves divided into 60 seconds gives the heart rate per minute. If the ventricular rhythm is irregular, the number of R waves in a given period of time (e.g. 10 seconds) are counted and the results are converted into the number per minute. [42]

PP interval: In regular sinus rhythm, the PP interval is the same as the RR interval. However, when the ventricular rhythm is irregular or when atrial and ventricular rates are different but regular, the PP interval is measured from the same point on two successive P waves and the atrial rate per minute computed in the same manner as the ventricular rate.

PR interval: It is a measure of the AV conduction time and includes the time required for atrial depolarization, the normal conduction delay in the AV node (approximately 0.07 second), and the passage of the impulse through the bundle of His and bundle branches to the onset of ventricular P wave to the beginning of the QRS complex. The normal value ranges from 0.12-0.20 sec (possibly up to 0.22 sec). A PR interval of 0.2 sec may be of no clinical significance with a heart rate of 60 beats per minute, but may well be significant with a heart rate of 100 beats per minute. [42]

QRS interval: This is the measurement of total ventricular depolarization time. It is measured from the onset of the Q wave (or R if no Q is visible) to the termination of the S wave. The upper limit of normal interval is 0.1 sec in frontal plane leads. Occasionally in precordial leads V2 or V3, this interval may be up to 0.11 sec.

Ventricular Activation Time (VAT): The time it takes an impulse to traverse the myocardium from the endocardial to the epicardial surface is assumed to be reflected in a measurement from the beginning of the Q wave to the peak of the R wave. The VAT should not exceed 0.03 sec in V1 and V2 and 0.05 sec in V5 and V6.

QT interval: This is measured from the onset of Q wave to the end of T wave. It measures the duration of electrical systole. The QT interval varies with the heart rate and must be corrected (QTc). For a heart rate of 60 beats per minute, QTc should not exceed 0.42 sec in men and 0.43 sec in women.

QU interval: This is the interval measured from the beginning of the Q wave to the end of the U wave. It measures total ventricular repolarization, including Purkinje fibers.

ST interval: This measures the interval from the QRS offset to beginning of RST segment.

PR segment: It is a portion of the ECG tracing from the end of the P wave to the onset of the QRS complex. It is normally iso-electric.

RST junction (J): It is the point at which QRS complex ends and the RST segment begins.

RST segment: It is usually called the ST segment. It is the portion from the J to the onset of the T wave. This segment is usually iso-electric but may vary from -0.5 mm to +2 mm in precordial leads. It is elevated or depressed in comparison with that portion of the base line that is between the termination of the T wave and the beginning of the P wave (TP segment) or when related to the level of the PR segment.

1.3 CARDIAC VECTORS

The term cardiac vector designates all of the electromotive forces of the heart cycle. It has known magnitude, direction, and polarity. At any given instant during depolarization and repolarization, electrical potentials are being propagated in many directions in space. Over 80% of these potentials are cancelled out by opposing forces, and only the net is recorded [42]. The instantaneous vector represents the net electrical force at a given instant. A mean vector of any given portion of the heart cycle (e.g. QRS) represents the mean magnitude, direction, and polarity for that period. A vector can be drawn for atrial depolarization (P), ventricular depolarization (QRS), and ventricular repolarization (T). Fig.1.7 shows different vectors in frontal plane and their normal ranges.

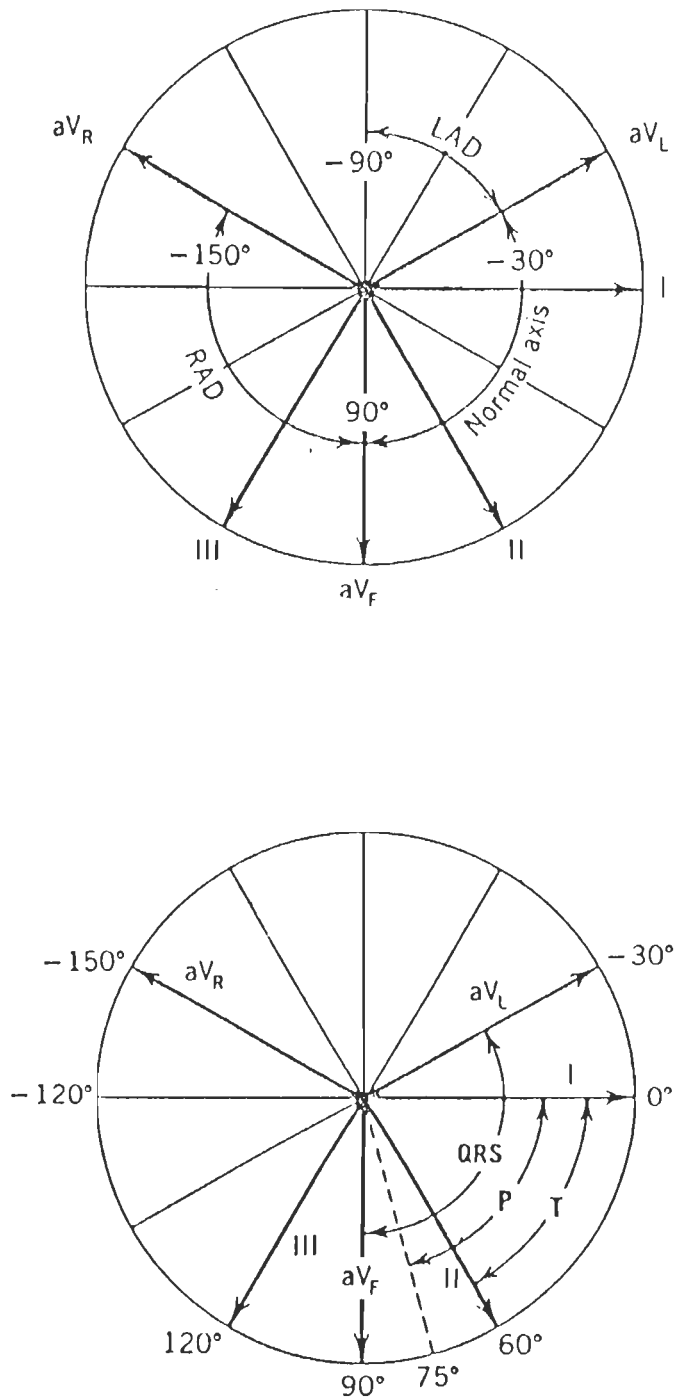


Fig.1.7 Cardiac vectors in frontal plane and their normal ranges

1.4 LEAD SYSTEMS

For diagnostic ECG recordings, several electrodes are attached to the body of patient. Specific lead configurations result from the combination of electrodes supplying signals to the amplifier. The details of lead definitions are given in the Table 1.1:

Table 1.1: Definition of ECG Leads [145]

Lead type	Electrodes used	Definitions
Bipolar or limb leads (Einthoven)	LA,RA,LL,RL	$I=LA-RA$ $II=LL-RA$ $III=LL-LA$
Augmented (Goldberger)	LA,RA,LL,RL	$aVR=RA-0.5(LA+LL)$ $aVL=LA-0.5(LL+RA)$ $aVF=LL-0.5(LA+RA)$
Unipolar chest leads (Wilson)	V1,V2,V3,V4,V5,V6	$V1=v1-(LA+RA+LL)/3$ $V2=v2-(LA+RA+LL)/3$ $V3=v3-(LA+RA+LL)/3$ $V4=v4-(LA+RA+LL)/3$ $V5=v5-(LA+RA+LL)/3$ $V6=v6-(LA+RA+LL)/3$
Orthogonal vector leads (Frank)	I,E,C,A,M,H,F	$X=0.610A+0.171C-0.781I$ $Y=0.655F+0.345M-1.000H$ $Z=0.133A+0.736M-0.264I-0.374E-0.231C$

The electrodes are connected to the amplifier directly or through resistive networks. The bipolar limb leads were first proposed by Einthoven. These are the three limb leads: I, II, and III. These derive signals from the left arm (LA), the right arm (RA), and the left leg (LL). The right leg (RL) electrode serves as common point of the amplifier. The augmented leads (aVR, aVL, aVF) were proposed by Goldberger, and these again derive signals from the limb leads [145]. Wilson proposed the unipolar chest leads which derive signals from six different chest locations. The reference input to the amplifier in these cases is known as the Wilson central terminal. The Wilson central terminal is formed by a resistive network that contributes equally weighted signals from each of the three limb electrodes (LA, RA, LL).

For diagnostic applications, recordings are obtained from all 12 leads (bipolar limb, augmented, and unipolar chest leads). For monitoring, usually one lead is selected and the ECG signal from that leads is displayed. Lead II is most commonly used for this purpose. Sometimes nonstandard chest leads are also being employed [145]. This is quite common in ambulatory ECG recording where the electrode locations on the chest are found to be quite convenient, as it generate less artifact. Monitoring during surgery may also require recording from a nonstandard lead, in case the usual lead configurations are not accessible.

1.5 SOURCES OF INTERFERENCE IN ECG RECORDING

For diagnostic quality ECG recordings, signal acquisition must be noise free. Since ECG signals are only of the order of 1 mV in amplitude, the ECG acquisition is susceptible to interference from other biological and environmental sources. The various sources of interference are motion artifacts, skin potentials, muscle noise, power-line interference, and radio frequency interference [71,144,145].

(i) Skin Potentials and Motion Artifacts:

The human skin is a source of electrical potentials and changes its characteristics with physiological causes or with external influences such as movement [145]. In general, about 25 mV of dc skin potential exists at the interface of the recording electrode and skin. The dc skin potentials do not prove to be a problem, as they are easily eliminated by high-pass filters. On the other hand, the motion artifacts generated by deformation of the skin or disturbance of the skin-electrode interface are difficult to eliminate from the ECG recording. Sometimes, the motion artifacts can resemble the QRS complexes in ECG recordings, making ECG interpretation difficult [Fig. 1.8(a)]. Other times, slow movement of electrodes or the body can result in baseline wander [Fig. 1.8(b)]. The slow base-line wander may not be filtered by the amplifier lower-corner frequency of 0.05 Hz and may result in saturation of the amplifier output. Many researchers found that the skin potentials and the motion artifacts can be reduced by abrasion or puncture of epidermal skin layers [145]. Good electrode design limit the relative movement between the electrodes and skin also helps in reduction of the motion artifact. The electrodes are designed so that the gel is recessed in a cup like structure [Fig. 1.9 (c), disposable foam electrode] and the adhesive maintains firm contact with the body.

(ii) Muscle Noise:

First, the human body itself generates muscle noise recorded as an electromyogram (EMG). The EMG noise is of the same order of amplitude as the ECG signals but occurs at higher frequencies [Fig.1.8(c)]. The amplitude of the EMG noise is proportional to the

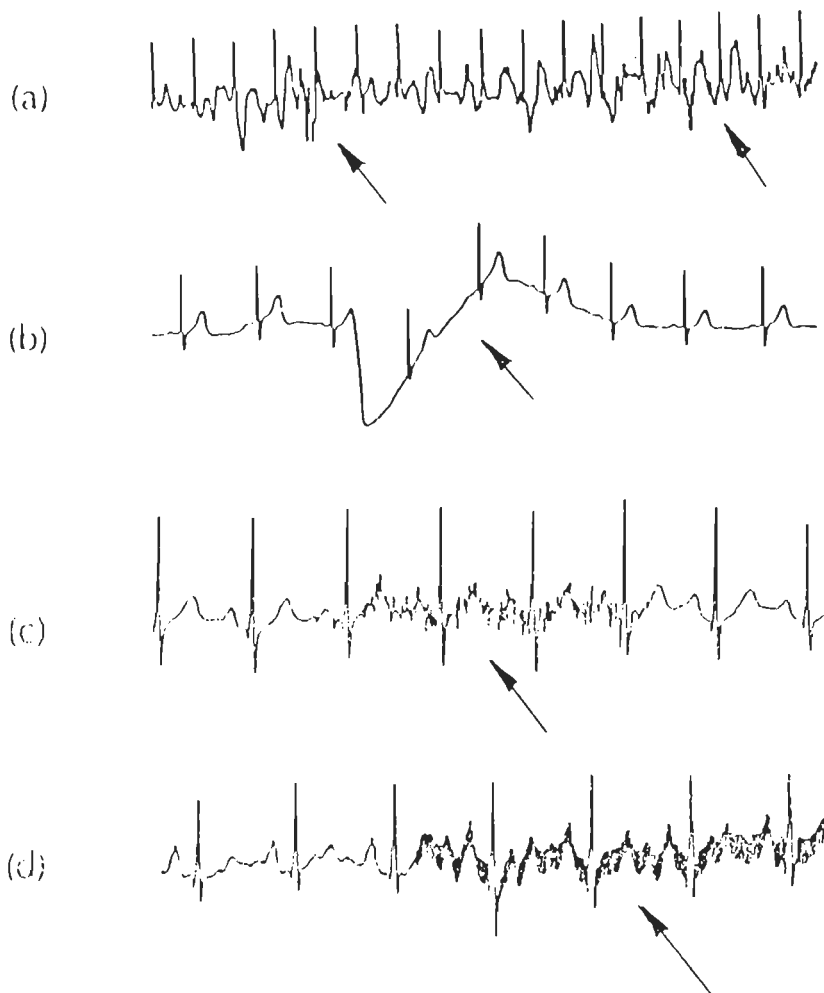
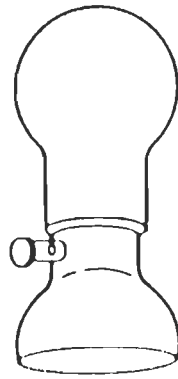
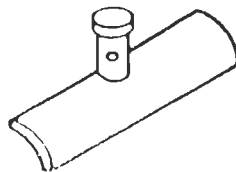


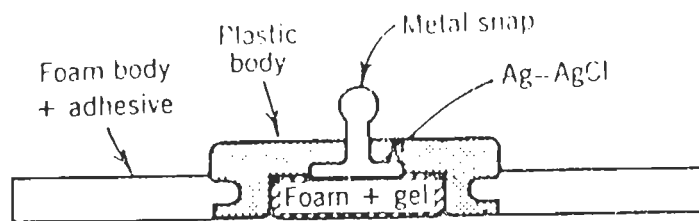
Fig.1.8 ECG waveforms in various recording situations: (a) motion artifact, (b) baseline wander, (c) EMG noise and (d) electrical interference
 [Webster J. G., 1988, (145)]



a) suction electrode



b) plate electrode



c) disposable foam electrode

Fig. 1.9 ECG electrodes

activity undertaken by the various muscle groups. Consequently, the EMG noise can be reduced by lowering down the muscle activity during the ECG recording and by judicious placement of ECG electrodes (away from large muscle groups), and by selective band-pass filtering (e.g. amplifying only the signals in a limited bandwidth range of 0.5-40Hz).

(iii) Environmental Sources of Interference:

The electrical interference induced by power lines [Fig. 1.8(d)] is probably the most pervasive problem in biopotential recording [145]. Surrounding power lines, electrical instruments, transformers, and so forth, radiate electrical interference, which becomes electrically or magnetically coupled to the body. There can be electrostatic coupling between the power-line sources and the body and electrode leads. The elimination of electrically induced interference is a difficult and tricky task. The human body, the electrode leads, and the ECG monitor form a loop and the magnetically induced currents are proportional to the area bounded by the loop. Therefore, this form of interference can be limited by twisting the leads together.

The other sources of environmental electrical interference are radio-frequency (RF) transformers. Several electrical and medical devices, such as electric motors and electrosurgical units, generate the interference signals indirectly. The electrosurgical units used in surgery emit signals of several hundred volts at about 1 MHz. Such interference is picked up by electrical conduction or induction. The RF interference frequencies are much higher than the ECG frequencies and therefore, can be filtered to some extent by shunt capacitors or blocked by series RF chokes.

As discussed above, electrical interference enters the recording system in many ways. Biological sources of noise and artifacts can be limited by proper design and placement of electrodes and proper skin preparation. The interference from most environmental sources can be reduced or eliminated by proper grounding, shielding, and wiring practice, leaving the most pervasive source of interference that form electrically induced differential and common-mode sources. The common-mode interference is rejected by the inherent property of the differential amplifier, which has very high common mode rejection ratio[145].

1.6 CLINICAL ASPECTS OF ECG

The ultimate application of ECG is in clinical diagnosis. Consequently, it is important for the engineers to be aware of the types of abnormalities and their electrophysiological character that arise, which are of clinical interest. Cardiac abnormalities can be divided in to two major groups, namely, those affecting the QRS morphology (contour) and those affecting

the rhythm. The changes, which arise from the abnormalities due to cardiac generators and the volume conductor, can be distinguished.

Through the statistical analysis of the normal ECGs, one can set up criteria by which the ECG is designated as the normal or abnormal type. It seems safe to assume that the electrical abnormalities reflected in the ECG imply the presence of clinical abnormalities. However, while objective criteria for abnormal ECGs exist, the clinical interpretations are less certain. The clinical experience, judgement, and collateral medical data play an important role in cardiac diagnosis. The emphasis here is primarily on the electrical abnormalities.

1.7 STANDARD ECG DATABASES

The algorithms developed in this work for the ECG analysis and interpretation have been evaluated by the single and multi-lead ECGs. The ECG records have been acquired from the CSE and the MIT/BIH data libraries and also from the indigenous data library created by the ECG recording in the laboratory.

1.7.1 Common Standards for Quantitative Electrocardiography (CSE) Database

There are three CSE reference data sets [147]. The first data set (CSE DS-1) consists of 3 lead ECGs, and has been recorded simultaneously in the standard sequence. In the second data set (CSE DS-2), all the leads i.e. standard 12 leads plus the 3 Frank leads are recorded simultaneously. A third CSE database (DS-3) has been developed for the assessment of diagnostic ECG and Vectorcardiogram (VCG) computer programs. This database comprises multi-lead recordings of the standard ECG and the VCG. All the data have been sampled at 500 Hz.

The DS-3 CSE measurement database consists of 250 original and 310 so called artificial ECG recordings. They have been divided into two equal sets i.e. data set one and data set two. The multi-lead measurement database is also composed of original and artificial ECG recordings. This database has been split into two equal sets i.e. data set three and data set four. The so-called artificial ECG data are out of strings of identical selected beats.

The onsets and offsets of P, QRS and T of these beats have been analyzed by a group of cardiologists during an extensive iterative Delphi review process in the CSE project. The results of this analysis have been released only for data set three. The data sets two and four are being used in CSE coordinating Center for testing purposes. For the diagnostic data set (CSE DS-5), only the digitized ECG data (1220 cases) have been released by the CSE

coordinating Center, not the clinical validated diagnoses. This database has been developed primarily for testing the performance of diagnostic ECG and VCG computer programs.

CSE three lead measurement library

SET	I	II
Original	125	125 (Number of patients)
Artificial	155	155 (Number of patients)

All the files corresponding to 3-lead CSE library start with the ASCII character E. Each record consists of minimum 5 seconds of data for each of the 4 standard ECG lead groups, followed by minimum 10 seconds data of X, Y, Z leads. The second character in the file name will be 'O' for original and 'A' for artificial. The third byte indicates whether the data belong to data set one (I) or data set two (II). The three bytes provide a sequential number, which goes from 001 to 125 for the original and from 001 to 155 for the files of the artificial ECG recordings.

The file names are as follows for the 3-lead CSE measurement database:

EO1-001.DCD to EO1-125.DCD

EA1-001.DCD to EO1-155.DCD

EO2-001.DCD to EO2-125.DCD

EA2-001.DCD to EA2-155.DCD

CSE multi-lead measurement library

SET	III	IV
Original	125	125 (Number of patients)
Artificial	125	125 (Number of patients)

File name starts with the character M. The record length for these cases is in principle 10 seconds for each lead. In some cases only 8 seconds will be significant. In these cases, the last significant sample has been repeated in order to fill up the last 2 seconds.

CSE Diagnostic Database

The multi-lead measurement database has all recordings of 10 seconds sampled at 500 Hz. The first character of all files is D, followed by a sequential number from 00001 to 01220. The full filenames for the diagnostic database are D-00001.DCD to D-01220.DCD.

1.7.2 Massachusetts Institute of Technology/ Beth Israel Hospital (MIT/BIH) Database

This database contains several hundred ECG recordings, extended over 200 hours in all [94]. Individual recordings contain one to three signals and range from 20 seconds to nearly 24 hours in length. Most of them have two signals and are of about 30 minutes long and are annotated beat-by-beat. About one-sixth of the CD containing the database is occupied by the MIT-BIH Arrhythmia Database, which is fully annotated. The disk also contains eight additional ECG databases. The recordings are found in ten directories:

mitdb	MIT-BIH Arrhythmia Database
cudb	Creighton University Ventricular Tachyarrhythmia Database
nstdb	MIT-BIH Noise Stress Test Database
stdb	MIT-BIH ST Change Database
vfdb	MIT-BIH Malignant Ventricular Arrhythmia Database
afdb	MIT-BIH Atrial Fibrillation/Flutter Database
cdb	MIT-BIH ECG Compression Test Database
svdb	MIT-BIH Supraventricular Arrhythmia Database
ltdb	MIT-BIH Long-Term ECG Database
odb	Other databases (excerpts from compatible CD-ROMs of physiologic signals)

Database Files

Most of the ECG recordings on this disk are represented by a header file, a signal file, and an annotation file. Together these three files comprise a 'record'. The records on this disk are organized into nine databases, each in its own directory e.g. directory 'odb' contains short records excerpted from several other databases. Each database record contains a continuous recording from a single subject. In this thesis work MIT/BIH Arrhythmia database has been used to evaluate the performance of software in feature extraction and HRV analysis. The details of database are given below.

MIT-BIH Arrhythmia Database

Record names:

100	105	111	116	122	200	207	213	220	230
101	106	112	117	123	201	208	214	221	231
102	107	113	118	124	202	209	215	222	232
103	108	114	119		203	210	217	223	233
104	109	115	121		205	212	219	228	234

\----- the '100 series' -----/ \----- the '200 series' -----/

This database consists of 48 annotated records, obtained from 47 subjects studied by the Arrhythmia Laboratory of BIH in Boston during 1975 and 1979. About 60% of the records were obtained from inpatients. The database contains 23 records (the '100 series') chosen at random from a set of over 4000 24-hour Holter tapes and 25 records (the '200 series') selected from the same set to include a variety of rare but clinically important phenomena that would not be well-represented by a small random sample. Several records in the 200 series were chosen specifically because features of the rhythm, QRS morphology, or signal quality may be expected to present significant difficulty to arrhythmia detectors.

Each record is slightly over 30 minutes in length. Each signal file contains two signals sampled at 360 Hz. The header files include the information about the leads used, the patient's age, sex, and medications.

1.8 LITERATURE REVIEW

1.8.1 Methods of ECG Analysis and Interpretation

Although the first attempt to automate ECG analysis by digital computer was made as early as in 1957 by Pipberger and his group, but the first industrial ECG processing system came in the market during seventies [80,151]. Since then many investigative and commercial minicomputer-based and microcomputer-based systems have become common in use. It took considerable time to develop operational computer programs than originally anticipated. However, over last 15 years, the computer programs were mainly developed by University research groups. In the last decade, the development has shifted to industry. Computers can assist a cardiologist in the task of ECG monitoring and interpretation. For example, in a cardiac intensive care unit (CICU), ECGs of several patients must be monitored continuously to detect any life-threatening abnormality that may occur. Since cardiologists are unlikely to be available to monitor the ECGs of all the patients during all 24 hours in a day, automated monitors programmed to detect abnormal heart rhythms are needed. Over the past several years, the computerized ECG monitors that provide complete 12-lead diagnostic quality ECG recordings and interpretations have become common. Computerized ECG monitoring and analysis are now carried out with bed side monitors, mobile carts equipped with ECG amplifiers and microcomputers, and portable ECG recorders hooked up via telephone networks. State-of-the-art systems are based on multiple microcomputers, which run, sophisticated arrhythmia analysis software, and are connected to central computer facilities where they share patient records and database.

In the past four decades, numerous computer programs have been developed for the automatic interpretation of ECG [147]. However, methods and independent databases to test the reliability of such programs are still scarce. Each ECG program has different principle with respect to analysis, for example, some measure single beats, whereas others analyze average beats. Until recent past, there were no standards in this field. There were no common definitions of waves, no standards for measurement or diagnostic classification, and no uniform terminology for reporting, transmission and processing of data. This has created a situation whereby large differences result in measurements by different computer programs and hampers the exchange of diagnostic criteria and interpretation results [150]. In addition, more and more microcomputer-based interpretative ECG machines are being put on the market without any prior independent validation.

In order to overcome some of these problems, a concerted action was started by the European Community (EC) in June 1980, striving towards 'Common Standards for Quantitative Electrocardiography' (CSE) [149].

Some of the internationally available ECG analysis and interpretation programs are the AVA program developed by Pipberger et al. [110], Nagoya program developed by Okajima et al. [102], MEANS program by Bommel et al. [15], Glasgow program developed by Macfarlane et al. [79], Dalhousie program developed by Rautaharju et al. [116], Hannover program developed by Zywiets et al. [156], Padova program developed by Degani and Bortolan [31], Lyon program developed by Arnaud et al. [9], Louvain program developed by Brohet et al. [22] and Porto program developed by Abreu-Lima and Marques de Sa' [1].

Pipberger et al. [110] developed an automatic vectorcardiographic analysis program during 1956. Signal recognition in this software is based on the spatial velocity function. Multivariate statistical analysis on orthogonal ECG leads assesses probabilities of nine alternative disease categories, based on QRS-T parameters. Okajima et al. developed an ECG analysis and interpretation program during 1960, named as Nagoya program. In Japan, it is being utilized, with some modifications, for interpreting or monitoring the VCG, exercise ECGs, arrhythmia detection in the CCU, ambulatory ECGs, and body-surface mapping of the ECG. Disease diagnosis is based on the use of scoring schemes. Bommel et al. had introduced their MEANS (modular ECG analysis system) in 1972 and first published in 1974. This system was intended to be applied both for the clinic use and population screening and the MEANS was able to classify according to conventional clinical criteria as well as the Minnesota code. They have used the technique of cross correlation with the template and a matched filter for detection of ECG waves and decision tree classifiers for disease diagnosis.

Macfarlane et al. [79] reported current Glasgow 12-lead ECG program. Its origin goes back to year 1977. It is designed to analyze from 3 to 15 simultaneously recorded leads with facilities for analysis of rhythm. Spatial velocity function is used for QRS detection and the wave typing is carried out using an iterative process and a set of rule-based criteria is used for interpretation of the (P)QRST morphology. The Dalhousie ECG analysis program (DALECG) is a collection of relatively loosely coupled program modules that can be combined in various ways for processing the rest and exercise ECGs. The program was designed particularly for research applications. Family of templates has been used for ECG analysis and the Minnesota code supplemented by several newer ECG classification schemes suitable for computer coding have been used by Rautaharju et al. [116]. The Hannover ECG program HES has been designed for measurement and interpretation of resting and exercise ECGs. In the signal analysis, the program follows an averaging strategy. For diagnostic classification, a hybrid model with decision trees and scoring algorithms has been used by the Zywiets et al. [156]. Methodology of ECG interpretation in the Padova program developed by Degani and Bortolan [31] is based on the use of spatial velocity functions for signal analysis and of fuzzy classifiers for disease interpretation.

Arnaud et al. [9] developed the Lyon program to interpret VCGs using heuristic procedures to extract not a simple and unique interpretation, but several diagnostic hypotheses in accordance with the spatio-temporal structure of the QRS-T electrical field. The Louvain program performs the analysis and interpretation of the VCG to increase the clinical utility of ECG analysis. Wave recognition techniques in which a mixture of threshold-crossings and template-matching methods are applied to filtered spatial velocity curves. A deterministic method is one in which the cardiologist's expertise is applied through Boolean algebra and decision tree logic in order to reach a diagnostic decision [22]. A computer program for ECG analysis and interpretation developed at the University of Porto in Portugal is reported by Abreu-Lima and Marques [1]. The program employs the three-lead Frank VCG and detection of QRS complexes is based on the double threshold method for the spatial velocity amplitude and its time derivative. The fiducial points of all the ECG wave components are then detected using an exhaustive sequential search algorithm. The decision tree logic is being used for diagnosis.

Programs reported above use ECG and/ or VCG and carry out interpretation based on decision logic or statistical analysis. Pipberger et al. [110] reported that the automated ECG diagnosis could be no better than the accuracy of the waveform detection that provides its measurement values. Similarly, Okajima et al. reported that there are still, many occasions of

mistakes in fiducial point recognition or contour classification agreed upon unanimously. The revisions and modifications of the program are continuously in progress. The modular ECG analysis system (MEANS) consists of modules for signal analysis and diagnostic classification. All modules underwent many changes as a function of experience, insight, and continuously changing information technology. Macfarlane has also reported that there will be continuous enhancement in the system if the more widely ECGs are interpreted on a particular system. Although diagnostic accuracy of computer programs is tending to reach a plateau, there is no doubt that many years hence, it will still be possible to report on recent developments in the programs. In all programs, there is every possibility that the work will always be enhanced, modifications for improvements be made and the use of new techniques like wavelet transforms be introduced for better results.

1.8.2 Feature Extraction of ECG Signal

The ECG signal is the graphical representation of the bioelectrical and biomechanical activities of the cardiac system. It provides valuable information regarding the functional aspects of the cardiac and cardiovascular systems. The QRS complex is the most characteristic wave set of all the waves in an ECG signal and represents depolarization of the ventricles. There are a number of methods, some of which deal with detection of ECG wave segments, namely P, QRS and T, while others deal with detection of the QRS complexes.

The QRS complex is the most prominent feature and its accurate detection forms the basis for extraction of other features and parameters from the ECG signal. The QRS wave is used as the basis for faithful heart disease diagnostics, for carrying out studies on HRV and for analysis of arrhythmia. A good amount of research work has been carried out during the last four decades for the accurate and reliable detection of QRS segment in the ECG signal. The QRS detection algorithms developed so far can be broadly placed into four categories; (i) syntactic approach, (ii) non-syntactic approach, (iii) transformative approach, and (iv) hybrid approach.

It is an established fact that QRS detection is taken as the basis for identification and extraction of various parameters of ECG signal [8,69,98,104,127,133,136,141,152]. A large number of software, hardware and hybrid techniques reported so far follow the procedure of filtering, squaring, and differentiation using decision rules like zero crossings, amplitude thresholds, sharp consecutive Q-R-S peaks, duration of QRS complex and R-R interval duration [8,104,127]. Most of the methods face difficulty due to wide variations in the physiological behaviour of the cardiac system. These changes are reflected in the

amplitudes, durations and slopes of the various segments of the ECG signal. These variations differ from beat-to-beat, lead-to-lead and patient-to-patient and are difficult to detect QRS complexes and to get satisfactory results for perfect diagnostics.

(i) Syntactic Approach

In syntactic approach of pattern recognition based QRS detection, the ECG signal is first reduced into a set of elementary patterns like peaks, durations, slopes, and interwave segments, and thereafter using rule based grammar. The signal is represented as a composite entity of peaks, duration, slopes and interwave segments. These patterns are then used to detect the QRS complexes in the ECG signal. The methods of this category are time consuming and require inference grammar in each step of execution for QRS detection. Even then the motivation for using a syntactic approach resides in the fact that human inspection of ECG waveforms is firstly an extraction of structural and qualitative information. Once this information has been obtained and some typical forms (like a QRS complex) have been recognized, the numerical values of the durations and amplitudes useful for diagnosis are measured [44,93,135].

Gustavo et al. [44] used the syntactic method to extract the time evolution of the rhythm using the energy of ECG derivatives and their coding by a look-up table method. Trahanias and Skordalakis [135] have reported a bottom-up approach to the recognition of ECG waveforms. This approach is based on the assumption that ECG waveforms are composite entities that can be decomposed into other simpler entities, further into other simpler ones, and so on, until peak patterns and segment patterns are obtained. After recognition of these primitive patterns, recognition of the ECG patterns using bottom-up procedure has been carried out. In their other paper [135], solutions to the sub-problems of primitive pattern selection, primitive pattern extraction, linguistic representation, and pattern grammar formulation are reported. They have observed that the primitive pattern extractor does not always accurately delineate the boundaries of the peak patterns. This type of error is propagated in the next stages and is responsible for many inaccurate results. Looking to the complex structure with infinite morphological variability, this approach faces difficulty in QRS detection.

(ii) Non-syntactic Approach

Most widely used class of ECG feature extraction techniques is of non-syntactic type. In this class, we find the use of amplitude, slope and threshold limit as well as the use of different filters, mathematical functions and models.

Okada [101] reported a five step digital filter, which removes components other than those of QRS complex from the recorded ECG. The final step of the filter produces a square wave and its on-intervals correspond to the segments with QRS complexes in the original signal. Thakor et al. [133] carried out power spectral analysis of ECG waveform, as well as of isolated QRS complexes and episodes of noise and artifacts. A band pass filter has been used to maximize the signal (QRS complex) to noise (T-waves, 60 Hz, EMG etc.) ratio to detect the QRS complex. Due to the inherent variability of ECG from different persons, as well as variability due to noise and artifacts, the filter design is suboptimal in specific situations. Pan and Tompkins [104] have developed a real-time algorithm for detection of the QRS complexes of ECG signals. It reliably recognizes QRS complexes based upon digital analysis of slope, amplitude, and width. Hamilton and Tompkins [45] have investigated the quantitative effects of number of common elements of QRS detection rules using the MIT/BIH arrhythmia database. Then they have developed a progressively more complex decision process for QRS detection by adding new detection rules and optimized decision rule process. Laguna et al. [69] developed a method to automatically determine the characteristic points (onsets and offsets) of the P, QRS, and T waves in the multilead ECG signals from the CSE DS-3 database. The method makes use of a differentiated and low pass filtered ECG signal. Escalona et al. [36] developed a QRS alignment technique which is based on the accurate detection of a single fiducial point in the bandpass filtered (3-30 Hz) QRS segment.

Urrusti and Tomkins [138] have described the use of moving window integral (MWI) filter for QRS detection. They have analysed MIT/BIH ECG database files for 13 MWI widths from 60 to 180 ms and found that the optimal MWI is application dependent. Dandapat and Ray [29] used the method of midprediction (MIDP) filtering for the detection of the spikes in the biomedical signals. They have observed that, in the MIDP error filtering method, the basewidth of the spike is retained in the error signal. The amplitude of the spike in the error signal and the basewidth of the spike together can be considered as the decision parameters to improve the reliability of the spike detection. A detection algorithm developed by Anti et al. [8] is based on optimized prefiltering in conjunction with a matched filter and dual edge threshold detection. Afonso et al. [3] have designed a multirate digital signal processing algorithm to detect heartbeats in the ECG. The algorithm incorporates a filter bank (FB) which decomposes the ECG into subbands with uniform frequency bandwidths and enables to perform independent time and frequency analysis on a signal. Gary et al. [41] evaluated nine different QRS detection algorithms for noise sensitivity. The noises were

electromyographic interference, 60 Hz power interference, baseline drift due to respiration, abrupt baseline shift, and a composite noise constructed from all other type of noises. None of the algorithms were able to detect all QRS complexes without any false positives with all types of noises at the highest level. Algorithm based on amplitude and slope had highest performance for the ECG corrupted with EMG. An algorithm using a digital filter had the best performance for the ECG corrupted with composite noise.

There are some algorithms, which work on the use of mathematical approaches like mixed mathematical basis functions, mathematical models, mathematical morphology, spatial velocity function, and averaging techniques [2,6,8,12,103]. Mathematical models are developed by considering the QRS segment as pulse shaped waveform and its variables as the number of peaks, arrival time, amplitudes and widths of various complexes [51]. The mixed mathematical functions like Gaussian, exponential, and straight line have been used to represent the composite ECG signal. Sornmo et al. [128] have considered the mathematical model for the occurrence of pulse shaped waveforms corrupted with coloured Gaussian noise. The number of waveforms, the arrival times, amplitudes and widths are regarded as unknown variables. Adaptivity of the detector is gained by utilizing past as well as future properties of the signal in determining thresholds for QRS acceptance. Tartakovsky et al. [132] reported the QRS detection technique used in TELVIN (Three-channel Evaluation of long-term ECG for Atrial and Ventricular Arrhythmia Identification and Validation) system. The algorithm for unsupervised template learning and fully automated rhythm monitoring implemented in the TELVIN system provides a reliable tool for long-term ECG analyses. Naima and Saxena [97,98] have presented two new approaches for feature extraction of the ECG signal for computer aided analysis. The first method is based on mixed mathematical functions and the second one on spline functions. The methods also identify and separate P, Q, R, S and T segments. These methods are good for memory-based manipulations and mapping type microcomputer based biomedical instruments. Park et al. [107] presented an algorithm detecting the presence of a fetal QRS complex. It computes the averaged magnitude of the difference between the fetal ECG signal and the reference signal to detect the fetal QRS event. Two approaches of normalizing the fetal ECG signal and the template are reported. Trahanias [136] suggested an approach based on mathematical morphology for QRS detection. This morphological operator works as a peak-valley extractor. Shaw and Savard [127] reported that the detection of subtle beat-to-beat variations in the morphology of the ECG is complicated by the effects of alignment errors and respiration. A method of directly estimating the alignment error (trigger jitter) from ECG is derived by relating the

variance to the squared slope of the averaged QRS complex. It was reported that the effects of respiration could be reduced by normalizing the amplitude of the QRS complexes. Maheshwari et al. [82] developed an analysis technique using the spatial velocity, which detects the QRS complexes, and thereafter, P and T waves.

Recently, some new techniques based on artificial neural network, fuzzy logic and genetic algorithms have also been developed for accurate QRS detection [23,40,65,141,152]. In these approaches, the basic methodology is to learn and later on to generalise the knowledge gained through the learning process to identify the known QRS complexes out of an exhaustive set of the ECG segments. The accuracy and reliability of QRS detection by these methods is dependent on the type of used training set. The artificial neural network (ANN) based method developed by Vijaya et al. [141], works on high prediction error to indicate the occurrence of QRS complexes.

As an improvement over the methods discussed above, the concept of adaptiveness has been introduced in the techniques used for QRS detection [44,51,66,69,152]. Adaptive thresholds for signal amplitude, slope, and durations, adaptive matched filtering, adaptive estimation of QRS segment features by the Hermite model, neural network based adaptive matched filtering and adaptive template building are some of the techniques in this category [66,132,140,152]. In these techniques, an algorithm configures itself to a unique QRS segment of a patient during an initial stage of learning. This adaptability approach enhances the QRS detection rate by a considerable extent and reduces the percentage of false detections, but at the same time, increases the computation as it involves learning phase (determination of adaptive model parameters) and repetitive calculations to optimise the threshold limits for amplitudes, slopes and durations.

Xue et al. [152] have developed an adaptive filtering algorithm based upon an ANN for QRS detection. The residual signal which contains mostly higher frequency QRS complex energy is then passed through a linear matched filter to detect the location of the QRS complex. This technique suffer from two problems: i) the pass band of the QRS complex is different for different subjects and even for different beats of the same subjects and ii) the noise and QRS complex pass-bands overlap. Adaptive Hermite Model Estimation System (AHMES) is presented by Laguna et al. [66] for on-line beat-to-beat estimation of the features of the ECG signal. The AHMES is based on the multiple-input adaptive linear combiner, using succession of the QRS complexes and the Hermite functions as inputs. The procedure has been incorporated to adaptively estimate a width related parameter. The system allows an efficient real-time parameter extraction for classification and data compression.

Different methods discussed above claim satisfactory results but methods like ANN based QRS detection and AHMES require exhaustive training, settings and estimation of model parameters, and hence, are computationally complex and time consuming. Jan et al. [51] have reported various algorithms for the detection of QRS complexes, atrial activity and artefacts. It was clearly demonstrated that the quality of the input signals influences the performance of the various detectors and the improvement in the performance of program MEANS is possible with better artefacts detectors.

(iii) Hybrid Approach

In the hybrid approach, the syntactic and non-syntactic approaches are combined to detect the QRS segment. These are not in common use, as in syntactic approach the trace is being made on actual morphology of the ECG signal and in non syntactic approach there is no consideration to maintain the morphology of the ECG signal.

(iv) Transformative Approach

The transformative techniques, namely Fourier transform, cosine transform, pole-zero transform, differentiator transform, Hilbert transform and wavelet transform are being used for the QRS detection [29,38,56,72,115,123]. The use of these transforms on ECG signal helps to characterise the signal into energy, slope, or spike spectra, and thereafter, the temporal locations are detected with the help of decision rules like thresholds of amplitude, slope, or duration. Murthy and Prasad [96] proposed a solution to the fundamental problem of ECG analysis, viz., delineation of the signal into its component waves. The DCT of a bell shaped biphasic function is approximated mathematically by a system function with two poles and two zeros. A one-to-one relation between the pole pattern in the z-plane and component wave pattern in the time signal is established.

Looking at the potential of using various approaches, it is very difficult to claim that a particular method or a particular category is always suitable for QRS detection. Due to the physiological variability of the QRS wave, and also due to the presence of noise and artifacts in the ECG signal, so far no QRS detection technique has been reported to provide 100% accuracy. In recent times, the use of wavelet transforms (WTs) in QRS detection has shown upper edge in terms of accuracy of detection, simplicity in calculations and no need of preprocessing [72].

Recently Rao [115] developed an algorithm based on discrete wavelet transform (DWT) to detect the R-peaks to compute R-R interval and to compress the ECG signal. This method has a very important advantage as it does not assume stationarity or quasi-stationarity of the ECG signal. Sahambi et al. [123,124] used the modulus maxima of the

WT using multiresolution analysis. Similarly Li et al. [72] reported an algorithm based on multiscale feature of WT. Kadambe et al. [56] described a QRS complex detector based on the dyadic wavelet transform which is robust to time-varying QRS complex morphology and noise. They observed that although no one algorithm exhibited superior performance in all situations, the DyWT-based detector compared well with the standard techniques and exhibited excellent performance. Li et al. [72] have reported a QRS detection technique using a quadratic spline WT. Better results are possible using this method because of the specific feature of the WT to characterize the local regularity of ECG signal. This feature is used to distinguish ECG waves from noise, artifacts and baseline drift. In principle, the WT cuts-up data into different components that are well localized in time and frequency. Each component with a resolution matched to its scale is used for analysis and diagnostics

Thus in the present time, a good amount of effort is being directed to perfect the WT based QRS detection techniques. The WTs have promising feature to characterize the local regularity of signals by decomposing the signal into elementary building blocks that are well localised both in time and frequency, and thereby, their robustness to noise make them ultimate choice for QRS detection. The feature of characterizing the local regularity of the signal is used to distinguish QRS segment from spurious noise, artifacts, baseline drift and high P and T waves.

In ECG analysis, the data transformation stage consists of the steps filtering and detection, typing and dominant beat selection and waveform recognition. For reasons of efficiency in communication and data storage, attention is also paid to data reduction [12,21,26,50,57,63,117].

1.8.3 Disease Diagnosis

Disease classification is being carried out by single lead or multi-lead analysis. The analysis of single lead ECGs mainly performed to check the rhythm (HR), variation in rhythm (HRV) and the rhythm related diseases like tachycardia, bradycardia, and arrhythmias. The single lead disease diagnosis is based on the analysis of rhythm and the rhythm is determined by detection of QRS (R-R) events. Multi-lead analysis based disease classification is based on complete analysis and extraction of ECG parameters from standard 12 leads and 3 Frank leads. In section 1.8.1, the discussion has been carried out about the analysis and interpretation of ECG programs which are based on 12 standard leads and 3 Frank leads. Discussion regarding HRV analysis using single lead ECG analysis is given here.

The HRV can be defined as the quantified fluctuations in the heart rate. The analysis of HRV is a well accepted method in two fields: firstly, in clinical situation, particularly in the ICU and in the coronary care unit and secondly, in the study of the neural cardiovascular system. The HRV often mirrors the effects of the underlying control activities and the information of these activities is obtained noninvasively, hence the HRV analysis is considered as an attractive source of information [28,39,53,84,121].

It is worth noting that R-R series is not constant but is characterized by oscillations of up to the 10% of its mean value. These oscillations are not casual but are the effect of the action of the autonomic nervous system in controlling the heart rate [146,153]. In this case, the parameter of interest is the variability of the SA node rhythm, which in fact, should be derived from the onset of the P waves. It has been shown, however, that the possible fluctuations in the intervals between the onset of P waves detection and QRS detection, which might cause errors, are within the considerable limits following from the inaccuracies of both the detection procedures [121,122]. The heart rate variability has become a topic of considerable interest for investigations of normal physiology and disease. The investigation of HRV has been the subject of many different studies. The effects of respiration on HR are mediated through the parasympathetic (vagal) system. The HRV related to respiration has been quantified by conventional time series techniques such as power spectrum analysis which separates the power on the basis of the frequency components in the interbeat interval (IBI) signal. Using this method, we can separate the average power associated with respiration (which we call vagal power) from the rest of the signal. The vagal influences on the heart can then be measured by finding vagal power under different conditions. These techniques have been used to understand the role of vagal control of the heart in normal (healthy) and diseased cases [48,84].

The review of the literature on HRV opens number of directions. Rompelman et al.[121, 122] have described the importance of HRV measurements in both clinical applications and the neural cardiovascular research. They have also shown that the fluctuations in HRV are related to both physiological and psychological factors. They have studied two groups of subjects characterized by a large difference in psychic state and psychiatric patients and normal ones. An investigation was conducted to know that up to what extent factors of neural cardiovascular control (for example, respiratory arrhythmia and blood pressure) are reflected in the HRV. Boer et al. [18,19] have presented a method to attribute the short-term variability of blood pressure and HR of resting subjects to their various causes, using spectral techniques. They have tried to extract information on properties

of the cardiovascular system from the relationship between spontaneous short-term variations in blood pressure and R-R intervals. Malik et al.[84] have pointed out that the reduced HRV has been reported as a predictor of mortality in recent MI patients, however, its automated assessment in long-term ECG recordings is complicated by recording noise and beat-recognition errors which necessitate filtering of the computer-established sequence of beat-to-beat intervals, and visual checking and manual editing of the long-term recording, making the whole method operator-dependent and cumbersome. They have used five filtering algorithms combined with three methods of expressing HRV numerically and used to compare two groups of patients undergoing 24 hour tape recording of the ECG within the first two weeks after MI. Mario et al. [90] have stated that the R-R interval measurement from digitized ECG contains an error due to the finite sampling frequency which may jeopardize the beat-to-beat analysis of the heart rate. They have developed a model to describe and quantitate this error. Craelius et al.[28] have estimated the autonomic nervous activity in three groups: Group A consists of patients who had experienced MI within 2-6 weeks before the tests; Group B consists of patients who had MI more than one year previously; Group C consists of patients who are free of cardiac disease. They have observed that relative to controls, Group A patients have reduced parasympathetic activity index (5+3 against 13+8) and an increased ratio of sympathetic to parasympathetic activity (17+17 against 4+2). Group B is not significantly different from Group A or C. The period of 2-6 weeks post-MI thus appears to be characterized by depressed parasympathetic activity which can be measured using HRV analysis. Malik et al. [85] have pointed out that the spectral-domain methods are known to be sensitive to artifacts in automatic recognition of long-term ECGs. Some of the time-domain methods are believed to be less sensitive, and others have only been used together with visual checking and manual editing of the automatic recognition. The visual verification and manual correction of the automatic recognition of a long-term ECG can be extremely time-consuming for 24 hour recordings. A perceived need for such a manual intervention discourages the assessment of HRV in routine clinical practice and confine the investigation of HRV to an academic setting. There is, therefore, a practical demand for fully automatic methods of HRV measurements which are robust and which provide clinically useful results for recordings of typical quality. This study evaluated the effects of the misrecognition artefact of automatic ECG analysis on five methods for time-domain HRV measurement, which have previously been shown to provide clinically relevant prognostic data in survivors of acute MI. Mandawat et al. [88] have measured HRV on 24 hour Holter recording from different patients by non-spectral methods and they have

observed that HRV is significantly reduced in patients with LVH secondary to hypertension or aortic valve disease. A continuous inverse relation exists between HRV and LV mass index. The impaired cardiac autonomic function in LVH may contribute to the mechanism of sudden death.

Fuenmayor et al. [39] have conducted research to determine whether R and R-R interval variability are modified by atrial pacing and whether these changes (if they do occur) are related to the inducibility of tachyarrhythmias during electrophysiological studies. They have observed in the patients who had normal ejection fraction and no structural cardiac damage that a significant decrease in R-R interval ($p=0.0002$) and in its SD ($p<0.005$) was observed following atrial pacing and no significant HR or R-R interval SD change was observed after pacing in the patients with structural heart disease. Jens et al.[53] have carried out the assessment of HRV by using different commercially available systems and concluded that the results of HRV analysis of the same Holter tape by using different commercially available systems are statistically noncomparable. These findings may be due to different levels of accuracy in removing ectopic beats and artifacts or to different algorithms for HRV analysis. Researchers urged to setup standards for proper assessment of HRV to avoid conflicting data due to different methodological approaches. Zhang et al. [154] have described an investigation into the phase dependence of HRV in response to respiration as a vagal input. This investigation offers considerable promise as a noninvasive scheme for phase-resetting experiments in humans. The estimated respiration response curve has succeeded in demonstrating the dynamic phase-entrainment and frequency dependence on respiration. Mainardi et al. [83] reported that due to limited data currently available on cardiovascular variability beat-to-beat series in ICU patients, they have analyzed both short-term and long-term variability parameters in ICU patients. Short-term parameters, obtained from HRV, showed decreased R-R interval values and an increased LF power in the five minutes following the AWS maneuver. Neither HF power nor RMSSD values increased, suggesting an increased sympathetic activity induced by AWS. These results indirectly confirm the R-R series as a most sensitive index of altered physiological status. Craelius et al. [28] stated that, in fact, time-varying HRV analysis applied to ICU monitoring has been found useful to detect the occurrence of physiological deterioration as well as the response to therapy, thus improving knowledge and control of patient status. To comply with these requirements, an adaptive scheme for the weighted-least-square (WLS) is proposed in which the forgetting factor is automatically driven by signal characteristics.

Yang and Liao [153] have used a wavelet transform to build a simulated model of an HRV signal and to create an algorithm for HRV signal decomposition. They have reviewed the characteristics of HRV signals and discussed an improved integral pulse frequency modulation model for the simulation of these signals. Hoyer et al.[48] have introduced a concept of nonlinear analysis of HR and respiratory dynamics that may improve the understanding of the underlying physiological processes of the autonomic nervous system (ANS), in comparison with the conventional linear analysis. Since HRV and RESP can be measured noninvasively, this concept may also be advantageous in diagnostic investigations of patients. Harel et al.[46] observed that the lower the sampling frequency is, the greater are the inaccuracies in R-R interval measurements and there is serious reduction in the quality of the power spectrum estimates of the HRV signal. They have reported a method to reduce the imprecision in R-R interval measurement caused by the low finite sampling frequency of ECG signals and to investigate the effect of noise on the accuracy of those measurements. They have implemented a robust algorithm to measure the R-R intervals with a high resolution accuracy despite the finite resolution of the sampled ECG signal. The main part of the algorithm is based on modeling the statistical properties of the R-R interval array. It does not operate via detection of the QRS complexes, i.e. it estimates the point process (HRV signal) directly from the raw ECG. Bates et al.[14] have compared the method using DFT with the nonequispaced Fourier transform(NeFT) method. The ability of both the methods to deal with noisy signals is investigated using a test signal with Gaussian white noise added. The test signal is developed using the integral pulse frequency modulation (IPFM) model. In addition, both the methods are used as the first step in an analysis using the discrete harmonic wavelet transform to provide better time resolution than spectral analysis using the DFT. Lund et al. [76] considered a growing interest in the analysis of beat-to-beat variations of the morphology (BBM) of cardiac waves in ECG and have introduced a method for extraction of beat-to-beat patterns and for noise reduction in the analysis of beat-to-beat variations of the morphology. They have observed that beat-to-beat variations in the QRS morphology are in general cyclic, with a main period of about four cardiac cycles. Narayan and Smith [99] have reported that sudden cardiac death affects over 3,00,000 individuals per annum in the United States alone and is predominantly thought to follow ventricular tachycardia (VT) or fibrillation (VF). The repolarization alternans (RPA) reflects alternate beat fluctuations in the morphology and timing of STU segment in the ECG and is used to identify risk to patients.

1.8.4 ECG Data Compression

The amount of Electrocardiogram data to be handled in Holter monitoring, ambulatory patients, central ECG monitoring, Intensive Coronary Care Units (ICCU), and from subjects for scientific studies is so large that it causes problems of efficient storage and management. The efficient transmission of this data for computer aided diagnosis and interpretation has become a standard requirement. Therefore, efficient ECG signal data compression without losing important morphological information of the signal has become an important requirement in almost all the computer based ECG diagnostics and interpretations. To record the standard 12-lead ECG signal in useful clinical bandwidth from 0.05 to 100 Hz, the sampling rate of 500 Hz is used. For monitoring applications in intensive care units and ambulatory patients, the useful bandwidth is limited between 0.5 to 50 Hz, as in these environments, the rhythm disturbances i.e. the arrhythmia are of principal interest [27,134]. The Common Standards for Quantitative Electrocardiography (CSE) working party has recommended that the sampling rate of 500 Hz should be used [61- 64]. But the recording of ECG signal with 500 Hz sampling rate acquires the redundant data in the low frequency zone containing the baseline, P, T and U waves, compared to the data in the high frequency zone i.e. the QRS complex [131]. Though the most clinical information is in the range of 0.05 to 100 Hz, the QRS waves are centered in a frequency band of 20 to 30 Hz and the P, T and U waves well below this frequency band. As per the sampling theorem, minimum required sampling frequency should be at least two times the frequency of the signal of interest [134]. To avoid the requirement of large memory storage and to facilitate the easy handling of data for transmission to higher medical centers for experts opinion for disease interpretation and advice, there is necessity of compressing the ECG data with no loss of information of diagnostic significance. For this purpose, a good number of data compression methods have been developed in the past [50,125], which can be mainly grouped into three categories, namely (i) direct data compression, ii) transformative and iii) parameter extraction techniques.

Amplitude Zone Time Epoch Coding (AZTEC), modified AZTEC, FAN, Scan Along Polygonal Approximation (SAPA), Coordinate Reduction Time Encoding System (CORTES), Turning Point (TP) are commonly used direct data compression techniques [27,50,129]. These methods attempt to reduce the redundancy in a data sequence by examining a successive number of neighboring samples. These techniques generally eliminate samples that can be implied by examining preceding and succeeding sample [50]. AZTEC decomposes raw ECG signal points into plateaus and slopes and its reconstructed signal is discontinuous (step like quantization) and is not acceptable to the cardiologist

[50,134]. In FAN algorithm, lines are drawn between the pairs of starting and ending points so that all intermediate samples are within some specified error tolerance [12,50,134]. The SAPA algorithm closely resembles the FAN algorithm. CORTES is hybrid of the AZTEC and TP algorithms [33,92,120]. It provides a way to reduce the effective sampling by half, by selectively storing important signal points (i.e. peaks, valleys or turning points).

In transformative compression techniques, the signal pre-processing is carried out by means of a linear orthogonal transformation and properly encoding the transferred output (expansion coefficients) and reducing the amount of data needed to adequately represent the original signal [55]. The reconstruction is performed by inverse transformation with a certain degree of error. Some of the commonly used techniques of this group are Karhunen-Loeve transform (KLT), Fourier Transform (FT), Cosine Transform (CT), Walsh transform (WT), Haar-transform (HT), the optimally warped transform, sub-band coding and the wavelet transform [26,47,70,77].

Linear transformations like FT, CT, and WT are applied to the signal and then compression via redundant sample reduction is applied in the transform domain rather than in the time domain. Typically, the transformation process produces a sequence of coefficients which reduce the amount of data needed to adequately represent the original signal. Out of different transforms, the KLT is the optimal transform[21], in the sense that the least number of orthonormal functions are needed to represent the input signal for a given RMS error. Moreover, the KLT results in decorrelated transform coefficients and minimizes the total entropy compared to any other transform. The computational time needed to calculate the KLT basis vectors is very intensive, which has given room for the use of sub-optimal transforms with fast algorithms (i.e. FT, WT, CT and HT).

In parameter extraction methods, namely peak-picking, cycle-pool-based, linear prediction, and neural network methods; the extraction of a set of useful parameters from the original signal is carried out and the same are used in the reconstruction process [12,50]. The idea is to quantize a small set of extracted signal features, finely enough to render an almost imperceptible distortion. For example, the peak-picking technique is based on the sampling of a continuous signal at peaks (maxima and minima) and other significant points of the signal. The basic operation of such technique involves the extraction of signal parameters that convey most of the signal information. These parameters include the amplitude and location of the maxima and minima points, slope changes, zero-crossing intervals, and points of intersection in the signal. These parameters are substituted in place of the original signal. In ANN based compression [125], the network is first trained with the large variety of data, and

the trained weights between different layers are stored during compression. This stored information requires less storage space and is used for retrieval of the original signal. Vector quantization (VQ) has also been used extensively in data compression [55]. It is employed in conjunction with any of the previously mentioned methods mainly as a way of quantizing the resulting data after compression. In most of all these data compression methods, a complicated procedure is involved to select the line segments, slope segments, segment lengths, amplitude of segment extreme points, setting of error thresholds, and coding schemes. Again a procedure is involved to decode the information stored in some coded form to reconstruct the signal.

In most of these methods, the compressed data is in the form of numerals, or codes and not in the form of signals. Even with the complex procedure and computations required for compression and decompression, performance-wise, no method can be placed in a category which satisfy all the requirements of compression and decompression. Thus there is still necessity to develop such techniques which can be a step still ahead in this direction. In the present work, a simple non-redundant-template direct data compression (NRT-DDC) method has been developed, which retains 100% information of compressed signal and provides a high compression ratio. In addition to this, wavelet transform based data compression has been extensively used in the present work to handle the large data for disease diagnosis and HRV analysis.

1.9 SCOPE OF PRESENT WORK

Computer aided feature extraction and analysis of the ECG signal for computer based cardiac disease diagnostics has become the necessity in the present time. The number of cardiac patients has increased too large and the number of cardiac specialists are so limited that it has become difficult to provide ECG based interpretation and diagnosis without the help of computer based expert systems. Looking to the need of time and by exposure through the exhaustive literature survey, it is clear that there is a need to enhance, modify the programs to cope up with the modern techniques and the information technology. To improve the performance of ECG analysis and interpretation, important aspects have been discussed in this thesis. Some of the highlighting factors of the work are as follows:

- i) There is a need of construction of new wavelets for QRS detection and make their use in identification and extraction of ECG parameters for better results.
- ii) There is a need of the use of existing scoring criteria for disease classification and development of modified scoring criteria.

- iii) There is a need to study existing data compression techniques and develop a new direct data compression technique for effective storage and transmission.
- iv) There is a need to study and analyse heart rate variability (HRV) and correlation with physical and psychophysical conditions.

1.10 ORGANIZATION OF THE THESIS

The first chapter deals with the introduction of the thesis problem, the ECG signal, its generation and the heart; lead system used to record 12-lead ECG; noise and artifacts in ECG recordings; CSE and MIT/BIH databases used for testing; literature review of the methods of ECG analysis and interpretation, feature extraction, data compression; heart rate variability and scope of present work.

Wavelet Transform is emerging as a very effective signal analysis technique in the field of biomedical engineering. It is effective for the analysis of non-stationary signals like ECG. Its extensive use is made in signal processing stages right from the noise reduction, feature extraction to disease interpretation. The useful theory and implementation steps of wavelet transform are discussed in the second chapter.

Third chapter deals with the detection of QRS complexes from the ECG signal. The QRS complex is the most prominent feature and its accurate detection forms the basis of identification and extraction of other features and parameters from the ECG signal. Results of the exhaustive evaluation of the wavelet transform based QRS detection software using CSE and MIT/BIH databases are given in this chapter.

Chapter four consists of the details of the feature extraction and determination of almost all diagnostically important parameters. The procedures adapted to measure different ECG wave and wave segments are also reported in this chapter.

The use of the ECG analysis for disease diagnostic and the strategy to use five beats from all the standard 12 leads are discussed in the fifth chapter. The use of existing scoring criteria for disease diagnosis is demonstrated and the methodology to develop modified scoring criteria is discussed in this chapter.

The discussion regarding the rhythm analysis and its use in heart rate variability analysis are given in the sixth chapter.

The ECG data compression using non-redundant templates and wavelet transform are reported in the seventh chapter.

The conclusions of the overall work, the findings and the guidelines for the future work are given in the last chapter.

WAVELET TRANSFORM

2.1 INTRODUCTION

Wavelet transform (WT) has a wide range of applications ranging from signal analysis to image or data compression. Compared to the classical Fourier-based transforms, it can play either the role of the short time Fourier transform (STFT) or the Gabor transform or that of discrete Fourier transform (DFT), or even that of a discrete cosine transform (DCT). Therefore, it is not astonishing that the tool referred to as 'wavelet transform' can take very different forms, depending upon the application [5,24,111,139].

Wavelets are mathematical functions that decomposes data into different frequency component, and then help in the study of each component with a resolution matched to its scale. They have advantages over traditional Fourier method in analyzing physical situations where the signal contains discontinuities and sharp spikes. Wavelet algorithms process data at different scales and resolutions. If we look at a signal with a large 'window', we would notice gross features. Similarly, if we look at a signal with a small window, we would notice detail features. In a generalized statement it can be stated that the result in wavelet analysis is to see both the forest and the trees [7].

The wavelet transform involves the use of a prototype wavelet function, called an analyzing wavelet or mother wavelet. The temporal analysis is performed with a contracted, high frequency version of the prototype wavelet, while frequency analysis is performed with a dilated, low frequency version of the same wavelet. Because the original signal or function can be represented in terms of a wavelet expansion, data operation can be performed using just the corresponding wavelet coefficients. If we further choose the best wavelets adapted to our data, or truncate the coefficients below a threshold, then data is sparsely represented. This sharp coding makes wavelets an excellent tool in the field of data compression.

In particular, the wavelet transform is of interest for the analysis of non-stationary signals, because it provides an alternative to the classical short-time Fourier transform or Gabor transform. The basic difference in STFT and WT is that, STFT uses a fixed analysis window, whereas, WT uses short windows for high frequencies and long windows for low frequencies. For some applications, it is desirable to see the WT as signal decomposition into a set of basis functions. In fact, basis functions are obtained from a single prototype wavelet by dilations and contractions (scaling) as well as shifts. Therefore, in a WT, the notation of

scale is introduced as an alternative to frequency, leading to a so called time-series representation [86].

2.2 WAVELET TRANSFORM Vs. FOURIER TRANSFORM

The FT and WT are both linear operations and the mathematical properties of the matrices involved in the transforms are also similar. For the FT, the basis functions used are sines and cosines and for the WT, more complicated basis functions called wavelets are used. Both the transforms have similarity, the basis functions are localized in frequency, making mathematical tools such as power spectra useful at picking-out the frequencies and calculating the power distributions. The most interesting dissimilarity between these two transforms is that the individual wavelet functions are localized in space while the Fourier sines and cosines functions are not. This localization feature, along with wavelet localization of frequency, makes many functions and operators using wavelets sparse when transformed into the wavelet domain. This sparseness, in turn, results in a number of useful applications such as data compression, ECG characterization, detecting features in images, and removing noise from time series.

An advantage of wavelet transform is its variable window. In order to isolate signal discontinuities, one would like to have some very short basis functions and at the same time, in order to obtain detailed frequency analysis, one would like to have some very long basis functions. A way to achieve this is to have short high-frequency basis functions and long low-frequency ones. This medium is exactly what we get with wavelet transforms. Wavelet transforms do not have a single set of basis functions like the FT, which utilizes just sine and cosine functions. Instead, wavelet transforms have an infinite set of possible basis functions. Thus wavelet analysis provides immediate access to information that can be obscured by other time-frequency methods such as Fourier analysis. Following are important features of wavelet transform:

1. In particular, WT is of interest for the analysis of non-stationary signals, because it provides an alternative to the classical short-time Fourier transform.
2. Wavelets have advantage over traditional Fourier methods in analyzing physical situations where the signal contains sharp spikes.
3. Wavelet algorithms process data at different scales or resolutions.
4. Basis functions are obtained from a single prototype wavelet by dilations and contractions (scaling) as well as by shifts.

- There are several types of wavelet transforms, and depending upon the application, one may be preferred over the others.

2.3 TYPES OF WAVELETS

There are numerous types of wavelets in general use. Following are some types of orthogonal wavelets [24]:

Type	Wavelet name
Haar	Haar
Daubechies	d4, d6, d8, d10, d12, d14, d16, d18, and d20
Symmlets	s4, s6, s8, s10, s12, s14, s16, s18, and s20
Coiflets	c6, c12, c24, and c30

Haar: The Haar wavelet is a square wave. It was discovered by the mathematician Haar in year 1910 [7,24], and provided the first known orthogonal wavelet series representation. The Haar wavelet has compact support and it is zero outside a finite interval. It is the only compact orthogonal wavelet, which is symmetric. However, unlike the other wavelets, the Haar wavelet is not continuous.

Daubechies: The daubechies were the first type of continuous orthogonal wavelet with compact support. This type of wavelet is named in honor of its discoverer Ingrid Daubechies, who is one of the pioneers in wavelet research.

Symmlets: The symmlets also have compact support, and were also constructed by Daubechies. While the daubechies are quite asymmetric, the symmlets were constructed to be as nearly symmetric as possible.

Coiflets: The coiflet were constructed by Daubechies to be nearly symmetric and also have additional properties thought to be desirable (vanishing moments for both ϕ and ψ). Daubechies used the name coiflets in honor of Ronald Coifman, another important contributor to the theory and application of wavelet analysis.

Biorthogonal wavelets are an important generalization of the orthogonal wavelet approximation. Biorthogonal wavelets are symmetric and do not introduce phase shifts in the coefficients, which can be important for certain, applications. However, a biorthogonal wavelet transform is not orthogonal. Following are the some biorthogonal wavelets.

Type	Wavelet name
B-spline	bs1.1, bs1.3, bs1.5 bs2.2, bs2.4, bs2.6, bs2.8 bs3.1, bs3.3, bs3.5, bs3.7, bs3.9
V-spline	vs1, vs2, vs3

B-spline: These are based on the simple polynomial spline function. The wavelet can have degree 0 (the Haar wavelet), degree 1 (a triangle function), or degree 2 (a quadratic function)[24,86,139]. The name of the b-spline wavelet has two numbers. The first number indicates the degree of the polynomial for the wavelets and the second number indicates the length of the support of the dual wavelet.

V-spline: These are variations on the b-spline designed to achieve near-orthogonality and support width, which is nearly the same for father and mother wavelets. There are three different v-splines. The numbers of the v-splines have no particular meaning.

2.4 WAVELET TRANSFORM

Wavelets are a mathematical function that decomposes data into different frequency components, and then help in the study of each component with a resolution matched to its scale. The interpretation of the scale as shown in Fig.2.1, is that when 'a' increases, the filter function $\Psi\left(\frac{t-b}{a}\right)$ becomes spread out in time and takes only long time behavior (low frequency) into account. That is, the scale factor 'a' can be interpreted as the scale in maps, very large scales mean global views, while very small scales mean detailed views. A related but different notation is that of resolution. The resolution of a signal is linked to its frequency content. However, in discrete-time signals, increasing the scale in the analysis involves sub-sampling, which automatically reduces the resolution. Decreasing the scale (which involves up-sampling) can be undone, and does not change the resolution. The interplay of scale and resolution changes in discrete-time signals. This kind of analysis of course works best if the signal is composed of high frequency components of short duration plus low frequency components of long duration, which is often the case with signals encountered in practice. A generalization of the concept of changing resolution at different frequencies is obtained with so called 'Wavelet packets', where arbitrary time-frequency resolution (within the uncertainty bound) are chosen depending on the signal.

The multi-resolution decomposition process shown in Fig.2.2 splits the signal into one detail and one low resolution signal. WT representation consists of computing coefficients

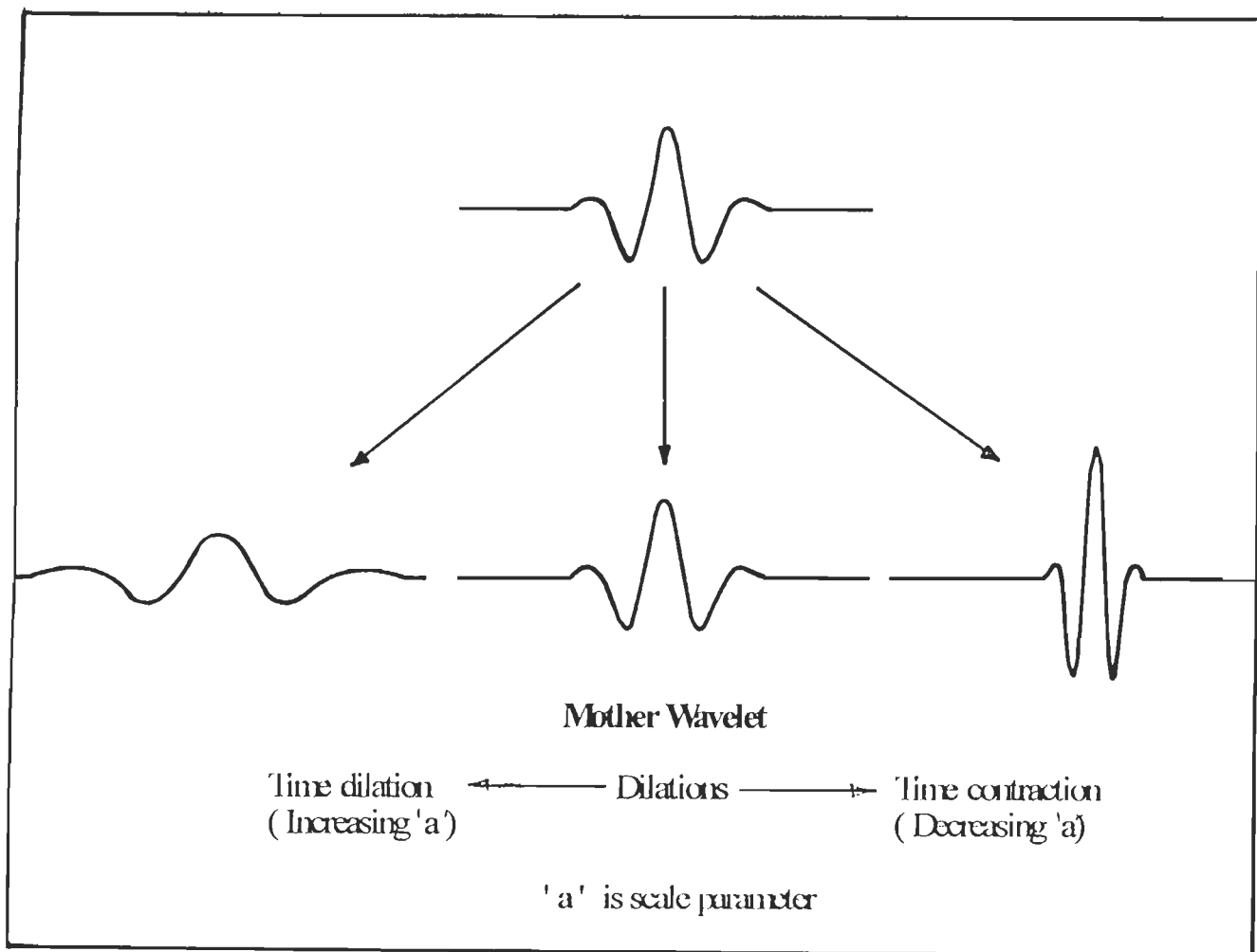


Fig.2.1 Mother wavelet and effect of time dilation and contraction on the amplitude

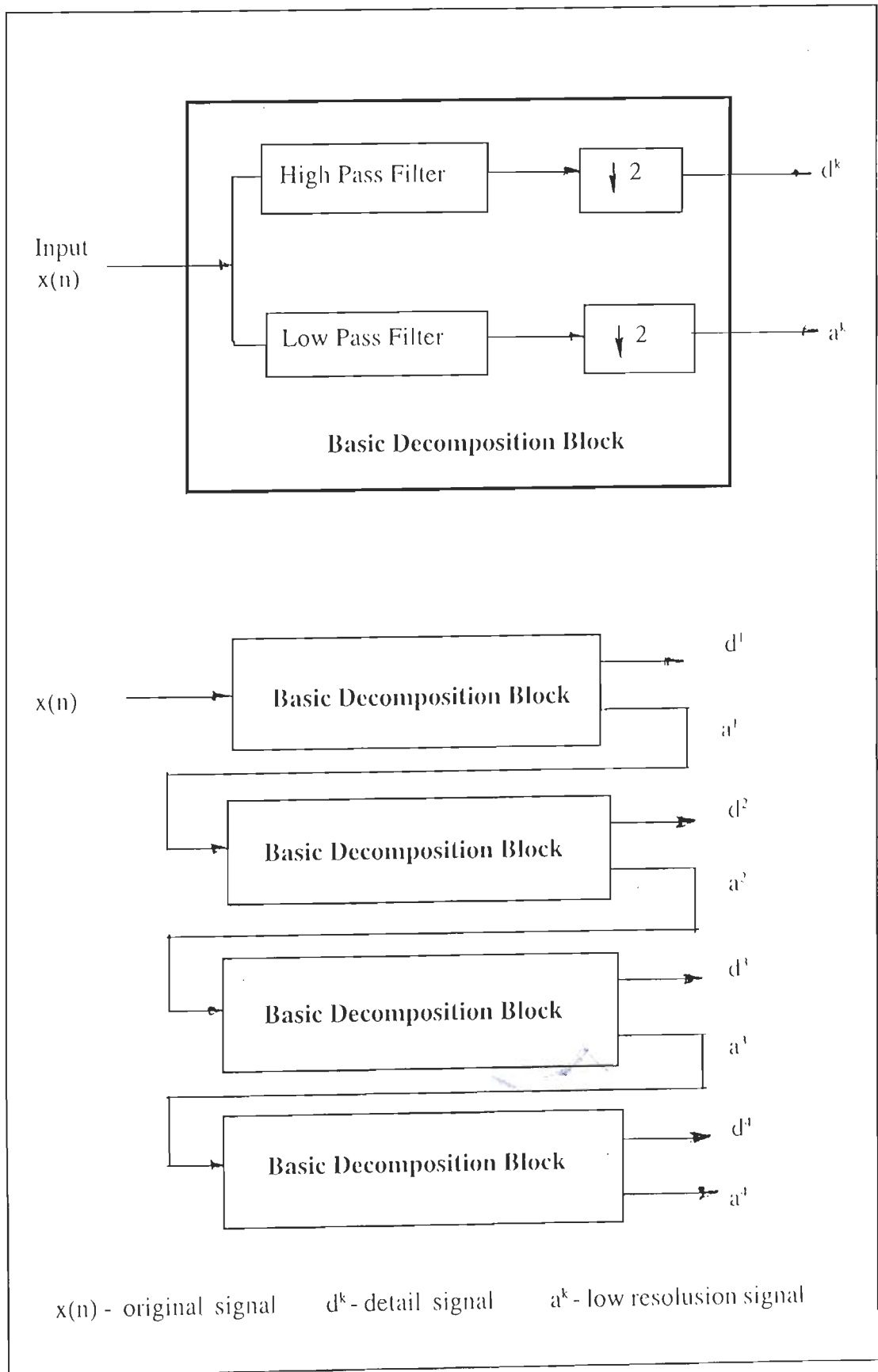


Fig.2.2 Implementation of wavelet transform

that are inner products of the signal and a family of wavelets. Wavelet corresponding to scale 'a' and time location 'b' is [115].

$$\Psi_{a,b}(t) = \frac{1}{\sqrt{a}} \Psi\left(\frac{t-b}{a}\right) \quad (2.1)$$

where, $\Psi(t)$ is the wavelet function and 'a' and 'b' are scale and shift related parameters, respectively.

The continuous wavelet transform (CWT) is given by the equation

$$\text{CWT}(x(t);a,b) = \frac{1}{\sqrt{a}} \int_{-\infty}^{\infty} x(t) \Psi^*\left(\frac{t-b}{a}\right) dt \quad (2.2)$$

where $x(t)$ is a signal and '*' stands for complex conjugate.

The discrete wavelet transform (DWT) has been recognized as a natural WT for discrete time signals by several investigators [5,114,139,]. Both time and time-scale parameters are discrete. The parameters 'a' and 'b' are discretised as $a = 2^j$ and $b = k 2^j$, where k and j are integers. Due to the use of scale 2^j , the WT is known as the dyadic wavelet transform (Dy WT). Since the CWT is sampled on a dyadic scale, the wavelets used are of the form

$$\Psi_{j,k}(t) = 2^{-j/2} \Psi(2^{-j}t - k) \quad (2.3)$$

The DyWT of a signal $x(t)$ is given by the equation

$$\text{DyWT}(b,2^j) = \frac{1}{2^j} \int_{-\infty}^{\infty} x(t) \Psi^*\left(\frac{t-b}{2^j}\right) dt \quad (2.4)$$

The DWT of discrete signal $x(n)$ achieves a multiresolution decomposition on a finite number of scales denoted by $j = 1, 2, \dots, J$ and the signal $x(n)$ is represented in terms of wavelet and scaling functions as

$$x(n) = \sum_{j=1}^J \sum_k d_{j,k} \Psi_{j,k}(n) + \sum_k a_{j,k} \Phi_{j,k}(n) \quad (2.5)$$

The $\Psi_{j,k}(n)$ are the synthesis wavelets, i.e. the discrete equivalent to $2^{-j/2} \Psi(2^{-j}t - k)$.

The DWT computes coefficients $d_{j,k}$ for $j = 1, 2, \dots, J$ and scaling coefficients $a_{j,k}$ given by

$$\begin{aligned} d_{j,k} &= \sum_m g(m - 2k) a_{j+1,m} \quad \text{and} \\ a_{j,k} &= \sum_m h(m - 2k) a_{j+1,m} \end{aligned} \quad (2.6)$$

The a's in a DWT are called the smooth coefficients and d's are the detail coefficients. The h and g are the discrete filters representing the scaling and wavelet functions, respectively. In wavelet transform implementation using digital filters, the general

strategy used is to pass a sampled signal $x(n)$ simultaneously through two specially designed filters, i.e., through a low pass filter and a high pass filter, and to then down sample the outputs. The process of low pass filtering involves the convolution of the signal $x(n)$ with a scaling function $\phi(t)$, whose Fourier transform appears as a low pass filter. The high pass filtering process involves the convolution of the signal $x(n)$ with a wavelet function $\psi(t)$, whose Fourier transform appears as a high pass filter. This process splits the signal into one detail signal d^1n ($n=0, \dots, N/2 - 1$) and one low resolution signal a^1n ($n=0, \dots, N/2 - 1$), here N represents the number of samples in the original signal. Signal a^1n ($n=0, \dots, N/2 - 1$) is also called an approximation function for $x(n)$. The low resolution signal can be further decomposed into a second detail signal and a lower resolution signal by passing a^1n ($n=0, \dots, N/2 - 1$) through the same two filters and down sampling. This procedure can be continued to get number of detail signals and a low resolution signal. This process of splitting a discrete signal $x(n)$, ($n = 0, \dots, N-1$) by DWT, decomposes $x(n)$ into a set of detail signals:

$$d^1n \ (n=0, \dots, N/2 - 1), \ d^2n \ (n=0, \dots, N/4 - 1), \ \dots, \ d^jn \ (n=0, \dots, N/2^j - 1)$$

and one low resolution signal a^jn ($n=0, \dots, N/2^j - 1$), where j is the decomposition scale.

2.5 PROPERTIES OF WAVELET FUNCTIONS

Selecting a wavelet requires a tradeoff between different properties such as smoothness, spatial localization, frequency localization, and the ability to represent local polynomial functions, orthogonality, and symmetry. These properties are discussed below:

Smoothness: The smoothness of the wavelet approximation is one of the properties that distinguish modern wavelet analysis. For many applications, the wavelet function must be sufficiently smooth to efficiently represent the characteristics of the underlying signal. The lack of smoothness is one of the main disadvantages of the Haar wavelet.

One measure of smoothness for a wavelet is given by the number of derivatives which exist for that wavelet. The Haar wavelet is discontinuous and hence is not differentiable. The $d4$ wavelet is continuous but also is not differentiable. The $d12$ wavelet, however, is twice differentiable [24,86].

Temporal and Spatial Localization: A central feature of wavelet analysis is the ability to localize features in time and space. The support width of a wavelet is closely related to its ability to localize features in time and space. Very compact wavelets, such as the Haar

wavelet, are very well localized in time and space. Support width is generally inversely related to the smoothness. The smoothest wavelet has the widest support width.

Vanishing Moments: A wavelet with a higher number of vanishing moments can better represent higher degree polynomial signals. The number of vanishing moments is also closely related to the smoothness of a wavelet. A mother wavelet ψ with M vanishing moments satisfies

$$\int t^m \psi(t) dt = 0 \quad m = 0, 1, \dots, M-1 \quad (2.7)$$

The coiflet has the unusual property of also having vanishing moments for the scaling function ϕ :

$$\int t^m \phi(t) dt = 0 \quad m = 1, \dots, M-1 \quad (2.8)$$

The zero moment for the father coiflet is always one.

Frequency Localization: Wavelet localizes features not only in time and space, but also in frequency. The Haar wavelet has very poor frequency resolution. In general, smoother wavelets have better frequency localization properties.

Symmetry: With the exception of the Haar wavelet, the orthogonal wavelets, which have compact support, are not symmetric; the daubelets are highly asymmetric and the symmlets and coiflets are nearly symmetric. All of the biorthogonal wavelets are either symmetric or anti-symmetric. Symmetric wavelets have the advantage of avoiding any phase shifts, the wavelet coefficients do not drift relative to the original signal.

Orthogonality: The orthogonality of the wavelet transform is a central feature for some applications. The biorthogonal wavelets lack the orthogonality property, although the v-spline biorthogonal wavelets are nearly orthogonal.

2.6 WAVELETS AND THEIR APPLICATIONS

As shown in Table 2.1, there exist an abundant variety of wavelets, and therefore, there is a fundamental problem of determining which one produces the best results for a particular application. Before selecting a particular wavelet, several standard wavelets are to be tried, and the one, which produces the best performance, should be used. The selection of a suitable wavelet is dependent on application, as is the case in pattern classification [35,87,]. A wavelet function is selected on the basis of the maximum number of correct classifications. In other applications, such as multi-scale modelling of stochastic process and signal coding, a good wavelet is the one which results in a small number of nonnegligible WT coefficients or a best approximation of a given signal upto a given scale. Thus, the scaling function

associated with a good wavelet usually has a shape similar to the shape of the given signal [87,114]. The other important aspects to be considered are less noise sensitivity and less quantization errors. The previous applications involving the optimization of wavelets for pattern classification include the work by Mallet et al. [87], who have optimized the shift and dilation parameters of discretization of wavelet. On the basis of exhaustive study and experience, it is possible to select a particular wavelet for a particular application.

In this work, a modified combined Wavelet Transforms technique has been used which is developed to analyze single and multi-lead electrocardiogram (ECG) signals for cardiac disease diagnostics. Two wavelets have been used i.e. a quadratic spline (QS) wavelet for QRS detection and the Daubechies six coefficient (D6) wavelet for P and T detection. Better results are possible using this method because of the specific feature of the wavelet transform to characterize the local regularity of ECG signal. This feature is used to distinguish ECG waves from noise, artifacts and baseline drift. WT decomposes data into different components that are well localized in time and frequency. Each component with a resolution matched to its scale is used for further analysis and diagnostics.

Wavelet transforms have become powerful alternative to Fourier transform methods in many medical applications, where the signals are non-stationary in nature. In addition to helping in the recognition and detection of key diagnostic features, they provide a powerful means for compressing medical images. Heart disease diagnosis, studies of fetal breathing, extraction of speech from background noise in digital hearing aids, detection of breast cancer, and medical image compression are the important application area of the wavelets [5,137].

Detecting coronary artery disease: Early detection of coronary artery disease has long been regarded as among the most vital areas of medical research. Diagnostic methods being used are traditional physical examinations and history-taking, electrocardiography, and echocardiography (ultrasonic imaging). Other invasive methods are thallium test and cardiac catheterization to inject a radio-opaque dye for X-ray examination.

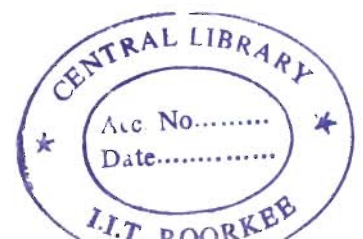
Wavelets applied to the analysis of heart sounds may provide useful information. It has been widely reported that turbulence to stenosis (narrowing) of the arteries creates audible sounds, which may be analysed to yield information about the nature and severity of the blockage.

Table 2.1 Wavelets and their application areas

Wavelet Filter Coefficients	Comments
1.0, 1.0 or 0.707107, 0.707107	Haar wavelets [47], used for data compression.
0.25, 0.375, 0.375, 0.25	Quadratic spline wavelet, [25,72,124], used for ECG characterization
$1/4(1+1/3)$, $1/4(3+1/3)$, $1/4(3-1/3)$, $1/4(1-1/3)$	Daubechies-4 wavelet[5,86], used for ECG analysis.
0.332671, 0.806891, 0.459877, -0.135011, -0.085441, 0.035226	Daubechies-6 wavelet, [5,47], used for data compression
-0.176777,0.353553,1.060660, 0.353553, -0.176777	[47], used for data compression
0.788486, 0.418092, -0.040689, -0.064539	[47], used for FBI fingerprint image coder
0.767245, 0.383269, -0.068878, -0.033475,0.047282,0.003759,-0.008473	[47], used for data compression
0.852699, 0.377402, -0.110624, -0.023849, 0.037828	[5,54,137] used for image compression
0.788486, 0.047699, -0.129078	[5,54,137] used for image compression
0.994369, 0.419845, -0.176777, -0.066291, 0.033145	[5,54,137] used for image compression
0.544089, 0.296844, 0.041409, 0.056710, 0.040100	[5,54,137] used for image compression

Detecting irregular heart beats: Although many people, especially the elderly, experience occasional abnormal or ectopic ventricular beats that cause no other symptoms An excess of premature ventricular contraction (PVCs) may indicate cardiac ischemia and lead to ventricular fibrillation, which may cause an acute heart attack. The detection and analysis of

G106215 .



PVCs is therefore of great interest. Recently, wavelets have been used to detect ectopic heart beats. In addition to this, wavelets have also been used to study beat-to-beat variations of the ECG signals and to monitor the status of patients after coronary angioplasty.

Alcohol and babies: It has been widely reported that chronic alcohol abuse during pregnancy may cause several kinds of problems in the newborn, including mental retardation and disorders of some facial nerves. Although the effects of alcohol have been examined extensively, the analyses have been limited to statistical descriptions of the time intervals between breathing events or to descriptions of short-term and long-term fluctuations in breathing activities using the fast Fourier transform. Wavelets can be used for quantifying and understanding the non-stationary fetal breathing process and how alcohol affect the time and frequency domain characteristic of fetal breathing [5,137].

Wavelets in hearing aids: Listeners with normal hearing could understand 50 percent of word lists (and 95% of sentences) with signal-to-noise ratio as low as -5 dB. By comparison, hearing-impaired listeners required S/N ratio of 9 dB to do as well. Several researchers have used a wavelet based method for extracting speech from the background noise. Both speech - to-noise ratio and the retention of consonants based on a wavelet packet algorithm looks promising as a preprocessor for hearing-loss compensation in digital hearing aids.

Early detection of breast cancer: In routine clinical examinations, physicians check for breast cancer by looking for abnormal skin thickening, malignant tissues, and microcalcifications. Small tumors and microcalcifications are difficult to detect because of the similarity of normal glandular tissues to those afflicted by malignant disease. Tremendous efforts have been made to enhance the diagnostic value of mammographic images by eliminating the noise in them. Wavelet transform methods have recently been developed to detect and classify tumors in digitized mammograms.

Medical image compression: The other great need in medical imaging is for data compression, There are lossless and lossy types of data compression methods. With lossless compression, a typical compression ratio of 3:1 can be achieved and the process is completely reversible [5,137]. Lossy compression, on the other hand, involves the loss of information and may not be reversible. It is, however, capable of much higher compression ratios. High compression ratio methods that do not lose medically important information could help the medical community. Wavelet can provide such a method. Because wavelet transform coefficients are localized in both space and frequency, they are better suited to image compression than other common transform methods.

In addition to these applications of wavelets, the other areas are the analysis of 1-D physiological signals obtained by phonocardiography, electrocardiography, and electroencephalography, including evoked response potentials. In signal processing, wavelets are being used for noise reduction, image enhancement, detection of microcalcification in mammograms, image reconstruction, tomography, magnetic resonance imaging (MRI) and multiresolution methods for the registration and statistical analysis of functional images of the brain (positron emission tomography (PET) and functional MRI).

Analysis of ECG: The crucial step in the analysis of ECG is the detection of the QRS complex. Wavelet based approach provides excellent performance in comparison to many other algorithms available [137]. The WT has used for discriminating normal and abnormal cardiac pattern [126] and also in detection of ventricular late potentials [119]. Wavelets are also applied to characterize beat-to-beat fluctuations of the heart rate under varying physiological conditions [142,146].

2.7 CONCLUSION

There are no definite rules for selecting a wavelet for a particular application. The use of different wavelets for a particular application gives different performance, hence the user has to see and select a particular wavelet, best suitable for the application of his interest. The overall choice for many applications can be met by the wavelet, which is orthogonal, smooth, nearly symmetric, and non-zero on relatively short interval. It is suggested by different researchers that the wavelets be constructed according to the application at hand [87,114].

DETECTION OF QRS COMPLEX

3.1 INTRODUCTION

Computer aided feature extraction and analysis of the ECG signal for computer based cardiac disease diagnostics has become the necessity in the present time. The number of cardiac patients has increased too large and the number of cardiac specialists are so limited that it has become difficult to provide effective cardiac care without the help of computer based expert systems. The first step in computer aided diagnostics is the identification and extraction of the features of ECG signal. The QRS complex is the most prominent feature in the ECG signal and its accurate detection forms the basis of extraction of other features and parameters from the ECG signal. A good amount of research work has been carried out during the last four decades for the accurate and reliable detection of QRS complex in the ECG signal. But still there is need to further carryout the work on a more efficient and reliable method which can increase the percentage of accurate and reliable QRS detection without leaving any doubt in respect of the automated system. The work carried out here is a concrete step in that direction.

3.2 METHODS OF QRS DETECTION

The QRS detection algorithms developed so far can be broadly classified into four categories; (i) syntactic approaches, (ii) non-syntactic approaches, (iii) hybrid approaches, and (iv) transformative approaches.

(i) Syntactic approaches

In syntactic approach, the ECG signal is first reduced into a set of elementary patterns like peaks, duration, slopes, and interwave segments, and thereafter, using rule based grammar, the signal is represented as a composite entity of peaks, duration, slopes and interwave segments. These patterns are then used to detect the QRS complexes in the ECG signal [44,105]. Mehta et al. [93] have used a syntactic approach to delineate peaks and boundaries. The accuracy of 99.83% in QRS identification and 96% in P and T wave identification has been reported in this work. Looking to the methodology used to delineate the wave components, it is clear that this method is suitable if the signal is smooth and regular in nature. Although the methods of this category are quite suitable to represent the ECG wave pattern and its parameters, but still lot of work is required to make these techniques perfect for the accurate and fully reliable detection of QRS complexes. Also the

syntactic methods are time consuming and require rule based grammar in each step of its execution for pattern classification [93,105].

(i) Non-syntactic approaches

The non-syntactic approaches are being widely used for the detection of QRS complexes. The algorithms are based on the band pass filters, mathematical models, artificial neural networks, adaptive techniques, and also on the use of amplitude, slope, power spectra, and spatial velocity functions [2,4,29,30,67,82,101,103]. Out of a number of available techniques in this category, the band pass filters are most widely used. The band pass filters remove the components other than those of the QRS complexes from the ECG signal. Thakor et al. [133] have used band pass filter to maximize the signal (QRS complex) to noise (T-waves, 60 Hz, EMG etc.) ratio to detect the QRS complexes. Due to the inherent variability of ECG from different persons, as well as variability due to noise and artifacts, the filter design is suboptimal in specific situations. An algorithm for the detection of QRS complexes, based upon digital analysis of slope, amplitude, and width has been developed by Pan and Tompkins [104]. For the standard 24 hour MIT/BIH arrhythmia database, the QRS detection rate has been reported as 99.3% by this method. This method faces difficulty when the P or T is higher in magnitude than the QRS complex and also with the non-QRS waves with highly unusual morphology. Hamilton and Tompkins [45] have used the MIT/BIH arrhythmia database to develop QRS detection. The resulting QRS detection algorithm has a sensitivity of 99.69% and positive predictivity of 99.77% when evaluated with the MIT/BIH arrhythmia database. Afonso et al. [3] have designed a filter bank (FB) to perform independent time and frequency analysis on the signal. The reported beat detection sensitivity is 99.59% and a positive predictivity of 99.56% against the MIT/BIH database. Gary et al.[41] have analysed different QRS detection algorithms for noise sensitivity. None of the algorithms are able to detect all QRS complexes without any false positive.

Some other methods make use of the differentiated low pass filtered ECG signal and thereafter its wave shapes for the QRS detection [67,69]. Escalona et al. [36] developed a technique which is based on the accurate detection of a single QRS fiducial point in the band pass filtered (3-30 Hz) QRS segment. Anti et al. [8] have reported a technique based an optimized prefiltering in conjunction with a matched filter and claimed a QRS detection error of 2.2% on record number 105 of the MIT/BIH Arrhythmia database. In most of these works it is claimed that the use of the digital filters improves the reliability of QRS detection in comparison to other methods [41,51]. The digital filter based QRS detection is accurate and reliable and can effectively handle the ECG signal even contaminated with noise and

interference. The digital filters can also handle those typical cases, which are otherwise difficult to handle by the algorithms based on the criteria of amplitude, slope, and zero crossings. There are difficulties with digital filter based algorithms where the pass band of the QRS complex varies with the heart beats, leads, and patients and also where the pass bands of the other segments and noise overlap with pass band of the QRS complex [152].

There are QRS detection techniques, which use the spatial velocity function, mixed mathematical basis functions, mathematical models, mathematical morphology and averaging [10,20,36,44,66,82,97,108,128]. Maheshwari et al. [82] developed an analysis technique using the spatial velocity to detect ECG wave components. The software reliably detects the QRS complexes and other component waves (P and T) with an accuracy of 90%. The technique developed by Trahanias [136] is based on mathematical morphology works as a peak-valley extractor. He has achieved a detection sensitivity of 99.38% and a positive predictivity of 99.48%. The method is based on the phenomenon of peak picking and is prone to noisy peaks. Although these techniques are suitable for most of the cases, but require exhaustive learning and training to form the mathematical model, and hence, are complex and time consuming, and find difficulty in on-line computer based ECG interpretation.

In recent times, artificial neural network based algorithms have been used in the detection of QRS complexes [141,152]. The basic methodology to use these techniques is to learn and later on to generalise the knowledge gained through the learning to identify the QRS complexes. The accuracy of detection of QRS complexes by these methods is dependent on the type of used training dataset. The method developed by Vijaya et al. [141] is based on an artificial neural network (ANN). It works on high prediction error to indicate the occurrence of QRS complexes. A sensitivity of 98.96% has been achieved by them using the CSE database DS-3. This algorithm is based on the amplitude error detection, hence gives false positive cases for high P and T components. Considering wide variability in ECG morphology, it is very difficult to cover all types of the patterns of QRS complex for training and to expect 100% accuracy of detection.

To optimize the performance of developed techniques, the concept of adaptiveness was introduced in the QRS detection [8,128,152]. The decision rules based on signal amplitude, slope, and duration are changed according to the signal at hand. Similarly, the terms adaptive matched filtering, adaptive estimation of QRS segment features by the Hermite model, neural network based adaptive matched filtering and adaptive template building are some of the techniques in this category [132]. Xue et al. [152] have developed an adaptive filtering algorithm based upon an ANN for the detection of the QRS complexes. The

use of ANN adaptive whitening filter has been made to model the lower frequencies of the ECG signal, which are inherently nonlinear and nonstationary. The residual signal that contains mostly higher frequency QRS complex energy is then passed through a linear matched filter to detect the location of the QRS complexes. The reported detection rate is 99.5% for the MIT/BIH arrhythmia database. In these techniques, an algorithm configures itself to a unique QRS segment of a patient during an initial stage of learning. This adaptability approach enhances QRS detection rate by a considerable extent and reduces the percentage of false detentions, but at the same time, increases the computation as it involves learning phase (determination of adaptive model parameters) and repetitive calculations to optimize the threshold limits for amplitudes, slopes and duration.

(iii) Hybrid Approaches

The syntactic and non-syntactic approaches are combined to detect the QRS complex. Syntactic techniques are based on the grammar rules used to model ECG signal as a group of straight lines and triangles. This requires having smooth ECG signal, but in practice this is not the case with wide variety of ECG morphologies. On the other hand in non-syntactic approach, there is no consideration to maintain the morphology of the signal. Gustavo et al. [44] used the syntactic method to extract the time evolution of the rhythm using the energy of ECG derivatives and their coding by a look-up table.

(iv) Transformative Approaches

The use of different transforms on ECG signal helps to extract the information in the form of energy, slope, or spike spectra, and thereafter, the ECG features are detected with the help of decision rules like thresholds of amplitude, slope or duration. Out of the available transforms, namely Fourier transform, cosine transform, pole-zero transform, differentiator transform, Hilbert transform, the use of wavelet transforms in the detection of QRS complexes, has shown optimum performance. Thus, the more effort is being put to develop the WT based techniques for QRS detection. Sahambi et al. [123] used the modulus maxima of the WT using multiresolution analysis for the detection of QRS complexes and the overall accuracy of the system to detect QRS complex is 98.8%. Similarly Li et al. [72] reported an algorithm based on multiscale feature of wavelet transform. They have reported 99.8% accuracy in QRS detection for the MIT/BIH arrhythmia database. Kadambe et al. [56] described a QRS complex detector based on the dyadic wavelet transform which is robust to time-varying QRS complex morphology and also to noise. They have observed that although no one algorithm exhibited superior performance in all situations, the DyWT based detector compares well with the standard techniques and exhibited excellent performance.

In the present work, the use has been made of multiresolution signal decomposition to evaluate the performance of the detection of QRS complexes with five different types of wavelets. Based on the evaluation study, a new wavelet has also been constructed.

3.3 WAVELET TRANSFORM

The WT is expressed as the time-integrated product of a signal with a set of analyzing basis functions [86,118,139]. The basis functions for the WT are dilated and shifted versions of a mother wavelet. The mother wavelet can have many different forms subject to certain constraints, such as the time average of the wavelet function be zero, i.e. $\int \psi(t)dt = 0$,

where $\psi(t)$ is a mother wavelet.

If the method is being used for data compression, certain restrictions are required on $\psi(t)$, so that the original signal can be recovered by the inverse WT.

The continuous wavelet transform is given by

$$\text{CWT}(x(t);a,b)=W(a,b) = \int x(t) \frac{1}{\sqrt{|a|}} \cdot \psi^* \left(\frac{t-b}{a} \right) dt \quad (3.1)$$

where $x(t)$ is a signal, ' * ' denotes complex conjugation and $\psi(t)$ is a wavelet function.

The CWT is closely related to time-frequency representations. The parameter 'b' is the time translation and the parameter 'a' is the dilation, or scale factor, and its reciprocal is similar to frequency. The equation 3.1 can be written in a more compact form by defining $\psi_{a,b}(t)$ for the WT as:

$$\psi_{a,b}(t) = \frac{1}{\sqrt{a}} \psi \left(\frac{t-b}{a} \right) \quad (3.2)$$

where $\psi_{a,b}(t)$ is a basis function, such as a Daubechies wavelet [47] or a quadratic spline wavelet [25,72], known as the mother wavelet. The basis functions consist of translations and dilations (or contractions) of the wavelet function. Increasing 'a' in equation (3.2) expands $\psi(t-b)$ along the t- axis, and hence is termed 'dilation'. Decreasing 'a' contracts the function. The parameter 'b' causes the function to translate along the time axis. As shown in Fig.2.1 (chapter II), amplitude increases with time contraction and decreases with time dilation to normalize energy. The duration of the wavelet defines its effective window width. Since this duration varies as 'a' varies, the WT uses windows of varying size. For large values of 'a', basis functions are broader, and the energy in their spectra is concentrated

at lower frequencies. The information in the low frequency end of the signal spectrum is captured by these basis functions. For smaller values of 'a', the basis functions are narrower, and their energy spectrum densities peak at higher frequencies with broader lobes so the information is captured in the high frequency end of the signal spectrum. The WT thus captures frequency information at various scales of frequency, and the representation provided by the WT is more accurately referred to as a 'time-scale' representation.

3.3.1 Implementation of Wavelet Transform

The Wavelet Transform is implemented using digital filters. As shown in Fig.2.2 (chapter II), the general strategy is to pass a sampled signal $x(n)$ simultaneously through two specially designed filters, i.e., through a low pass filter and a high pass filter, and then to down sample the outputs. The process of low pass filtering involves the convolution of the signal $x(n)$ with a scaling function $\phi(t)$, whose Fourier transform appears as a low pass filter. The high pass filtering process involves the convolution of the signal $x(n)$ with a wavelet function $\psi(t)$, whose Fourier transform appears as a high pass filter. This process splits the signal into one detail signal d^1n ($n=0, \dots, N/2 -1$) and one low resolution signal a^1n ($n=0, \dots, N/2 -1$), here N represents the number of samples in the original signal. The output of high pass filter is a detail signal and low pass, is a approximate signal or called as coarse signal. The signal a^1n ($n=0, \dots, N/2 -1$) is also called an approximation function for $x(n)$. The low resolution signal can be further decomposed into a second detail signal and a lower resolution signal by passing a^1n ($n=0, \dots, N/2 -1$) through the same two filters and down sampling. This procedure can be continued to get number of detail signals and a low resolution signal. This process of splitting a discrete signal $x(n)$, ($n = 0, \dots, N-1$) by DWT, decomposes $x(n)$ into a set of detail signals and a low resolution signal as:

Detail signals: d^1n ($n=0, \dots, N/2 -1$), d^2n ($n=0, \dots, N/4 -1$),..., d^jn ($n=0, \dots, N/2^j -1$)

Low resolution signal: a^jn ($n=0, \dots, N/2^j -1$)

where j is the decomposition scale.

3.3.2 Identification of ECG waves

Fig.3.1 shows the implementation of the WT for ECG analysis. Firstly the original signal $x(n)$, sampled at 500 Hz, is convolved with coefficients of the scaling function $\phi(t)$ and the wavelet function $\psi(t)$ to get low pass and high pass filtered outputs, respectively. The output from the low pass filter is down sampled by 2 to get the low resolution signal a^1n ($n=0, \dots, N/2 -1$) and the output from the high pass filter is used

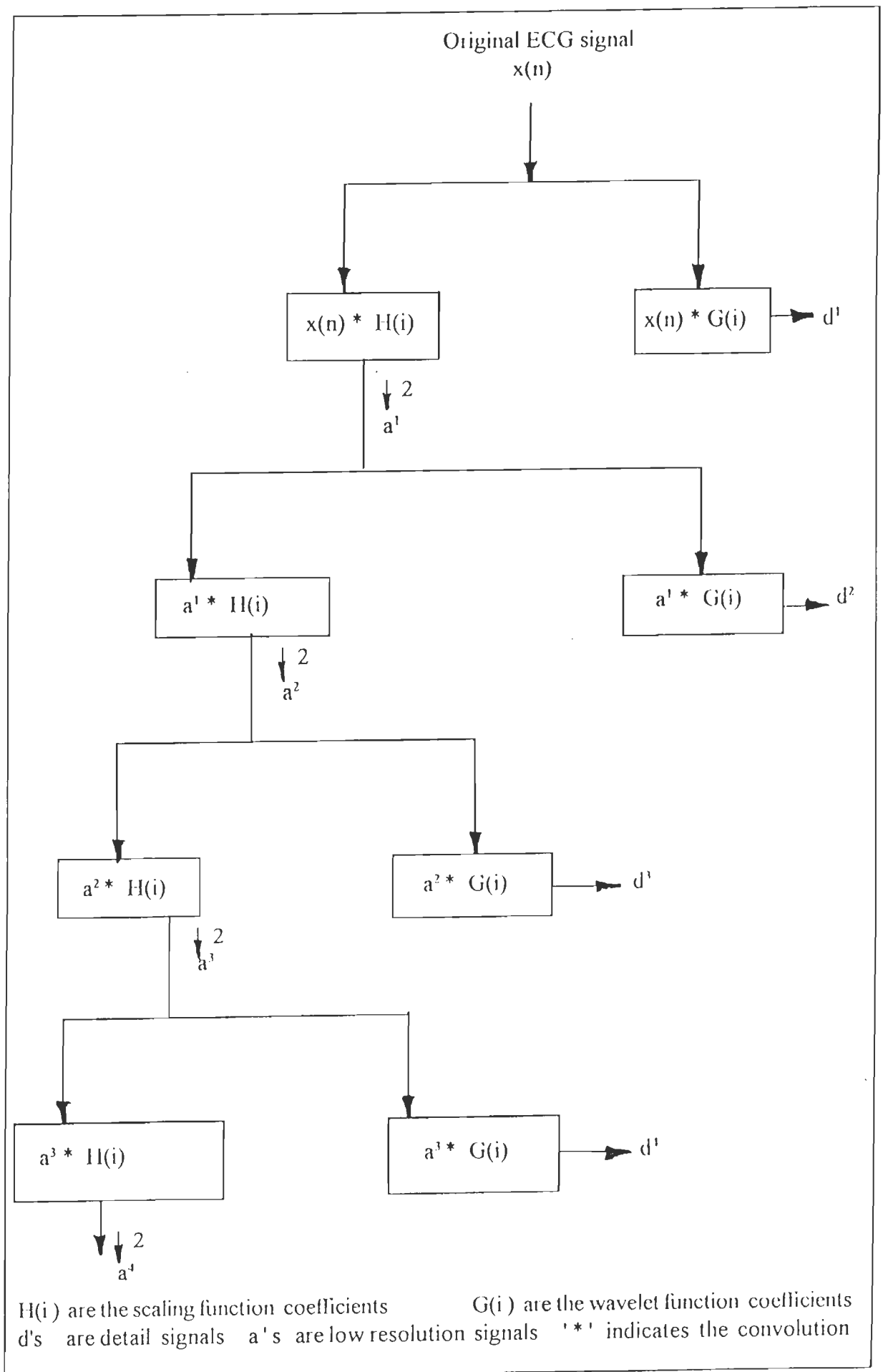


Fig.3.1 Extraction of detail signals at different scales

without down sampling to get the detail signal d^1n ($n=0, \dots, N-1$). It is observed that the accurate detection rate of QRS complex is increased by avoiding the down sampling of the output of high pass filter as it reduces the loss of information. This first decomposition process splits the original signal's bandwidth in half; i.e., the low resolution signal contains the low frequency components of the input signal and the detail signal contains the high frequency components of the input signal. In the second decomposition, the new low resolution signal a^1n ($n=0, \dots, N/2 - 1$) is convolved with the coefficients $\phi(t)$ and down sampled to get the next low resolution signal a^2n ($n=0, \dots, N/4 - 1$). Convolution of a^1n ($n=0, \dots, N/2 - 1$) with $\psi(t)$ without down sampling produces the detail signal d^2n ($n=0, \dots, N/2 - 1$). The same decomposition procedure is repeated to extract the d^3n ($n=0, \dots, N/4 - 1$) and d^4n ($n=0, \dots, N/8 - 1$) detail signals. The nature of these detail signals is shown in Fig. 3.2, which indicates a gradual increase in the energy of the QRS complexes from the lowest scale (2^0) to the highest scale (2^3). The clear extraction of QRS complexes can be seen in detail signal d^4 (2^3) at which the detection of QRS complexes has been carried out. The fifth stage of signal decomposition ($d^5(2^4)$) is also shown in the Fig.3.2, where some of the QRS complexes are missing as this stage emerge lower frequency ECG components signal.

3.4 SELECTION OF WAVELETS FOR QRS DETECTION

There exists an abundant variety of wavelets, and therefore, there is a fundamental problem to determine as which wavelet is to produce the best results for a particular application. There are no fixed rules to select a wavelet. In practice, before selecting a particular wavelet, several standard wavelets are usually tried, and the one, which produces the best performance, is used. The selection of a suitable wavelet is application dependent as is the case in pattern classification [87,126]. A wavelet function is selected on the basis of the maximum number of correct classifications. In other applications, such as multi-scale modeling of stochastic process and signal coding, a good wavelet is the one which results in a small number of non-negligible WT coefficients or a best approximation of a given signal up to a given scale. Thus, the scaling function associated with a good wavelet usually has a shape similar to the shape of the given signal [87,126]. The other important aspects to be considered are less noise sensitivity and less quantization errors. The previous applications involving the optimization of WTs for pattern classification include the work by Mallet et al.[87]. Mallet et al. optimized the shift and dilation parameters of the discretization of a chosen wavelet. On the basis of exhaustive study and experience with wavelets, it is

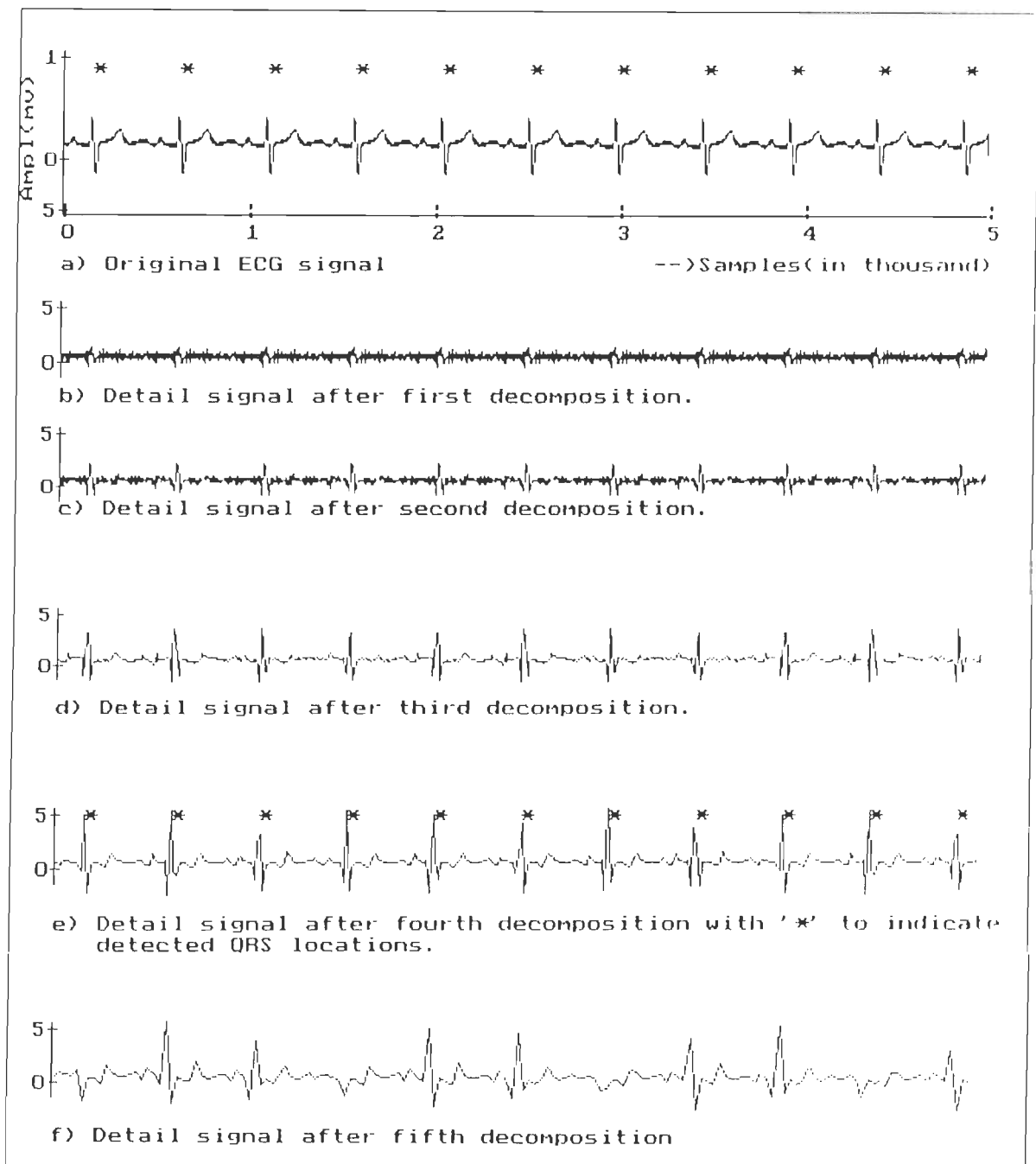


Fig.3.2 Wavelet transform based QRS detection steps

recommended that the faithful QRS detection can be performed by selecting the following characteristic features:

(i) Signal splitting by multiresolution decomposition

The WT feature is used to split the ECG signal into different frequency bands. It needs optimization in the scale of signal decomposition because the QRS energy emerging at different scales by the different wavelets is different.

(ii) Compact and symmetric wavelet

The use of compact and symmetric wavelet produces less phase shift in the QRS fiducials of detail signal d^4 compared to the original signal.

(iii) Magnitude of wavelet-filter coefficients

The energy emerging at different decomposition levels is dependent on the magnitude of the wavelet filter coefficients, therefore, the optimization of the magnitude of the wavelet filter coefficients is needed to emerge the optimum energy in the detail signal corresponding to the frequency band of the QRS complexes.

(iv) Detection of QRS at the extreme of data segment

The use of wavelet with finite support avoids the difficulty in the detection of QRS complexes falling in the extreme of ECG data array.

The performance evaluation for the different wavelets, given in Table 3.1, has been carried out using the CSE DS-3 database. The results are given in Table 3.2. Among the five existing and a new wavelets, given Table 3.1, QSWT and WT6 have been found to be the best suitable wavelets for QRS detection, as they give a higher rate of QRS detection. For further analysis, we used the quadratic spline wavelet. The QSWT has two high pass filter coefficients, namely -2.0 and +2.0, which are high in magnitude and are on either side of the reference line (zero crossing). These two high magnitude coefficients help to emerge modulus maxima lines corresponding to ECG samples, particularly from the QRS complexes, which also have samples on either side of the reference line. It is also observed that the use of the QSWT to detect P and T waves by extracting detail signals at higher scales 2^3 or $> 2^3$, gives more cases of failure, as the detail signals get affected by base line wander and low frequency noise. Also there are a larger number of modulus maxima lines and these create difficulty in the distinction of P and T waves. The Daubechies six coefficient (DU6) wavelet has been found to be more successful in detection of P and T wave segments. Its moderate filter length and moderate coefficient values, compared to the other listed wavelets, provide more smoothing and less shift in the ECG fiducials.

Table 3.1 Details of wavelet filters analysed for QRS detection

Wavelet No.	Lowpass h(n)/ Highpass g(n) Filters	Wavelet filter coefficients	Reference
WT1	H(n) G(n)	=0.160102,0.603829,0.724309,0.138428, -0.242295,-0.032245,0.077571,-0.006241, -0.012581,0.003336 = $(-1)^n h(L-1-n)$	F.Yang et.al[153] Daubechies WT
WT2	H(n) G(n)	=0.035226,-0.085441,-0.135011,0.459878, 0.806892,0.332671 = $(-1)^n h(L-1-n)$	M.L.Hilton[47] Daubechies WT
WT3	H(n) G(n)	=0.125,0.375,0.375,0.125 =-2.0,2.0	B.C.B.Chan et.al.[25] Qaudratic Spline WT
WT4	H(n) G(n)	= -0.176777,0.353553,1.060660,0.353553, -0.176777 = 0.707107,0.353553	M.L.Hilton[47]
WT5	H(n) G(n)	=0.707107,0.707107 = $(-1)^n h(L-1-n)$	M.L.Hilton[47]
WT6	H(n) G(n)	=0.25,0.5,0.25 = $(-1)^n h(L-1-n)$	New Wavelet

L – filter length

Table 3.2 QRS detection performance of six wavelets
(using first 25 records of CSE DS-3 database)

Record No.	No. of QRS present	WT1	WT2	WT3	WT4	WT5	WT6 New
01	132	132	132	132	164*	132	132
02	228	228	228	228	228	226*	228
03	204	204	204	204	261*	204	204
04	144	144	144	144	144	144	144
05	192	192	192	192	192	192	192
06	180	180	180	180	180	180	180
07	201	201	200*	201	201	200*	201
08	120	120	118*	120	120	120	120*
09	144	143*	144	144	182*	144	144
10	072	072	072	072	072	072	072
11	168	168	168	168	182*	168	168
12	156	156	156	158*	183*	156	156
13	144	144	144	144	144	144	144
14	096	096	096	096	126*	096	096
15	084	072*	072*	083*	083*	082*	083*
16	192	192	186*	192	208*	192	190*
17	120	120	120	120	120	120	120
18	156	156	156	156	156	156	156
19	156	156	156	156	156	156	156
20	264	252*	260*	264	264	264	264
21	096	094*	094*	096	164*	090*	095*
22	144	144	144	144	174*	144	144
23	096	090*	092*	096	100*	096	096
24	120	120	120	120	243*	120	120
25	108	108	108	108	108	108	108
Total	3717	3684	3686	3718	4155	3706	3707
Rate of QRS Detection (%)		99.11	99.16	99.91	88.18	99.70	99.89

* indicates the error in QRS detection

Rate of QRS detection = (actual-failed)/ (actual)

3.5 QRS DETECTION USING EXISTING WAVELETS

Algorithm

After the selection of a suitable wavelet for the detection of QRS complexes, the procedure described above (section-3.3.1) is used to implement the WT representation. In the present work, the QRS complex has been detected by six wavelets, five existing ones WT1-WT5 and one newly developed WT6 given in Table-3.1. Firstly, the WT1 has been selected to observe the performance. The steps are explained in the Fig.3.1. The signal decomposition scheme, shown in Fig.3.1, splits the ECG signal $x(n)$ sampled at 500 Hz into different detail signals $d^1, d^2, d^3,$ and d^4 at scales 2^j ; $j = 0, 1, 2,$ and $3,$ respectively. The WT of signal $x(n)$ at scale 2^j is a filtered signal of $x(n)$ that passes through a digital band pass filter (or high pass filter for scale 2^j). This process of splitting a discrete signal $x(n), (n=0, \dots, N-1)$ by DWT decomposes $x(n)$ into a set of detail signals.

$$d^1 (n=0, \dots, N-1), d^2 (n=0, \dots, (N/2)-1), d^3 (n=0, \dots, (N/2^2)-1),$$

$$d^4 (n=0, \dots, (N/2^3)-1),$$

and one low resolution signal

$$a^j = (n=0, \dots, (N/2^j)-1).$$

Where, N is the number of samples and j is the decomposition scale.

The nature of these detail signals for WT1 is shown in Fig. 3.2, which indicates the gradual increase in energies of QRS complexes from low scale 2^0 to higher scale 2^4 . The detection of QRS complexes has been carried out by using detail signal d^4 . The detail signal d^4 , as shown in Fig. 3.2(e), is used to perform the detection of QRS complex fiducial points by amplitude threshold of 0.5ϵ , where ϵ is the adaptive threshold parameter. The value of ϵ is determined by scanning the first ECG cycle and by updating the threshold value ϵ as per the signal amplitude using the equation

$$\epsilon = \max(d^j[k]), \quad 60(n-1) < k < 60n, j=4$$

where, $n = 1, 2, \dots, N/60$, and represents the number of ECG cycles and 60 represents the number of samples per cycle in the d^4 signal. N is the number of samples in detail signal d^4 and $d^j[k]$ are the detail signal samples at scale 2^j .

The absolute value of d^4 has been used to detect the QRS peak by using the threshold of 0.5ϵ (i.e. 50% of max. amplitude of d^4). This is equivalent to using +ve as well as -ve thresholds. The detection of R or S peak of QRS complex was carried out by the equation.

$$S[j] = k, \text{ if } |d^4[k]| \geq 0.5\epsilon$$

where, $S[j]$ represents the QRS complex fiducial locations.

To avoid the detection of more than one QRS complex fiducial from the same QRS segment,

after detecting first fiducial QRS from a QRS complex, a window equivalent to 100 ms is skipped in d^4 signal.

After detecting QRS locations in d^4 and by considering the phase shift as detailed in Table-3.3, the original ECG signal $x(n)$ is scanned at all the detected QRS fiducials by scanning a window of 50 ms on either side of detected QRS location to detect the real peak location and its amplitude as shown in Table-3.4. The detected locations are indicated by an asterisk (*) in Fig. 3.2. After detecting QRS locations, effort is made to detect QRS -onsets and -offsets using all the wavelets.

3.5.1 Test results with existing wavelets

In this study, the detection of QRS complexes by different wavelets has been carried using standard 12 lead ECGs of first 25 records of CSE DS-3. In all, 3717 number of beats of 300 ECGs (25 records x 12 leads) with wide morphologies have been analyzed. It has been found that even with the wide variability of ECG morphologies, the detection of QRS complex has been carried out accurately. The details of success and failure in QRS detection by different wavelets are given in Table-3.2 and the QRS detection by all wavelets in a record are demonstrated in the Fig. 3.3.

The first wavelet WT1 having high and low pass filter coefficients, gives QRS detection rate of 99.11%. The performance of WT2 is similar to WT1 and gives QRS detection rate of 99.16. These long filter length wavelets usually fail to detect QRS complex, if it present at the start or end of data as shown in Fig.3.4. The compact wavelet WT3 is computationally simple, faces less difficulty in detecting the end point QRS complexes, and gives high detection rate of 99.91%. The fourth wavelet WT4 faces difficulty in detecting QRS complex when the signal amplitude is low, and gives QRS detection rate of 88.18%. The WT5 is computationally suitable for detection of end point QRS complexes, and gives detection rate of 99.70%.

3.6 CONSTRUCTION OF NEW WAVELET

After studying the effect of wavelets on ECG signal and its QRS detection as discussed in section-3.5, the ability of some other wavelets to know their effectiveness on ECG signal and to detect QRS complex has been carried out. Results of QRS detection with different wavelets are listed in Table-3.2. The experience and knowledge obtained from this evaluation was then used to construct a new wavelet given in the following section.

Table 3.3 Detection of QRS peak amplitude and location in d^4 signal by six wavelets (Using CSE DS-3 Record No. MA-001.DCD.)

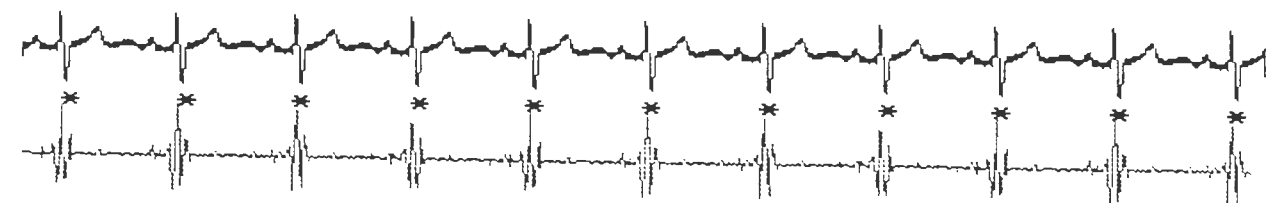
Lead No	Original Amp/ Loc	WT1	WT2	WT3	WT4	WT5	WT6 New
1L1	0.370 158	0.386 160(2)	0.357 160(2)	0.428 160(2)	0.2498 168(10)	0.505 168(10)	1.053 160(2)
1L2	0.512 151	0.666 152(1)	0.658 152(1)	0.823 152(1)	0.441 160(9)	0.884 160(9)	1.907 152(1)
1L3	0.355 151	0.811 152(1)	0.742 152(1)	0.905 152(1)	0.662 144(7)	0.907 160(9)	2.113 152(1)
1aVR	0.195 176	0.150 176(0)	0.272 176(0)	0.281 184(8)	0.204 178(2)	0.292 184(8)	0.822 176(0)
1aVL	0.448 164	0.442 160(4)	0.470 160(4)	0.582 168(4)	0.337 168(4)	0.630 176(12)	1.234 168(4)
1aVF	0.434 151	0.737 152(1)	0.697 152(1)	0.865 152(1)	0.533 152(1)	0.896 160(9)	2.007 152(1)
1V1	1.013 177	1.115 176(1)	0.940 176(1)	0.654 176(1)	0.244 176(1)	0.920 184(7)	2.435 176(1)
1V2	1.537 157	1.417 160(3)	1.348 160(3)	1.225 160(3)	0.810 152(5)	1.644 160(3)	3.689 160(3)
1V3	1.107 157	1.592 160(3)	1.464 160(3)	1.508 160(3)	1.025 152(5)	1.573 160(3)	4.131 160(3)
1V4	1.102 156	1.162 160(4)	1.006 160(4)	1.304 160(4)	0.728 152(4)	1.427 160(4)	3.006 160(4)
1V5	0.570 154	0.608 160(6)	0.521 152(2)	0.899 160(6)	0.640 160(6)	0.983 160(6)	1.568 152(2)
1V6	0.146 152	0.342 152(0)	0.382 152(0)	0.615 160(8)	0.642 160(8)	0.659 168(16)	1.121 152(0)

Figures in brackets show shift in QRS location (detected in d^4) from the real.
 Loc: Location in samples Amp: Amplitude in mV

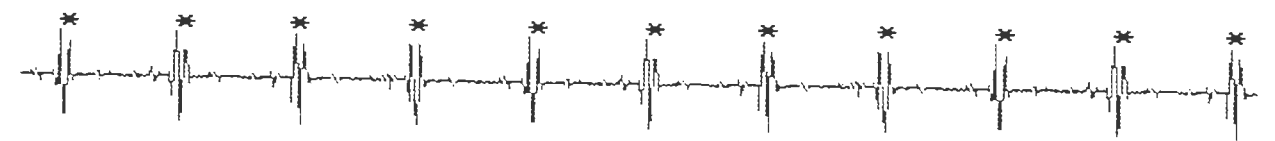
Table 3.4 Detection of QRS peak amplitude and location by mapping the detected locations in d^4 with original ECG signal (MA-001.DCD)

L ead No.	Original	WT1	WT2	WT3	WT4	WT5	WT6
1L1	0.370 158	0.370 158	0.370 158	0.370 158	0.370 158	0.370 158	0.370 158
1L2	0.512 151	0.512 151	0.512 151	0.512 151	0.512 151	0.512 151	0.512 151
1L3	0.355 151	0.355 151	0.355 151	0.355 151	0.355 151	0.355 151	0.355 151
1aVR	0.195 176	0.207 177	0.207 177	0.207 177	0.207 177	0.207 177	0.207 177
1aVL	0.448 164	0.448 164	0.448 164	0.448 164	0.448 164	0.448 164	0.448 164
1aVF	0.434 151	0.434 151	0.434 151	0.434 151	0.434 151	0.434 151	0.434 151
1V1	1.013 177	1.013 177	1.013 177	1.013 177	1.013 177	1.013 177	1.013 177
1V2	1.537 157	1.537 157	1.537 157	1.537 157	1.537 157	1.537 157	1.537 157
1V3	1.107 157	1.107 157	1.107 157	1.107 157	1.107 157	1.107 157	1.107 157
1V4	1.102 156	1.102 156	1.102 156	1.102 156	1.102 156	1.102 156	1.102 156
1V5	0.570 154	0.570 154	0.570 154	0.570 154	0.570 154	0.570 154	0.570 154
1V6	0.146 152	0.146 152	0.146 152	0.146 152	0.146 152	0.146 152	0.146 152

Original Signal



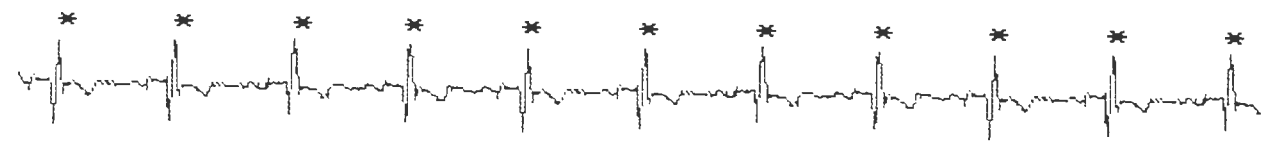
WT1



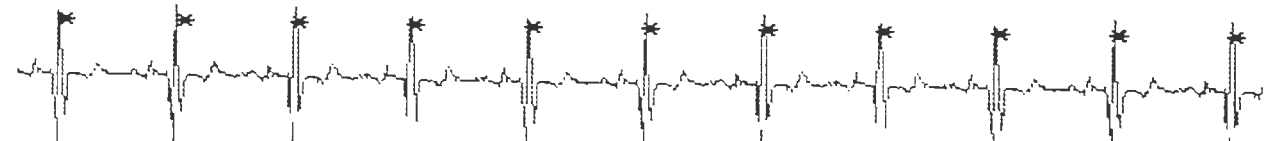
WT2



WT3



WT4



WT5



WT6 (best)

Fig.3.3 Normal ECG and accurate detection of QRS segments by six WTs
(Record No. MA-001.DCD, lead I)

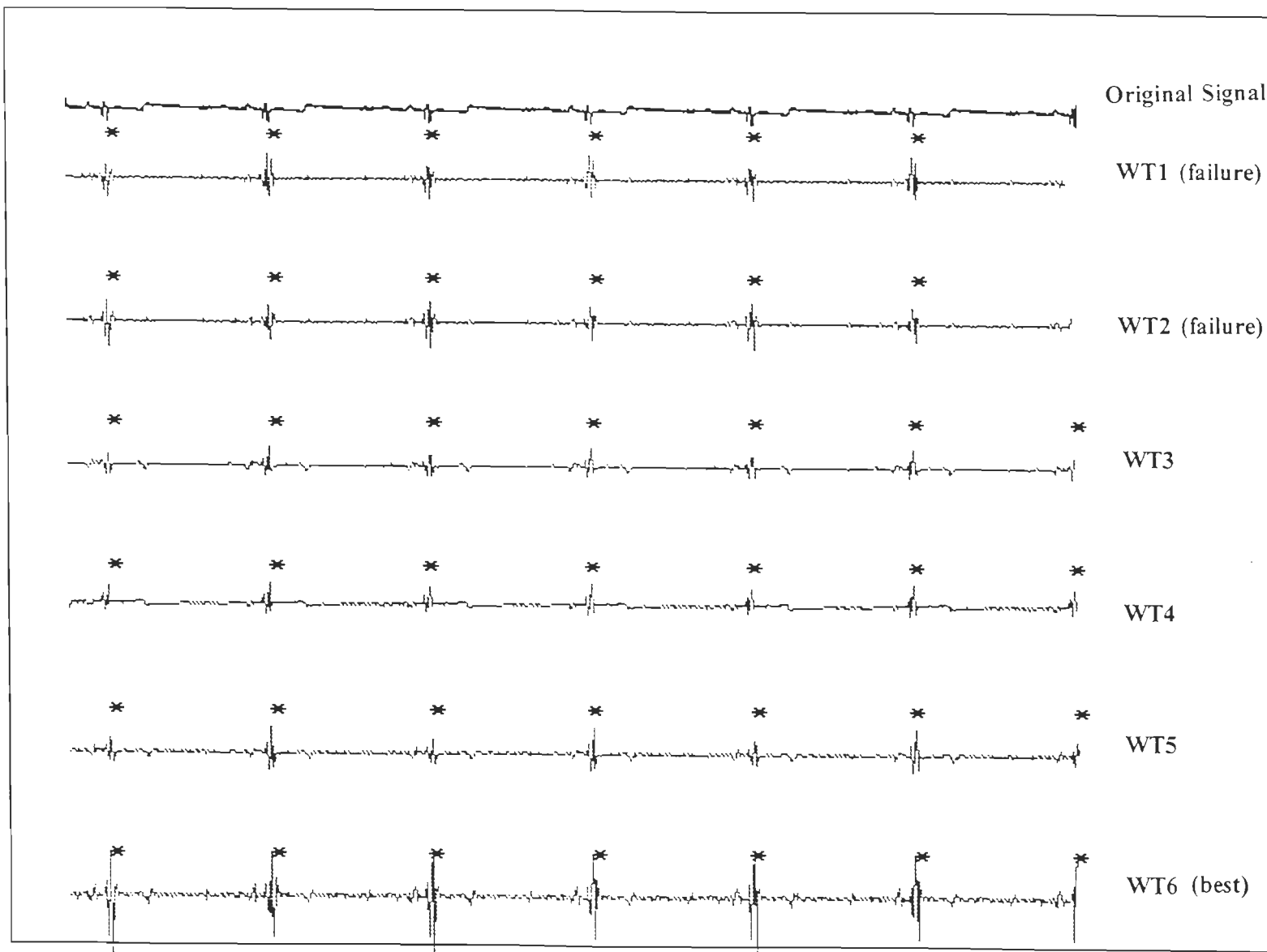


Fig.3.4 Small amplitude ECG with QRS segment present at extreme of data
(Record No. MA-015.DCD₃ lead aL)

3.6.1 Construction

After an exhaustive performance evaluation of existing five wavelets (WT1-WT5) and also by keeping in view the selection guidelines for wavelets, a new wavelet has been constructed for the detection of QRS complexes. This new constructed wavelet is named as WT6. The WT6, as given in Table-3.1, satisfies the requirements of having symmetric compact support with the scaling function of QRS complex shape. This has three low and three high pass filter coefficients and these coefficients are optimized by carrying out tests on large number of the ECG data for the detection of QRS complexes. The final values of coefficients are 0.25, 0.5, 0.25 for low pass filter and -0.25, 0.5, -0.25 for high pass filter. It is observed that if the two extreme coefficients out of three are half in magnitude to middle one then the performance to detect the QRS complex is optimum. This is due to similar characteristic of QRS complex i.e. approximately Q and S being 20-50% of R-wave and three coefficients which are in the form of three consecutive peaks like the three consecutive peaks of Q-R-S complex. The QRS complex rate achieved by using WT6 is the second best (next to QSWT). The detection rate is 99.89% because of the concept that a good wavelet is the one, which has the shape of scaling function similar to QRS complex in the ECG signal. This is also supported by its symmetry and less number of computations.

3.6.2 Test Results

In this work, the CSE DS-3 multi-lead and the MIT/BIH database have been used to evaluate the performance of the software. The CSE database contains ECG recordings of 15 leads recorded simultaneously from 125 patients at 500 Hz for 8-10 seconds. The CSE working party has constructed a multi-lead artificial (MA) series database from multilead original (MO) series database by selecting a section of beats from all the 15 leads of the MO series [147].

To study and analyse the effects of WTs on amplitude and phase shifts, first ECG cycle of CSE DS-3 record No. MA-001.DCD has been used and details of the measurements are given in the Tables 3.3 and 3.4. Table-3.3 shows the comparison of locations measured by wavelets with the real locations of first QRS segment. These measurements of Table-3.3 are carried out using d^4 signal of all the six wavelets, hence, according to the wavelet filter lengths and the magnitude of filter coefficients, the measurements show shifts in QRS locations. The QRS location shifts measured by different wavelets are shown in brackets in Table-3.3. The cases of failure shown in Table 3.3 for WT4 are due to its two positive high pass filter coefficients, which are less effective in reducing the baseline wander. To measure

exact QRS locations, the fiducial locations measured using d^4 signal (Table 3.3) are mapped with original ECG signal. The results of this mapping are given in Table-3.4. In all measurements, the QRS locations and amplitudes measured by wavelets are leadwise same, for example in lead I, QRS location and amplitude measured after mapping by all the wavelets is 0.37 mV at 158th sample number.

The QRS detection performance of all the wavelets is shown in the Figs. (3.3-3.7). In Fig.3.3, a normal ECG is shown with the detection of QRS complex by all the six wavelets. It is observed that there is no failure by any of the six wavelets (WT1-WT6), but the QRS energies extracted out of the original ECG signal by different wavelets are different. It can be observed that more is the energy with low amplitude signal, and thereby, better is the performance of detection. The energy extracted by new wavelets is moderate (as per the amplitude of ECG signal) compared to other wavelets.

Some special cases are considered in Figs.3.5-3.7. Fig.3.4 shows the failure of the wavelets (WT1-WT2) due to long filter length. It can be seen that the last beat of the ECG is not being detected due to more number of coefficients. Fig.3.5 shows a signal, in which, it is very difficult to detect QRS segments as it is noisy with high P and T and low QRS segment. The major failure of WT4 is found due to non-concentrated extraction of modulus maxima lines corresponding to real QRS segments and is because of two positive high pass filter coefficients (Table -3.1).

Fig.3.6 is another typical example, wherein, basic concept of splitting ECG signal to detect QRS usually fails because it contains some other non-QRS complexes of same frequency which also emerge with the QRS complexes in d^4 signal. The possible failure is reduced by skipping the portion of ECG for 100 ms after the detection of a fiducial from the QRS segment. Even with this precaution, the failure has occurred with WT4.

A record with high frequency noise (noisy spikes) is shown in Fig.3.7. The better performance of new wavelet is observed in this case. It gives very clear extraction of QRS segment with the optimized modulus maxima lines. This is also observed in all the cases shown in Figures 3.3-3.7, where use of WT6 gives very clear moderate energy extraction of QRS complex.

3.7 DISCUSSIONS

From the analysis of results given in Table-3.3, it can be stated that the use of WT1, WT2, WT3, WT5 and WT6 gave approximately the same QRS location when measured in detail signal d^4 . The performance of the new wavelet WT6 is comparable to that of WT3

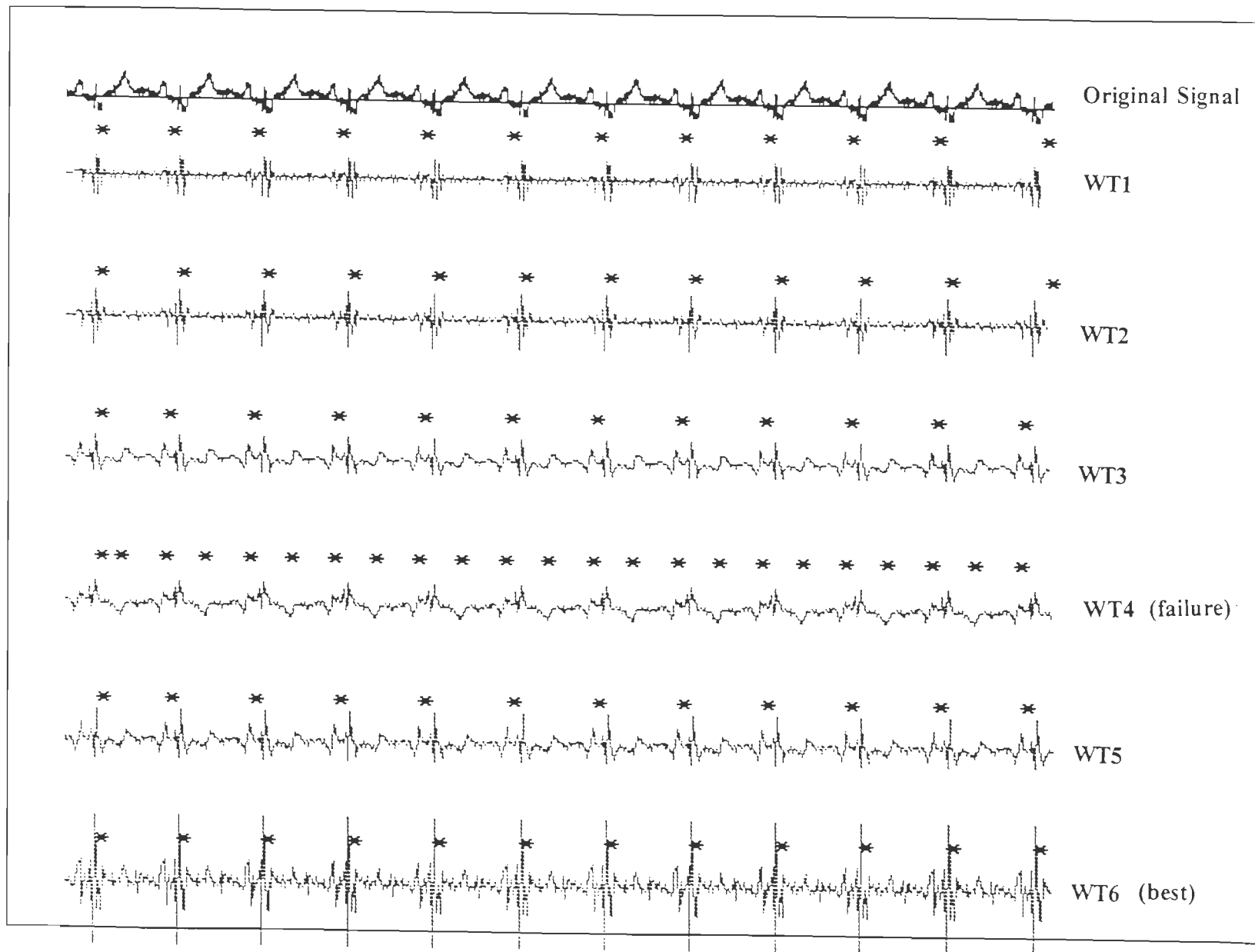


Fig.3.5 Typical ECG with high P and T waves
(Record No. MA-009.DCD, lead II)

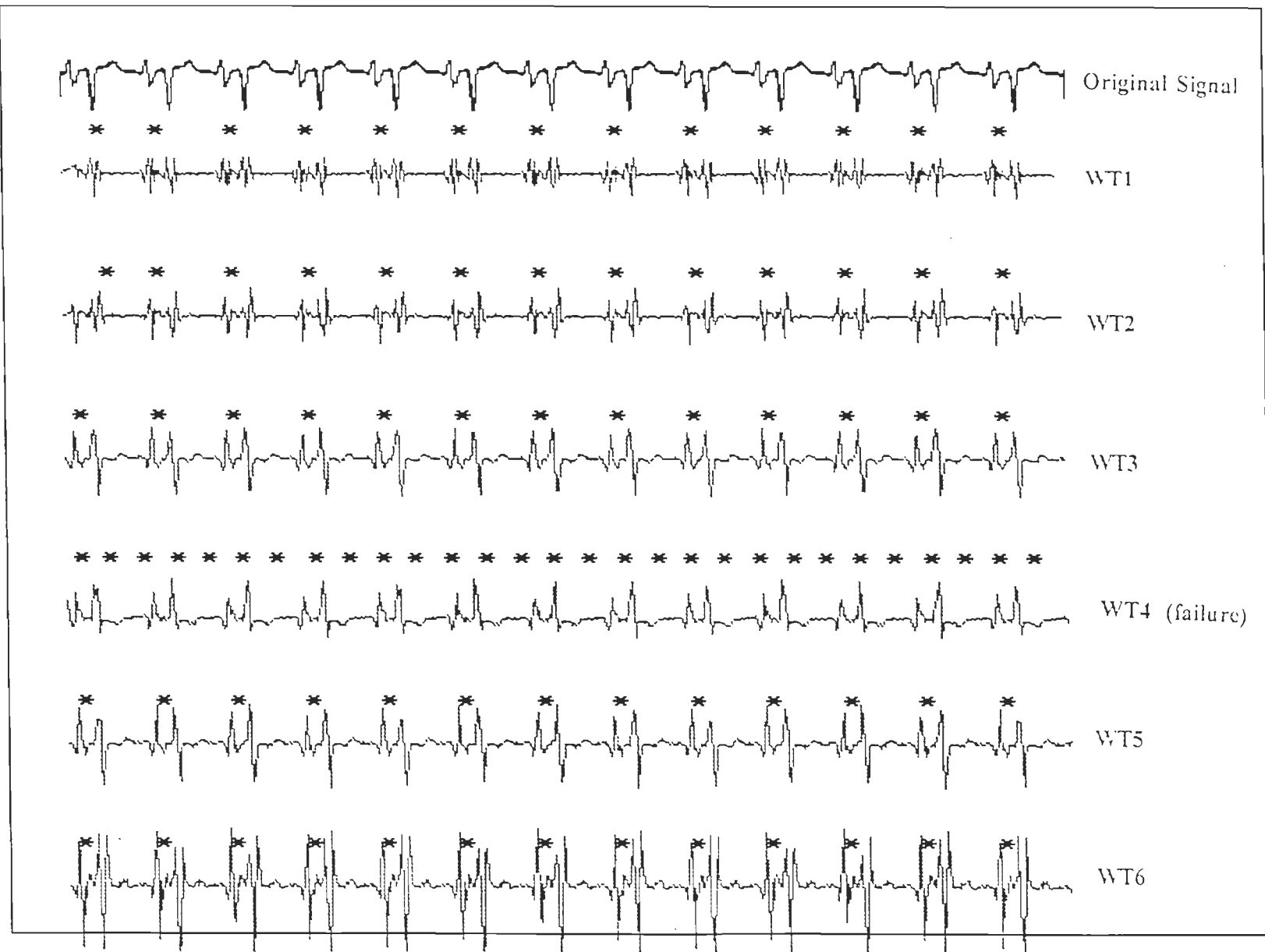


Fig.3.6 ECG with like QRS segments having same frequency
(Record No. MA-012.DCD, lead V1)

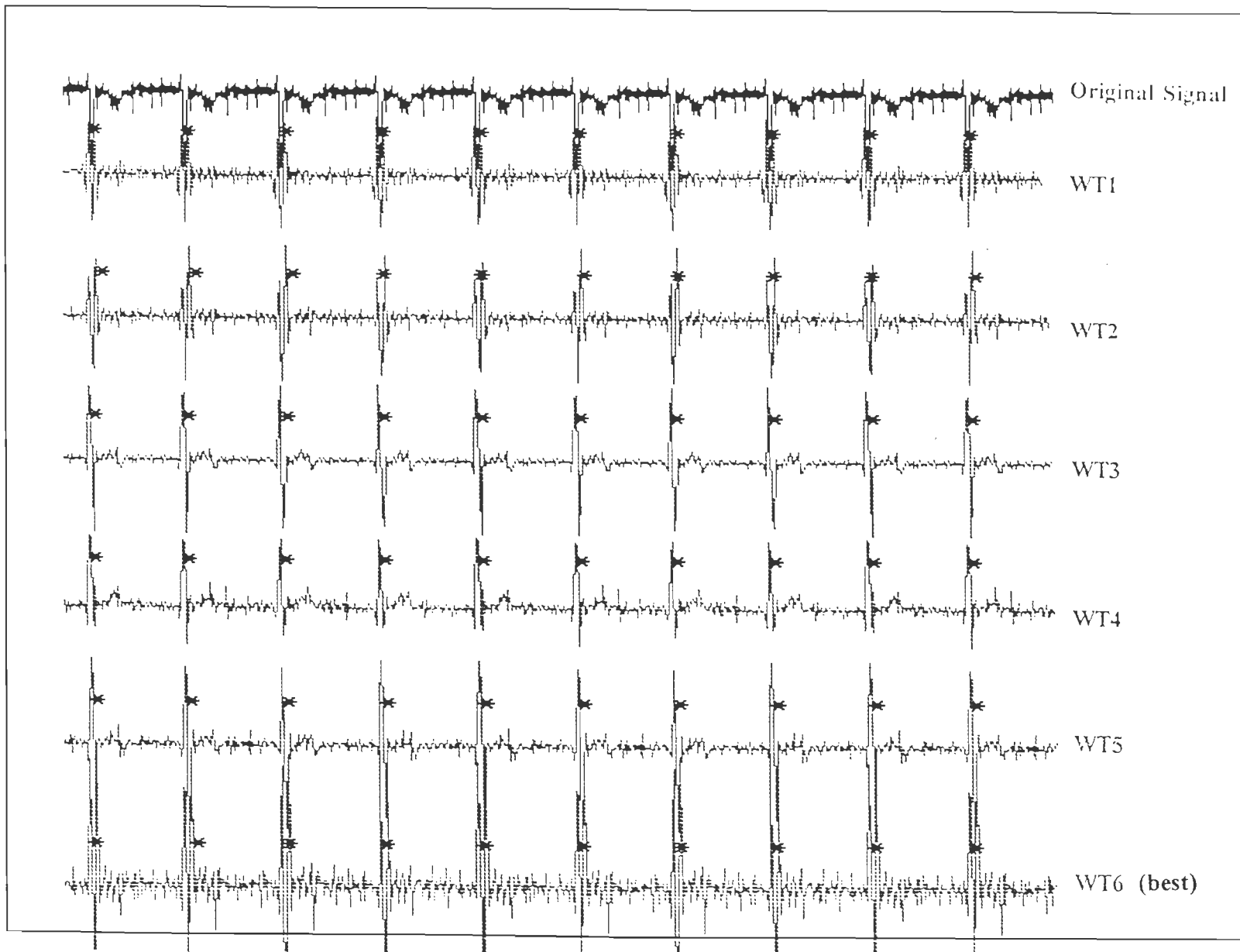


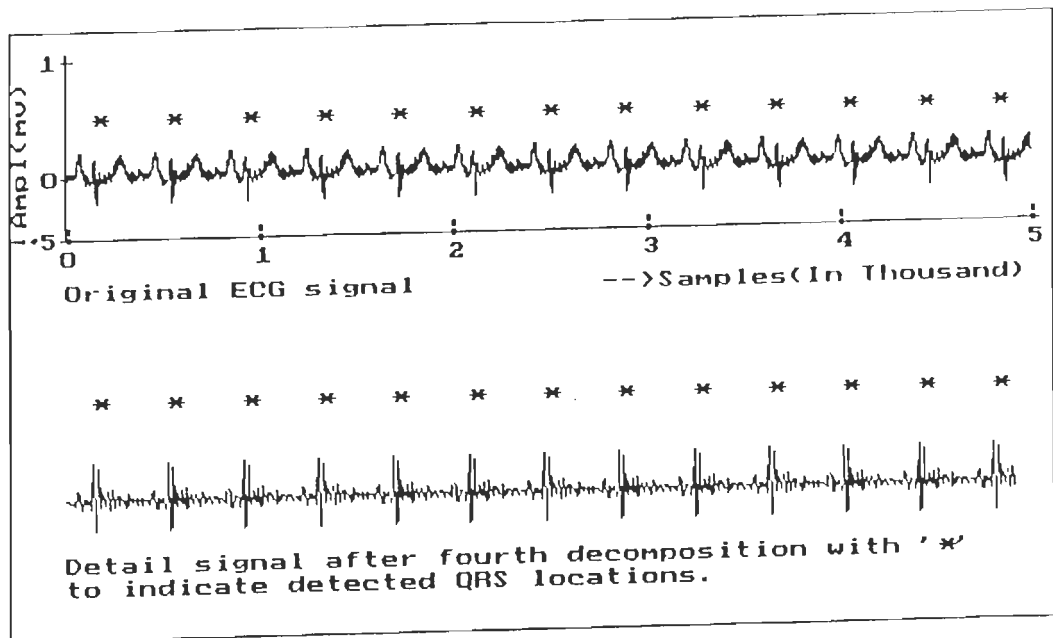
Fig.3.7 ECG with high frequency noise
(Record No. MA-120.DCD, lead II)

which gives the highest rate of QRS detection. This is due to its compact support and the required shape of scaling function for QRS detection. Hence, these two wavelets are found suitable for the detection of QRS complex.

After this analysis and the confirmation that the QSWT and WT6 are the suitable wavelets for QRS detection, it is observed that even with the wide variety of ECG morphologies and with noise and artifacts, the software detects QRS complexes in all (125 records) except 3 records accurately, when scanned by quadratic spline wavelet.

Fig.3.8 shows ECG record number MA-032.DCD lead aVF of CSE DS-3 and the detail signal extracted at the fourth decomposition with the scale 2^3 . Even with high amplitude P and T waves, the detail signal emerges with modulus maxima lines accurately corresponding to QRS locations in the original ECG signal. The QRS fiducials are detected by adaptive amplitude threshold. To observe the correctness, detected QRS locations are indicated by asterisks '*' on the original, as well as the detail signal. In a record length of 5000 samples, the software detects all 13 QRS complexes. The detected QRS locations and their amplitudes are shown in the Table 3.5. Fig.3.9 shows CSE DS-3 record number MA-108.DCD lead V3, which exhibits an unusual morphology with depressed large amplitude T waves, low amplitude QRS complexes and shift in the baseline. Other algorithms fail to detect QRS fiducials in such types of signals. As can be seen in Fig.3.9, this algorithm detects all 16 QRS complexes correctly, indicated by asterisks in the figure. The locations and amplitudes are shown in Table 3.6.

ECG records from the MIT/BIH Arrhythmia database have also been used to evaluate the performance of algorithm. Figs.3.10 and 3.11 show the original ECG signals with their corresponding detail signals extracted by taking the WT of the ECG signals with scale 2^3 . Fig.3.10 shows an ECG with high QRS amplitude and drift in the baseline. Fig.3.11 shows ECG having irregular beats with positive and negative QRS peaks. It can be seen in the figures that even with variable heart rate, with +ve or -ve QRS peaks, the software detects all QRS complexes correctly. Table 3.7 shows locations and amplitudes of the 17 detected QRS fiducials of record 100. Table 3.8 shows 21 QRS fiducials with positive and negative QRS peaks from record 200. Fig.3.12 shows the exceptional cases of ECG signals with the accurate detection of the QRS complexes in the presence of noise and artifacts using the MIT/BIH database. Fig.3.13 shows the false positive detection of the QRS complexes due to noise present in the frequency band of QRS complexes. The noise components emerged in d^4 signal as modulus maxima lines caused failure.

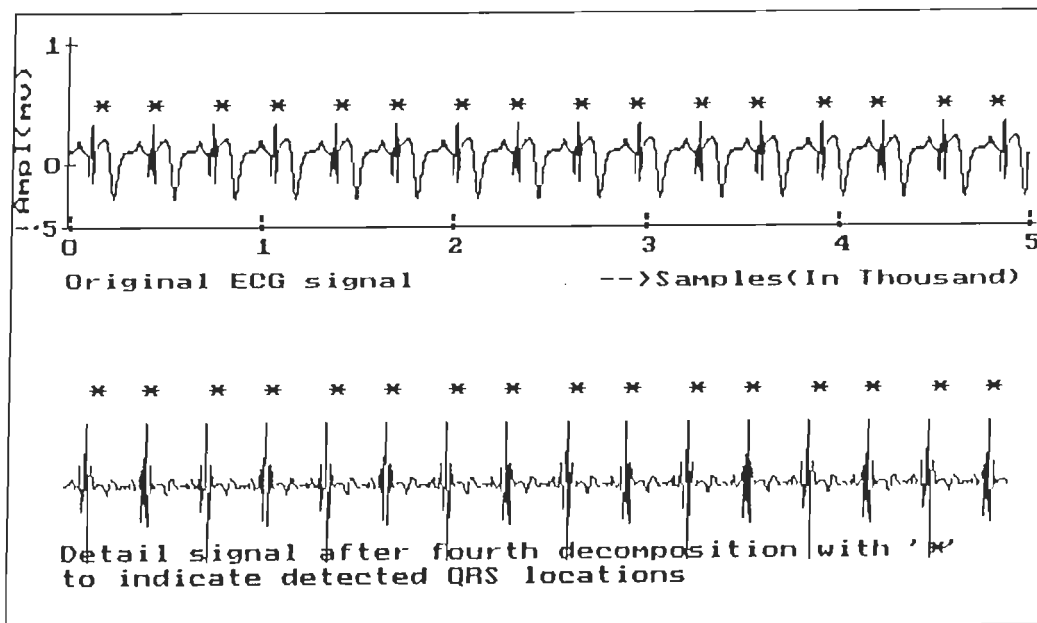


Record: MA-32.DCD, lead aF.

Fig.3.8 QRS detection in high amplitude P and T waves ECG using QSWT

Table 3.5 WT Based QRS Detection
(Record MA-032.DCD, Lead aF)

Sr. No.	Sample No.	QRS peak (mv)
1	169	-0.268
2	561	-0.268
3	953	-0.268
4	1345	-0.268
5	1737	-0.268
6	2129	-0.268
7	2521	-0.268
8	2913	-0.268
9	3305	-0.268
10	3697	-0.268
11	4089	-0.268
12	4481	-0.268
13	4873	-0.268

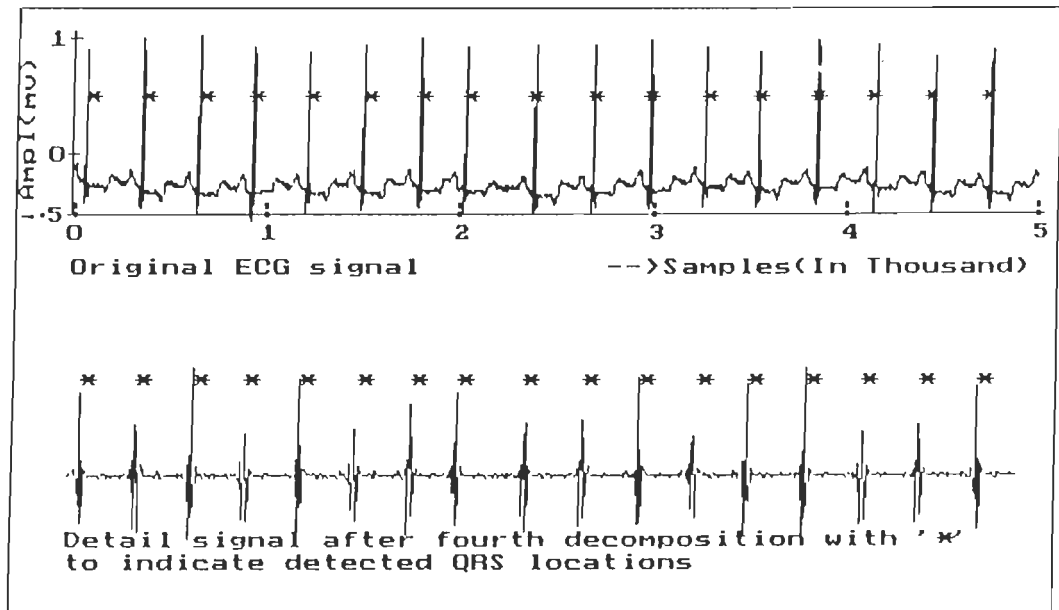


Record: MA-108.DCD, lead V3.

Fig.3.9 QRS detection in inverted T wave ECG using QSWT

Table 3.6 WT Based QRS Detection
(Record MA-108.DCD,Lead V3)

Sr. No.	Sample No.	QRS peak (mV)
1	132	0.290
2	448	0.290
3	764	0.290
4	1080	0.290
5	1396	0.290
6	1712	0.290
7	2028	0.290
8	2344	0.290
9	2660	0.290
10	2976	0.290
11	3292	0.290
12	3608	0.290
13	3924	0.290
14	4240	0.290
15	4556	0.290
16	4872	0.290

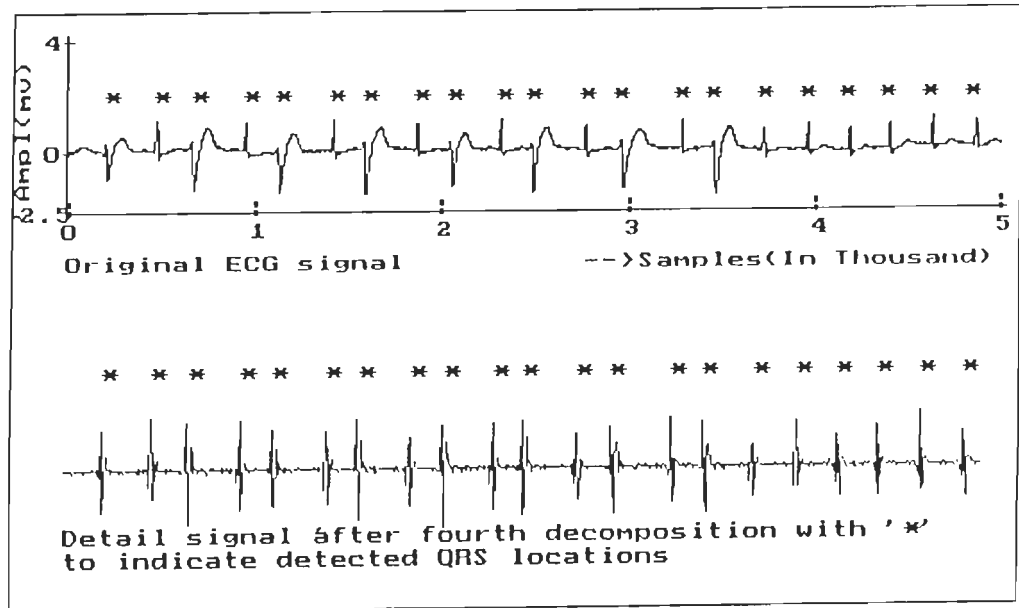


Record: MIT/BIH-100.dat

Fig.3.10 Sample record of MIT/BIH database

Table 3.7 WT Based QRS Detection
(Record MIT/BIH 100)

Sr. No.	Sample No.	QRS peak (mv)
1	77	0.840
2	370	0.940
3	663	0.960
4	947	0.860
5	1231	0.820
6	1515	0.885
7	1809	0.945
8	2045	0.875
9	2403	0.885
10	2706	0.890
11	2998	0.925
12	3283	0.865
13	3560	0.835
14	3863	0.935
15	4171	0.890
16	4466	0.795
17	4765	0.850



Record: MIT/BIH-200.dat

Fig.3.11 Sample record of MIT/BIH database

Table 3.8 WT Based QRS Detection
(Record MIT/BIH 200)

Sr. No.	Sample No.	QRS peak (mV)
1	224	-1.505
2	488	1.110
3	689	-2.010
4	965	1.025
5	1147	-2.080
6	1434	1.115
7	1608	-2.135
8	1883	0.945
9	2072	-1.915
10	2332	1.155
11	2504	-2.175
12	2786	0.855
13	2988	-1.965
14	3302	1.030
15	3748	0.650
17	3976	0.790
18	4201	0.665
19	4417	0.870
20	4647	1.125
21	4880	0.960

The developed software has the facility to detect QRS complexes on all standard 12 leads in a single execution. Table 3.9 shows the results of QRS detection of record MA-010.DCD of CSE DS-3. This record has 72 QRS complexes (6*12 leads) and software detects all these complexes. Table 3.9 shows their fiducial position and amplitude for each detected QRS complex. For this particular case, the rate of QRS detection is 100% as all 72 QRS complexes of record MA-010.DCD get detected. The accuracy in the amplitude measurements in 69 QRS complexes is 100%, but in 3 complexes, as there has been a wrong mapping of reference QRS complexes (d^4 signal) with the real QRS complexes (original signal), there is an error of 0.58 mV (25.43%). This case is of a very wide QRS complex (about 85 samples), which emerged more number of modulus maxima lines, hence in 3 beats the reference QRS complexes have not mapped correctly with the QRS peaks in the original signal.

Tables 3.10 and 3.11 show the summary of results of QRS detection using the CSE and the MIT/BIH databases, respectively. As shown in the tables, the detection rates of QRS complexes are 99.866% using the CSE database and 99.806% using the MIT/BIH database by the quadratic spline wavelet. The sensitivity of QRS detection using the CSE DS-3 database is 100% and using the MIT/BIH database is 99.904%.

There are some typical ECG signals, where most of the QRS detection methods fail to detect QRS complexes. The ECG waveform shown in Fig.3.9 of CSE DS-3 has high P and T wave segments compared to the QRS complex, and the one shown in Fig.3.9 has large amplitude inverted T wave segments. With such ECGs, QRS detection methods based on amplitude threshold, squaring or slope criteria, or AN network fail, as these work on the criteria of amplitude-error-detection [45,104,127,135].

The other two typical ECG records of MIT/BIH database are shown in Figs.3.10 and 3.11. Fig.3.10 shows high amplitude QRS complexes with baseline wander and Fig. 3.11 shows irregular beats with positive and negative QRS peaks. In such cases, methods, which scan a fixed window width to detect the QRS complexes, and the methods which use decision rules like zero crossing fail due to consecutive Q-R-S peaks. Also in pattern recognition based detection of QRS complexes, the ECG signal is first reduced into a set of elementary patterns like peaks, durations, slopes, and interwave segments, and thereafter, using rule based grammar, the signal is represented as a composite entity of peaks, durations, slopes and interwave segments. These patterns are then used to detect the QRS complexes in the ECG signal. This category methods are time consuming and require inference grammar in each step of execution for detection of QRS complexes [93]. The comparative results of QRS

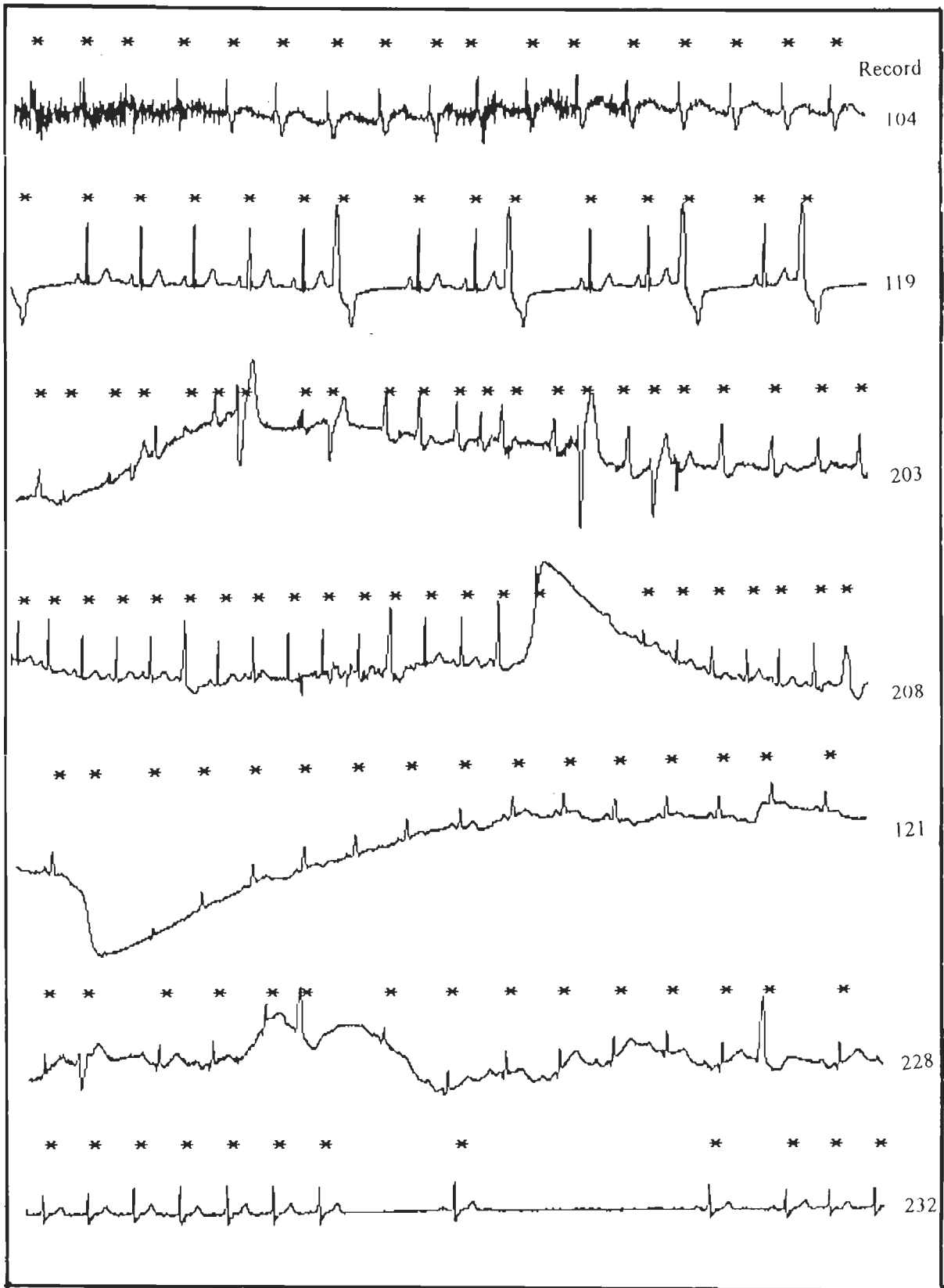


Fig.3.12 Detection of QRS complexes using the MIT / BIH database

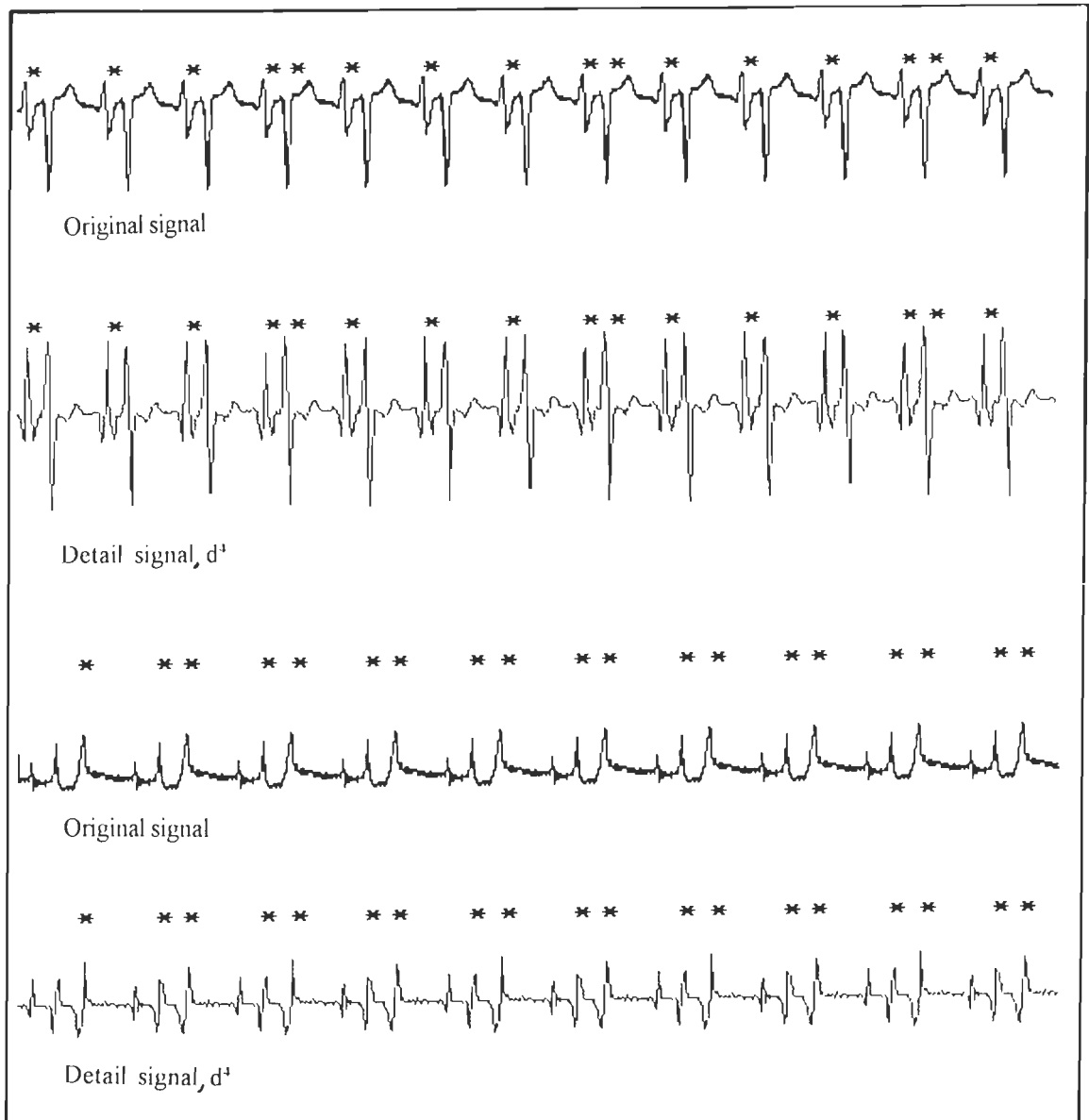


Fig.3.13 False positive detection of QRS complexes using the CSE database

Table 3.9 WT based QRS detection of record No. MA-010.DCD

Lead No.	No. of QRS	QRS - 1 Pos\Amp	QRS - 2 Pos\Amp	QRS - 3 Pos\Amp	QRS - 4 Pos\Amp	QRS - 5 Pos\Amp	QRS - 6 Pos\Amp
10L1	6	181 0.99	989 0.99	1797 0.99	2605 0.99	3413 0.99	4221 0.99
10L2	6	186 -2.90	994 -2.90	1802 -2.90	2610 -2.90	3418 -2.90	422 -2.90
10L3	6	184 -3.81	992 -3.81	1800 -3.81	2608 -3.81	3416 -3.81	4224 -3.81
10aVR	6	188 1.02	996 1.02	1804 1.02	2612 1.02	3420 1.02	4228 1.02
10aVL	6	182 2.40	990 2.40	1798 2.40	2606 2.40	3414 2.40	4222 2.40
10aVF	6	185 -3.34	993 -3.34	1801 -3.34	2609 -3.34	3417 -3.34	4225 -3.34
10V1	6	210 2.28	1018 2.28	1826 2.28	2616 1.70	3424 1.70	4232 1.70
10V2	6	185 3.30	993 3.30	1801 3.30	2609 3.30	3417 3.30	4225 3.30
10V3	6	185 3.80	993 3.80	1801 3.80	2609 3.80	3417 3.80	4225 3.80
10V4	6	185 3.99	993 3.99	1801 3.99	2609 3.99	3417 3.99	4225 3.99
10V5	6	181 2.59	989 2.59	1797 2.59	2605 2.59	3413 2.59	4221 2.59
10V6	6	179 1.67	987 1.67	1795 1.67	2603 1.67	3411 1.67	4219 1.67

Pos: Position in sample number Amp: Amplitude in mV

Table 3.10 Results of QRS detection by using quadratic spline wavelet
(records of the CSE DS-3, use of 12 leads)

Lead No.	Total no. of QRS complexes	QRS complexes detected	True positive (TP)	False positive (FP)	False Negative (FN)
I	1502	1507	1502	05	00
II	1502	1502	1502	00	00
III	1502	1502	1502	00	00
aVR	1502	1502	1502	00	00
aVL	1502	1502	1502	00	00
aVF	1502	1512	1502	10	00
V1	1502	1502	1502	00	00
V2	1502	1502	1502	00	00
V3	1502	1502	1502	00	00
V4	1502	1502	1502	00	00
V5	1502	1511	1502	09	00
V6	1502	1502	1502	00	00
Total	18024	18048	18024	24	00

Detection rate of QRS complexes – 99.866 %
(actual-failed)/(actual)

Percentage of false detection = 00.133 %

Sensitivity of QRS detection = 100.00%
Sensitivity = TP / (TP+FN)

Table 3.11 Results of QRS detection for the MIT/BIH database

Record No.	Total beats	Detected QRS	TP	FP	FN
100	2141	2142	2141	01	00
101	1735	1735	1735	00	00
102	2069	2069	2069	00	00
103	1952	1951	1951	00	01
104	2113	2111	2111	00	02
105	2428	2415	2408	07	20
106	1890	1890	1890	00	00
107	2044	2044	2044	00	00
108	1669	1673	1669	04	00
109	2402	2402	2402	00	00
111	2019	2019	2019	00	00
112	2399	2399	2399	00	00
113	1706	1706	1706	00	00
114	1772	1750	1750	00	22
115	1815	1815	1815	00	00
116	2221	2221	2221	00	00
117	1459	1459	1459	00	00
118	2143	2143	2143	00	00
119	1863	1863	1863	00	00
121	1732	1732	1732	00	00
122	2344	2344	2344	00	00
123	1390	1390	1390	00	00
124	1486	1486	1486	00	00
200	2431	2424	2424	00	07
201	1949	1970	1949	21	00
202	2024	2032	2024	08	00
203	2871	2868	2868	00	03
205	2526	2526	2526	00	00
207	1950	1960	1943	17	07
208	2837	2834	2834	00	03
209	2869	2869	2869	00	00
210	2514	2516	2511	05	03
212	2620	2620	2620	00	00
213	3112	3112	3112	00	00
214	2136	2138	2136	02	00
215	3231	3231	3231	00	00
217	2105	2103	2103	00	02
219	2034	2043	2032	11	02
220	1887	1887	1887	00	00
221	2295	2295	2295	00	00
222	2337	2329	2326	03	11
223	2468	2467	2467	00	01
228	1920	1926	1909	17	11
230	2121	2121	2121	00	00
231	1503	1503	1503	00	00
232	1662	1668	1662	06	00
233	2945	2941	2941	00	04
234	2624	2624	2624	00	00
Totals	103763	103766	103664	102	99

Rate of QRS detection = 99.806%

Percentage of false detection = 00.193%

Sensitivity of QRS detection = 99.904%

Table 3.12 Comparison of ECG analysis results

Sr. No.	Method	Reference	Sensitivity / Rate of QRS detec.(%)	Type of data used
01	Template construction for QRS classification.	Tartakosky et.al.[132]	98.600 / ----	Their own database. (900000 beats)
02	A real-time QRS detection based upon digital analysis of slope, amplitude & width.	Pan et.al.[104]	99.761/ 99.300	24 h MIT/BIH arrhythmia database.
03	QRS detection using the optimised decision rule process	Hamilton et.al.[45]	99.690/ 99.461	MIT / BIH database. (109267 beats)
04	NN based adaptive matched filtering for QRS detection	Xuc et.al.[152]	---- / 99.500	MIT / BIH database. (record 105)
05	An approach to QRS detection using mathematical morphology.	Trahanias [136]	99.380/ ----	CSE DS-1 (1492 beats)
06	Detection of ECG characteristic points using wavelet transform.	Li et.al.[72]	99.904/ 99.847	MIT / BIH database. (116137 beats)
07	An integrated pattern recognition method.	Melhta et.al.[93]	----/ 99.830	CSE database.
08	QRS detection based on optimized prefiltering in conjunction with matched filter & dual edge threshold	Antti et.al.[8]	----/ 97.800	MIT/BIH database. (2572 beats)
09	Use of wavelet transform for ECG characterization.	Sahambi et.al.[123]	----/ 98.780	MIT / BIH (14481 beats)
10	Predictive neural network based technique to detect QRS complexes.	Vijaya et.al.[141]	98.960/ ----	CSE DS-3 (3657 beats.)
11	Present method: WT based QRS detection.	-----	100 / 99.866 99.904/ 99.806	CSE DS-3 (18024 beats) MIT/BIH database (103763 beats)

detection are given in Table 3.12. The percentages of sensitivity/ rate of accurate QRS detection in this table are not directly comparable, because, different databases or different number of beats have been used by different workers.

3.8 CONCLUSIONS

The present algorithm works satisfactorily in all typical morphologies of ECG signal. Among the wavelets evaluated for the detection of QRS complexes, QSWT and WT6 are found the best suitable. Looking to the performance of the developed algorithm, which gives the detection rate of 99.806% using all 48 records of the MIT/BIH Arrhythmia database and 99.866% using the CSE DS-3, prove the utility of the wavelets for the detection of QRS complexes. In addition to this, the results reported by Li et al. [72] and Kadambe et al. [56] also suggest that the use of wavelet has found distinct place for itself in field of computer aided ECG analysis and interpretation.

Important conclusions on the basis of the work presented in this chapter are:

- (i) The compact wavelets are most suitable for QRS detection and give better performance than long length wavelet filters. Also the computationally compact wavelets are comfortable. The phase-shift is more in asymmetric than symmetric wavelets.
- (ii) Even with noisy signals, QRS detection by wavelets need no additional signal processing to remove baseline wander, noise, and artifacts. It is observed that the failure occurs when ECG signal contains noise in the frequency range of QRS complex, because these noise components also emerge with the QRS complex in detail signal d^4 .
- (iii) Even with higher P and T wave segments, the detection of QRS by WT is accurate due to the signal splitting.
- (iv) The main cases of failure are due to the emergence of small amplitude modulus maxima lines when the signal amplitude is very low or with the high amplitude signal, where more number of modulus maxima lines get extracted throughout the ECG signal.
- (v) The wavelet transform implementation requires values from the future and the past. This causes trouble at the beginning and the end of a finite-length signal. This problem can be resolved by extending the signal either periodically or symmetrically. In case of ECG, this problem can be overcome easily by starting the transformation leaving few samples at the beginning and end of ECG data array, and making use of these samples later on to establish symmetry around QRS complex.
- (vi) It has been observed that the QSWT and the new wavelet produce best results in QRS detection.

FEATURE EXTRACTION OF ECG SIGNAL

4.1 INTRODUCTION

The ECG signal is the graphical representation of the bioelectrical and biomechanical activities of the cardiac system. It provides valuable information regarding the functional aspects of the cardiac and cardiovascular systems. The QRS complex is the most characteristic wave set in the ECG signal, and represents depolarization of the ventricles. During this phase, the heart pumps out blood at maximum pressure to the circulatory and pulmonary systems.

During the past four decades, a number of computer programs have been developed for the automatic interpretation of cardiac disorders using ECG signals [150]. However, still the state of perfection is yet to reach in this vital area of cardiac disease diagnostics. The methods and independent databases are needed in large number and wide variety to test the reliability of such programs. All ECG computer analysis programs are basically composed of two parts. The first one dealing with the accurate identification and measurement of characteristic features of ECG signal and the second one dealing with the diagnostic interpretation. The main task in the measurement is to find exact location of the major reference points, i.e., the onsets and offsets of P, QRS and T waves. The following section covers various techniques developed so far for such purpose.

4.2 FEATURE EXTRACTION TECHNIQUES

As discussed in earlier chapters I and III, the key of the ECG feature extraction is the detection of QRS complex and is taken as the basis for identification and extraction. The main groups of techniques, as discussed earlier, are based on the different approaches, namely syntactic, non-syntactic, hybrid and transformative types. Using these approaches, number of software, hardware and hybrid techniques have been developed. These techniques follow the procedure of filtering, squaring, and differentiation using decision rules like zero crossings, amplitude thresholds, sharp consecutive Q-R-S peaks, duration of QRS complex and R-R interval duration [8,104]. Most of these methods face difficulty due to wide variations in the physiological behaviour of the cardiac system. To overcome the limitations of existing methods, new methods are being developed to obtain better results. One such powerful technique is based on the WTs which has been reported by different researchers, namely Li et al. [72], Rao [115], Shahambi et al. [123] and Kadambe et al. [56]. The QRS complex has

components of higher frequency and P and T waves have low frequency contents, therefore, the signal splitting nature of WT is of immense help in ECG feature extraction.

This chapter deals with a modified wavelet transform technique, which has been developed to analyze multi-lead electrocardiogram signals for cardiac disease diagnostics. Two wavelets have been used, i.e. a quadratic spline (QS) wavelet for QRS detection and Daubechies six coefficient (DU6) wavelet for P and T detection. The modified combined wavelet approach first extracts the QRS complex as discussed in chapter III, and thereafter, its onset and offset and the P and T waves and their onsets and offsets. After detecting the fundamental ECG components, the ECG parameters namely, P-on, P-position, P-off, QRS-on, QRS-peak, QRS-off, Q-on, Q-peak, Q-off, R-on, R-peak, R-off, S-on, S-peak, S-off, R' -peak, T- peak and T-end are extracted. From these fundamental measurements, the parameters of diagnostic significance, namely, the heart rate, P-amplitude, PR-interval, QRS-interval, QT-interval, QRS peak-to-peak amplitude, ventricular activation time (VAT), and frontal plane axis (FPA) are identified and extracted. Software was validated by extensive testing using CSE dataset-3 (DS-3) and dataset-5 (DS-5) obtained from Belgium [147].

4.2.1 Feature Extraction

Feature extraction becomes the important stage in automated disease diagnosis as it has responsibility to tender the particular disease. The determination of wave amplitude and location is the basis to measure ECG features. The accurate measurement of wave amplitude and location is dependent on the proper selection of reference level. The steps of feature extraction are as follows:

- i) Reference level (baseline) determination
- ii) Minimum wave requirements and wave labeling
- iii)Parameter extraction: It consists of basic measurements like amplitude and duration of waves segments and intervals and determination of parameters like areas, ratios, axes, vectors and spatial parameters.

ECG features (wave duration and amplitude) are used by most cardiologists in their programs. For the classification of 12-lead ECG, processing systems might use up to 40 parameters per lead, i.e., a total of 300 to 500 parameters. Even with all these considerations, different programs perform differently on different diagnostic categories [78,150]. Therefore, a conclusion from this observation is that so far neither an uniform optimal set of classification features (diagnostic criteria) nor a generally optimal classification procedure can be defined.

With respect to above listed areas, The CSE Working Party and American Heart Association (AHA) have framed guidelines and recommendations to facilitate the researchers and to have common platform for the comparison of different methods and the results and to make possible the exchange of ECG measurements for development of diagnostic programs. Keeping this in view, in the present work, the recommendations and suggestions from these to organizations have been considered to carryout the work from the stage of signal acquisition to interpretation.

It was recommended by the AHA [149] that the ST segment, the T wave and the P wave, should all be measured with respect to the iso-electric part of the tracing before the P wave. However the CSE Working Party recommends that, from an electrophysiological point of view, it is not appropriate to use separate baselines for measuring QRS and ST-T complexes. It recommends strongly the uniform use of a horizontal baseline, determined in an interval before QRS onset for all QRS and ST-T measurements in such a way as to avoid the problem arising in the AHA recommendations in which there is a discontinuity in the implied baseline immediately after the J point. In the AHA recommendations it is stated that: ‘The reference level for the measurement of the S-T junction (point J) should be the P-R segment at the beginning of the QRS. The level of reference for measurements of the S-T segment, the T wave, and the U wave should be the level at the termination of the T-P or U-P interval when this can be determined’. The AHA recommendations further states that: ‘ The latter may not be possible at very high heart rates, particularly in maximal or sub-maximal exercised tests since the T wave and the succeeding P wave tend to fuse, and a T-P or U-P interval cannot be detected any more. In such cases, the level of reference should be the P-R segment at the beginning of QRS complex, both for the resting ECG and the recording at higher heart rates.

4.2.2 Interpretation

The diagnostic classification is the ultimate aim of the ECG signal analysis. The interpretation of diseases is being carried out mainly by heuristic knowledge and partly by statistical analysis.

4.3 SELECTION OF BEATS

Automated ECG signal analysis can use the redundancy of complexes available in the sampled ECG to optimize the accuracy of measurements. Considering the redundancy of the ECG wave complexes, one form of averaging or another is carried out in general approach of

measurement. Normally, a set of beats of similar configuration is grouped together and an average beat is formed [78]. Measurements are then made on this average beat. There are alternative approaches available where a set of measurements is obtained and an average value is determined. In some other approaches, simply a beat is used for the analysis.

Three techniques are currently in use to select beats for measurements. The first one locates the “best complex” for analysis. All of the complexes of a given lead set are required to locate this best complex. Then the complex with the least noise and baseline wander is chosen for the analysis. In the second technique, some time-coherent averaging is done of all the complexes that are considered to be morphologically of the same type. This procedure reduces the random noise on the signal. Detailed wave recognition and measurement extraction is then made on the average complex. The third technique makes detailed wave recognition on every complex in the lead set and subsequently averages the measurements of similar dominant complexes [78].

Until now there is no fixed approach for the types of beats to be used. Jan et al. [51] in his findings showed favor for the second technique, but the findings are unable to show any significant difference in QRS duration if wave recognition is performed on single complex or averaged complexes and computed using beat alignment. Based on the results of extensive noise tests performed in a CSE project, a measurement strategy that uses selective averaging has recently been recommended for diagnostic ECG computer programs [149].

The use of averaging, however, theoretically leads to improved signal-to-noise ratio and hence, more accurate amplitude measurements. The accuracy of computer-derived durations is still under discussion, but it should be noted that, if a reference point is incorrectly determined (the QRS onset, for example), then any amplitude measured with respect to such a point is prone to an error. To minimize such errors, most programs find a reference level by averaging in the vicinity of the QRS onset or else fit a smooth curve from which the reference can be taken. From these guidelines, the strategy of using selected beats has been considered in this work to measure the ECG parameters in five different beats (five beats per lead). The regular beats are detected from the average R-R intervals, and individual beat is used to determine its individual baseline.

4.4 AMPLITUDE MEASUREMENT PROCEDURE

As per the recommendations of The CSE Working Party, baseline is determined from the PR segment and the onset of QRS, the QRS onset is used as a reference for all QRS and

ST-T amplitude measurements [149]. To detect the PR segment and the QRS onset, a window (30% of R-R interval) preceding to R peak is scanned to detect positive and negative peaks and isoelectric segments.

4.5 INTERVAL MEASUREMENT PROCEDURE

Fig.1.6 demonstrates different ECG wave components and their pictorial representation.

The **P duration** is measured from the beginning to the end of the P wave. The P duration may vary between lead groups, as a result of a perpendicular orientation of initial or terminal excitation vectors on the corresponding leads and on account of wave recognition problems, especially in noisy recordings. Measurements in orthogonal or multiple leads are therefore more accurate. In case of 12 lead ECG recordings with conventional 3-channel equipment, the longest of the duration in the extremity lead groups is recommended as the best estimate, for reasons of measurement stability [149]. Indeed, inter- and intra-observer variability, as well as reproducibility figures and a comparison of program with visual results in the CSE project have demonstrated that P onset and P offset determined are most reliably performed in the peripheral leads. This is in conformity with the direction of the major P wave vectors, which follow a superior- inferior course in the frontal plane in most of the cases.

The **P-R (or P-Q) interval** is measured from the beginning of the P wave to the beginning of QRS. This interval may also vary between lead groups, in view of the possible perpendicular orientation of initial activation vectors on the corresponding leads. Ideally the PR interval should be measured from the earliest P deviation to the earliest onset of QRS complex in any of the leads, as can be derived from multi-channel recordings in which all ECG channels, i.e. all 12 conventional leads or at least 8 independent standard leads are recorded simultaneously.

The **P-R (or P-Q) segment** is that part of the ECG between the end of the P-wave and the beginning of the QRS complex. The duration of the segment is calculated by subtracting the P duration from the P-R interval.

The **QRS duration** is measured from the earliest onset to the latest end of QRS complex when leads are recorded simultaneously. For the same reasons listed above, multichannel recorders and quasi orthogonal leads are preferred.

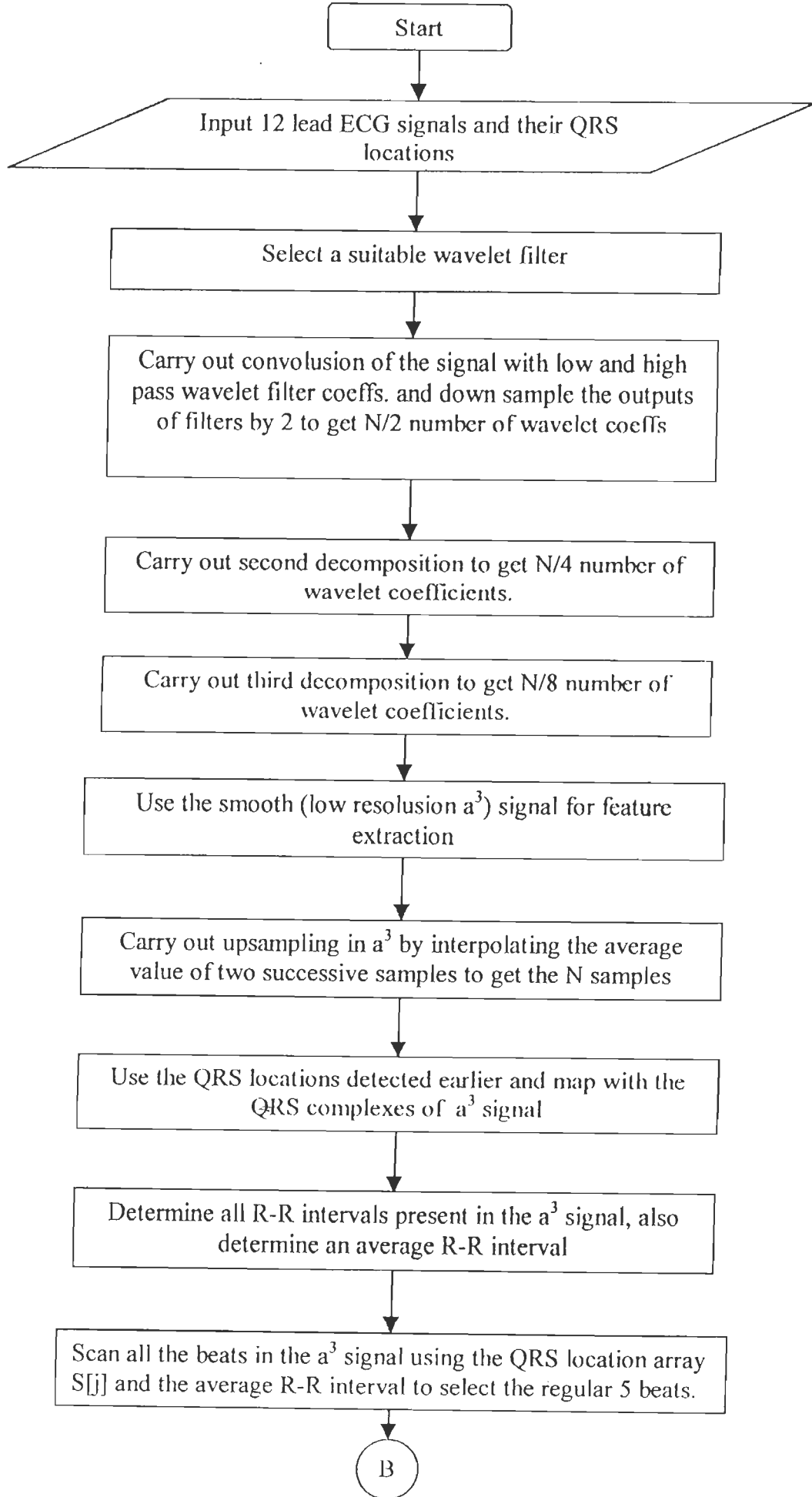
The **Q-T interval** is measured from the beginning of QRS complex to the end of T wave. When obtained from the conventional lead groups, the longest interval found is

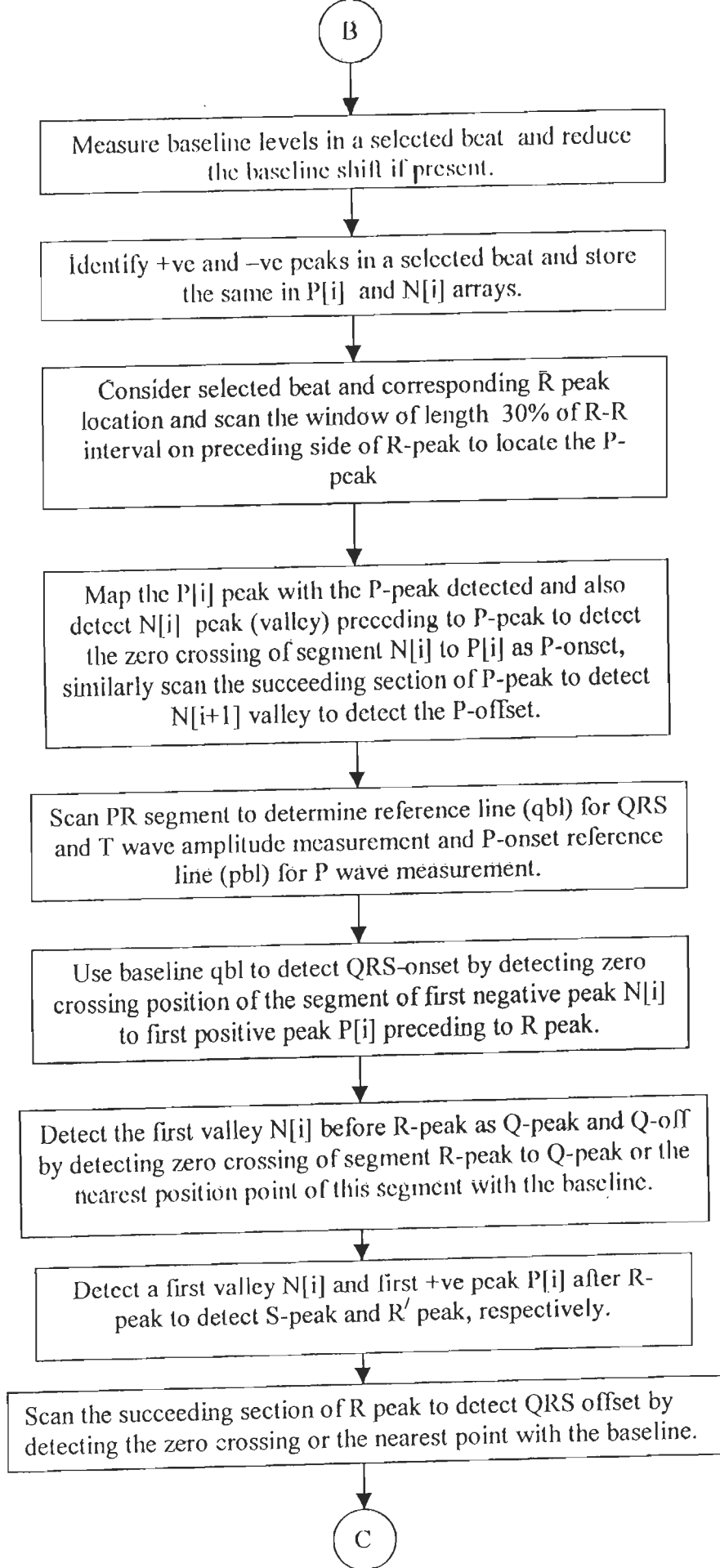
regarded as nearly correct. However, the Q-T interval is usually measured accurately in precordial leads V1 to V3 [42,149].

4.6 P, Q-R-S AND T WAVES DETECTION

4.6.1 Method

An algorithm for P, Q-R-S and T waves identification using wavelet transform decomposition is given in the form of flowchart in Fig.4.1. The low resolution signals extracted using DU6 wavelet are shown in Fig.4.2. It indicates the splitting of the original ECG signal into three signals a^1 to a^3 . The use of DU6 wavelet makes the signal smoother [47,86]. Out of the three signals shown in Fig.4.2, a^3 signal is extracted without down sampling the output of preceding low pass filter. Extraction of a^3 without down sampling leads to smooth and avoid loss of information from the a^3 signal. It is observed that the accuracy of measuring onsets and offsets of ECG wave segments is greater when the a^3 signal is extracted without down sampling. The a^3 signal is used to measure all the ECG wave fiducials by referring to the already detected QRS locations. Firstly, the QRS peak in the a^3 signal is mapped with the reference QRS by scanning through a 50 ms window on either side of the reference. This detects the QRS peak in a^3 signal. If the detected QRS peak in the a^3 signal is a positive maxima, then the peak is an R wave and the preceding first negative peak is the Q wave. To the left of the Q peak, the first point close to the reference line is the QRS- onset. If the detected QRS peak is a negative maxima, the peak is an S wave and the preceding first positive peak is an R wave. To the left side of the R wave, the first negative peak is the Q wave. Following the R wave, the first negative peak is the S wave and to the right side of the S wave, the first positive peak, if present, is the R' wave. First point close to the reference line is the QRS - offset. After detecting all waves of the QRS complex, the P wave is detected by scanning through a window of length equal to 30% of the R-R interval on the left-side of QRS- peak. The P- peak is obtained by detecting the absolute maximum peak in the defined window and P-on and P -off by identifying first points close to the reference line on either side of P peak. Identification of biphasic P wave has been carried out by a procedure, that if algebraic sum of P wave (i.e. net P deflection which is sum of sample amplitudes from P-onset to P-offset) samples, firstly increases and then decreases or vice-versa, the wave is biphasic. If the algebraic sum of sample amplitudes increases or decreases from P-onset to P-offset, the wave is uniphasic. Similarly, the T wave is detected by





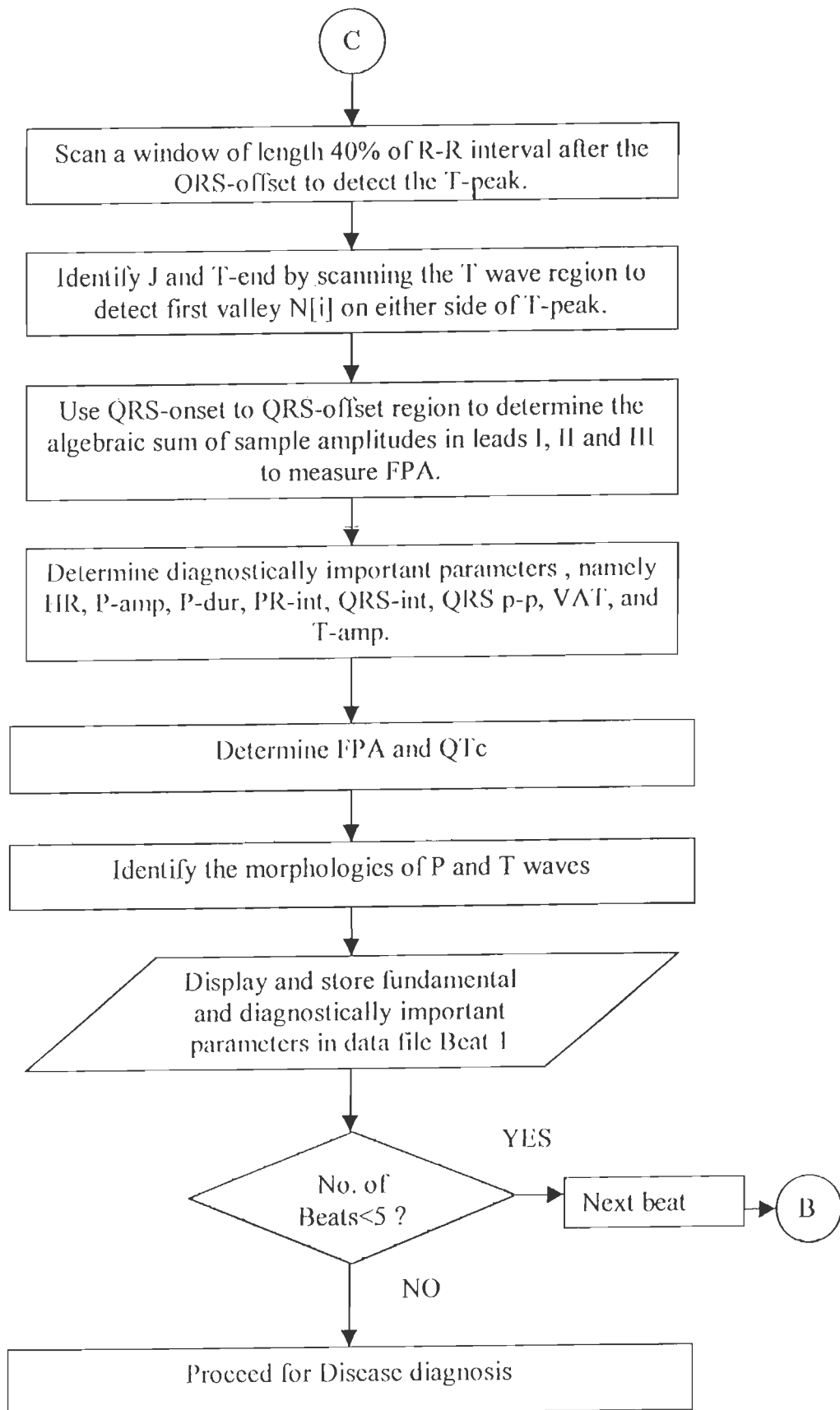


Fig. 4.1 Flow chart for WT based ECG feature extraction

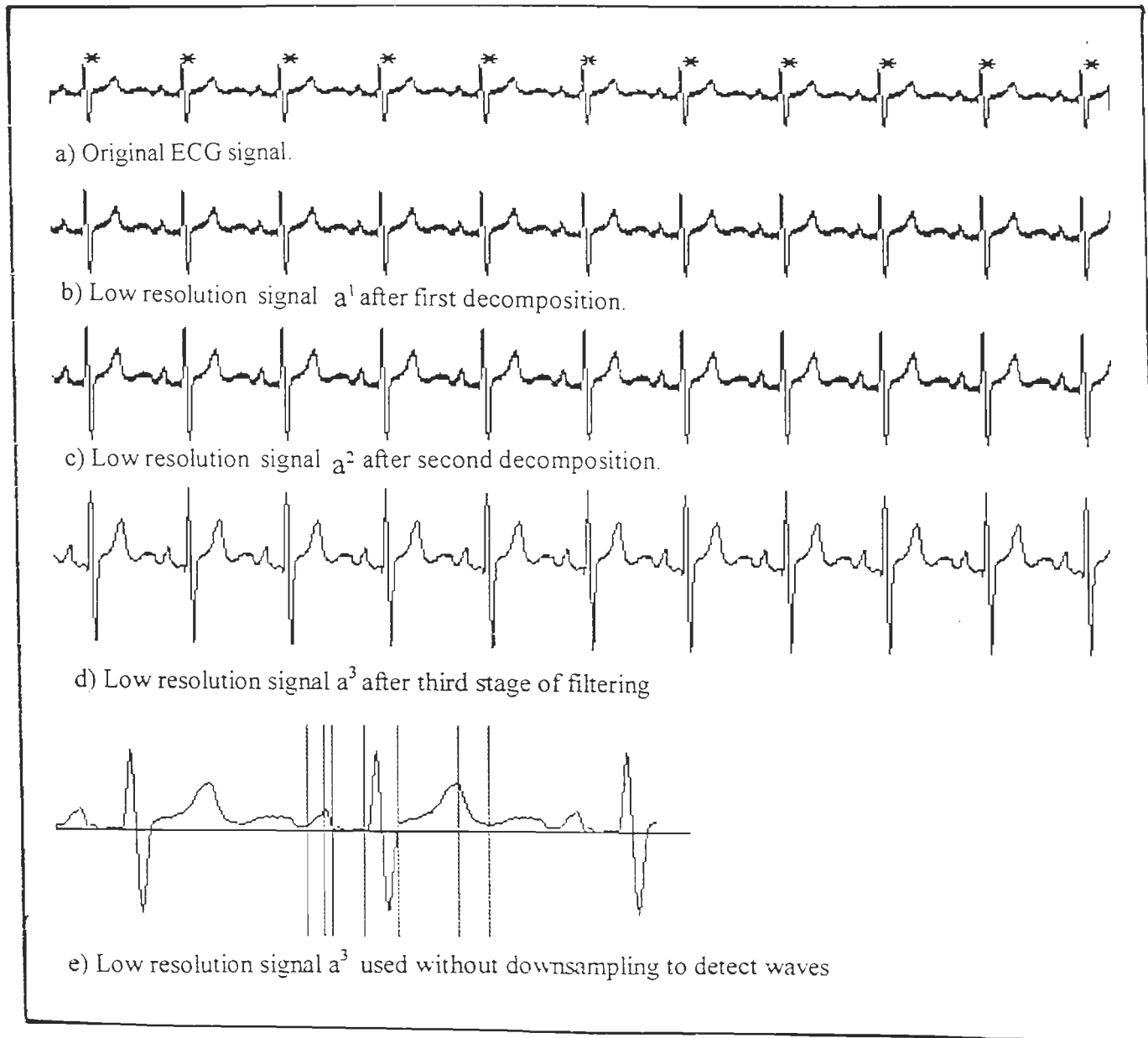


Fig. 4.2 Detection of ECG waves

scanning through a window of length equal to 40% of the R-R interval on right-side of QRS peak to detect the T-peak and the T-end.

The detection of the P, QRS and T waves is shown in Fig.4.3 by vertical lines at the P-onset, P-peak, P-off, QRS-on, QRS-off, T-peak and T-end positions. The software has a facility to scan complete length of recording in 12 standard leads and select 5 beats from each lead. As shown in Fig.4.3(a), five ECG beats from lead I from record MA-001.DCD have been selected to carryout complete analysis. The CSE dataset 3 is such, in which the complete record length of 8 to 10 seconds is constructed by copying the same beat repeatedly, hence all beats are same in a particular lead. This can be seen from the Fig. 4.3(a-c), where first three leads of record MA-001.DCD have been selected. At the bottom of these figures, the parameter estimates are given, which are same for all five beats in lead I. Same is the case with lead II and III.

4.7 DIAGNOSTIC PARAMETERS

After detecting the ECG wave fiducials, as shown in Table 4.1, the ECG signal parameters of diagnostic value, namely, heart rate, P- amplitude, P- duration, PR- interval, QRS- interval, QRS peak-to-peak amplitude, QT and QTc - interval, Ventricular Activation Time (VAT), T- amplitude and Frontal Plane Axis (FPA) are obtained. Table 4.2 shows the leadwise parameters measured from first beat of record MA-001.DCD of CSE DS-3. The detail description of measurement procedures used in this thesis work for the extraction of diagnostically important parameters from the fundamental measurements (Table 4.1) is given as below:

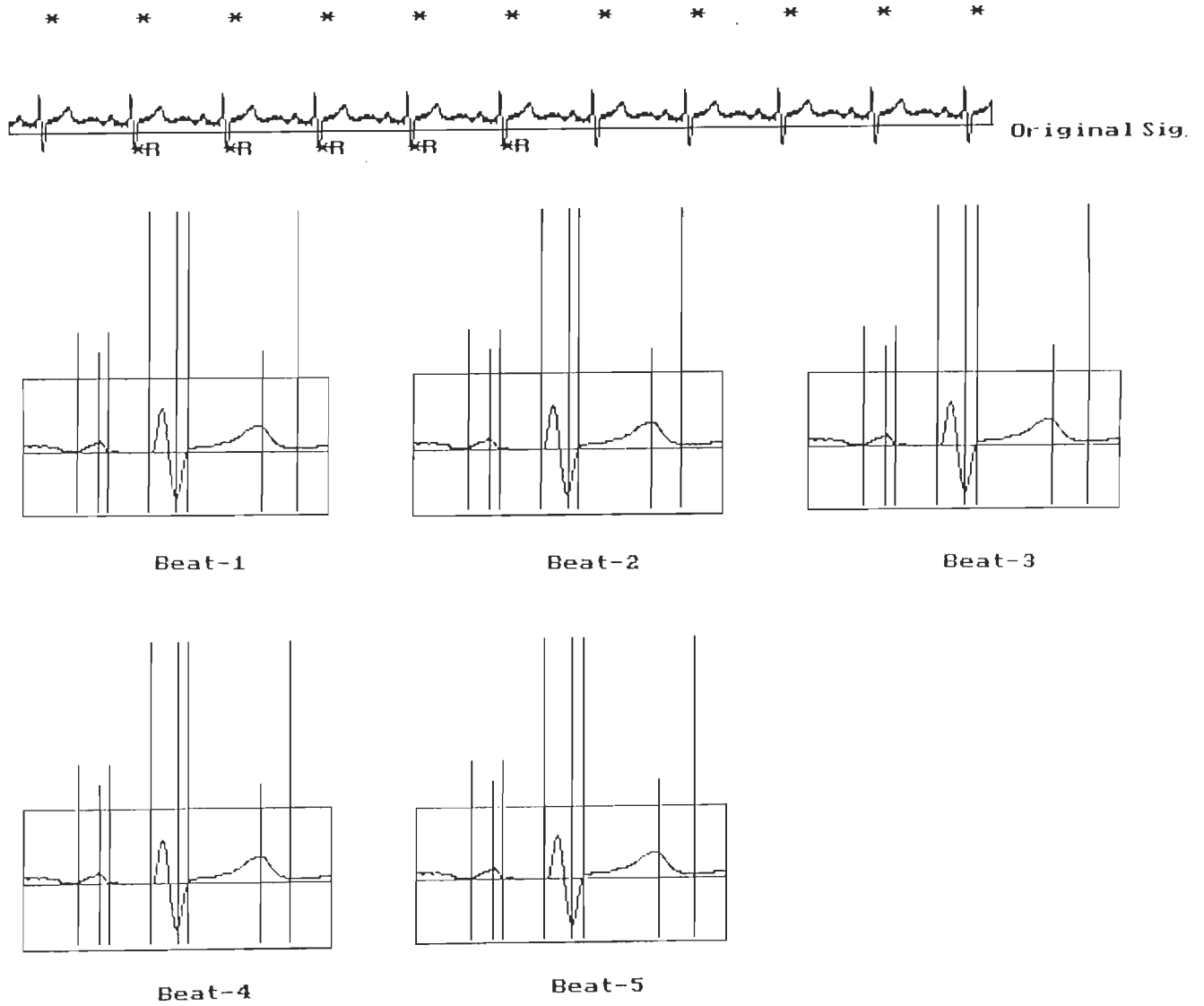
4.7.1 Heart Rate (HR) is determined from the measurements of R-R intervals as

$$\text{Heart Rate (BPM)} = 60 / (\text{R-R interval in sec})$$

4.7.2 Ventricular Activation Time (VAT) is measured from the measurements i.e. QRS onset and the R peak position as

VAT (in ms) = (R peak position - QRS onset position) x 2 (ms), where 2ms is sampling time [42].

Here, as shown in the Table 4.1, wave location measurements are given in the sample numbers and the wave amplitude in mV. Therefore, the VAT duration is measured from the difference of sample number of R peak location and the QRS onset location.



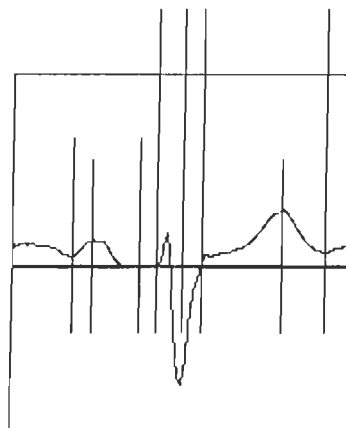
ECG Parameters of Diagnostic Significance

HR BPM	P-A mv	Pdur sec	Print sec	QRSint sec	QRSp-p mv	QT-int sec	VAT sec	T-A mv	NetD mv	
63.83	0.06	0.10	0.23	0.12	0.64	0.46	0.04	0.18	-0.63	Beat=1
63.83	0.06	0.10	0.23	0.11	0.65	0.42	0.03	0.18	-0.60	Beat=2
63.83	0.06	0.10	0.23	0.12	0.64	0.46	0.04	0.18	-0.63	Beat=3
63.83	0.06	0.10	0.23	0.11	0.65	0.42	0.03	0.18	-0.60	Beat=4
63.83	0.06	0.10	0.23	0.12	0.64	0.46	0.04	0.18	-0.63	Beat=5

Fig. 4.3 (a) Analysis of 5 beats in a ECG signal (CSE DS-3 record MA-001.DCD, Lead I)



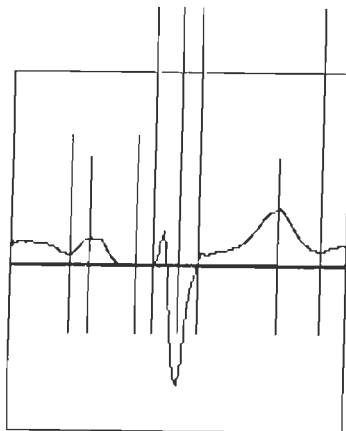
Beat-1



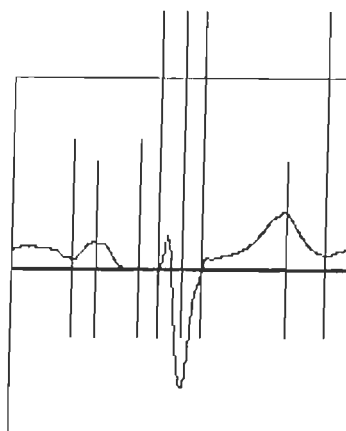
Beat-2



Beat-3



Beat-4

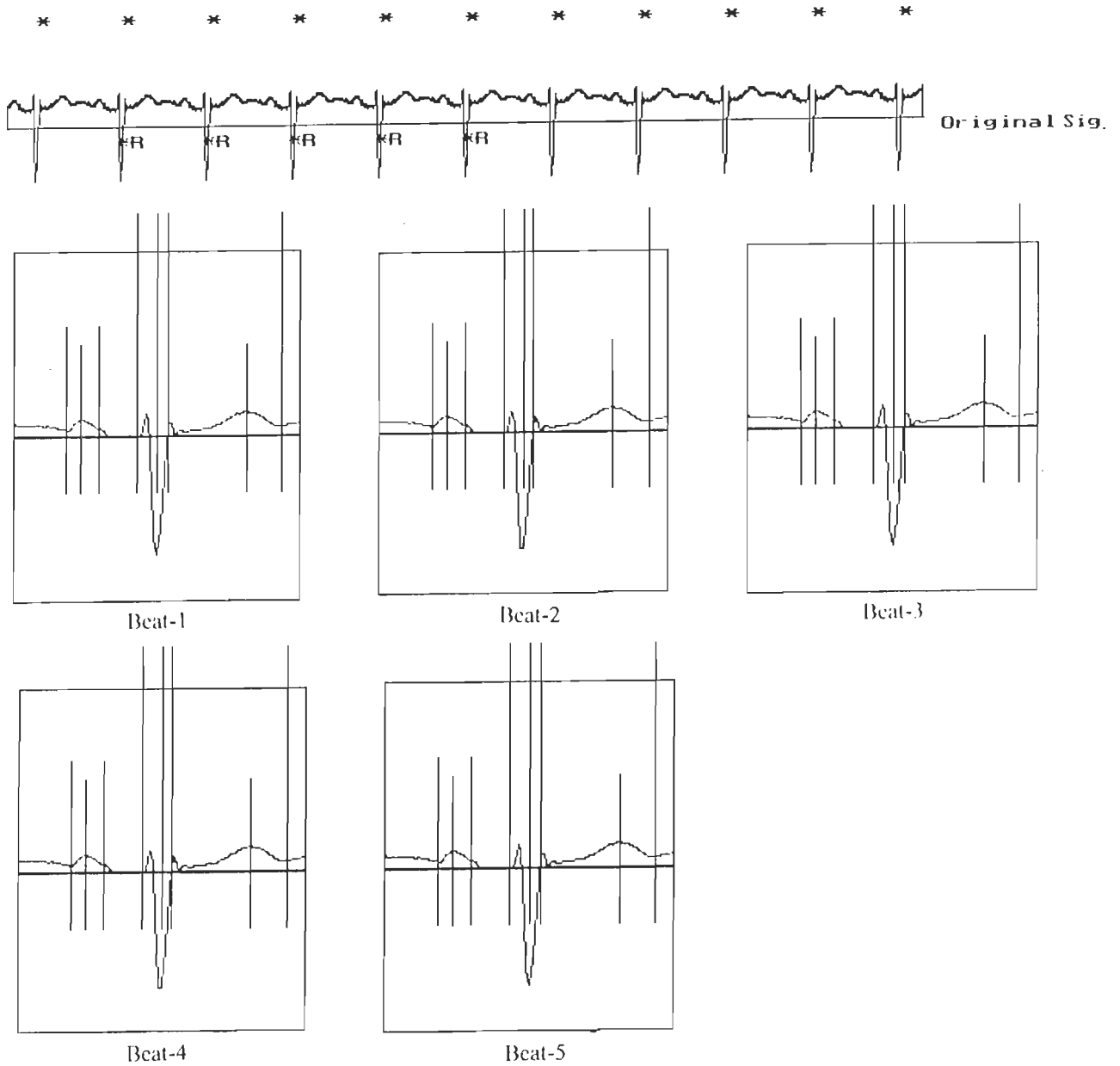


Beat-5

ECG Parameters of Diagnostic Significance

HR BPM	P-A mv	Pdur sec	Print sec	QRSint sec	QRSp-p mv	QT-int sec	VAT sec	T-A mv	NetD mv	
63.83	0.07	0.18	0.24	0.12	0.62	0.46	0.02	0.24	-8.81	Beat=1
63.83	0.07	0.18	0.23	0.13	0.63	0.47	0.03	0.24	-8.79	Beat=2
63.83	0.07	0.18	0.24	0.12	0.62	0.46	0.02	0.24	-8.81	Beat=3
63.83	0.07	0.18	0.23	0.13	0.63	0.47	0.03	0.24	-8.79	Beat=4
63.83	0.07	0.18	0.24	0.12	0.62	0.46	0.02	0.24	-8.81	Beat=5

Fig. 4.3(b) Analysis of 5 beats in a ECG signal (CSE DS-3 record MA-001.DCD, Lead II)



ECG Parameters of Diagnostic Significance

HR BPM	P-A mv	Pdur sec	PRint sec	QRSint sec	QRSp-p mv	QT-int sec	QT sec	T-A mv	NetD mv	
63.83	0.05	0.10	0.24	0.10	0.66	0.47	0.03	0.11	-8.51	Beat=1
63.83	0.05	0.10	0.23	0.10	0.64	0.47	0.02	0.11	-8.49	Beat=2
63.83	0.05	0.10	0.24	0.10	0.66	0.47	0.03	0.11	-8.51	Beat=3
63.83	0.05	0.10	0.23	0.10	0.64	0.47	0.02	0.11	-8.49	Beat=4
63.83	0.05	0.10	0.24	0.10	0.66	0.47	0.03	0.11	-8.51	Beat=5

Fig.4.3(c) Analysis of 5 beats in a ECG signal (CSE DS-3 record MA-001.DCD, Lead III)

Table 4.1 Measurement of ECG parameters by using wavelet transform of record No. MA-001.DCD

Lead No.	Pon pos	P pos	P mv	Poff pos	QRSon pos	Q pos	Q mv	Qoff pos	R pos	R mv	Roff pos	S pos	S mv	R' pos	R' mv	QRSoff pos	T pos	T mv	Tend pos	Net QRS defl., mv
1L1	36	68	0.07	84	148	148	0.00	156	168	0.25	180	188	-0.26	00	0.00	208	320	0.15	376	-0.45
1L2	18	50	0.14	110	138	138	0.00	142	150	0.17	158	170	-0.61	206	0.06	210	314	0.30	370	-11.87
1L3	18	42	0.11	70	134	134	0.00	138	150	0.14	158	166	-0.72	190	0.09	198	314	0.15	370	-12.19
1aR	62	110	0.09	134	150	154	-0.04	158	178	0.44	266	206	0.05	210	0.05	238	314	-0.13	370	10.94
1aL	42	90	0.04	118	146	150	-0.01	154	166	0.49	182	186	-0.13	00	0.00	198	302	0.04	338	5.87
1aF	18	42	0.14	90	134	134	0.01	134	150	0.17	158	170	-0.62	190	0.01	194	314	0.24	370	-10.0
1V1	10	34	0.06	58	150	166	-0.27	174	178	0.46	190	194	-0.25	206	0.03	214	334	0.13	410	-0.57
1V2	10	66	0.04	90	142	146	-0.04	150	158	0.52	166	174	-0.83	206	0.00	210	318	0.20	398	-18.20
1V3	42	66	0.05	90	142	142	-0.01	146	158	0.71	166	174	-0.86	206	0.00	210	314	0.26	394	-15.11
1V4	30	66	0.06	90	138	138	0.01	138	158	0.60	166	174	-0.78	00	0.00	202	314	0.30	374	-13.29
1V5	30	62	0.07	118	138	138	0.00	142	154	0.37	166	178	-0.63	00	0.00	202	310	0.27	370	-13.43
1V6	30	62	0.09	122	138	138	0.00	142	154	0.23	166	178	-0.48	00	0.00	202	306	0.25	366	-11.69
PGM	30	64	---	90	140	140	---	144	158	---	166	176	---	190	---	205	314	---	370	---
REF	22	--	---	87	139	---	---	---	---	---	---	---	---	---	--	202	---	---	370	---

PGM (median of 12 lead measurements)- Program results. FPA(Frontal Plane Axis) = 88.08 degrees.
 REF - CSE Refree results.

Table 4.2 ECG parameters of CSE DS-3 record No. MA-001.DCD

Lead No.	HR BPM	P-A mv	P-dur sec	PR-int sec	QRS-int sec	QRS p-p mv	QT-int sec	VAT sec	T-A mv
1L1	64.66	0.067	0.096	0.264	0.120	0.518	0.456	0.040	0.152
1L2	63.83	0.140	0.184	0.264	0.144	0.781	0.464	0.024	0.300
1L3	63.83	0.110	0.104	0.264	0.128	0.863	0.472	0.032	0.152
1aR	63.83	0.092	0.144	0.232	0.176	0.489	0.432	0.056	-0.134
1aL	63.83	0.042	0.152	0.248	0.104	0.624	0.376	0.040	0.042
1aF	63.83	0.138	0.144	0.264	0.120	0.793	0.472	0.032	0.242
1V1	63.83	0.056	0.096	0.336	0.128	0.708	0.488	0.056	0.132
1V2	63.83	0.042	0.160	0.296	0.136	1.350	0.504	0.032	0.202
1V3	63.83	0.054	0.096	0.232	0.136	1.568	0.504	0.032	0.258
1V4	63.83	0.063	0.120	0.256	0.128	1.377	0.472	0.040	0.303
1V5	63.83	0.074	0.176	0.248	0.128	1.000	0.464	0.032	0.272
1V6	63.83	0.086	0.184	0.248	0.128	0.711	0.456	0.032	0.248
QTc = 0.478 sec (Using the median values of heart rate and QT interval)									

4.7.3 Uniphasic/ Biphasic P and T Waves

Identification of P wave as uniphasic or biphasic has been carried out by measuring the area under the wave. A procedure as explained in the flowchart Fig.4.4 has been evolved to determine the algebraic sum of P wave samples by scanning the window from P-onset to P-offset. Decision regarding the morphology of the wave has been taken from the nature of profile of the area under the P wave, i.e., if the algebraic sum of samples firstly increases and then decreases or vice-versa, the wave is biphasic. If the algebraic sum of sample amplitudes only increases or only decreases from P-onset to P-offset, the wave is uniphasic. Same procedure has been followed for T wave identification. Figure 4.5 depicts the identification of uniphasic and biphasic P and T wave segments.

4.7.4 Frontal Plane Axis

There have been many suggested methods to measure the QRS axis [78]. However, the adhoc Task Force of the World Health Organization (WHO) and the International Society and Federation for Cardiology has recently recommended that the QRS axis should be determined by measuring the areas under the QRS complex in leads I, II and III. Any two pairs of leads can be selected from the three leads in three different ways. The recommendation is that QRS axis be calculated from the average value of three measurements in three different pairs out of I, II, and III leads.

An alternative approach is to utilize the sum of the signed Q wave (negative), R wave (positive) and S wave (negative) amplitudes in these leads to calculate a QRS axis. In either case, a function $f(I)$, for example, can be used to represent the measurement (area or component sum) derived in this case from lead I. The flowchart given in Fig.4.6 and the following calculation shows as how the use of the three standard limb leads I, II, III from which three measurements $f(I)$, $f(II)$, $f(III)$ are obtained allows an estimate of a frontal plane axis and avoids the need for repeated calculation and averaging as suggested by the WHO Task Force.

Consider that leads I, II and III with lead direction as conceived in the Eithoven triangle as shown in the Fig.4.7, are superimposed on a Cartesian coordinate system. Then $OL = f(I)$, $OM = f(II)$ and $ON = f(III)$ represent the amplitude of the projection of desired axis (or vector OA) onto the lead axes I, II, III as shown in the same Fig.4.7. Thus, the Cartesian coordinates of these projections; that is, the coordinates of L, M, N are as follows:

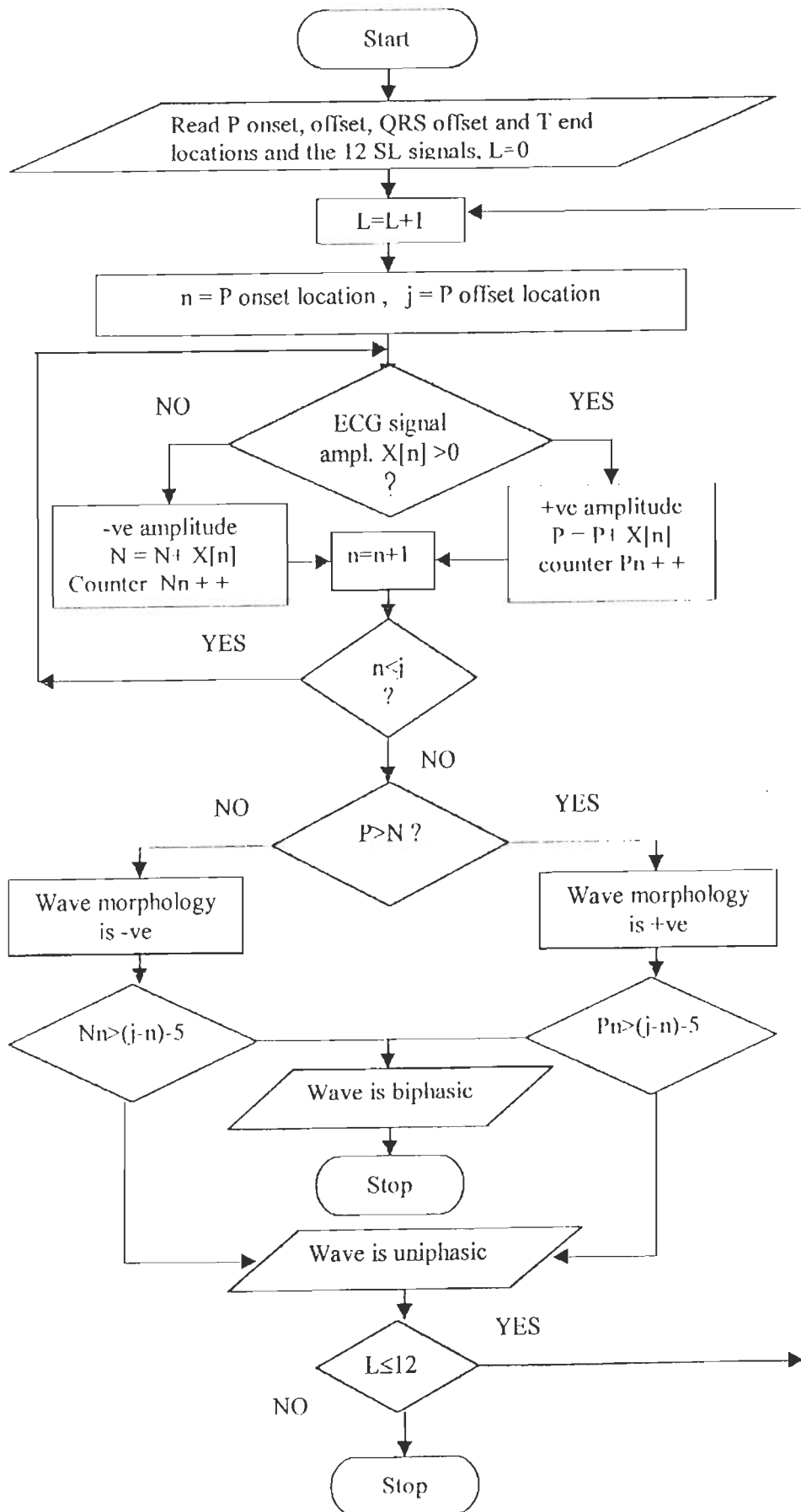
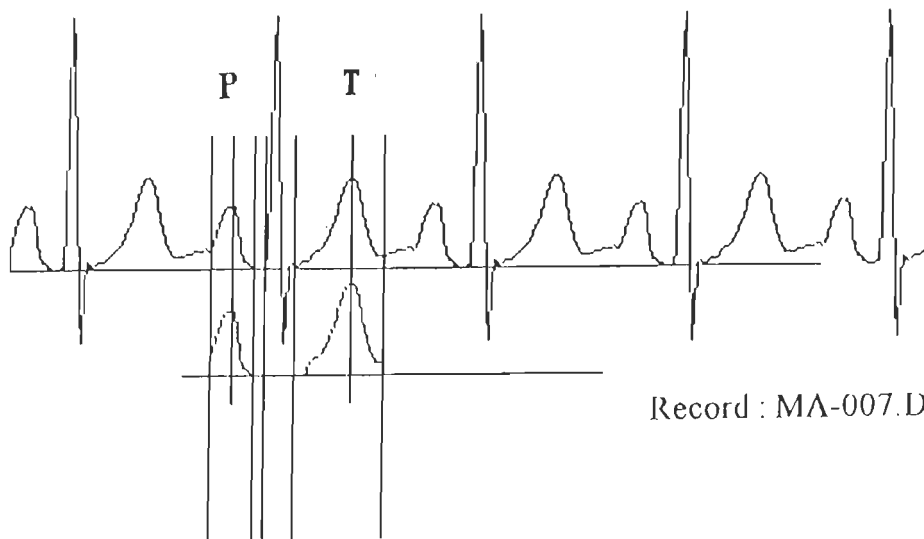


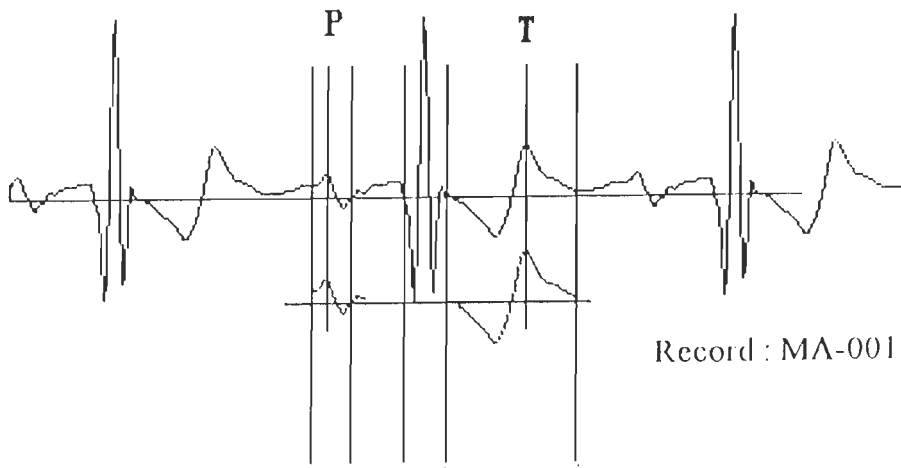
Fig. 4.4 Flowchart to identify uniphasic or biphasic P and T waves



Record : MA-007.DCD Lead LI

P: wave net +ve deflection=4.23 mV
and net -ve deflection=0.00 mV--> P is Uniphasic

T: wave net +ve deflection=9.04 mV
and net -ve deflection=0.00 mV--> T is Uniphasic



Record : MA-001.DCD Lead VI

P: wave net +ve deflection=1.03 mV
and net -ve deflection=-0.20 mV--> P is biphasic

T: wave net +ve deflection=4.09 mV
and net -ve deflection=-3.59 mV--> T is biphasic

Fig. 4.5 Identification of biphasic P and T waves

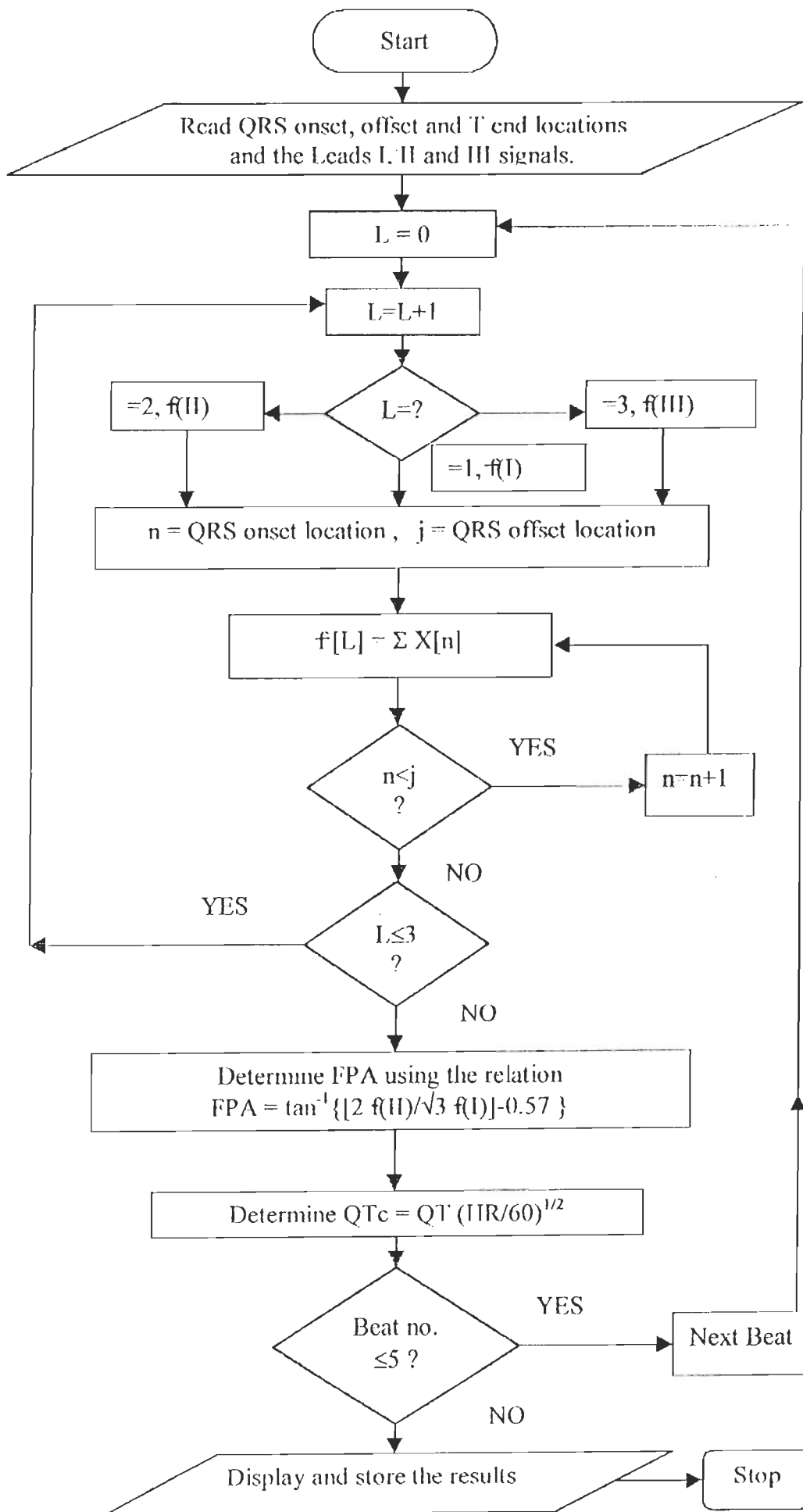


Fig.4.6 Flowchart for determination FPA and QTc

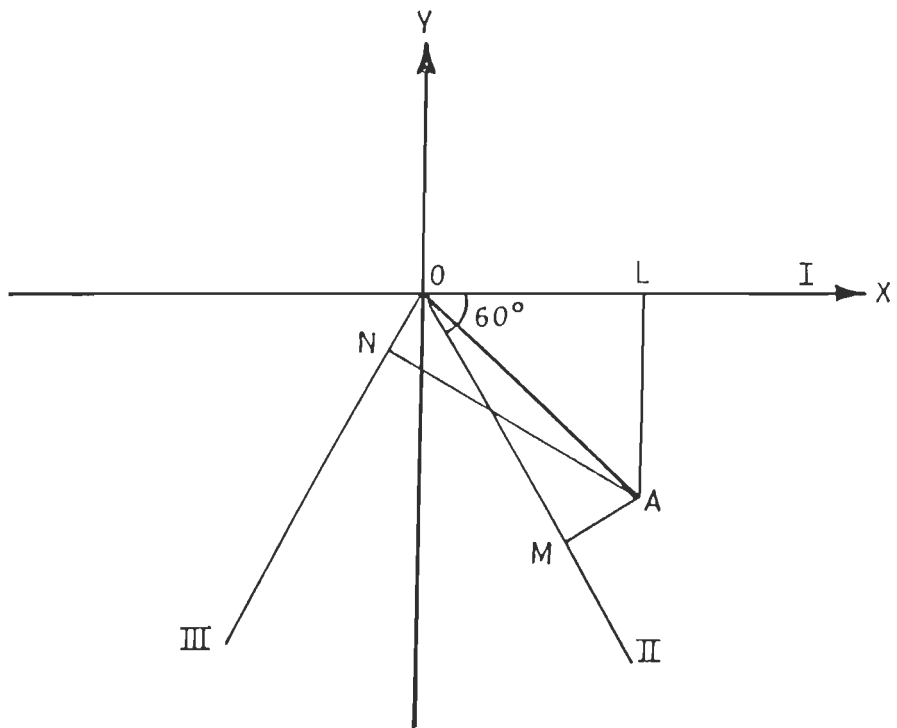
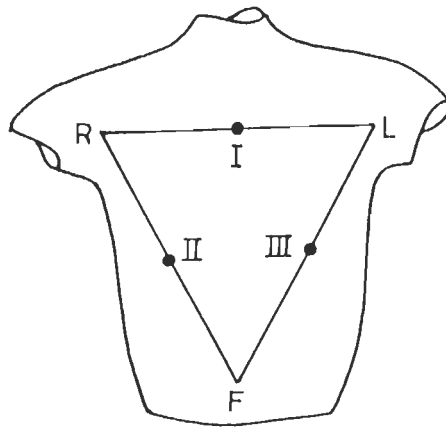


Fig. 4.7 Determination of FPA from the QRS complex in leads I, II, and III

axis projection on lead I: $L = (f(I), 0)$

axis projection on lead II: $M = (f(II) \cos 60^\circ, f(II) \sin 60^\circ)$

axis projection on lead III: $N = (- f(III) \cos 60^\circ, f(III) \sin 60^\circ)$

It should be noted that the functions $f(I)$, $f(II)$ and $f(III)$ are signed values.

The coordinates of the desired mean axis, that is, OA on a circle of suitably small radius R intercepting all vectors, are given by the average component values.

$$R/3.OA \{ [f(I) + f(II) \cos 60^\circ - f(III) \cos 60^\circ], [f(II) \sin 60^\circ + f(III) \sin 60^\circ] \}$$

$$= R/3.OA \{ f(I) + 1/2 [f(II) - f(III)], \sqrt{3}/2 [f(II) + f(III)] \}$$

The required angle is obtained from the arctangent of the ratio of the two components [78]:

$$FPA = \tan^{-1} \{ \sqrt{3}/2 (f(II) + f(III)) / f(I) + 1/2 [f(II) - f(III)] \}$$

$$= \tan^{-1} \{ \sqrt{3} [f(II) + f(III)] / [2 f(I) + f(II) - f(III)] \}$$

$$= \tan^{-1} \{ 2 [f(II)/\sqrt{3} f(I)] - 0.57 \}$$

where $f(I)$ and $f(II)$ indicate net QRS complex deflection in leads I and II, respectively.

4.7.5 QT Interval

Accurate determination of the QT interval, whether by computer methods or by manual methods, is difficult. For example, the variation between cardiologists estimating P, QRS and T reference points in the CSE study was greatest when they manually estimated the end of the T wave. Likewise, computer programs in the same study also showed greatest variation when finding the T wave termination. Furthermore, many researchers wish to monitor QT interval changes over a period of time by making use of ambulatory monitoring equipment.

It is well known that the QT interval varies significantly with the heart rate and a number of formula have been derived for correcting the QT interval. The most commonly used formula is [78].

$$QTc = QT \times (\text{rate}/60)^{1/2}$$

4.8 TEST RESULTS USING CSE DS-3 AND DISCUSSIONS

After developing an algorithm for reliable detection of the QRS complex, the ECG analysis software measures the fundamental ECG parameters by using the QRS location as a sharp time reference. To validate this algorithm, CSE data set-3 was used. Table 4.1 shows the basic ECG parameters measured by the program developed. Table 4.1 shows the ECG parameters extracted from the 12 standard leads of CSE DS-3 record MA-001.DCD, which

includes P-on, P-peak, P-off, QRS-on, Q-peak, Q-off, R-peak, R-off, S-peak, R' -peak, QRS-off, T-peak and T-end. At the bottom of table, five wave fiducials estimated by the software namely P-on, P-off, QRS-on, QRS-off and T-end, are compared with those given in the CSE reference. The results estimated by the programme and symbolized by 'PGM' is a median value determined from the wave measurements of the 12 standard leads and the estimates symbolized by 'MREF' is a median value of results given by CSE referee.

The comparison of software measurement results with referee results has been given in Table 4.3. The CSE committee has published measurement results of 25 records out of 125, hence the Table 4.3 shows only those 25 records. The comparison given in Table 4.3, of five wave fiducial points namely, P-on, P-off, QRS-on, QRS-off and T-end, shows that the most of the values are well within the tolerance limits suggested by the CSE working party. These tolerance limits are derived from the median values of results submitted by five human referees [147]. As indicated by small circles in Table 4.3, 11 out of 123 comparisons (i.e. 5 wave fiducials x 25 cases, excluding two estimates of record 111, whose referee results are not given by the CSE) are found outside the tolerance limits. Thus the overall accuracy of the software in the measurement of five wave fiducials is about 91.00%. Therefore, the parameters estimated by present software are found well within the recommended tolerances given by the CSE Working Party.

Table 4.2 shows a comparison of the program estimate (symbolized as PGM) of the five ECG fiducials: P-onset, P-offset, QRS-onset, QRS-offset, T-end with the corresponding median of the same ECG fiducials with the corresponding median MREF, of estimates given by five CSE referees. At the end of the table, the recommended tolerances (T-limit), i.e., the CSE recommended average standard deviations of these five ECG fiducials in milli-seconds (ms) is cited by the CSE Working Party [147]. The results are shown in Fig 4.8(a-g).

The sampling frequency used in the CSE data base is 500Hz, a recommended tolerance of 12 ms for P onset, would mean that a difference of 6 samples positions between the statistical median of the five referees estimate and the program estimates is admissible. It may be noted from the Table 4.3 that, in record nos. 6, 16, 21, 26, 31, 51, 56, 66, 71, 81, 91, 96, 106, 116 and 121, all five fiducials estimated using the developed software, are well within the recommended tolerance limits from their respective median referee values. Thus, in a total of 125 measurement estimates reported in Table 4.3, over 91% of the program's estimates are well within the recommended tolerance limit. This can be easily verified from Fig.4.8(a-g). Figures 4.8(a-g) show the normalized deviation w.r.t. median (MRRF) of the parameters,

Table 4.3 Summary of ECG analysis results of 25 cases of CSE DS-3 database

Rec No.	Pon		P pos	Poff		QRSon		Q pos	R pos	S pos	R' pos	QRSoff		T pos	Tend	
	PGM	REF		PGM	REF	PGM	REF					PGM	REF		PGM	REF
01	30	22	64	90	87	140	139	140	158	176	190	205	202	314	370	370
06	23	22	51	79	74	85	87	87	107	119	123	127	129	211	267	270
11	25	22	53	73	77	89	97	101	121	135	137	145	145	237	281	281
16	31	35	59	80	86	101	102	107	119	131	141	147	144	233	279	283
21	99	105	131	167	164	177	181	177	203	219	219	233	233	355	419	420
26	41	40	69	105	99	145	141	153	185	209	--	222	225	303	365	365
31	41	38	73	105	100	123	124	133	149	161	167	173	173	265	309	311
36	45	53	81	101	106	123	124	123	147	161	--	179	185	263	331	320
41	57	56	81	109	106	131	127	135	149	161	170	179	193	287	337	340
46	27	26	63	91	80	101	104	103	127	155	--	167	172	275	343	340
51	13	13	43	73	68	91	90	91	105	119	131	137	135	199	253	246
56	79	78	107	135	132	167	170	169	191	203	211	219	218	329	385	391
61	51	53	91	127	123	175	165	175	191	201	203	211	210	311	369	366
66	67	63	93	119	120	140	137	147	167	179	---	187	190	291	347	353
71	43	44	77	102	97	123	119	129	143	157	157	165	161	243	299	301
76	39	35	65	97	99	127	124	131	149	165	173	183	199	269	321	320
81	37	40	57	105	100	125	122	125	149	163	--	175	180	237	325	326
86	41	38	69	100	94	121	120	121	141	165	175	189	186	295	347	370
91	37	36	69	99	96	113	116	119	141	157	166	177	175	277	317	331
96	19	21	45	73	79	138	142	138	163	177	----	199	201	285	329	340
101	25	24	57	85	76	93	93	93	113	129	----	137	134	217	269	268
106	65	65	97	121	120	127	130	139	155	169	173	177	177	297	345	346
111	55	—	83	103	—	103	96	103	119	133	---	139	145	207	255	307
116	51	50	79	103	109	116	120	127	141	153	161	167	163	265	315	314
121	25	25	61	89	85	123	124	125	153	167	169	179	182	283	329	325
TLimit	—6—			—6—		—4—						—6—			—15—	

PGM (median) - Results of our program (in sample numbers).

REF - CSE Refree results.

TLimit - Tolerance limit recommended by CSE (in sample numbers).

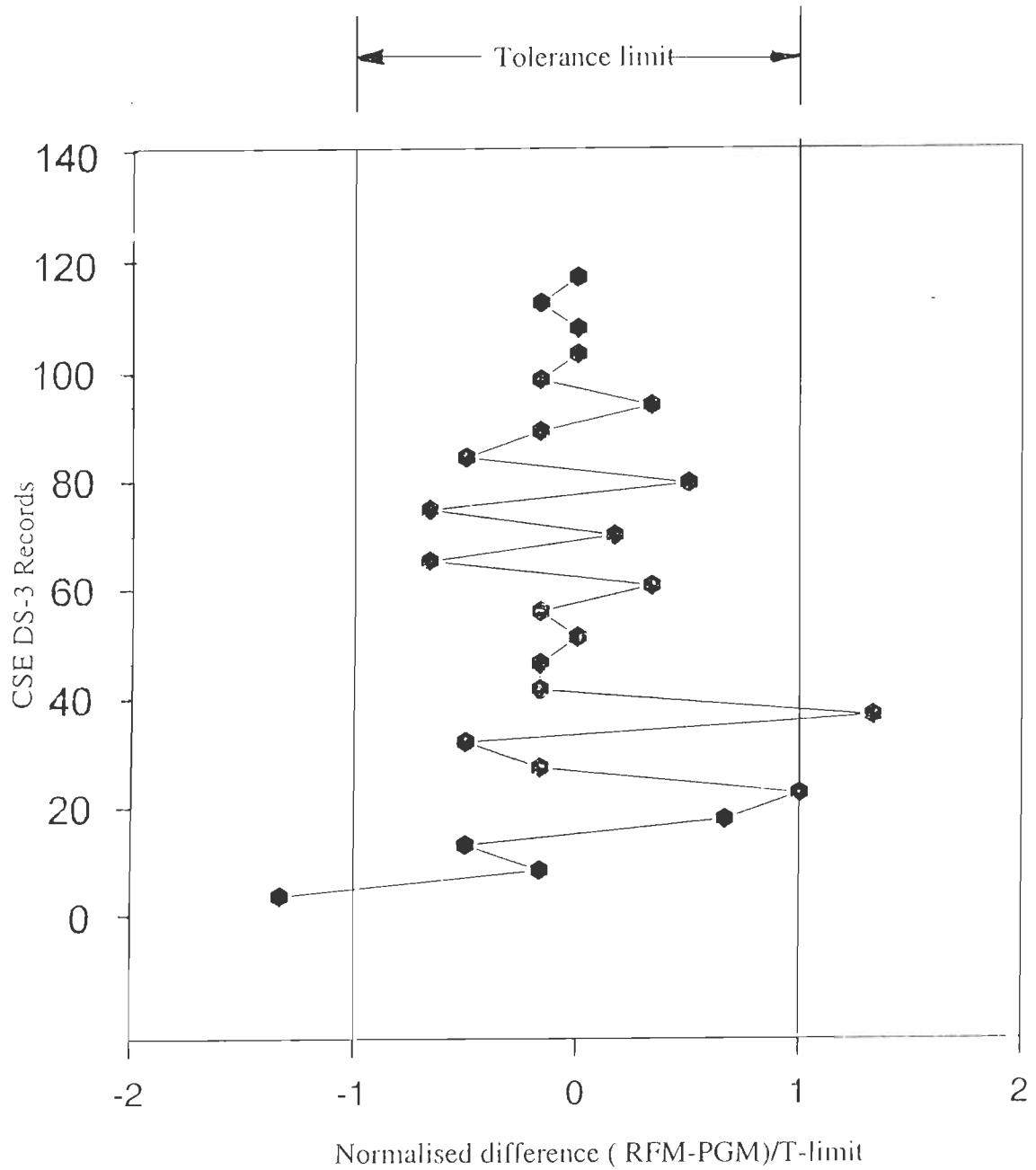


Fig. 4.8(a) Comparison of P-onset program measurements with referee results

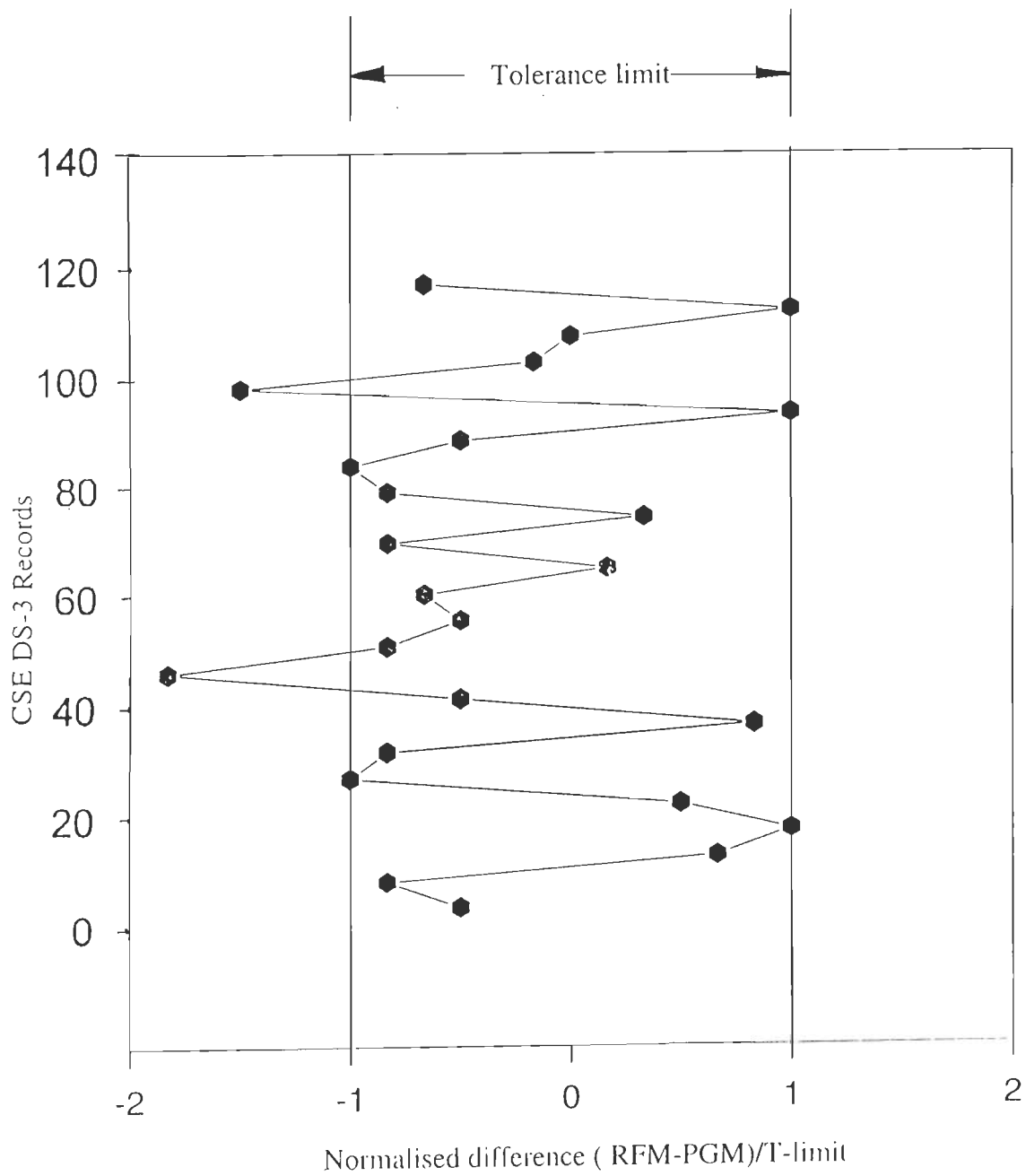


Fig.4.8(b) Comparison of P-offset program measurements with referee results

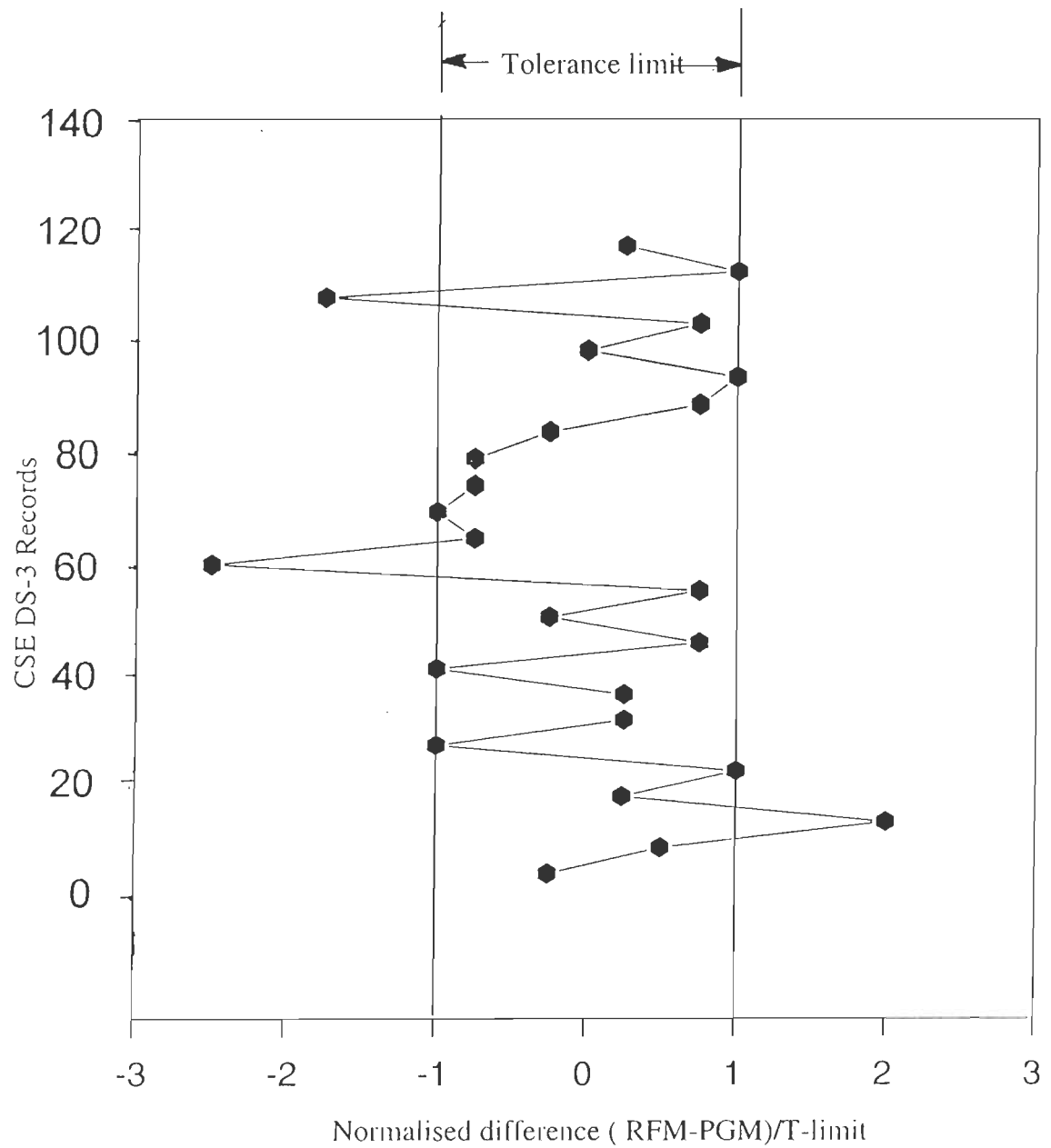


Fig.4.8(c) Comparison of QRS-onset program measurements with referee results

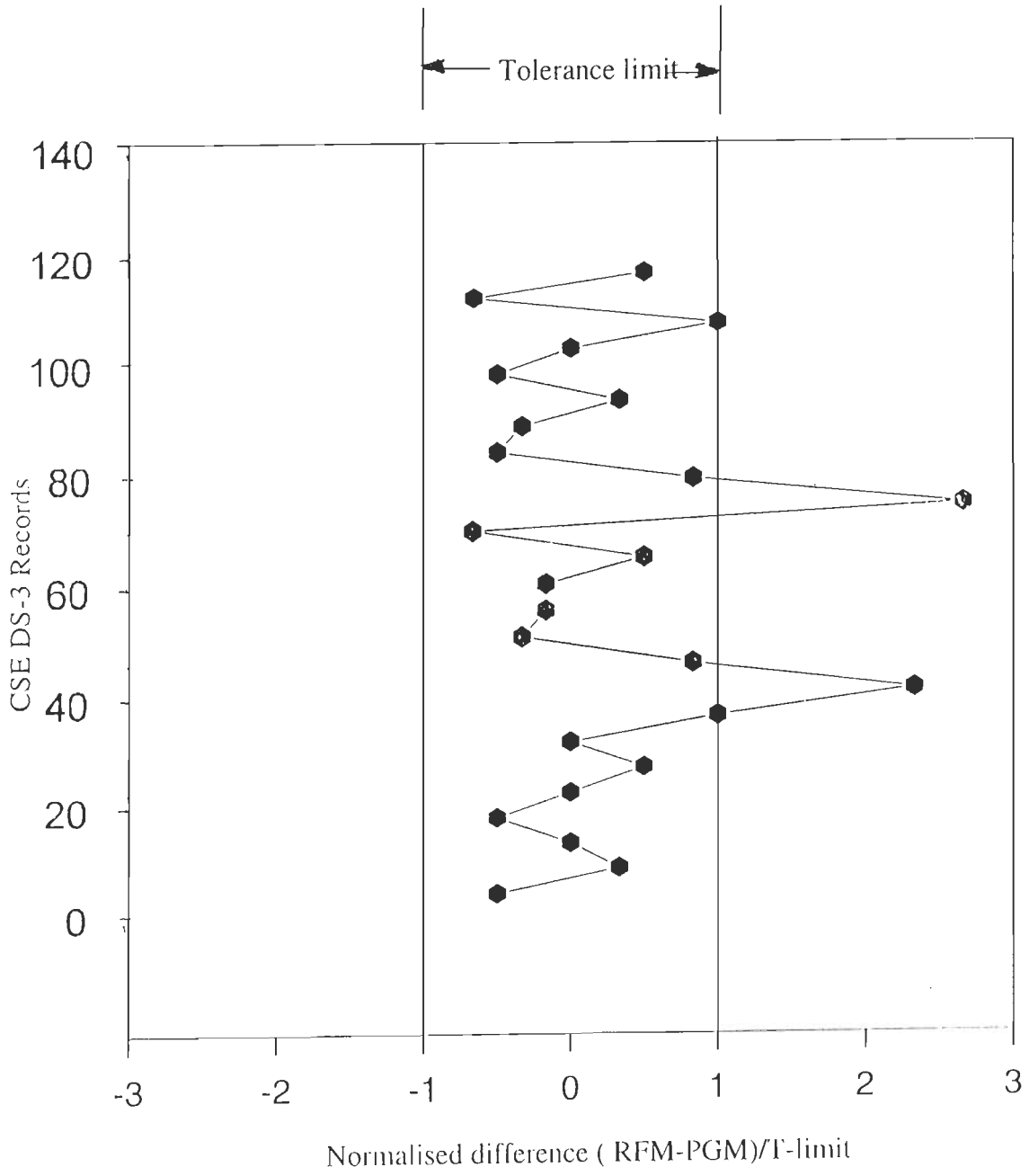


Fig.4.8(d) Comparison of QRS-offset program measurements with referee results

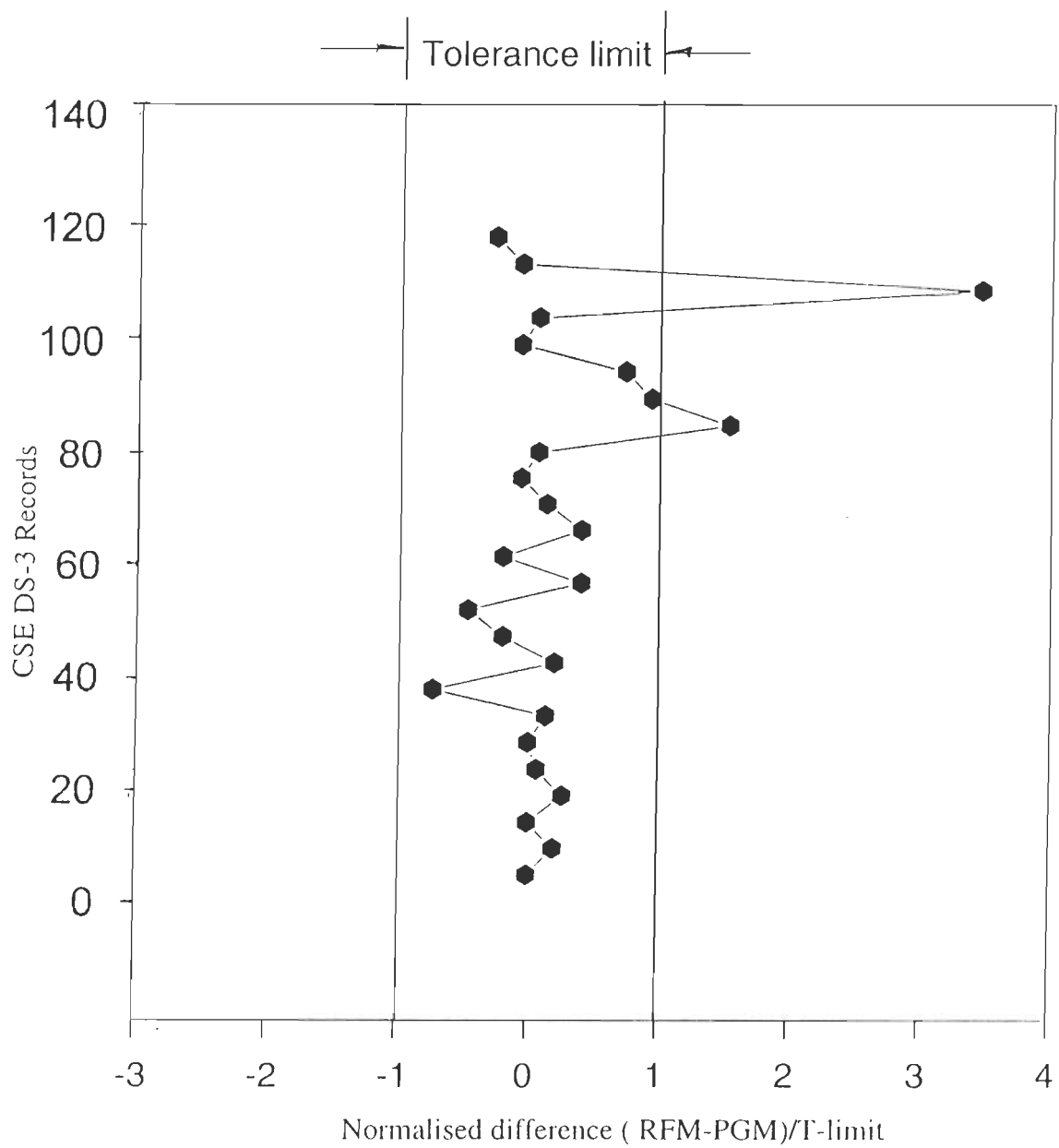


Fig.4.8(c) Comparison of T-end program measurements with referee results

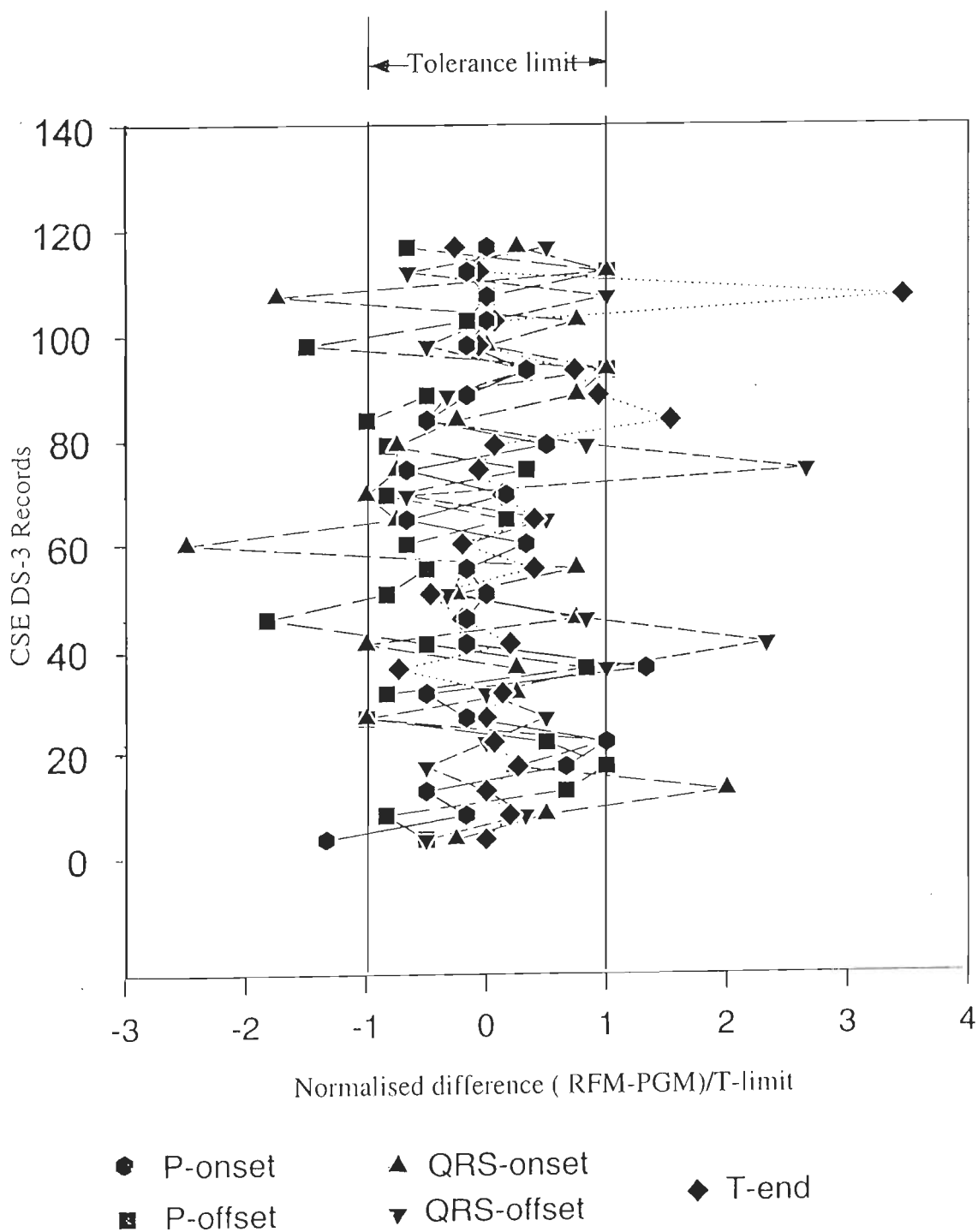


Fig.4.8(f) Comparison of five fiducial program measurements with referee results.

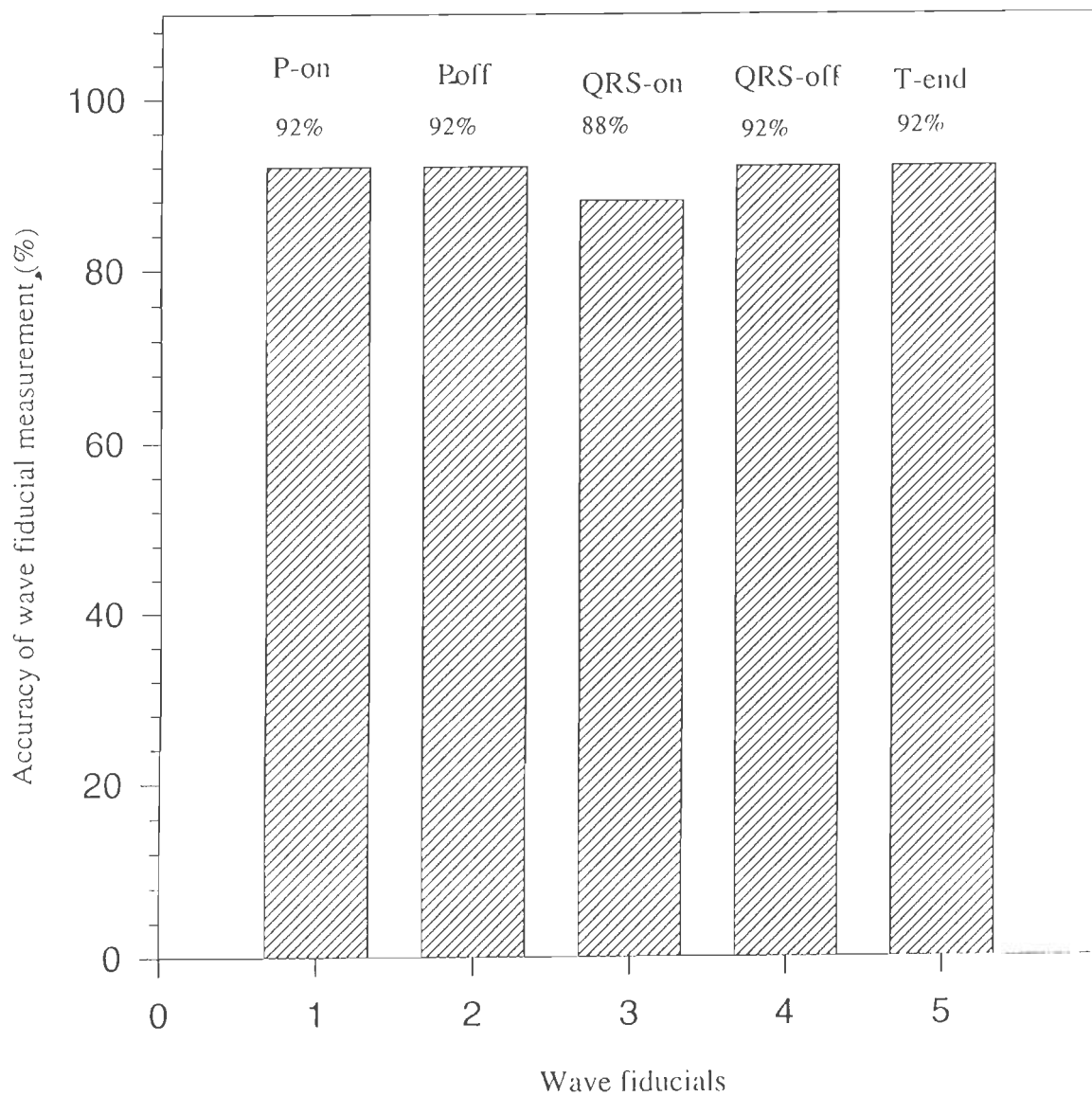
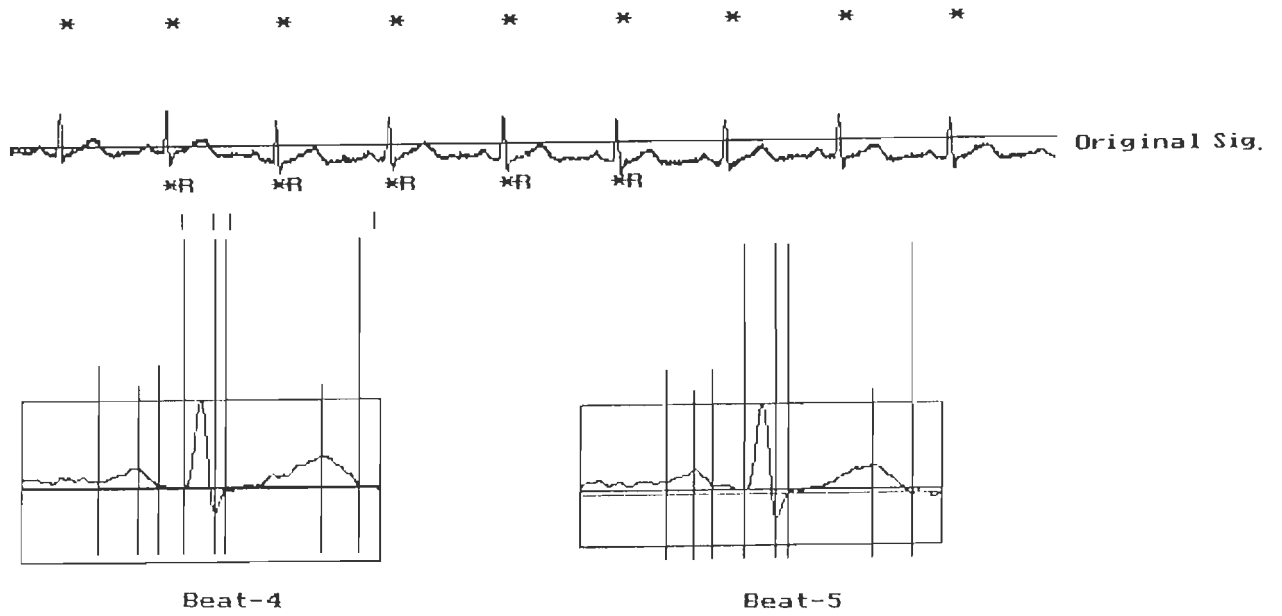


Fig.4.8(g) Comparison of ECG wave fiducial measurements of CSE DS-3 record

namely P onset, P offset, QRS onset, QRS offset and T end for the CSE multi-lead ECG records of DS-3, for which the visual estimates are known. The parameters on the ordinate of the graph is the record numbers and on the abscissa are normalized deviation of a parameter (say P onset), that is, a parameter deviation ($|MREF-PGM|$) from the median value of the visual estimates provided by the human referees of the CSE database, is normalized with respect to the tolerances of the measurement standards, given by The CSE Working Party [149]. It can be observed from the Figs. 4.8(b-f) that the program's estimate of the parameters P-onset, P-offset, QRS-onset and T-end are well within the recommended tolerances except in case of 5 records for onset measurements and 6 records for offset measurements of ECG waves.

From Table 4.3 and the Fig. 4.8(b), it can be observed that in two records, namely: 46 and 101, P-offset deviates by 5 samples (10 ms) and 3 samples (6 ms), respectively more than the specified tolerance. The tolerance limits specified by the CSE for the ECG wave fiducials P-onset, P-offset, QRS-onset, QRS-offset, T-end are 6, 6, 4, 6 and 15 samples, respectively. A similar observation reveals that the estimation of the QRS onset in record number 6 deviates by 4 samples (8 ms), in record 61 by 6 (12 ms) samples and record in record 111 by 3 (6 ms) samples. In the QRS-offset in record numbers 41 and 76, the deviation is of 8 samples. Out of a total 123 fiducial location estimates (i.e. five wave fiducial locations in each of the 25 ECG records, except two estimates), 11 estimates deviate from the tolerance as shown in Fig. 4.8(f). Hence it does not significantly affect the estimation of the diagnostically significant parameters of the ECG analysis. Thus, the algorithm estimation is within the tolerance band in 91.0% of the estimates.

The software has also been tested using the ECGs recorded in the laboratory. Some sample records are given in the Figures 4.9(a-e). Fig. 4.9(a) shows Lead I recording from a subject and the * markings on complete recording indicates the detection of QRS complexes. Out of 9 beats present in the record, 5 beats have been scanned for feature extraction and the resulting diagnostic parameters are given at the bottom of the same Fig. 4.9(a). Looking to the fundamental measurements indicated by vertical lines and the diagnostic parameters extracted from 5 beats, it is clear that the software is reliable to work with indigenous database. Estimated parameters from the five beats, namely heart rate is in the range of 84 to 89 BPM, QRS duration is in the range of 0.08 to 0.09 sec and VAT is in the range from 0.03 to 0.04 sec. In addition, all other parameters are in the normal range. The verification of the actual heart rate measured by pulse rate matches 100% with the median value of heart rate estimate

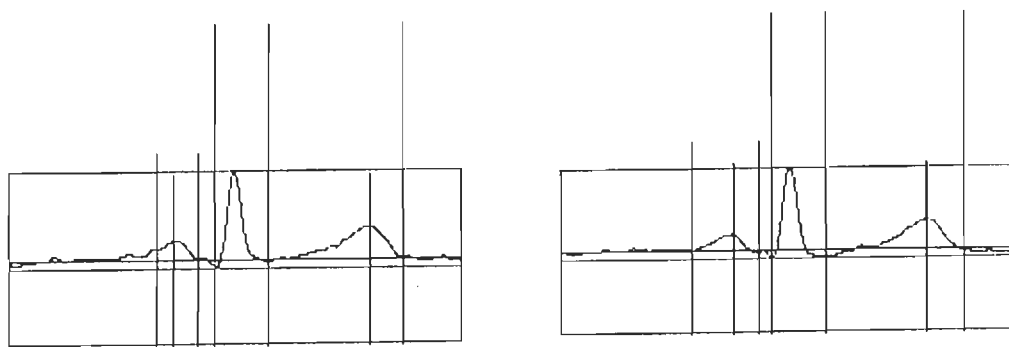
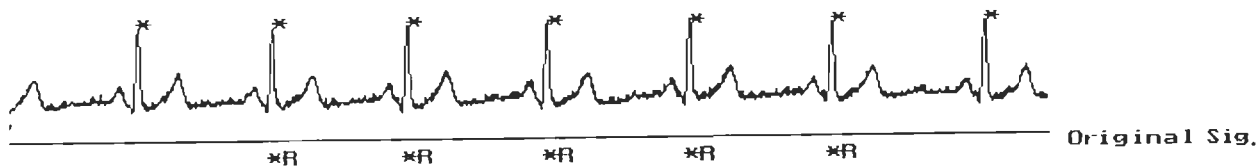


ECG Parameters of Diagnostic Significance

HR BPM	P-A mv	Pdur sec	PRint sec	QRSint sec	QRSp-p mv	QT-int sec	UAT sec	T-A mv	NetD mv	
89.27	0.05	0.11	0.14	0.09	0.47	0.36	0.04	0.05	1.09	Beat=1
88.25	0.02	0.07	0.17	0.08	0.44	0.36	0.04	0.14	6.58	Beat=2
85.15	0.05	0.11	0.15	0.08	0.45	0.36	0.03	0.17	8.43	Beat=3
84.84	0.04	0.11	0.16	0.08	0.47	0.33	0.03	0.14	7.29	Beat=4
85.63	0.04	0.09	0.15	0.08	0.46	0.31	0.03	0.11	9.28	Beat=5

Fig. 4.9(a) Analysis of a ECG signal recorded in the laboratory

(Subject Information : Age 48, Sex Male)



Beat-4

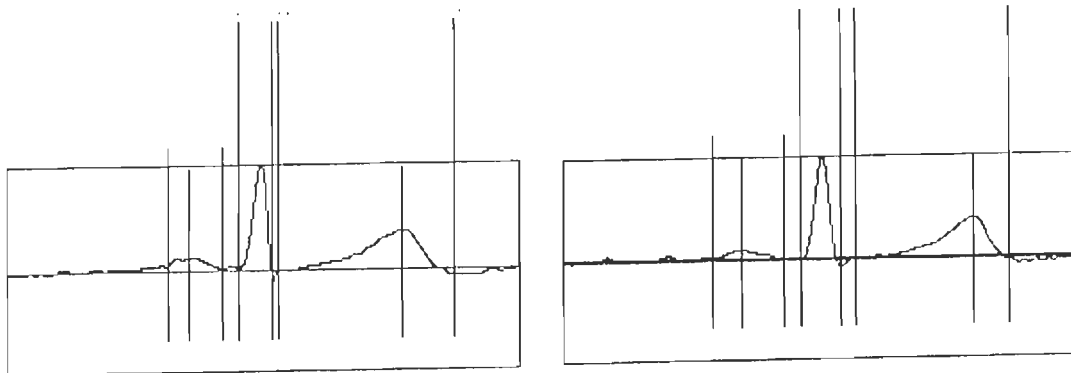
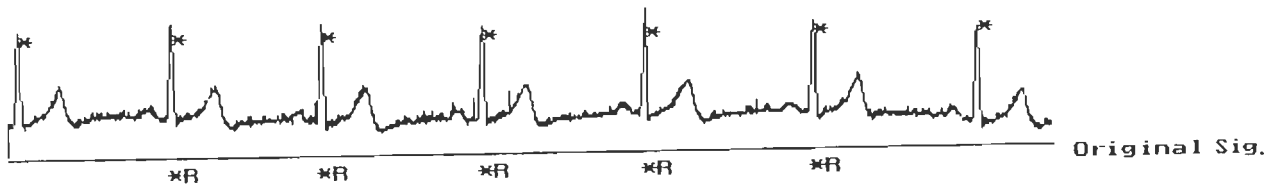
Beat-5

ECG Parameters of Diagnostic Significance

HR BPM	P-A mv	Pdur sec	PRint sec	QRSint sec	QRSp-p mv	QT-int sec	UAT sec	T-A mv	NetD mv	
70.36	0.01	0.12	0.12	0.09	0.82	0.37	0.03	0.34	24.77	Beat=1
71.23	0.05	0.12	0.16	0.11	0.86	0.37	0.04	0.37	29.35	Beat=2
68.07	0.04	0.13	0.13	0.10	0.82	0.37	0.03	0.31	27.49	Beat=3
67.67	0.02	0.08	0.12	0.10	0.82	0.35	0.04	0.33	26.40	Beat=4
67.18	0.07	0.12	0.15	0.10	0.75	0.36	0.03	0.30	23.16	Beat=5

Fig. 4.9(b) Analysis of a ECG signal recorded in the laboratory

(Subject Information : Age 26, Sex Male)



Beat-4

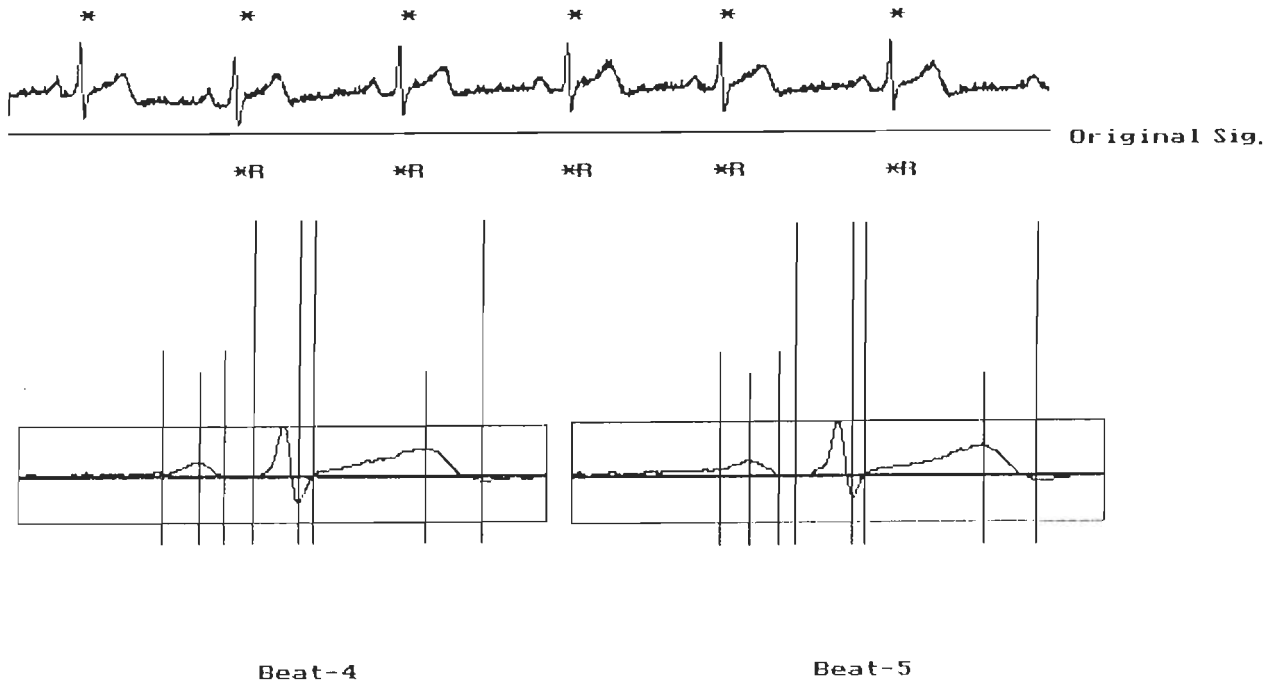
Beat-5

ECG Parameters of Diagnostic Significance

HR BPM	P-A mv	Pdur sec	Print sec	QRSint sec	QRSp-p mv	QT-int sec	UAT sec	T-A mv	NetD mv	
62.62	-0.01	0.05	0.12	0.09	0.89	0.41	0.04	0.25	18.93	Beat=1
63.92	0.00	0.08	0.13	0.09	0.93	0.41	0.04	0.32	22.42	Beat=2
60.10	0.06	0.09	0.19	0.08	0.88	0.41	0.04	0.35	23.07	Beat=3
59.17	0.06	0.10	0.14	0.07	0.96	0.40	0.04	0.33	20.17	Beat=4
57.48	0.05	0.14	0.17	0.10	0.88	0.38	0.04	0.34	20.29	Beat=5

Fig. 4.9(c) Analysis of a ECG signal recorded in the laboratory

(Subject Information : Age 38, Sex Male)

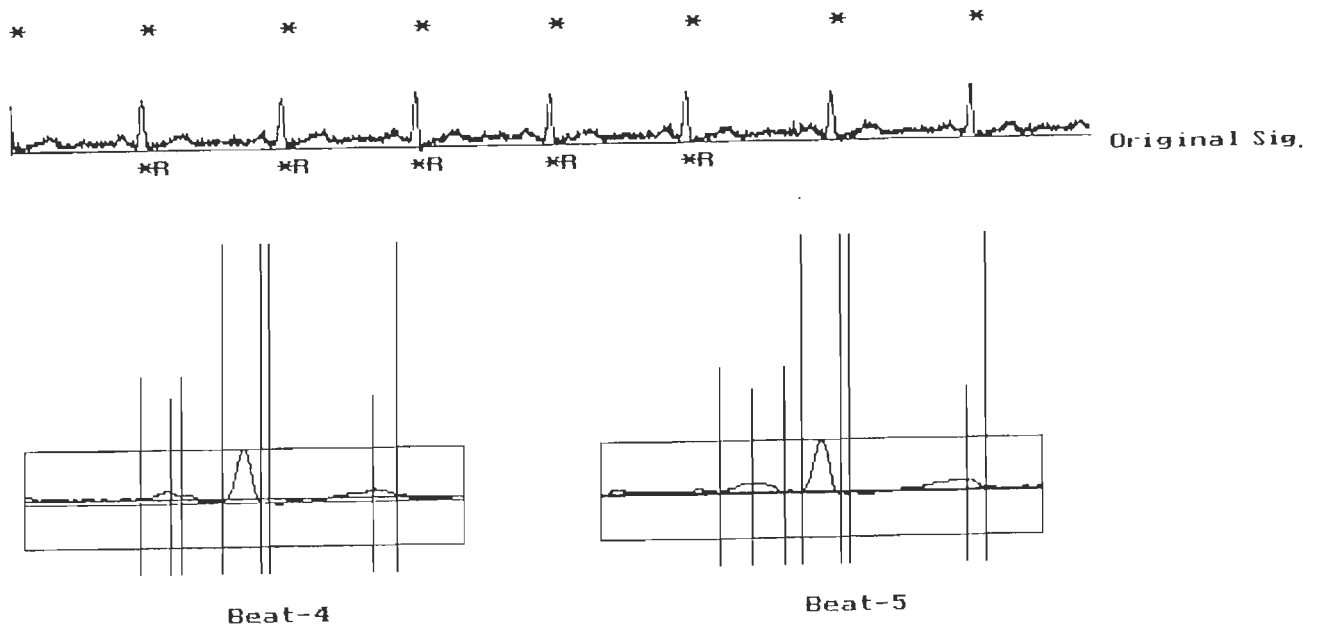


ECG Parameters of Diagnostic Significance

HR BPM	P-A mv	Pdur sec	PRint sec	QRSint sec	QRSp-p mv	QT-int sec	VAT sec	T-A mv	NetD mv	
60.33	0.07	0.09	0.15	0.11	0.64	0.42	0.05	0.43	20.42	Beat=1
59.40	0.08	0.11	0.17	0.10	0.63	0.40	0.05	0.29	11.10	Beat=2
57.33	0.09	0.14	0.19	0.11	0.62	0.43	0.06	0.26	7.86	Beat=3
62.88	0.08	0.11	0.17	0.11	0.61	0.43	0.05	0.22	6.79	Beat=4
57.05	0.06	0.11	0.14	0.13	0.62	0.45	0.08	0.25	10.01	Beat=5

Fig. 4.9(d) Analysis of a ECG signal recorded in the laboratory

(Subject Information : Age 55, Sex Male)



ECG Parameters of Diagnostic Significance

HR BPM	P-A mv	Pdur sec	Print sec	QRSint sec	QRSp-p mv	QT-int sec	VAT sec	T-A mv	NetD mv	
75.29	0.00	0.05	0.10	0.10	0.43	0.34	0.04	0.10	12.24	Beat=1
71.01	0.03	0.12	0.14	0.08	0.44	0.35	0.04	0.11	10.98	Beat=2
74.56	0.04	0.11	0.14	0.09	0.50	0.33	0.04	0.07	9.26	Beat=3
73.96	0.04	0.07	0.15	0.09	0.43	0.32	0.04	0.09	11.47	Beat=4
73.26	0.05	0.11	0.15	0.09	0.45	0.33	0.04	0.09	11.45	Beat=5

Fig. 4.9(e) Analysis of a ECG signal recorded in the laboratory

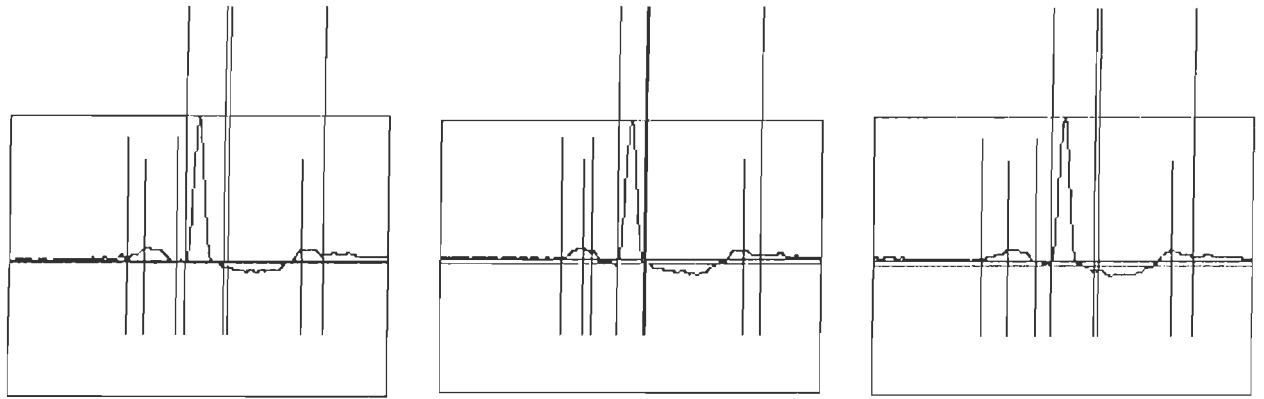
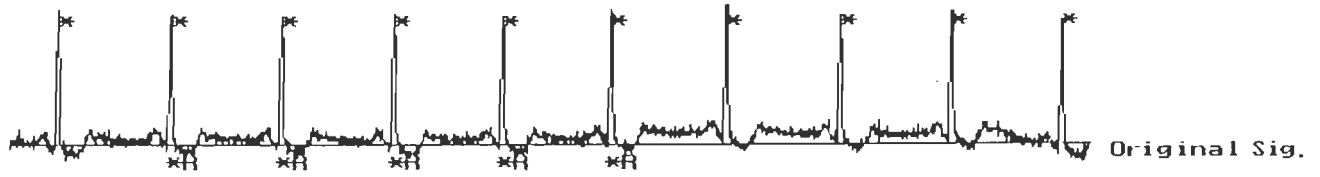
(Subject Information : Age 35, Sex Male)

from 5 beats. Other four ECGs recorded from four different subjects are shown in Figs. 4.9(b-e). The ECG parameter estimates from these records are given and the accuracy in identification of ECG wave segments can be visually observed from the vertical lines at the main wave fiducial locations (P-on, P-peak, P-off, QRS-on and -off, T-peak and -end).

4.9 TEST RESULTS USING CSE DS-5 AND DISCUSSIONS

As explained in the first chapter, the CSE DS-3 is called a measurement data set because CSE has published the measurement results of this data set. Therefore, to evaluate the performance of the developed software, the results can be compared with the results published by the CSE group. This database is such, in which, a section of beats in all 12 standard leads having least noise and baseline wander has been selected and copied repeatedly to construct the complete record of length 8-10 seconds. This is in consideration that the original recordings usually contain a lot of beat-to-beat variability and give beatwise variations in the parameter values. Hence the comparison of various programs becomes difficult as they give different results on the same data set. Though, it is not artificial but constructed from the real recording, the DS-3 is called an artificial data set.

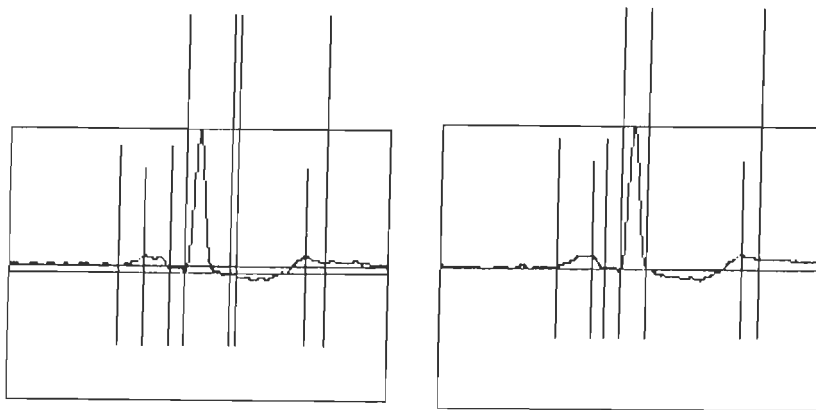
After confirmation of the reliability of software using CSE DS-3, diagnostic dataset (CSE DS-5) has been used for analysis and disease diagnosis. As shown in Fig. 4.10(a-c), three ECGs of record D-0001.DCD from CSE DS-5 are given. Here five beats from each ECG lead have been scanned to extract the parameters. As in the case of CSE DS-3 records, measurements from 5 beats show the same parameters with no variable values as all beats in an ECG remained to be the same (hence it may be called as artificial dataset). The CSE DS-5 contains original recordings and show variations in the parameter estimates, these are shown at the bottom of Fig. 4.10(a). For example, in lead I (Fig. 4.10(a)), heart rate readings are 56.82 BPM for beat-1, 58.25BPM for Beat-2 and 57.69, 59.76 and 60.24 BPM for remaining three beats, respectively. In the same manner, other parameters namely, P-amplitude, P-duration, PR-interval, QRS-interval, QRS-p-p, QT-interval, VAT, T-amplitude and the net QRS deflection show variations as per the beat measurements. Five main wave fiducials measured from five beats of D-00001.DCD record are given below to compare measurements of same fiducials in different beats. The median values of wave onsets and offsets mentioned in sample numbers for P, QRS and T end estimates from five beats are almost in the same range, indicating the exact measurements.



Beat-1

Beat-2

Beat-3



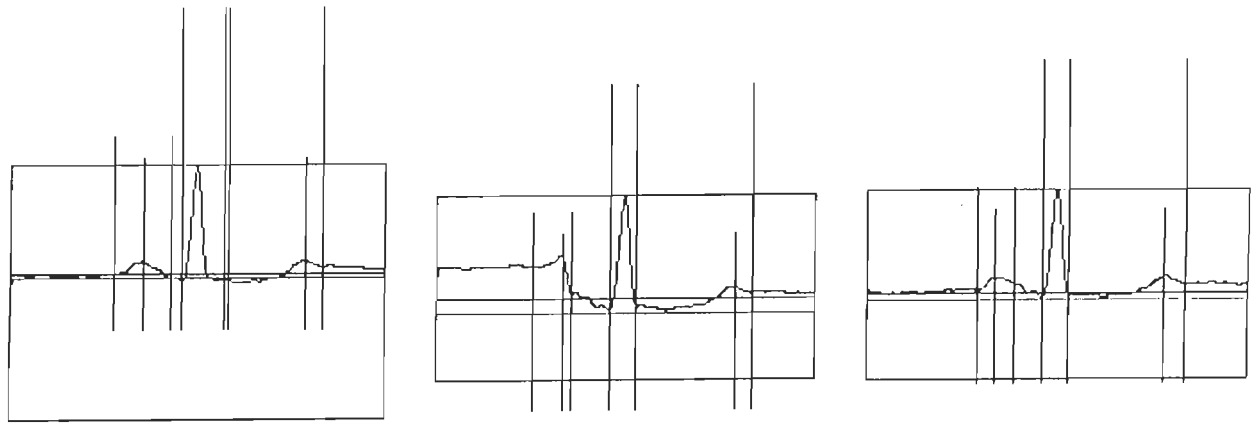
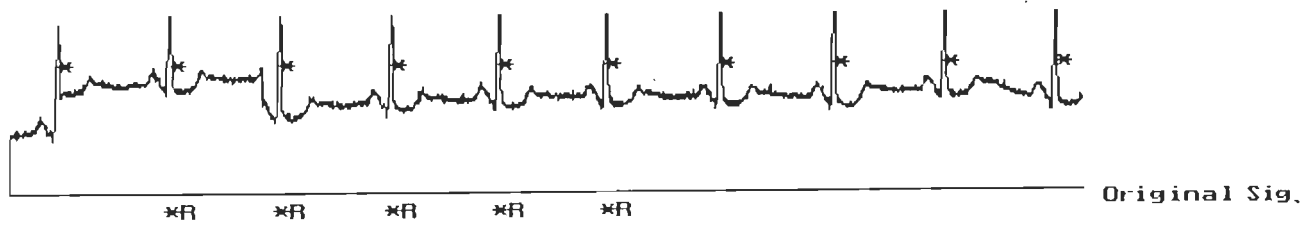
Beat-4

Beat-5

ECG Parameters of Diagnostic Significance

HR BPM	P-A mv	Pdur sec	Print sec	QRSint sec	QRSp-p mv	QT-int sec	VAT sec	T-A mv	NetD mv	
56.82	0.08	0.14	0.16	0.12	1.16	0.38	0.04	0.12	19.80	Beat=1
58.25	0.03	0.08	0.16	0.08	1.10	0.40	0.04	0.11	19.68	Beat=2
57.69	0.05	0.15	0.20	0.14	1.19	0.40	0.04	0.12	20.96	Beat=3
59.76	0.06	0.14	0.19	0.14	1.13	0.39	0.04	0.13	19.92	Beat=4
60.24	0.08	0.14	0.18	0.07	1.11	0.38	0.03	0.12	18.56	Beat=5

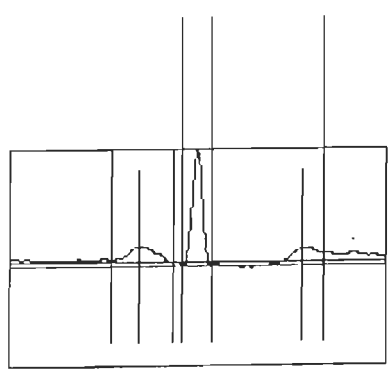
Fig. 4.10(a) Analysis of 5 beats in a ECG signal (CSE DS-5 record D-00001, Lead I)



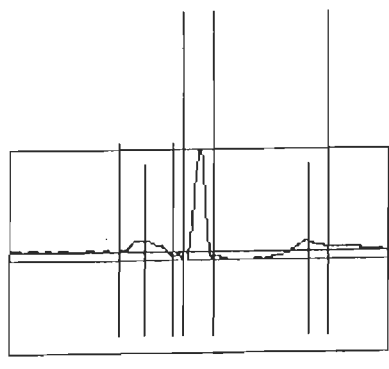
Beat-1

Beat-2

Beat-3



Beat-4

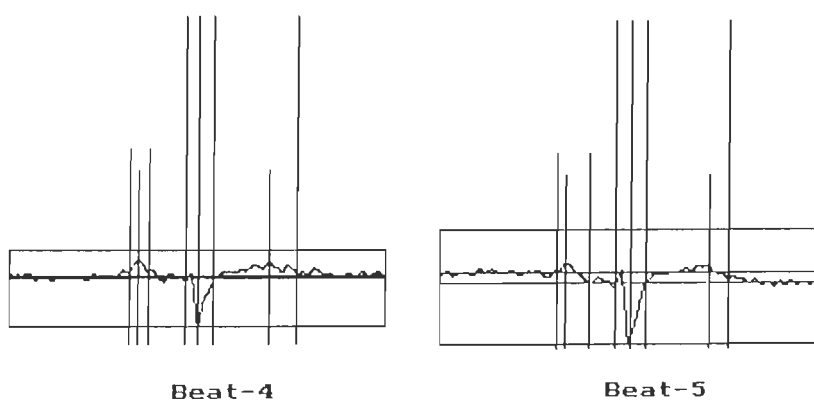
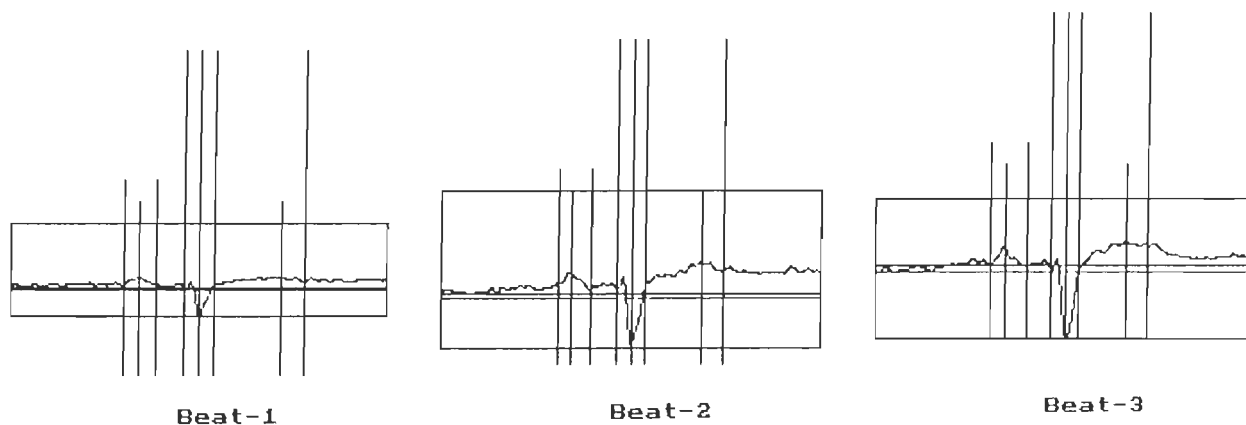
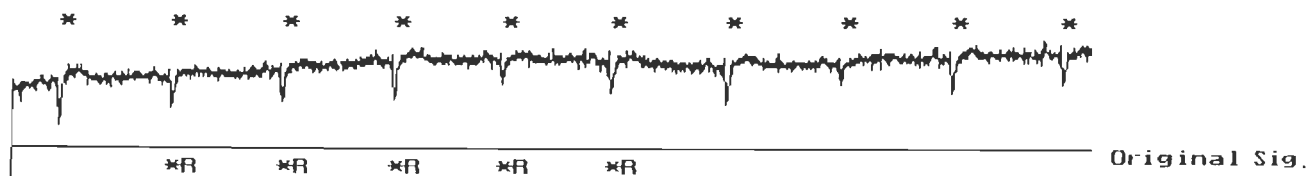


Beat-5

ECG Parameters of Diagnostic Significance

HR BPM	P-A mv	Pdur sec	PRint sec	QRSint sec	QRSp-p mv	QT-int sec	QAT sec	T-A mv	NetD mv	
57.03	0.08	0.16	0.20	0.13	0.92	0.39	0.04	0.12	14.73	Beat=1
58.14	0.00	0.10	0.22	0.07	0.89	0.39	0.04	0.07	15.00	Beat=2
57.80	0.06	0.10	0.19	0.07	0.84	0.39	0.04	0.12	14.27	Beat=3
59.76	0.07	0.18	0.21	0.08	0.92	0.39	0.04	0.10	15.03	Beat=4
59.88	0.03	0.15	0.19	0.08	0.86	0.40	0.04	0.09	14.86	Beat=5

Fig. 4.10(b) Analysis of 5 beats in a ECG signal (CSE DS-5 record D-00001, Lead II)



ECG Parameters of Diagnostic Significance

HR BPM	P-A mv	Pdur sec	PRint sec	QRSint sec	QRSp-p mv	QT-int sec	VAT sec	T-A mv	NetD mv	
57.14	0.07	0.09	0.18	0.08	0.27	0.34	0.02	0.07	-3.51	Beat=1
58.37	0.04	0.09	0.16	0.08	0.27	0.30	0.02	0.11	-2.29	Beat=2
57.58	0.06	0.10	0.17	0.08	0.32	0.27	0.02	0.10	-3.86	Beat=3
60.00	0.04	0.06	0.16	0.08	0.20	0.31	0.02	0.06	-1.97	Beat=4
59.64	-0.00	0.09	0.17	0.08	0.29	0.31	0.02	0.04	-3.43	Beat=5

Fig. 4.10(c) Analysis of 5 beats in a ECG signal (CSE DS-5 record D-00001, Lead III)

Beat	P -on	P -off	P (off-on)	QRS -on	QRS -off	QRS (off-on)	T -end	T -end to QRS-on
1	112	156	44	196	238	42	396	200
2	106	157	51	193	236	43	392	199
3	102	158	56	195	235	40	392	197
4	110	160	50	196	236	40	392	196
5	110	159	49	195	236	41	394	197

4.10 STATISTICAL ANALYSIS OF ECG PARAMETERS

Statistical analysis in Tables 4.4 (a-e) is given for the program estimates carried using the CSE DS-5. The median values are calculated from the measurements of standard 12 leads ECGs in all 5 beats, separately, as well as for all combined five beats [95]. This includes main five wave fiducials i.e. P -onsets and -offsets, QRS -onsets and -offsets, and T end. From a record, five regular beats per lead are selected and about 29 parameters per beat per lead are extracted. Hence total parameters of a beat from a record containing 12 leads result in $12 \times 25 = 348$ measurements. The software extracts the parameters from five such beats in 12 standard leads.

Results are produced in the form wave onsets and offsets, various listings and tables containing comparisons of individual 5 beats results with median program results. Mean, Standard Error (SE), Median, Mode, Standard Deviation (SD) and Standard Variance (SV) are calculated for both the data sets DS-3 and DS-5. For DS-3, as the different beats in a lead are same, there is no point in giving details of mean, SE, median and SD. For DS-5, parameter statistics is performed to evaluate mean differences and variances between individual and median values of program results. With respect to interval and amplitude measurements of various components of the QRS complex (Q, R, S, R', S' waves) as well as of the P wave and ST-T complex, a median value of program results from 12 SL is used as a reference to compare individual results. The average measurements of P, PR, QT, and QRS duration obtained from the 12 lead were compared with the median values. These details are given at the bottom of Tables 4.4(a-e).

The median results derived from combined 12 lead measurements proved to correlate in the best way with the results of the visual analysis. The statistical parameters, namely, SE

and SD derived from 12 SL measurement show the best performance of the ECG analysis. For example, in beat-1 of CSE DS-5 Record D-0001.DCD (Table 4.4(a)), for heart rate estimates the mean value is 56.8058 BPM, variance is 0.3503, SE is 0.170 and SD 0.5918; for P-amplitude, the mean value is 0.1075 mV, variance is 0.0008, SE is 0.008, and SD is 0.0292; for P-duration, the mean value is 0.0975 sec, variance is 0.0008, SE is 0.008 and SD is 0.0295; for PR-interval, the mean value is 0.1533 sec, variance is 0.0011, SE is 0.009 and SD is 0.0336; for QRS-interval, the mean value is 0.1108 sec, variance is 0.0009, SE is 0.009 and SD is 0.0314; for QRS p-p, the mean value is 1.2950 mV, variance is 0.4928, SE is 0.202 and SD is 0.7020; for QT-interval, the mean value is 0.3941 sec, variance is 0.0038, SE is 0.017 and SD is 0.0620; for VAT, the mean value is 0.0433 sec, variance is 0.0004, SE is 0.006 and SD is 0.0210, and for T amplitude, the mean value is 0.21 mV, variance is 0.0575, SE is 0.069 and SD is 0.2398. As expected, the duration related parameters in a beat (beat 1 of all 12 SL) showed small variations in value of parameters as compared to amplitude related parameters. This is because a wave in different leads has different amplitude values and nearly same duration values [42,74].

The SD for different parameters (Table 4.4(a), beat 1) varies from 0.021 to 0.702. The highest SD (0.702) belongs to QRS p-p and the lowest belongs to S position, therefore, the parameter estimates from individual 12 SL are coinciding best with overall program median.

4.11 CONCLUSIONS

The ultimate aim of the ECG analysis is the disease diagnosis. In general, the automated disease diagnostic is being carried out by observing the limits of the ECG parameters and by applying different scoring criteria for the disease classification. Therefore, the reliability of the disease diagnosis is totally dependent on accuracy of the ECG parameter estimates. As discussed earlier, the check has been made by comparing the program results with the referee results in case of CSE DS-3 dataset and statistical analysis has been used to see that the measurements are reliable and accurate.

On the basis of the outcomes of the present work, it can be stated that the use of the combined wavelets in the ECG analysis has the following advantages:

- (i) The WT detects the QRS complexes with high sensitivity and eliminates baseline wander, artifacts and noise. This avoids the use of additional filters for noise reduction.

- (ii) The approach of combined wavelets proved very powerful as it gives high sensitivity for QRS, P and T detection compared to other existing methods of detection even with signals corrupted with baseline wander, noise and artifacts.
- (iii) The aspect of avoiding down-sampling the output of high-pass filter reduces the loss of information.
- (iv) The smoothing feature of the DU6 wavelet makes it more suitable than the QS wavelet to detect P and T wave fiducials.
- (v) Usually, the fixed window width concept fails due to variability in the heart rate, therefore, the use of a variable window width determined from the R-R interval gave accurate results.
- (vi) Due to high accuracy of R-R interval measurement, this method may find wider use in the detection of arrhythmia and heart rate variability and the use of WT will definitely find distinct place for itself in the field of computer aided ECG analysis and interpretation.

DISEASE DIAGNOSIS USING MULTILEAD ECG

5.1 INTRODUCTION

The number of cardiac patients are increasing at an alarming rate and it is not practically possible to take care of all of them by the limited number of existing expert cardiologists. This situation is not only true for India, but exists in every country in the world. Computer aided interpretation and diagnostics is the only solution to this problem. This problem was anticipated by the researchers as long as about 43 years ago and the first attempt to automate ECG analysis by digital computer was made in 1957 by Pipberger et al.[110]. During last 40 years, computer based ECG processing and analysis has gained tremendous momentum and the developments related to computer aided analysis of ECG signals have gone hand-in-hand with the advances in computing technology [80]. Computerized ECG analysis and interpretation requires signal conditioning, data acquisition, processing, feature extraction, inferencing and disease diagnosis. Drazen reported that in the year 1987 over 50 million ECG signals were analyzed using computer based technique in North America only. Macfarlane et al. [80] reported that this level at least doubled by the year 1990. This itself indicates the utmost necessity of the computer based systems for the cardiac disease diagnostics.

The ultimate aim of ECG analysis is disease diagnosis. The diseases namely, Left Ventricular Hypertrophy (LVH), Right Ventricular Hypertrophy (RVH), Myocardial Infarction (MI), Right Bundle Branch Block (RBBB), Left Bundle Branch Block (LBBB), Tachycardia and Bradycardia are the common heart diseases seen in the heart patients. Therefore, the same diseases are considered in the present work. In general, disease diagnosis is carried out by observing the limits of ECG parameters, i.e. application of different scoring criteria for disease classification. The reliability of disease classification is based on accuracy of the measured parameters and the use of more than one criterion simultaneously [78,102].

A good number of techniques have been developed for the feature extraction which are broadly classified (as discussed in earlier chapters) into four categories, namely i) syntactic, ii) non-syntactic, iii) hybrid and iv) transformative techniques. Currently WT based feature extraction techniques have gained lot of attention of researchers and are being exploited for effective and dependable tools for computer aided diagnostics. One of the reasons in favour of WTs is that, they characterize the local regularity of signals by decomposing the signal into elementary building blocks that are well localized both in time

and frequency, and thereby, make them robust to eliminate noise. It is being felt by the researchers that in future, WT may be the ultimate choice for ECG feature extraction.

To see that the measured parameters provide correct diagnosis, we have used firstly the CSE DS-3 data records and the alternate scoring criteria for the same disease [93,102]. If both the criteria give the same diagnostic statement for the same input parameters, then this reflects the accuracy of the estimated measurements. This is due to the fact that different scoring criteria use different ECG parameters to diagnose the same disease. The scoring criteria to detect LVH and RVH used by Marriot [91], S.S. Mehta et al. [93], and Maheshwari et al. [82], have been used and are given in Tables 5.1 - 5.3. The use of two criteria has been made to cross check and confirm the disease diagnostics. The detection of tachycardia or bradycardia is made on the basis of heart rate, if it is above 100 beats/min, it is the case of tachycardia and if it is below 60 beats/min, it is the case of bradycardia [42].

This chapter deals with a computer based cardiac disease diagnosis system which has been developed using the wavelet transforms for QRS detection and for logical interweaved inferences for Left Ventricle Hypertrophy (LVH), Right Ventricle Hypertrophy (RVH), Myocardial Infarction (MI), Right Bundle Branch Block (RBBB) and Left Bundle Branch Block (LBBB). The system has been tested for its diagnostic performance for the above diseases using modified scoring criteria developed in this work. The results are compared with the diagnostic results reported by the CSE Working Party and existing scoring criteria reported by other workers. The developed system with the combined use of wavelets and the modified scoring criteria is expected to establish itself as an ideal solution for computer aided diagnostics of cardiac diseases.

5.2 CARDIAC DISEASES

More common cardiac diseases namely, LVH, RVH, MI, RBBB and LBBB have been considered in this work. This section explains the commonly used interpretation criteria for a particular disease.

5.2.1 Electrical Axis of QRS

As previously stated, the total electrical activity produced by ventricular depolarization may be expressed as a vector, i.e., the mean QRS vector. In the plane of the limb leads (frontal plane), it can be represented as an arrow originating from the center of the Einthoven's triangle. This arrow is called the mean manifest QRS electrical axis or the mean QRS axis in the frontal plane.

Table 5.1 Scoring criteria for RBBB and LBBB

Criteria	Point score
RBBB Criteria	
QRS duration in V1 ≥ 0.12 sec	01
VAT in V1 ≥ 0.08 sec	01
R' $>$ R in V1	01
T in V1 < -0.1 mV (inverted T)	01
Q in V1 $\neq < -0.01$ mV &	01
Q duration = 0 sec (No Q in V1)	
	If Total score ≥ 3 , RBBB
LBBB Criteria	
QRS duration in V5 or V6 ≥ 0.12 sec	01
VAT in V5-6 ≥ 0.08 sec	01
R' $>$ R in V5-6	01
T in V5-6 < -0.1 mV	01
Q in V5-6 $\neq < -0.01$ mV &	01
Q duration = 0 sec	
	If Total score ≥ 3 , LBBB

Table 5.2 Existing and modified LVH scoring criteria

A	Mehta et al.[93]	score	Diagnostics
01	Minimal criteria : RaVL > 11 mm or RV5, V6 > 27 mm or SV1 + RV5, V6 >35 mm	03	If total score is = 3, LVH possible = 4, LVH probable ≥ 5 with minimal criteria satisfied, LVH definite.
02	VAT in V5, V6 > 0.05 s	01	
03	QRS duration > 0.1 s	01	
04	ST- segment depression & T inversion in V5, V6	01	
05	RI + SIII > 26 mm in horizontal heart (-30° < QFPA < 0°)	01	
06	RaVF > 20 mm in vertical heart (75° < QFPA ≤ 110°)	01	
07	Frontal plane QRS axis superior to -30°	02	
B	Okajima et al.[102]		
01	RV6 > 2.6 mV	03	If total score is > 4, with abnormal ST-T on leads V5, V6 or RV5, V6 > 4.0 mV, definite LVH >6, definite LVH
02	RV5 > 2.6 mV	03	
03	RaVL > 1.2 mV	02	
04	RI,II,III,aVF > 2.5 mV	01	
05	QV5 < QV6 & QV6 < -0.5 mV	02	
06	RV6 + SV1 > 3.5 mV	03	
07	RV5 + SV1 > 3.5 mV	02	
08	RI > 1.5 mV	02	
09	-30° ≥ axis > -90°	01	
10	-5° ≥ axis > -30° (< 11 years)	01	
C	Marriot [91]		
01	R or S in limb lead ≥20 mm or SV1,V2 ≥30 mm or RV5, V6 > 30 mm	03	If total score is = 4, probable LVH = 5, definite LVH
02	Any ST shift (without digitalis) Typical 'strain' ST-T (with digitalis)	03 01	
03	LAD (-30° or more)	02	
04	QRS interval ≥ 0.09 s	01	
05	I.D. in V5, V6 ≥ 0.05 s	01	
06	P – terminal force in V1 > 0.04	03	
D	Modified Scoring Criteria		
01	RI + SIII > 2.5mV with horizontal heart	02	If total score is > 4, LVH possible ≥ 6, LVH probable ≥ 8, LVH definite
02	RV5 + RV6 + SV1 ≥ 3.5mV	02	
03	RV5, V6 > 2.6mV	02	
04	RaVL > 1.1 mV with horizontal heart or RaVF >2.0mV with vertical heart	02	
05	ST- segment depression & T inversion in V5, V6	01	
06	VAT in V5, V6 > 0.05 s	01	
07	QRS duration > 0.11 s	01	
08	LAD (-30° to -90°)	01	
09	Q wave present in V1, V2	01	

Table 5.3 Existing and modified RVH scoring criteria

A	Mehta et al.[93]	Score	Diagnostics
01	Minimal criteria RAD or Rs (R/S > 1) or qR (R/Q > 1) with VAT > 0.03 s in V1	03	If total score is = 3, RVH possible = 4, RVH probable ≥ 5 with minimal criteria satisfied, RVH definite
02	Persistent S-peak in V5, V6	01	
03	ST- segment depression & T inversion in V1	01	
04	ST- segment depression & T inversion in V2	01	
05	ST- segment depression & T inversion in V3	01	
06	ST- segment depression & T inversion in II & III	01	
07	RaVR ≥ 5 mm	01	
08	RaVF ≥ 5 mm with ST-T inversion in aVF	01	
B	Okajima et al.[102]		
01	RV1 > 0.5 mV	03	If total score is = 3, possible RVH ≥ 4, probable RVH ≥ 6, definite RVH
02	R'V1 > 1.0 mV & RV1 ≥ SV1 & negative T V1 ≤ -0.2 mV	03	
03	Q ≤ -0.1 mV & RV1 > SV1	01	
04	Both R ≤ S/2 and Rv4 ≥ 0 mV	01	
05	RV5 < SV6 or RV5, V6 < -1.5 mV	01	
06	SV5, V6 ≤ -1.5 mV	01	
07	RAD	01	
C	Maheshwari et al.[82]		
01	Axis > 90° (begin scoring)	03	If total score is ≥ 4, cannot rule out RVH ≥ 6, possible RVH ≥ 8, definite RVH
02	Axis > 110°	03	
03	RV5, V6 > 2.6 mV	01	
04	RI, II, III, aVF > 2.5 mV	02	
05	RV1 or R'V1 > 0.5 mV	01	
06	ST depression > 0.2 & TV1, V2, V3 < -0.1 each	01	
07	RV4 < S/2 and RV4 > 0 mV	01	
08	R/S < or R < 1.5 mV in V5, V6 or S < -0.5 mV in V5, V6	02	
D	Modified RVH Scoring Criteria		
01	RV1 + SV5 ≥ 1.05 mV or RV1 + SV6 ≥ 1.05 mV	01	If total score is > 4, RVH possible ≥ 6, RVH probable ≥ 8, RVH definite
02	RV1 > 0.7 mV	01	
03	RaVR > 0.5 mV	01	
04	SV1 < -0.2 mV	01	
05	ST- segment depression & T inversion in V1	01	
06	VAT in V1 > 0.035 s	01	
07	QRS duration > 0.11 s	01	
08	RAD (90° to -150°)	01	
09	Q wave present in V1	01	

An accurate determination of the QRS axis can be made utilizing the QRS deflection in any two of the three standard limb leads. The net area enclosed under the QRS in each given lead is first calculated. The net area is the algebraic sum of the negative and positive areas. This is expressed in microvolts-seconds. The calculated net area of each given lead is then appropriately represented on the Einthoven's triangle [74,78].

5.2.2 Significance of the QRS Axis

Axis is expressed in degrees as a deviation from the 3 O'clock axis (lead I at 0°). Left axis deviation (LAD) is to exist when the axis lies between -90° and -30° (clockwise) and right axis deviation (RAD) is present when the axis lies between $+90^\circ$ and -150° through 180° . The normal range of frontal plane QRS axis (FPA) is between -30° and 90° through 0° . However, the electrical axis in some normal individuals has been found to range from -30° to 90° . Conversely, the people with definite evidence of heart disease, such as ventricular hypertrophy (VH), may display a normal axis. Because of this fact, many authors felt that the electrical axis had little value in diagnosis [74,145]. However, FPA lying outside the range between -30° and 90° , indicates the probability of ventricular hypertrophy, conduction defect, or myocardial infarction.

It is obvious that the QRS axis varies with the age, body built and different diseases [42,74]. In RVH with congenital heart disease, the QRS axis may be found between -90° and -150° . In LVH, the QRS axis is often present between 0° and -45° , although it may deviate rightwards as far as between $+60^\circ$ and $+90^\circ$ (particularly in adolescent rheumatic aortic disease, where coexisting right ventricular prominence may account for the lack of LAD). In RVH, the QRS axis usually deviates rightwards, to lie between $+90^\circ$ and $+150^\circ$, although no axis deviation may be present. In LBBB, the QRS axis is usually between 0° and -75° . In general, the greater the block, the greater is the left axis deviation. In RBBB, the QRS axis may be found between $+90^\circ$ and -90° , depending on the type of RBBB; also, occasionally LAD in the extremity leads (QRS axis around -75°) may be mistaken for LBBB, but the chest leads establish the diagnosis of RBBB. In MI, the QRS axis also undergoes a deviation, since the QRS vector forces tend to move away from the "dead zone". The explanation for this statement is that, under normal conditions the vector forces in a given ventricular wall are at least, partially neutralized by those forces produced in the opposite wall. In MI, the necrotic zone of muscle becomes electrically inactive, so that the electrical forces in the opposite healthy wall are transmitted unopposed, with no forces to counterbalance them, and the vector force tends to move away from the zone of infarcted muscles. An anterolateral MI will

have a QRS axis pointing upward, around -60° , away from the infarcted area. Thus the QRS axis can be a useful adjunct, if used intelligently, in the analysis of the clinical electrocardiogram [74].

5.2.3 Left Ventricular Hypertrophy

The electrocardiographic interpretation of ventricular abnormalities particularly hypertrophy, bundle branch block (BBB) and MI, has been greatly simplified by the application of the unipolar scalar technique. The chest leads are less influenced by position. They offer more favorable advantage points and record a more valid picture (morphology) of altered myocardial potentials as they are close to heart. For example, in LVH and LBBB, the left precordial leads demonstrate characteristic abnormal morphologic patterns. Similarly, the right precordial leads reflect diagnostic alterations in RVH and in RBBB. It is important to remember that, the entire ECGs (the standard extremity leads and the chest leads) must be analyzed and correlated with the panoramic morphologic picture in order to reach a valid interpretation. In the abnormal, as well as the normal heart, one should always try to explain the morphology in each unipolar lead in terms of sequence of activation, from both the scalar and the vectorial approach. Specific morphologic patterns exist for hypertrophy and for bundle branch block [42,74,145].

Diagnostic Electrocardiographic signs of LVH:

(i) **Increased voltage of QRS deflection:** In the production of the normal left ventricular surface pattern in leads V5 and V6, the R deflection results from the stimulus traveling through the left ventricular wall toward the electrode. Similarly, in the recording of the normal right ventricular surface pattern in lead V1, the S wave is also produced by the activation wave in the left ventricular wall traveling away from the electrode. In the presence of ventricular hypertrophy with increased electrical forces from the hypertrophied left chamber, leads over the left precordium, V5 and V6 show high-amplitude R waves, and the right precordial lead V1 shows a deep S wave. The limb leads usually show left axis deviation. Attention was drawn to the diagnostic significance of high-voltage QRS complexes in the standard limb leads [74]. If the total voltage of the R wave in lead I and the S wave in lead III equals 2.5 mV or more, LVH is suggested. This is true only when the hypertrophied heart is in the horizontal position. However, the precordial leads, are more diagnostic of cardiac hypertrophy than the limb leads. The presence of LVH in adults is suggested in the unipolar leads when i) the sum of the left ventricular potentials (R wave in leads V5 and V6 and S wave in lead V1) totals 3.5 mV or more; ii) the voltage of the R wave in precordial

lead V5 or V6 exceeds 2.6 mV; iii) the voltage of the R wave in lead aVL in the horizontal heart exceeds 1.1 mV, or the R wave in lead aVF in the vertical heart exceeds 2 mV. It must be pointed out, however, that diagnosis of VH is open to an error when based solely on the voltage of the QRS complex [74].

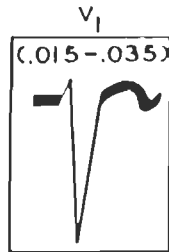
(ii) **S-T Segment and T wave changes over the Left Ventricle:** The S-T segment is depressed and the T wave is inverted in leads V5 and V6, or other leads over the left ventricle. In the right precordial leads (V1, V2), where the QRS is predominantly negative, the T wave is upright and the S-T segment may be slightly elevated. The changes in S-T segment and T wave of this type are secondary and presumably result from the altered ventricular depolarization process in the presence of LVH [42,74].

(iii) **Delayed onset of intrinsicoid deflection over the Left Ventricle:** The onset of the intrinsicoid deflection is measured from the onset of the QRS to the peak of the R wave and represents the time interval for passage of the impulse through the ventricles to the epicardium underlying the exploring electrode. An increased mass of myocardium, as in LVH, prolongs the time interval for the passage of the stimulus to the epicardial surface. The onset of the intrinsicoid deflection in LVH thus occurs later than it would normally be in the left precordial leads V5 and V6. The onset of the intrinsicoid deflection over the right precordium is early [74].

(iv) **Increased duration of QRS complex:** As a consequence of the increased muscle mass, the activation wave must travel longer than normal course, and hence, the QRS complex is widened. The normal duration of the QRS interval in the standard limb leads may be prolonged to 0.11 sec or even to 0.12 sec; however, it may also be 0.10 sec or less and still compatible with the diagnosis of LVH. For example, a normal QRS interval in the range of 0.06 or 0.07 sec is possible, and in such a case, a duration of 0.08 or 0.09 sec could represent its prolongation. Other factors which may be responsible for the increased duration of the QRS complex are: i) lengthening of the conduction time required for spread of activation over the endocardium in the dilated and hypertrophied ventricle and ii) incomplete LBBB. It is also stated that 90 per cent of cases with first-degree LBBB (incomplete LBBB) have left ventricular hypertrophy. Fig 5.1 illustrates the distinctive features of the precordial leads in left ventricular hypertrophy.

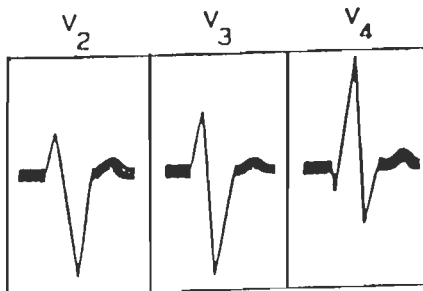
(v) **Left Axis Deviation:** In LVH, the mean QRS axis usually, but not always, shows left axis deviation, between -30° and -90° . The reasons for this are: i) great increase in the left ventricular muscle mass; ii) frequent occurrence of counterclockwise rotation around the anteroposterior axis (horizontal position); iii) presence of counterclockwise rotation around

LVH



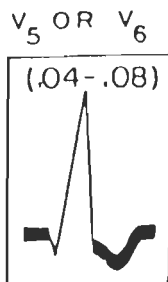
Lead V1:

Normal VAT
Small R wave or absent
Increased S wave amplitude
S-T Segment may or may not be elevated.



Leads V2, V3, V4 :

The R wave increases in amplitude and the S waves decreases in amplitude in leads progressing across the precordium from right to left.



Lead V5 or V6:

Late VAT
Increased R wave amplitude
Widened QRS
Depressed S-T segment
Inverted T

Fig. 5.1 Precordial leads in LVH

[Lipman B.S, and Massie E.(74)]

the longitudinal axis, due to which the free wall of the left ventricle is directed upward, backward and to the left; and iv) in many cases, existence of some degree of LBBB, which means that the septal forces are transmitted from right-to-left rather than in the normal left-to-right manner. This alteration helps to deviate the QRS axis to the left. [74]

5.2.4 Right Ventricular Hypertrophy

Three main patterns usually considered suggestive of right ventricular hypertrophy are: i) right axis deviation; ii) certain P wave abnormalities produced by atrial enlargement which, by inference, were believed associated with RVH; and iii) a pattern consisting chiefly of deep S waves [74].

Diagnostic Electrocardiographic signs of RVH:

(i) **Amplitude of QRS complex and R/S ratio:** In RVH, there is increased amplitude of those deflections produced by the right ventricular forces and decreased amplitude of those deflections produced by left ventricular forces. Thus, the R wave in the right chest lead V1 and the S wave in the left precordial leads V5 and V6 are of greater amplitude than normal one. In the normal adult heart, the R/S ratio in lead V1 is less than 1 and the R/S ratio in lead V5 or V6 is greater than 1. In RVH, the reverse is true; the R/S ratio in lead V1 is greater than 1 and in lead V5 or V6 is less than 1. Fig 5.2 illustrates the distinctive features of the precordial leads in right ventricular hypertrophy.

The RVH in adults is suggested in the V leads when i) the sum of the right ventricular potentials (R wave in lead V1 and S wave in lead V5 or V6) totals 1.05 mV or more; ii) the voltage of the R wave in precordial lead V1 exceeds 0.7 mV; iii) the amplitude of the R wave in lead aVR is 0.5 mV or more; iv) the S wave in lead V1 is less than -0.2 mV. It should be pointed out again that diagnosis of ventricular hypertrophy is doubtful when dependent solely on the voltage of the QRS complex [74].

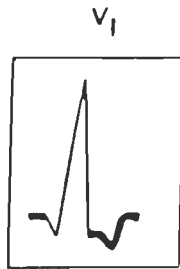
(ii) **S-T segment and T wave changes over the right ventricle:** In chest lead V1, the S-T segment may be depressed and the T wave inverted over the hypertrophied right ventricle, for reasons identical with those given under S-T and T changes in left ventricular hypertrophy.

(iii) **Delayed onset of intrinsicoid deflection over the right ventricle:** In precordial lead V1, the onset of the intrinsicoid deflection occurs later in RVH than it does normally (0.035 sec or more).

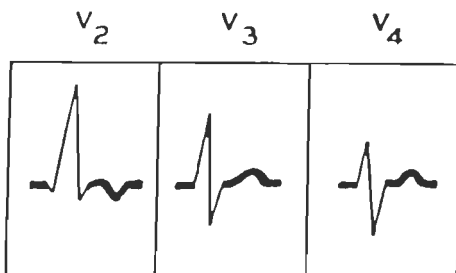
(iv) **Duration of QRS complex:** In contrast to the pattern in LVH, the QRS duration seldom is prolonged, because even with hypertrophy, the thickness of the right ventricle does not exceed that of the left one. The QRS duration may measure 0.10 sec or more.

RVH

Lead V1:

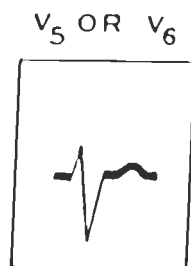


- R/S ratio > 1
- Tall R wave
- Small S wave or absent
- Depressed S-T segment
- Inverted T wave
- Late VAT
- Q wave present



Leads V2, V3, V4 :

The R wave decreases in amplitude and the S wave increases in amplitude in leads progressing across the precordium from right to left.



Lead V5 or V6:

- R/S < 1
- Small R wave
- Deep S wave
- Isoelectric S-T segment
- Upright T wave
- Normal VAT

Fig. 5.2 Precordial leads in RVH

[Lipman B.S, and Massie E.(74)]

(v) **Right axis deviation:** The mean QRS axis usually deviates rightward in RVH so that the axis lies between $+90^\circ$ and -150° . On the other hand, in some cases of RVH, there is no axis deviation.

5.2.5 Intraventricular Conduction Delay

Bundle branch block is primarily an electrocardiographic diagnosis. It occurs when the spread of the excitation wave is delayed or obstructed in the bundle of His tissue below the bifurcation into right and left main branches. The entire duration of the ventricular depolarization process is called the intraventricular conduction time and is represented on the ECG by the QRS interval. When the intraventricular conduction time is prolonged (widened QRS complex), bundle branch block (BBB) may be considered to exist [37,74]. If the QRS interval is 0.12 sec or more, complete BBB may be diagnosed. If the intraventricular conduction time is prolonged but is less than 0.12 sec, incomplete BBB is said to exist.

Right Bundle Branch Block: Bundle branch block has been logically divided into right and left block, each is recognized electrocardiographically by characteristic precordial lead morphologies. Referring to Fig.5.3, following are the criteria being used to diagnose the right bundle branch block.

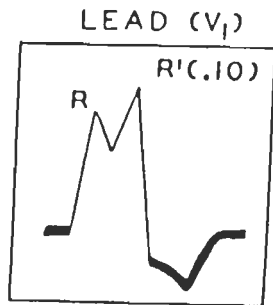
1. QRS widened to 0.12 sec or more.
2. Late onset of intrinsicoid deflection (VAT) in leads over the right ventricle: VAT in the right precordial leads may be as late as 0.10 sec or more (normal activation time 0.015-0.035 sec). The delayed VAT is a fundamental criterion of RBBB and must be present to make the diagnosis.
3. Increased amplitude of intrinsicoid deflection (R') in right precordial leads.
4. S-T segment and T wave changes in leads over the right ventricle.
5. Initial positivity in leads over the right ventricle: Q wave (initial cavity negative) in leads over the right ventricle is usually ruled out right bundle branch block.

Left Bundle Branch Block: To diagnose the LBBB, same five criteria as explained for RBBB but with different leads are used. Scoring schemes developed from these criteria are given in Table 5.1.

5.2.6 Myocardial Infarction

Localized myocardial damage is one condition, in which the ECG if used correctly, can be considered for clinical diagnostic assistance. The degree of myocardial damage may be classified as first degree (mild), second degree (moderate), and third degree (severe).

RBBB



Lead V1:

QRS interval ≥ 0.12 sec

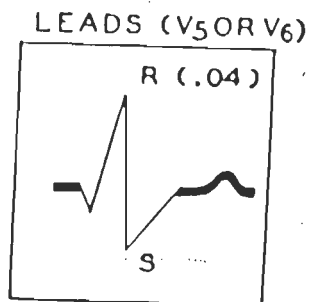
VAT ≥ 0.08 sec

Increased R' amplitude

Depressed S-T segment

Inverted T wave

Q wave is absent



Lead V5 or V6:

Broad slurred S wave

Normal VAT

S-T segment is isoelectric

Upright T wave

Normal Q wave

Fig. 5.3 Right and Left precordial leads in RBBB

[Lipman B.S, and Massie E.(74)]

Table 5.4 Existing and modified MI scoring criteria

A		Okajima et al.[102]										
Position criteria		Anterior			Lateral			Inferior				
		V2	V3	V4	I	V5	V6	II	III	aVF		
01	Q/R≥1/3 & Q≥36 msec	3	3	3	3	3	3	3	2	3		
02	Q/R≥1/3 & Q≥28 msec	2	2	2	2	2	2	2	1	2		
03	Q/R≥1/4 & Q≥24 msec	1	1	1	1	1	1	1	0	1		
04	with all three leads T< -0.1	3			3			3				
05	with all two leads T< -0.1	2			2			2				
06	with all one leads T< -0.1	1			1			1				
		≥4, cannot rule out infarction			≥6, possibility of infarction			≥8, definite infarction				
B 54 criteria/ 32 points , Macfarlane et al. [78]												
Lead	Criteria	Ponts	Score	Lead	Criteria	Ponts	Score					
I	Q≥30 ms	1	2	V3	R≥50 ms or R≥1.5 mV	1						
	R/Q≤1 or R≤0.3mV	1			S≤0.4 mV	1						
II	Q≥40 ms or	2	2	V4	any Q or R≤20ms	1	1					
	Q≥30 ms	1			R≤0.2mV or RV3≤RV1	1						
aVL	Q≥30 ms	1	2	V5	Q≥20 ms	2	3					
	R/Q≤1	1			R/Q≤0.5 or R/S≤0.5	1						
aVF	Q≥50 ms	3	5	V6	R/Q≤1 or R/S≤1 or	1						
	or Q≥40 ms	2			R≤0.7mVor notched R	1	3					
V1	or Q≥30 ms	1		V6	Q≥30 ms	2						
	R/Q≤1	2			R/Q≤1 or R/S≤1	1						
V2	or R/Q≤2	1		V6	R/Q≤2 or R/S≤2 or	1						
	Anterior any Q	1	2		R≤0.7 mV, notched R	1						
V2	S≥1.8 mV	1	4	V6	Q≥30 ms	1	3					
	Posterior R/S≥1	1			R/Q≤1 or R/S≤1	2						
V2	R≥50ms & R≥1mVor	2		V6	R/Q≤3 or R/S≤3 or	1						
	R≥40 ms & R≥0.6mV	1			R≤0.6 mV, notched R	1						
V2	S≤0.3 mV	1										
	Anterior any Q or	1	1									
V2	R≤10msorR≤0.1mV	1	4									
	Posterior R/S≥1.5	1										
V2	R≥60 ms & R≥2 mV	2										

							32					
Interpretation : %MI =Total score * 3												
C Modified MI scoring criteria		Anterior				Lateral			Inferior			
		V2	V3	V4	V5	V6	I	aVL	V6	II	III	aVF
01	Q/R >= 1/4 & Q >= 0.04 sec	4	4	4	4	4	4	4	4	4	4	
02	Inverted T wave	1	1	1	1	1	1	1	1	1	1	
		>5, possible anterior MI				>4, possible lateral MI			>4, possible inferior MI			
		≥9, probable. anteriorMI				≥7, probable lateral MI			≥7, probable inferior MI			
		≥17, definite anterior MI				≥11, definite lateral MI			≥11, definite inferior MI			

Electrocardiographically, first degree damage is ischemia (T wave change); second degree damage is injury (S-T change); and third degree damage is infarction (QRS change).

The important diagnostic electrocardiographic finding in MI is an abnormal Q wave (or QS complex) [42]. Small q waves are normal in many leads. They are commonly recorded in leads I, aVF, and V4-6, and are not over 0.02 sec in duration, and the Q:R ratio is less than 25%. The electrocardiographic recording at any given moment in time represent the mean of electrical forces going in many spatial directions. Because of this, approximately 90% of such forces are cancelled, leaving only 10% to be recorded. When MI of significant extent occurs, the forces of depolarization from that area will be lost. The result will be a change in direction of the mean forces which will now be directed away from the site of infarction. This is most significant during the initial 0.04-0.05 sec of ventricular depolarization and results in the abnormal Q wave (or QS complex) in leads overlying the infarct zone. An abnormal Q wave is defined by the criteria Q duration of 0.04 sec or greater and Q:R ratio 25% or greater [74].

The first electrocardiographic finding in MI is ST segment elevation in a lead overlying the area of infarction. Within the first few hours of infarction, 'giant' upright T waves may be seen in leads overlying the infarct. After a period of hours or days, the ST segment returns to the isoelectric line and T wave change occurs. The T waves begin to invert in those leads that showed ST segment elevation [54,81,106].

By applying the criteria for recognition of infarction to specific leads, one can determine the site of infarction as mentioned below:

Site of infarct	Leads that reflect the infarct
Anterior	V2-6
Inferior	aVF (and II and III)
Lateral	I, aVL, and V6

5.3 EXISTING AND MODIFIED DISEASE DIAGNOSTIC CRITERIA

Out of the two classification methods, namely decision and fuzzy classifiers, decision classifiers are in common use for ECG interpretation [16,43,59,155]. In this work, three important cardiac diseases LVH, RVH and MI (Anterior, Lateral and Inferior) are considered. An exhaustive performance evaluation study of existing scoring schemes for disease diagnostic interpretation has been carried out. In addition to the basis given in the literature, data and recommendations published/ reported domestically or internationally; an exhaustive

study of existing scoring schemes reported by Marriot et al.[91], Okajima et al.[102], Macfarlane et al.[79], Maheshwari et al.[82] and Mehta et al.[93], was carried out to construct the modified scoring schemes and the decision tree classifier using modified scoring schemes for LVH, RVH and myocardial infarction.

The performance study of the existing criteria has been carried out using the records of the CSE DS-3 and CSE DS-5 dataset. The existing and modified scoring criteria are given in Tables 5.2 – 5.4. In LVH criteria ‘A’ [93], the use has been made of 7 criteria with total score of 10 points. Out of 7 criteria, 5 are amplitude and 2 duration based criteria. Seven leads, namely I, III, aVL, aVF, V1, V5 and V6 have been used. The use of FPA is made and no consideration to Q wave. The scoring scheme ‘B’ [102] in Table 5.2 consists of 10 criteria with maximum score of 20 points. All 10 used criteria are amplitude dependent, and there is no consideration to durations. In all, 8 leads, namely I, II, III, aVL, aVF, V1, V5 and V6 have been used. The use of Q and FPA is also made and diagnostic interpretation is carried out from the total score as detailed in Table 5.2.

Marriot’s LVH scoring scheme ‘C’ in Table 5.2 consists of 7 criteria with total score of 14 points. In all, 5 amplitude and 2 duration criteria are used. There is a use of P-terminal force and FPA, but no use of Q wave. Ten leads, namely I, II, III, aVR, aVL, aVF, V1, V2, V5 and V6 have been used.

On the basis of the study of existing scoring criteria and details available in the literature, a modified LVH scheme ‘D’, as given in Table 5.2 has been constructed.

On the similar lines, three existing RVH and two MI scoring criteria, given in Tables 5.3 and 5.4 are studied to develop the modified RVH and MI scoring schemes. All these scoring schemes are based on amplitudes and durations of ECG waves. To extract these parameters, the software discussed earlier, analyses 12 standard leads and generates five output data files. Each data file contains four measurements, namely wave peak location, peak amplitude, onset and offset of 6 ECG waves (P, Q, R, R', S, and T), hence first data file corresponding to first beats in all 12 leads gives 288 measurements (i.e. 4 wave measurements x 6 ECG waves x 12 leads). Using these measurements, the performance evaluation of existing LVH, RVH and MI scoring schemes have been carried out to develop modified scoring schemes to construct a decision tree classifier (shown in Fig. 5.4).

While developing the modified scoring schemes, following points have been kept under consideration:

- i) Common scoring criteria being used in existing schemes have been identified.

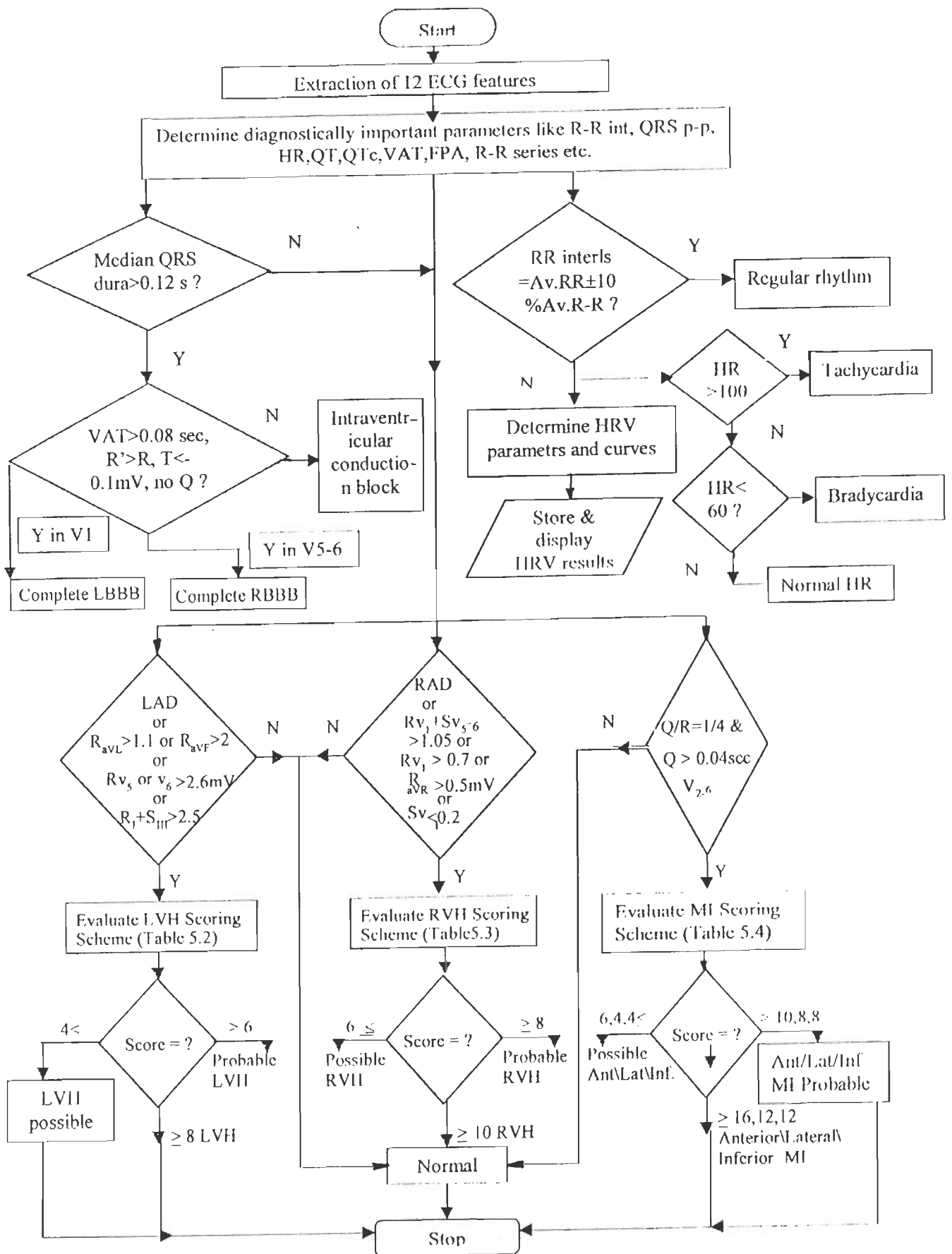


Fig. 5.4 Decision tree classifier using modified scoring criteria for LVH, RVH and MI

- ii) Additional criteria from the text books, data and recommendations from the published reports, which are must and are not present in the existing schemes, have been identified and included.
- iii) For fixing the scoring thresholds values for interpretation, an exhaustive analysis has been carried out using the CSE DS-3 and DS-5 data sets.

The modified scoring criteria contain all the required points given by other workers and clearly bring out the diagnosis without any ambiguity. Software has been developed to extract the ECG parameters of five beats from each lead using the standard 12 leads and extended to implement the existing as well as modified scoring schemes for LVH, RVH and MI diseases.

5.4 SOFTWARE DEVELOPMENT

Feature extraction software is extended to implement the existing as well as modified scoring schemes for LVH, RVH and MI diseases. After validation of the modified scoring criteria, the complete procedure of diagnostic as cited in a decision tree classifier has been implemented. This classifier tree classifies the diseases by using the modified scoring criteria and the criteria for LBBB, RBBB, Tachycardia, Bradycardia and also checks the rhythm and heart rate variability (HRV). Details of HRV are discussed in the next chapter.

Algorithm:

- i) As discussed in the earlier chapter, the diagnostic parameters, namely R-R interval, P amplitude, P terminal force, QT, QTc, QRS p-p, QRS net deflection, FPA, HR and VAT are determined.
- ii) The diseases like Tachycardia, Bradycardia, LBBB and RBBB have been interpreted. The HRV analysis is carried out by spectral and non-spectral indices. The curves like interval tachogram, distribution density curve and PSD are obtained.
- iii) To avoid the complicated computations in evaluating the point scoring for LVH, RVH, MI, LBBB and RBBB, firstly minimal criteria (shown in Fig.5.4) are applied, and if satisfied, then the remaining paths to add scoring points are considered.
- iv) The thresholds defined for interpretation of diseases are to classify the disease.
- v) Considering the parameters from the first data file, the diagnostic interpretation procedure as give above is applied to classify diseases into LVH, RVH, MI (Anterior, Lateral and Inferior), LBBB, and RBBB diseases or Normal. The procedure is repeated for remaining four data files.

- vi) From a 12 leads ECG record of a patient, five individual beats are measured and interpreted to result in five independent decisions. This may include LVH (possible/ probable/ definite) and/ or RVH (possible/ probable/ definite) and/ or MI (anterior, Lateral, Inferior) (possible/ probable/ definite) and/ or normal, and /or left bundle branch block, right bundle branch block.

From these five individual results, the best of five interpretation results drawn from five data files of five different beats are considered as the final diagnosis. These steps are more clear from the example given in the following section:

5.5 TEST RESULTS AND DISCUSSIONS

5.5.1 Disease Diagnosis using CSE Dataset -3

Disease diagnostic testing has been carried out on all 125 cases of CSE DS-3 database. As an illustrative examples, detailed diagnostic results of 25 cases are shown in Table 5.5. This shows the results of the criteria for LVH and RVH. The first set of criteria, i.e. LVH criteria-I and RVH criteria-I, are the ones used by Mehta [93], and the second set of criteria, i.e. LVH criteria-II and RVH criteria-II, are the ones used by Marriot [91] and Maheshwari et al.[82] and are given in Tables 5.2 – 5.4. As the diagnostic interpretation of the ECGs from the CSE DS-3 database is not yet disclosed by the CSE, two alternate diagnostic criteria have been used to enable the validation of the disease classification. It is observed that the final diagnostic results obtained according to the score and the thresholds used by both the criteria are the same. Overall disease diagnostic results obtained out of all 125 cases of CSE DS-3 are given below:

No. of cases of LVH (definite)	16
No. of cases of LVH (probable)	25
No. of cases of LVH (possible)	28
No. of cases of RVH (definite)	18
No. of cases of RVH (probable)	11
No. of cases of RVH (possible)	09
No. of cases of Tachycardia	07
No. of cases of Bradycardia	26

Some of the above listed cases are multidisease cases with overlap of more than one disease.

Table 5.5 Heart disease diagnostic results using CSE DS-3 database

Record No.	Heart Rate (BPM)	Net Deflection in Leads (mv)		FPA (degrees)	LVII Score		RVII Score	
		I	II		Cr-I	Cr-II	Cr-I	Cr-II
01	63.83	-0.45	-11.10	88.08	01	01	00	00
06	89.29	0.96	0.53	1.84	00	00	00	00
11	81.08	11.34	1.36	-23.34	01	01	00	00
16	93.75	-0.27	0.24	57.93	01	02	03	09 RVH
21	47.47 B	-1.87	-4.52	65.79	01	01	00	00
26	47.47 B	-1.87	-4.52	65.79	07	04 LVH	03	00 PoRVII
31	64.94	1.58	-1.19	-72.53	04	04 PrLVII	00	00
36	68.18	4.11	-5.59	-64.95	02	02	00	00
41	66.67	-0.14	-0.4	-6.13	03	03 PoLVII	01	00
46	69.44	6.46	3.67	4.95	02	02	01	00
51	114.5 T	-8.07	-3.63	-2.89	01	01	01	00
56	62.50	1.28	0.83	10.18	00	01	00	00
61	76.53	2.31	3.61	50.99	00	00	00	00
66	63.03	10.08	7.94	18.75	01	01	01	00
71	78.53	0.93	8.05	9.41	01	01	00	00
76	81.08	2.98	-13.22	-80.03	03	03 PoLVII	00	00
81	71.09	0.73	2.56	73.96	02	02	00	00
86	61.22	6.01	-23.01	-78.67	07	06 LVH	01	00
91	73.17	9.76	4.82	0.01	02	04 PrLVII	02	00
96	62.76	-1.49	7.85	81.45	02	02	03	12 RVII
101	103.4 T	7.66	11.19	48.16	01	01	00	00
106	66.08	1.2	2.38	59.82	01	02	01	00
111	107.1 T	-0.91	6.52	-83.54	00	00	03	09 RVII
116	75.00	2.26	0.77	-10.01	02	02	00	00
121	76.14	4.03	2.42	7.03	00	00	02	00

Cr - Criteria	B - Bradycardia	T - Tachycardia
LVH - Left Ventricular Hypertrophy	PoLVII - Possible LVH	PrLVH - Probable LVII
RVH - Right Ventricular Hypertrophy	PoRVII - Possible RVII	PrVII - Probable RVII

Table 5.6 Disease Diagnosis using Existing Scoring Schemes (First 10 records of CSE DS-5)

ECG beat	LVH			RVH			MI					Final diagnosis	
	SSM PS DI DI5	OKJ PS DI DI5	EST PS DI DI5	SSM PS DI DI5	OKJ PS DI DI5	RMA PS DI DI5	OKJ ANT LAT INF DI DI5			McF PS %MI			
1B1	01 NL NL	00 NL NL	01 NL NL	00 NL RS	01 NL NL	00 NL NL	00	00	00	NL	NL	23 69	RVH-PS.MI- PS.NL-PS
1B2	00 NL	00 NL	00 NL	00 NL	00 NL	00 NL	00	00	00	NL		19 57	
1B3	00 NL	00 NL	00 NL	03 RS	01 NL	00 NL	00	00	01	NL		18 54	
1B4	00 NL	00 NL	00 NL	03 RS	00 NL	00 NL	00	00	01	NL		17 51	
1B5	00 NL	00 NL	00 NL	00 NL	00 NL	00 NL	00	00	01	NL		20 60	
2B1	01 NL NL	00 NL NL	01 NL LS	00 NL NL	00 NL NL	00 NL NL	00	00	00	NL	NL	23 69	LVH-PS.MI- PS
2B2	01 NL	00 NL	01 NL	01 NL	00 NL	00 NL	00	00	00	NL		18 54	
2B3	02 NL	00 NL	04 LR	00 NL	00 NL	00 NL	00	01	00	NL		24 72	
2B4	00 NL	00 NL	00 NL	00 NL	00 NL	00 NL	00	00	01	NL		23 69	
2B5	00 NL	00 NL	00 NL	00 NL	00 NL	00 NL	00	00	00	NL		15 45	
3B1	05 LH LS	01 NL NL	07 LH LH	03 RS RS	01 NL NL	01 NL NL	04	04	04	MIX	MIX PS	20 60	LVH-DF. RVH-PS. MIX MI- PS
3B2	02 NL	00 NL	05 LH	03 RS	00 NL	00 NL	04	02	01	AMS		17 51	
3B3	02 NL	00 NL	04 LR	03 RS	00 NL	00 NL	04	02	00	AMS		16 48	
3B4	01 NL	00 NL	04 LR	03 RS	00 NL	00 NL	04	02	00	AMS		14 42	
3B5	02 NL	00 NL	05 LH	02 NL	00 NL	00 NL	04	02	00	AMS		12 36	
4B1	02 NL NL	02 NL NL	04 LR LS	03 RS RS	01 NL NL	08 RH RH	00	04	01	LMS	LMS/ IMS	20 60	RVH-DF. LVH-PS. LMI-PS. IMI-PS
4B2	01 NL	02 NL	03 NL	03 RS	01 NL	08 RH	00	02	04	IMS		20 60	

Table 5.6....continued

4B3	01 NL	00 NL	03 NL	03 RS	01 NL	09 RH	00 02 00 NL	20 60	
4B4	01 NL	00 NL	03 NL	00 NL	00 NL	00 NL	00 00 00 NL	20 60	
4B5	00 NL	00 NL	00 NL	00 NL	00 NL	00 NL	00 00 04 IMS	20 60	
5B1	05 LH LH	02 NL NL	04 LR LH	01 NL NL	00 NL NL	00 NL NL	00 00 02 NL IMS	17 51	LVH-DF, IMI-PS
5B2	05 LH	04 NL	04 LR	00 NL	00 NL	00 NL	00 00 02 NL	14 42	
5B3	05 LH	04 NL	00 NL	00 NL	00 NL	00 NL	00 00 02 NL	16 48	
5B4	03 LS	02 NL	00 NL	00 NL	00 NL	00 NL	01 00 02 NL	17 51	
5B5	07 LH	03 NL	06 LH	01 NL	00 NL	00 NL	00 00 04 IMS	21 63	
6B1	03 LS LS	01 NL NL	03 NL NL	00 NL RS	00 NL NL	00 NL NL	00 00 04 IMS IMS	18 54	LVH-PS RVH-PS IMI-PS
6B2	02 NL	01 NL	03 NL	03 RS	00 NL	00 NL	00 00 04 IMS	14 42	
6B3	01 NL	00 NL	01 NL	00 NL	00 NL	00 NL	00 00 02 NL	22 66	
6B4	00 NL	00 NL	01 NL	03 RS	00 NL	00 NL	00 00 01 NL	22 66	
6B5	00 NL	00 NL	00 NL	00 NL	00 NL	00 NL	00 00 01 NL	22 66	
7B1	00 NL NL	00 NL NL	00 NL NL	04 RR RR	00 NL NL	00 NL NL	00 00 00 NL NL	13 39	RVH-PR
7B2	01 NL	00 NL	01 NL	04 RR	00 NL	00 NL	00 00 00 NL	13 39	
7B3	00 NL	00 NL	00 NL	04 RR	00 NL	00 NL	00 00 00 NL	11 33	
7B4	00 NL	00 NL	00 NL	03 RS	00 NL	00 NL	00 00 00 NL	12 36	
7B5	00 NL	00 NL	00 NL	03 RS	00 NL	00 NL	00 00 00 NL	14 42	
8B1	06 LH LH	13 LH LH	08 LH LH	00 NL NL	01 NL NL	00 NL NL	00 04 01 LMS LMS	16 48	LVH-DF LMI-PS
8B2	05 LH	13 LH	07 LH	00 NL	01 NL	00 NL	00 04 01 LMS	17 51	
8B3	05 LH	13 LH	07 LH	00 NL	01 NL	00 NL	00 02 01 NL	15 45	

Table 5.6....continued

									Table 5.6 continued.....
8B4	06 LH	13 LH	08 LH	00 NL	01 NL	00 NL	00 02 01 NL	15 45	
8B5	06 LH	13 LH	08 LH	00 NL	01 NL	00 NL	00 02 01 NL	15 45	
9B1	02 NL LS	00 NL NL	04 LR LH	03 RS RS	00 NL NL	00 NL NL	00 01 00 NL NL	12 57	LVH-DF RVH-PS MI-PS
9B2	03 LS	00 NL	05 LH	03 RS	00 NL	00 NL	00 01 00 NL	19 57	
9B3	01 NL	00 NL	01 NL	01 NL	00 NL	00 NL	02 00 00 NL	20 60	
9B4	02 NL	00 NL	04 LR	01 NL	01 NL	00 NL	00 02 01 NL	17 51	
9B5	02 NL	00 NL	04 LR	02 NL	01 NL	00 NL	02 01 01 NL	22 66	
10B 1	01 NL NL	00 NL NL	01 NL NL	00 NL RS	00 NL NL	00 NL NL	00 00 00 NL NL	23 69	RVH-PS, MI-PS
10B 2	00 NL	00 NL	00 NL	00 NL	00 NL	00 NL	00 00 00 NL	22 66	
10B 3	00 NL	00 NL	00 NL	03 RR	00 NL	00 NL	00 00 00 NL	18 54	
10B 4	00 NL	00 NL	00 NL	00 NL	00 NL	00 NL	00 00 00 NL	20 60	
10B 5	00 NL	00 NL	00 NL	00 NL	00 NL	00 NL	00 00 00 NL	17 51	

5.5.2 Disease Diagnosis using CSE Dataset -5

After the reliable testing of the software using the CSE DS-3, the use of CSE DS-5 diagnostic data set has been made. Feature extraction results of every fifth record of the CSE DS-3 are given by the CSE Working Party, hence, the confirmation of feature extraction by the software is firstly made to proceed for the disease diagnosis using the alternate scoring criteria. With this type of analysis of software, in which actual measurements are known for comparison and if the use of alternate scoring schemes give same diagnostic interpretation, it may be stated that the software is reliable to use further. After testing of the software on CSE DS-3, disease diagnosis using CSE DS-5 records and the ECGs recorded from different subjects in the laboratory, have been carried out.

As an illustrative example, first 10 records of the CSE DS-5 are considered whose diagnostic truth is reported by the CSE and the opinions obtained from the medical experts have been used as the reference. Table 5.6 gives the disease diagnosis results interpreted by using existing scoring schemes on the CSE DS-5 records. As given in Table 5.6, final diagnostic statement is a resultant statement based on the results of existing three LVH, three RVH and two MI schemes. The strategy used by CSE [148] to give final diagnosis statements has been followed here. The procedure used to draw a final decision out of existing schemes will be clear from the example given below:

The first criteria of LVH [93] gives following point score for record no.1 of CSE DS-5.

Beat No.	Point score	
1B1	01/ NL	where 1B1 represents beat 1 of record no.1 and the point score 01, which interpret the case as normal (NL)
1B2	00/ NL	
1B3	00/ NL	
1B4	00/ NL	
1B5	00/ NL	

If we consider the resultant of these five scores, say best of five, then it gives 00/ NL, means the final diagnostic result given by first scoring scheme [93] is a normal case checked against the left ventricular hypertrophy. Similarly, as given in the Table 5.6, other two scoring schemes given by Okajima and Marriot give the disease interpretation as normal case as against LVH investigation.

After these three results by three diagnostic schemes, the final result is determined by weights. The weights are decided by counting number of normal, number of possible LVH, probable LVH and definite left ventricular hypertrophy. Out of three results from three

schemes, the highest one is considered as the net result of all three LVH schemes. This final result is an effective result of 5 beats x 3 schemes i.e. 15 individual results. If the final count is ≥ 1 and < 5 for a particular disease, then the diagnostic weightage is given as a possibility for that particular disease. If the count is > 5 then the diagnosis is carried out according to number of definite or probable results.

Right ventricular hypertrophy scoring results are also given in Table 5.6, out of which, the results for the first record of CSE DS-5 are considered here, as follows:

Beat no.	SSM criteria score	OKJ criteria score	RMH criteria score
01	00/ NL	01/ NL	00/ NL
02	00/ NL	00/ NL	00/ NL
03	03/ RVH possible	01/ NL	00/ NL
04	03/ RVH possible	00/ NL	00/ NL
05	00/ NL	00/ NL	00/ NL

In this case, all three existing scoring schemes in all five beats analysis conclude that the investigation as against the RVH is normal except in Mehata's [93] criteria. For third and fourth beats, this criteria gives the score of 03 and as per the threshold limits used to check the disease in the SSM criteria, the resulting interpretation is RVH possible. But for remaining three beats, the same scoring scheme gives the results as normal, hence, ultimate diagnosis is the normal-possible and RVH-possible case. To be on safer side, if the scoring show a disease in one or two beats, then that particular disease is graded as possible and not definite or probable. The overall count of normal in three schemes shown above is the highest, hence, the net interpretation as against the RVH interpretation is a normal case, and RVH possible is indicated by two beats in one scoring scheme (Mehta et al.[93]), therefore, this normal interpretation is referred to as normal-possible and RVH-possible.

To know about the MI (Anterior, Lateral, Inferior), two existing scoring diagnostic criteria [78,102] are used. The point scoring by these two scoring schemes is as follows:

Beat no.	OKJ criteria		Macf criteria		
	Anterior	Lateral	Inferior	score	% MI
01	00/ NL	00/ NL	00/ NL	23	69
02	00/ NL	00/ NL	00/ NL	19	57
03	00/ NL	00/ NL	01/ NL	18	54
04	00/ NL	00/ NL	01/ NL	17	51
05	00/ NL	00/ NL	01/ NL	20	60

From all these scores of Okajima's diagnostic criteria, the net diagnosis interpretation as against the MI is the normal case. This is because Okajim's criteria gives the scores resulting the normal case, while Macfarlane's MI scoring scheme gives a score of above 50%, indicating the possibility of MI.

The overall final diagnosis for this first case is now decided from the three net results of three LVH, three RVH and two MI scoring schemes, hence, for the first case as detailed in Table 5.6, the final diagnosis is RVH-possible/ MI possible/ Normal-possible. For other records, the procedure explained above to diagnose the disease using the parameter estimates in five beats is used and the results are given in Table 5.6, and the results are displayed according to the priority. Suppose the net results of three diagnostic criteria are say, LVH probable/ RVH definite/ MI possible, then this is rearranged as RVH definite/ LVH probable/ MI possible. Using the same strategy of disease diagnosis, the results of diagnosis interpretation for the first 10 records of the CSE DS-5 have been carried out by using existing as well as modified scoring schemes. The complete details of disease diagnosis scoring and interpretation of 10 records using existing scoring schemes are given in Table 5.6 and the complete procedure to diagnose the diseases using the developed software are outlined in the Table 5.7. In addition to this comparison, the comparison is also carried out with the results obtained from the panel of experts.

A typical record D-0008.DCD from the CSE DS-5 has been used and the five data files of ECG parameters and the corresponding disease interpretation by existing as well as modified scoring schemes are given in Table 5.7. From the first beat ECG parameter results, the determined heart rate is 53 BPM, which indicates that the case is of Bradycardia. From the RBBB and LBBB diagnostic scoring criteria as detailed in Table 5.1 and used in decision tree classifier (Fig. 5.4), the parameters of beat-1, give the interpretation that the case is not of RBBB or LBBB. The FPA, determined from the net QRS deflections measured in leads I, II, and III, is -0.4168 degree and is used in LVH and RVH interpretation. For LVH interpretations, three existing and one modified scoring schemes have been used (as shown in Table 5.7) and all these criteria interpret that the case is of LVH (definite). Similarly for RVH, no decision against RVH is given, indicating that the case is not of RVH. Two existing and one modified MI scoring schemes also give no indication of MI. Like this, the software undergoes the procedure to diagnose the disease repeatedly using five different parameter files from five different beats. For remaining four beats, the diagnostic results are also detailed in the same table.

From the beat-2 measurements, displayed results are as follows:

HR is 53 BPM, FPA is 0.0716 degree and the case is of Bradycardia, LVH (definite), no RVH and no MI.

From the beat-3 parameter measurements, interpretation results are as follows: HR is 56 BPM, FPA is 17.74 degree and the case is of Bradycardia, LVH (definite), no RVH and no MI.

From beat-4 parameters, the diagnostic results are HR is 56 BPM, FPA is 23.45 degree and the case is of Bradycardia, LBBB, LVH (definite), no RVH and no MI.

For 5th beat diagnostic results are HR=56 BPM, FPA=15.24 degree and the case is of Bradycardia, LBBB, LVH (definite), no RVH and Anterior MI-possible.

The ultimate result is then displayed from the net result of five interpretations given by modified scoring schemes. This final result are given at the end of Table 5.7, as the case is abnormal with LVH definite, Bradycardia, LBBB-possible and Anterior MI-possible.

Diagnostic results determined by the modified diagnostic scoring criteria using decision tree classifier are given in Table 5.8. The results of this evaluation are compared with the results determined by existing scoring schemes and also with the diagnostic truth given by CSE group. Comparison of the disease diagnosis results is given in Tables 5.9-5.10

Using the strategy of disease diagnostics from the features of five ECG beats, the validation of the software is carried out by using the number of records from the CSE database. The results of this evaluation are compared with the results obtained by the existing scoring schemes and also with the diagnostic truth. The CSE Working Party has considered the case as normal even if the record shows minor abnormalities such as non-specific ST-T changes, incomplete right or left BBB, left anterior fascicular block, minor intraventricular conduction defects (QRS <120ms) or even myocardial ischemia, as a single statement without making reference to any of the seven primary categories Normal, LVH, RVH, BVH AMI, IMI, and MIX MI [148]. To compare the results of existing and modified scoring schemes with the CSE results, the diseases Bradycardia, Tachycardia, RBBB, and LBBB diseases are not considered. From the comparison given in Table 5.9 and the diagnostic opinion obtained from the medical experts as given in Table 5.10, the diagnostic interpretation performed by existing criteria matches with the truth in 60% of the cases and by the modified criteria in about 80% of the cases, thereby resulting a gain of 20% reliability in the disease diagnosis. The gain is due to the three factors; use of combined WT's for feature extraction, use of five beats in place of one beat for analysis, and the use of modified scoring schemes having required number of criteria. After the confirmation of reliable diagnosis from the use of multiple scoring schemes reported by different researchers and the opinion of a

Table 5.7 Complete Procedure to Interpret the ECG by Decision Tree Classifier using 'Five Beats' of a Record CSE D-00008.DCD

BEAT - 1 Parameter

(Wave position is given in sample Nos. and Wave amplitude in mV)

Lead	P Wave					QRS Complex										T Wave				
	Pon	Ppos	Pamp	Poff	QRSon	Qpos	Qamp	Qoff	Rpos	Ramp	Roff	Spos	Samp	Soff	R'	QRSoff	Tpos	Tamp	Tend	NetD
L1	79	131	0.07	147	199	199	-0.06	200	231	1.39	246	251	-0.23	256	--	267	359	-0.37	451	27.64
L2	91	123	0.14	167	167	167	-0.02	168	231	1.38	243	251	-1.27	256	--	279	367	-0.09	423	13.47
L3	80	108	0.11	132	152	152	0.07	157	212	0.79	221	232	-2.14	237	--	248	360	0.33	440	-11.53
aR	119	159	0.10	199	199	199	0.23	199	203	0.23	211	231	-0.95	236	--	244	367	0.45	431	-10.23
aL	111	127	0.03	143	207	207	-0.05	209	231	1.80	247	251	-0.08	256	--	259	355	-0.22	447	33.86
aF	76	104	0.13	128	148	148	0.02	152	212	1.02	221	232	-1.63	237	--	245	360	0.12	436	0.35
V1	87	103	-0.03	119	195	195	0.32	195	203	0.40	210	231	-2.03	236	--	253	367	0.72	435	-24.40
V2	90	106	0.07	126	198	198	0.02	198	210	0.37	215	230	-4.02	235	--	259	366	0.64	438	-77.50
V3	90	106	0.04	126	178	178	0.13	178	210	0.66	216	230	-4.33	235	--	261	366	0.75	438	78.33
V4	85	109	0.05	157	173	173	-0.10	174	209	1.01	219	233	-3.17	238	--	260	389	0.12	437	59.04
V5	82	118	0.06	162	202	202	-0.11	202	230	3.94	241	250	-2.37	255	--	274	374	-0.84	438	25.60
V6	75	123	0.08	163	207	207	-0.32	207	231	3.39	245	251	-1.76	256	--	279	379	-1.12	439	1.20

=====DIAGNOSTIC RESULTS=====

HR(BPM)=53.000 Bradycardia
 FPA=0.416829 Degrees

-----LVH-----

LVH Criteria-I(SSM) Score=6 LVH DETECTED
 LVH Criteria-II(OKJ) Score=13 LVH
 LVH Criteria-III(MAR) Score=8 LVH
 LVH Criteria-IV(MOD) Score=11 LVH DETECTED

-----RVH-----

RVH Criteria-I(SSM) Score=0 NO RVH
 RVH Criteria-III(OKJ) Score=1 NO RVH
 RVH Criteria-II(RMII) Score=0 NO RVH
 RVH Criteria-IV(MOD) Score=3 NO RVH

-----MI Criteria-I(OKJ)-----

Anterior MI Score=0
 Anterior MI Score=0
 Anterior MI Score=0
 Total Anterior MI Score=0 NO AMI

Lateral MI Score=1
 Lateral MI Score=1
 Lateral MI Score=1
 Total Lateral MI Score=3 NO LMI

Inferior MI Score=0
 Inferior MI Score=1
 Inferior MI Score=0
 Total Inferior MI Score=1 NO IMI

Table 5.7continued

-----MI Criteria-2(MOD)-----

Anterior MI Score=0
 Anterior MI Score=0
 Anterior MI Score=0
 Anterior MI Score=1
 Anterior MI Score=1
 Total Anterior MI Score=2 NO AMI

Lateral MI Score=1
 Lateral MI Score=1
 Lateral MI Score=1
 Total Lateral MI Score=3 NO LMI

Inferior MI Score=0
 Inferior MI Score=1
 Inferior MI Score=0
 Total Inferior MI Score=1 NO IMI

-----Criteria-3(MACF)-----

Total score=16 and MI =48 %

BEAT - 2 Parameters

Lead	Pon	Ppos	Pamp	Poff	QRson	Qpos	Qamp	Qoff	Rpos	Ramp	Roff	Spos	Samp	Soff	R'	QRSoff	Tpos	Tamp	Tend	NetD
L1	79	131	0.06	147	199	199	-0.08	200	231	1.30	247	251	-0.23	256	--	267	359	-0.38	423	25.55
L2	95	127	0.18	175	203	203	0.01	203	231	1.37	244	251	-1.26	256	--	267	427	0.04	459	12.64
L3	76	108	0.15	128	180	180	0.10	180	208	0.76	219	232	-2.04	237	--	244	356	0.34	440	-11.60
aR	119	171	0.09	195	195	195	0.26	195	199	0.26	213	231	-0.93	236	--	244	367	0.46	427	-6.61
aL	111	127	0.05	175	207	207	-0.05	211	231	1.65	247	251	-0.11	256	--	259	355	-0.25	435	30.00
aF	76	108	0.17	156	156	156	0.02	158	212	1.06	222	232	-1.65	237	--	246	356	0.13	400	1.61
V1	79	103	-0.02	127	191	191	0.26	191	207	0.35	212	231	-2.05	236	--	255	367	0.66	427	25.25
V2	86	106	0.05	126	190	190	0.04	190	206	0.35	212	230	-3.77	235	--	257	362	0.60	430	12.68
V3	86	110	0.06	126	170	170	0.13	172	210	0.70	214	230	-4.18	235	--	258	362	0.72	438	-75.27
V4	81	109	0.07	153	165	165	-0.04	167	209	1.21	217	233	-3.21	238	--	257	389	0.20	441	-52.88
V5	94	122	0.06	166	206	206	-0.04	206	230	4.13	243	250	-2.35	255	--	274	374	-0.80	442	33.63
V6	86	107	0.19	122	207	207	0.26	208	231	4.09	242	247	-1.13	252	--	275	375	-0.79	439	53.00

=====RESULTS=====

HR(BPM)=53.000 Bradycardia

FPA=0.071606 Degrees

=====LVH=====

LVH Criteria-I(SSM) Score=5 LVH DETECTED
 LVH Criteria-II(OKJ) Score=13 LVH
 LVH Criteria-III(MAR)Score=7 LVH
 LVH Criteria-IV(MOD) Score=10 LVH DETECTED

====RVH====
 RVH Criteria-I(SSM) Score=0 NO RVH
 RVH Criteria-III(OKJ) Score=1 NO RVH
 RVH Criteria-II(RMH) Score=0 NO RVH
 RVH Criteria-IV(MOD) Score=3 NO RVH

====MI Criteria-1(OKJ)====
 Anterior MI Score=0
 Anterior MI Score=0
 Anterior MI Score=0
 Total Anterior MI Score=0 NO AMI

Lateral MI Score=1
 Lateral MI Score=1
 Lateral MI Score=1
 Total Lateral MI Score=3 NO LMI

Inferior MI Score=0
 Inferior MI Score=1
 Inferior MI Score=0
 Total Inferior MI Score=1 NO IMI

====MI Criteria-2(MOD)====
 Anterior MI Score=0
 Anterior MI Score=0
 Anterior MI Score=0
 Anterior MI Score=1
 Anterior MI Score=1
 Total Anterior MI Score=2 NO AMI

Lateral MI Score=1
 Lateral MI Score=1
 Lateral MI Score=1
 Total Lateral MI Score=3 NO LMI

Inferior MI Score=0
 Inferior MI Score=1
 Inferior MI Score=0
 Total Inferior MI Score=1 NO IMI

====Criteria-3(MACF)====
 Total score=17 and MI =51 %

Table 5.7continued

BEAT - 3 Parameters

Lead	Pon	Ppos	Pamp	Poff	QRson	Qpos	Qamp	Qoff	Rpos	Ramp	Roff	Spos	Samp	Soff	R'	QRSoff	Tpos	Tamp	Tend	NetD
L1	79	131	0.06	159	199	199	-0.09	200	231	1.18	247	251	-0.25	256	--	267	363	-0.39	427	21.75
L2	87	123	0.18	163	183	183	0.02	183	231	1.45	241	247	-1.18	252	--	263	359	-0.08	423	16.76
L3	80	108	0.15	144	172	172	0.12	172	212	0.90	220	232	-1.91	237	--	244	356	0.35	420	-4.59
aR	119	167	0.10	231	175	175	0.26	175	183	0.26	213	231	-0.92	236	--	244	363	0.46	423	-0.26
aL	111	127	0.01	155	211	211	-0.10	213	231	1.54	249	251	-0.10	255	--	255	443	0.08	499	28.61
aF	76	108	0.17	144	168	168	0.07	168	212	1.17	223	232	-1.54	237	--	246	356	0.15	420	5.73
V1	83	103	-0.03	127	195	195	0.14	195	207	0.22	212	231	-2.12	236	--	256	367	0.48	431	-33.14
V2	90	106	0.05	126	190	190	0.08	190	206	0.37	212	230	-3.62	235	--	257	362	0.62	430	-68.45
V3	86	106	0.04	130	190	190	0.11	190	210	0.65	214	230	-4.16	235	--	259	362	0.69	434	-80.08
V4	81	109	0.07	125	165	165	0.01	165	209	1.25	217	233	-3.17	238	--	257	389	0.24	433	-49.61
V5	90	122	0.07	138	206	206	-0.05	206	230	4.14	243	250	-2.29	255	--	278	374	-0.85	434	34.89
V6	91	119	0.04	163	207	207	0.93	207	231	4.96	243	251	-0.33	256	--	279	375	0.11	451	6.00

=====RESULTS=====

HR(BPM)=56.000 Bradycardia

FPA =17.742389 Degrees

=====LVH=====

LVH Criteria-I(SSM) Score=5 LVH DETECTED
 LVH Criteria-II(OKJ) Score=13 LVH
 LVH Criteria-III(MAR) Score=7 LVH
 LVH Criteria-IV(MOD) Score=10 LVH DETECTED

=====RVH=====

RVH Criteria-I(SSM) Score=0 NO RVH
 RVH Criteria-III(OKJ) Score=1 NO RVH
 RVH Criteria-II(RMH) Score=0 NO RVH
 RVH Criteria-IV(MOD) Score=3 NO RVH

=====MI Criteria-I(OKJ)=====

Anterior MI Score=0
 Anterior MI Score=0
 Anterior MI Score=0
 Total Anterior MI Score=0 NO AMI

Lateral MI Score=1
 Lateral MI Score=1
 Lateral MI Score=0
 Total Lateral MI Score=2 NO LMI

Inferior MI Score=0
 Inferior MI Score=1
 Inferior MI Score=0
 Total Inferior MI Score=1 NO IMI

Table 5.7continued

=====MI Criteria-2(MOD)=====

Anterior MI Score=0
 Anterior MI Score=0
 Anterior MI Score=0
 Anterior MI Score=1
 Anterior MI Score=0
 Total Anterior MI Score=1 NO AMI

Lateral MI Score=1
 Lateral MI Score=0
 Lateral MI Score=0
 Total Lateral MI Score=1 NO LMI

Inferior MI Score=0
 Inferior MI Score=1
 Inferior MI Score=0
 Total Inferior MI Score=1 NO IMI

=====Criteria-3(MACF)=====

Total score=15 and MI =45 %

BEAT - 4 Parameters

Lead	Pon	Ppos	Pamp	Poff	QRson	Qpos	Qamp	Qoff	Rpos	Ramp	Roff	Spos	Samp	Soff	R'	QRsoff	Tpos	Tamp	Tend	NctD
L1	79	131	0.05	151	203	203	-0.08	203	231	1.16	250	255	-0.24	260	--	267	363	-0.39	435	23.32
L2	95	123	0.18	163	203	203	0.09	203	231	1.55	243	251	-1.15	256	--	267	423	0.12	451	20.27
L3	80	108	0.14	128	188	188	0.18	188	212	0.97	222	232	-1.87	237	--	247	356	0.42	436	3.26
aR	119	155	0.11	171	187	187	0.22	187	195	0.22	212	231	-0.96	236	--	243	371	0.43	435	6.05
aL	111	127	-0.00	151	211	211	-0.10	212	231	1.59	247	247	-0.09	252	--	252	435	0.07	503	29.55
aF	76	104	0.16	144	184	184	0.13	184	212	1.23	221	232	-1.44	237	--	244	352	0.21	432	7.93
V1	83	99	-0.02	123	195	195	0.11	195	203	0.17	210	231	-2.11	236	--	255	367	0.48	435	35.31
V2	86	102	0.05	126	198	198	0.11	198	210	0.44	215	230	-3.60	235	--	260	362	0.68	438	66.88
V3	86	114	0.04	158	198	198	0.10	198	210	0.60	216	230	-4.14	235	--	261	362	0.66	438	81.78
V4	85	109	0.06	153	193	193	0.12	193	209	1.23	219	233	-3.01	238	--	261	389	0.33	441	-44.84
V5	90	118	0.07	138	170	170	-0.12	170	230	4.24	242	250	-2.31	255	--	274	370	-0.91	438	30.60
V6	91	127	0.06	163	211	211	0.95	211	231	4.87	246	251	-0.30	256	--	279	375	0.24	447	5.60

=====RESULTS=====

HR(BPM)=56.000 Bradycardia LBBB

FPA =23.457230 Degrees

=====LVH=====

LVH Criteria-I(SSM) Score=6 LVH DETECTED
 LVH Criteria-II(OKJ) Score=13 LVH
 LVH Criteria-III MAR Score=8 LVH
 LVH Criteria-IV(MOD) Score=11 LVH DETECTED

Table 5.7continued

=====**RVH**=====

RVH Criteria-I(SSM) Score=0 NO RVH
RVH Criteria-III(OKJ) Score=1 NO RVH
RVH Criteria-II(RMH) Score=0 NO RVH
RVH Criteria-IV(MOD) Score=3 NO RVH

=====**MI Criteria-1(OKJ)**=====

Anterior MI Score=0
Anterior MI Score=0
Anterior MI Score=0
Total Anterior MI Score=0 NO AMI

Lateral MI Score=1
Lateral MI Score=1
Lateral MI Score=0
Total Lateral MI Score=2 NO LMI

Inferior MI Score=0
Inferior MI Score=1
Inferior MI Score=0
Total Inferior MI Score=1 NO IMI

=====**MI Criteria-2(MOD)**=====

Anterior MI Score=0
Anterior MI Score=0
Anterior MI Score=0
Anterior MI Score=5
Anterior MI Score=0
Total Anterior MI Score=5 NO AMI

Lateral MI Score=1
Lateral MI Score=0
Lateral MI Score=0
Total Lateral MI Score=1 NO LMI

Inferior MI Score=0
Inferior MI Score=1
Inferior MI Score=0
Total Inferior MI Score=1 NO IMI

=====**Criteria-3(MACF)**=====

Total score=15 and MI =45 %

Table 5.7....continued

BEAT - 5 Parameters

Lead	Pon	Ppos	Pamp	Poff	QR	Son	Qpos	Qamp	Qoff	Rpos	Ramp	Roff	Spos	Samp	Soff	R'	QRSoff	Tpos	Tamp	Tend	NetD
L1	71	131	0.06	147	199	199	-0.04	200	231	1.29	248	251	-0.21	256	--	267	363	-0.37	439	26	22
L2	79	119	0.16	159	187	187	0.05	187	231	1.46	241	247	-1.18	252	--	286	367	-0.04	423	19	13
L3	72	108	0.13	124	172	172	0.12	172	212	0.90	219	232	-2.08	237	--	245	356	0.37	444	-7.70	
aR	119	175	0.09	231	183	183	0.20	183	187	0.20	213	231	-0.96	236	--	245	371	0.41	477	7	10
aI	111	127	-0.01	43	211	211	-0.08	213	231	1.68	251	251	-0.07	254	--	254	359	0.21	447	33	11
aF	60	108	0.15	124	172	172	0.09	172	212	1.18	223	232	-1.63	237	--	247	356	0.17	414	4	18
V1	75	99	-0.04	123	195	195	0.12	195	207	0.21	212	231	-2.21	236	--	256	367	0.51	431	4	78
V2	86	106	0.04	126	198	198	0.17	198	210	0.45	216	230	-3.05	235	--	261	362	0.77	438	-56	79
V3	82	102	0.05	122	194	194	0.21	194	210	0.72	214	230	-4.22	235	--	258	362	0.87	434	-78	31
V4	81	97	0.06	117	177	177	0.16	180	209	1.30	216	233	-2.92	238	--	259	389	0.33	429	-41	11
V5	86	114	0.05	138	186	186	-0.09	186	230	4.06	240	246	-2.19	251	--	274	370	-0.87	442	32	75
V6	159	191	0.07	207	207	207	1.05	207	231	5.05	244	251	-0.12	256	--	264	453	1.62	479	6	00

=====RESULTS=====

HR(BPM)=56.000 Bradycardia LBBB

FPA =15.248838 Degrees

=====LVH=====

LVH Criteria-I(SSM) Score=6 LVH DETECTED
 LVH Criteria-II(OKJ) Score=13 LVH
 LVH Criteria-III(MAR) Score=8 LVH
 LVH Criteria-IV(MOD) Score=11 LVH DETECTED

=====RVH=====

RVH Criteria-I(SSM) Score=0 NO RVH
 RVH Criteria-III(OKJ) Score=1 NO RVH
 RVH Criteria-II(RMH) Score=0 NO RVH
 RVH Criteria-IV(MOD) Score=3 NO RVH

=====MI Criteria-I(OKJ)=====

Anterior MI Score=0
 Anterior MI Score=0
 Anterior MI Score=0
 Total Anterior MI Score=0 NO AMI

Lateral MI Score=1
 Lateral MI Score=1
 Lateral MI Score=0
 Total Lateral MI Score=2 NO LMI

Inferior MI Score=0
 Inferior MI Score=1
 Inferior MI Score=0
 Total Inferior MI Score=1 NO IMI

Table 5.7continued

=====MI Criteria-2(MOD)=====

Anterior MI Score=0

Anterior MI Score=0

Anterior MI Score=0

Anterior MI Score=9

Anterior MI Score=0

Total Anterior MI Score=9 AMI -probable

Lateral MI Score=1

Lateral MI Score=1

Lateral MI Score=0

Total Lateral MI Score=2 NO LMI

Inferior MI Score=0

Inferior MI Score=1

Inferior MI Score=0

Total Inferior MI Score=1 NO IMI

=====Criteria-3(MACF)=====

Total score=15 and MI =45 %

RESULTANT DIAGNOSIS FROM THE 5 BEATS ITERPRETATIONS BY A
STRATEGY OF BEST OF FIVE RESULTS.

LVH definite score = 5

LVH probable score = 0

LVH possible score = 0

RVH definite score = 0

RVH probable score = 0

RVH possible score = 0

MI Anterior definite score = 0

MI Anterior probable score = 1

MI Anterior possible score = 0

MI Lateral definite score = 0

MI Lateral probable score = 0

MI Lateral possible score = 0

MI Inferior definite score = 0

MI Inferior probable score = 0

MI Inferior possible score = 0

LVH definite Bradycardia LBBB -possible Anterior MI possible

=====

Case is Abnormal

Table 5.8 Disease diagnosis using modified scoring criteria (on CSE DS-5)

ECG beat	LVH			RVH			MI					Final Diagnosis
	PS	DI	DI5	PS	DI	DI5	ANT	LAT	INF	DI	DI5	
1B1	04	NL	NL	04	NL	NL	00	01	04	NL	IMS	Bradycardia, Inferior MI possible, NL possible
1B2	02	NL		02	NL		00	01	04	NL		
1B3	02	NL		01	NL		00	00	01	NL		
1B4	02	NL		01	NL		00	00	05	IMS		
1B5	02	NL		02	NL		00	01	01	NL		
2B1	02	NL	NL	01	NL	NL	00	00	12	IMD	IMD	Inferior MI definite
2B2	01	NL		00	NL		00	00	12	IMD		
2B3	02	NL		02	NL		01	00	08	IMR		
2B4	00	NL		01	NL		00	00	05	IMS		
2B5	00	NL		00	NL		00	00	00	NL		
3B1	04	NL	NL	03	NL	NL	13	03	03	AMR		Bradycardia, LBBB, Anterior MI probable
3B2	02	NL		01	NL		13	02	01	AMR		
3B3	02	NL		02	NL		09	02	04	AMS		
3B4	01	NL		01	NL		13	02	04	AMR		
3B5	04	NL		01	NL		13	02	04	AMR		
4B1	02	NL	NL	03	NL	NL	02	03	08	IMR	IMR	Inferior MI -probable
4B2	01	NL		03	NL		01	03	08	IMR		
4B3	02	NL		03	NL		01	03	08	IMR		
4B4	01	NL		02	NL		00	01	08	IMR		
4B5	01	NL		03	NL		00	00	08	IMR		
5B1	06	LR	LR	01	NL	NL	00	00	14	IMD	IMD	LVH probable, Inferior MI definite
5B2	06	LR		01	NL		04	00	14	NL		
5B3	04	NL		01	NL		04	00	14	IMD		
5B4	04	NL		01	NL		00	00	06	IMS		
5B5	05	LS		01	NL		01	00	07	IMR		
6B1	01	NL	NL	01	NL	NL	04	00	07	IMR	IMD	Bradycardia, Inferior MI definite
6B2	01	NL		01	NL		04	00	03	NL		
6B3	01	NL		03	NL		04	00	18	IMD		
6B4	00	NL		02	NL		00	00	09	IMR		
6B5	00	NL		02	NL		00	00	09	IMR		

Table 5.8 continued

Table 5.8 continued...						
7B1	01 NL NL	03 NL NL	20 08 04 AMD/LMR AMD I.M.S	Anterior MI definite. Lateral MI possible		
7B2	02 NL	03 NL	20 04 04 AMD			
7B3	00 NL	01 NL	16 04 04 AMR			
7B4	00 NL	01 NL	16 04 04 AMR			
7B5	00 NL	02 NL	16 04 04 AMR			
8B1	11 LH LH	03 NL NL	02 03 01 NL AMS	Bradycardia, LBBB, LVI definite. Anterior MI possible		
8B2	10 LH	03 NL	02 03 01 NL			
8B3	10 LH	03 NL	01 01 01 NL			
8B4	11 LH	03 NL	05 01 01 NL			
8B5	11 LH	03 NL	09 02 01 AMR			
9B1	02 NL NL	01 NL NL	13 01 12 AMR/IMD AMR IMD	Bradycardia, Inferior MI definite. Anterior MI probable		
9B2	02 NL	02 NL	13 01 12 AMR/IMD			
9B3	01 NL	01 NL	14 01 12 AMR/IMD			
9B4	02 NL	03 NL	14 01 13 AMR/IMD			
9B5	03 NL	04 NL	15 00 13 AMR/IMD			
10B1	00 NL NL	02 NL NL	00 00 04 NL NL	Normal		
10B2	00 NL	02 NL	00 00 04 NL			
10B3	02 NL	02 NL	00 00 00 NL			
10B4	02 NL	02 NL	00 00 04 NL			
10B5	00 NL	02 NL	00 04 04 NL			

Table 5.9 Comparison of results

Rec no.	Diagnostic truth	Existing criteria results	Modified criteria results
01	NL -PR	R-PS,MI-PS,NL-PS	IMI-PS, NL PS
02	NL -PR/ IMI-PS	L-PS, MI-PS	IMI-DF
03	AMI-DF	L-DF,R-PS,MIX MI-PS	AMI-PR
04	IMI-PR/ NL -PS	R-PF, L-PS,LMI-PS,IMI-PS	IMI-PR
05	AMI-DF	L-DF,IMI-PS	L-PR, IMI-DF
06	NL -PS/ IMI-PS	L-PS,R-PS,IMI-PS	IMI-DF
07	MIX -DF/ AMI	R-PR	AMI-DF,LMI-PS
08	L-DF,BVH,non specific	L-DF,LMI-PS	L-DF, AMI-PS
09	AMI-DF	L-DF,R-PS,MI -PS	IMI-DF, AMI-PR
10	NL -PR	R-PS,MI-PS	NL

SC - score, DI - diagnostic interpretation, DI5 - DI from five beats, NL- normal,
L- LVH, R - RVH, PS - possible, PR - probable,
DF- definite, AMI-anteriorMI, LMI - lateral MI, IMI - inferior MI

Table 5.10 Comparison of program results with experts opinion

Record no.	Diagnostic truth (CSE)	Experts opinion		Modified scoring criteria results
		Exprt-I	Exprt-II	
01	NL -PR	NL	NL	IMI-PS, NL PS
02	NL -PR/ IMI-PS	IMI-PR	1 st DEG. AV BLOCK	IMI-DF
03	AMI-DF	AMI-DF	LVH strain	AMI-PR
04	IMI-PR/ NL -PS	NL	Non-specific	IMI-PR
05	AMI-DF	IMI-PS, RBBB	IMI (Ischemia)	L-PR, IMI-DF
06	NL -PS/ IMI-PS	NL-PR	NL (Appeared)	IMI-DF
07	MIX -DF/ AMI	AMI-PR, LBBB	Inferolateral infarct, incomplete RBBB	AMI-DF, LMI-PS
08	L-DF, BVH, Non-specific	LVH-DF, LBBB	LVH Strain	L-DF, AMI-PS
09	AMI-DF	AMI-DF	Antero septal infarct	IMI-DF, AMI-PR
10	NL -PR	RBBB	NL (Appeared)	NL

SC - score, DI - diagnostic interpretation, DI5 - DI from five beats,
 L- LVH, R - RVH, PS - possible,
 DF- definite, AMI-anteriorMI, LMI - lateral MI,

NL- normal,
 PR - probable,
 IMI - inferior MI

Table 5.11 Disease Diagnostic results from the Best of 5 Interpretations using Decision Tree Classifier (25 records of CSE DS-5)

LVH - Left Ventricular Hypertrophy, **RVH** - Right Ventricular Hypertrophy,
MI - Myocardial Infarction, **D** - Definite, **PR** - Probable, **PO** - Possible

Record No. 1

LVH			RVH			Anterior			MI Lateral			Inferior		
D	PR	PO	D	PR	PO	D	PR	PO	D	PR	PO	D	PR	PO
0	0	0	0	0	0	0	0	0	0	0	0	0	0	1

Bradycardia, Inferior MI -possible
Case is abnormal -possible

Record No.2

LVH			RVH			Anterior			MI Lateral			Inferior		
D	PR	PO	D	PR	PO	D	PR	PO	D	PR	PO	D	PR	PO
0	0	0	0	0	0	0	0	0	0	0	0	0	0	1

Inferior MI -possible
Case is normal -possible

Record No.3

LVH			RVH			Anterior			MI Lateral			Inferior		
D	PR	PO	D	PR	PO	D	PR	PO	D	PR	PO	D	PR	PO
0	0	0	0	0	0	0	3	0	0	0	0	0	0	0

Bradycardia, MI anterior -probable, LBBB
Case is abnormal

Record No. 4

LVH			RVH			Anterior			MI Lateral			Inferior		
D	PR	PO	D	PR	PO	D	PR	PO	D	PR	PO	D	PR	PO
0	0	0	0	0	0	0	0	0	0	0	0	0	1	3

Inferior MI -probable
Case is abnormal

Record No. 5

LVH			RVH			Anterior			MI Lateral			Inferior		
D	PR	PO	D	PR	PO	D	PR	PO	D	PR	PO	D	PR	PO
0	2	1	0	0	0	0	0	0	0	0	0	0	1	2

LVH -probable, Inferior MI -probable
Case is abnormal

Table 5.11....continued ..

Record No. 6

LVH			RVH			MI					
						Anterior	Lateral	Inferior			
D	PR	PO	D	PR	PO	D	PR	PO	D	PR	PO
0	0	0	0	0	0	0	0	0	0	0	0

Bradycardia

Case is normal -possible

Record No. 7

LVH			RVH			MI					
						Anterior	Lateral	Inferior			
D	PR	PO	D	PR	PO	D	PR	PO	D	PR	PO
0	0	0	0	0	0	0	0	0	0	0	3

Inferior MI -probable

Case is Abnormal

Record No. 8

LVH			RVH			MI					
						Anterior	Lateral	Inferior			
D	PR	PO	D	PR	PO	D	PR	PO	D	PR	PO
5	0	0	0	0	0	0	0	0	0	0	0

Bradycardia, LVH -definite, Anterior MI -possible, LBBB

Case is abnormal

Record No. 9

LVH			RVH			MI					
						Anterior	Lateral	Inferior			
D	PR	PO	D	PR	PO	D	PR	PO	D	PR	PO
0	0	0	0	0	0	0	0	0	0	0	0

Bradycardia

Case is abnormal -possible

Record No. 10

LVH			RVH			MI					
						Anterior	Lateral	Inferior			
D	PR	PO	D	PR	PO	D	PR	PO	D	PR	PO
0	0	0	0	0	0	0	0	0	0	0	0

Case is normal

Record No. 11

LVH			RVH			MI					
						Anterior	Lateral	Inferior			
D	PR	PO	D	PR	PO	D	PR	PO	D	PR	PO
0	0	0	0	0	0	0	0	0	0	0	1

Inferior MI -possible

Case is normal

Table 5.11....continued

Record No. 12

LVH			RVH			Anterior			MI Lateral			Inferior		
D	PR	PO	D	PR	PO	D	PR	PO	D	PR	PO	D	PR	PO
0	0	0	0	0	2	0	0	0	0	0	0	0	0	0

Bradycardia

Case is abnormal -possible

Record No. 13

LVH			RVH			Anterior			MI Lateral			Inferior		
D	PR	PO	D	PR	PO	D	PR	PO	D	PR	PO	D	PR	PO
0	0	0	0	0	0	0	0	1	0	0	0	0	0	1

Anterior MI -possible, Inferior MI -possible

Case is normal -possible

Record No. 14

LVH			RVH			Anterior			MI Lateral			Inferior		
D	PR	PO	D	PR	PO	D	PR	PO	D	PR	PO	D	PR	PO
0	0	0	0	0	0	0	0	0	0	0	0	0	0	1

Bradycardia, Inferior MI -possible

Case is abnormal -possible

Record No. 15

LVH			RVH			Anterior			MI Lateral			Inferior		
D	PR	PO	D	PR	PO	D	PR	PO	D	PR	PO	D	PR	PO
0	0	0	0	0	0	0	0	2	0	0	0	0	0	1

Bradycardia, Anterior MI -possible

Case is abnormal

Record No. 16

LVH			RVH			Anterior			MI Lateral			Inferior		
D	PR	PO	D	PR	PO	D	PR	PO	D	PR	PO	D	PR	PO
0	0	0	0	0	0	0	0	0	0	0	0	0	0	1

Inferior MI -possible

Case is normal

Record No. 17

LVH			RVH			Anterior			MI Lateral			Inferior		
D	PR	PO	D	PR	PO	D	PR	PO	D	PR	PO	D	PR	PO
0	0	0	0	0	0	0	0	0	0	0	0	0	0	1

Inferior MI -possible

Case is normal -possible

Table 5.11....continued

Record No. 18

LVH			RVH			Anterior			MI Lateral			Inferior		
D	PR	PO	D	PR	PO	D	PR	PO	D	PR	PO	D	PR	PO
0	0	0	0	0	0	0	0	0	0	0	0	0	0	0

Case is normal

Record No. 19

LVH			RVH			Anterior			MI Lateral			Inferior		
D	PR	PO	D	PR	PO	D	PR	PO	D	PR	PO	D	PR	PO
0	0	0	0	0	0	0	3	0	0	1	1	0	0	0

Tachycardia, Anterior MI -probable, Lateral MI -probable

Case is abnormal

Record No. 20

LVH			RVH			Anterior			MI Lateral			Inferior		
D	PR	PO	D	PR	PO	D	PR	PO	D	PR	PO	D	PR	PO
0	0	0	0	0	0	0	0	0	0	0	0	0	0	0

Case is normal

Record No. 21

LVH			RVH			Anterior			MI Lateral			Inferior		
D	PR	PO	D	PR	PO	D	PR	PO	D	PR	PO	D	PR	PO
0	0	0	0	0	0	0	0	0	0	0	0	0	0	0

Bradycardia

Case is abnormal -possible

Record No. 22

LVH			RVH			Anterior			MI Lateral			Inferior		
D	PR	PO	D	PR	PO	D	PR	PO	D	PR	PO	D	PR	PO
0	0	3	0	0	0	0	0	0	0	0	1	0	0	0

LVH possible

Case is abnormal

Table 5.11....continued

Record No. 23

LVH			RVH			Anterior			MI Lateral			Inferior		
D	PR	PO	D	PR	PO	D	PR	PO	D	PR	PO	D	PR	PO
0	0	0	0	0	0	4	1	0	0	0	0	0	0	0

Bradycardia, Anterior MI -definite

Case is abnormal

Record No. 24

LVH			RVH			Anterior			MI Lateral			Inferior		
D	PR	PO	D	PR	PO	D	PR	PO	D	PR	PO	D	PR	PO
0	1	2	0	0	0	0	1	1	0	0	0	0	3	2

Bradycardia

LVH -probable, Anterior MI -probable, Inferior MI -probable

Case is abnormal

Record No. 25

LVH			RVH			Anterior			MI Lateral			Inferior		
D	PR	PO	D	PR	PO	D	PR	PO	D	PR	PO	D	PR	PO
0	5	0	0	0	0	0	0	0	0	0	0	0	0	0

Bradycardia, LVH -probable

Case is abnormal

Table 5.12 : Disease diagnosis using the ECGs recorded in the laboratory

Record No. 1vk

LVH			RVH			Anterior			MI Lateral			Inferior		
D	PR	PO	D	PR	PO	D	PR	PO	D	PR	PO	D	PR	PO
0	0	0	0	0	0	0	0	0	0	0	0	0	0	0

Case is Normal

Record No. 2raj

LVH			RVH			Anterior			MI Lateral			Inferior		
D	PR	PO	D	PR	PO	D	PR	PO	D	PR	PO	D	PR	PO
0	0	0	0	0	0	0	0	0	0	0	0	0	0	0

Case is normal

Record No. 3saad

LVH			RVH			Anterior			MI Lateral			Inferior		
D	PR	PO	D	PR	PO	D	PR	PO	D	PR	PO	D	PR	PO
0	0	0	0	0	0	0	0	0	0	0	1	0	0	0

Lateral MI possible

Case is normal possible

Record No. 4mish

LVH			RVH			Anterior			MI Lateral			Inferior		
D	PR	PO	D	PR	PO	D	PR	PO	D	PR	PO	D	PR	PO
0	0	0	0	0	0	0	0	0	0	0	0	0	0	0

Case is normal

Record No. 5mustf

LVH			RVH			Anterior			MI Lateral			Inferior		
D	PR	PO	D	PR	PO	D	PR	PO	D	PR	PO	D	PR	PO
0	0	0	0	0	0	0	0	0	0	0	0	0	0	0

Case is normal

Record No. 6sth

LVH			RVH			Anterior			MI Lateral			Inferior		
D	PR	PO	D	PR	PO	D	PR	PO	D	PR	PO	D	PR	PO
0	0	0	0	0	0	0	0	0	0	0	0	0	0	0

Case is normal

team of expert cardiologist regarding the performance of developed software, testing has been carried out on number of records from the DS-5 and the detailed diagnosis results are given for 25 cases in Table 5.11. The disease diagnosis was also carried out on the ECGs recorded in the laboratory and the results are given in the Table 5.12.

5.6 CONCLUSIONS

The strategy of disease interpretation using decision tree classifier gives 80% accuracy in disease diagnosis. Therefore, to use the system in actual clinical practice it needs to undergo an exhaustive training under the supervision of medical experts. As the diagnosis results of CSE DS-5 records are not disclosed by the CSE, the accuracy obtained is based on a few numbers of cases whose diagnostic truth is known. The 80% accuracy is because of the reliable feature extraction by WT and also because of the new approach of analyzing the five consecutive beats per lead of a record. The use of modified scoring schemes, which includes required number of criteria, strengthens the reliability of cardiac disease diagnostics.

The results of diagnosis given in Tables 5.11 and 5.12 make it clear that, as there is advantage in using of multiple beats (5 beats). It helps to confirm the disease if indicated by a beat or more than that. Also it is equivalent to seeking the second, third or more opinions about a cardiac disease by different cardiac experts. There is low possibility of incorrect opinion as the final disease diagnosis is dependent on the analysis and confirmation of disease by exiting as well as modified disease scoring criteria on the five beat analyses.

DISEASE DIAGNOSTICS USING RHYTHM ANALYSIS

6.1 INTRODUCTION

The human heart rate (HR) or rhythm has for a long time been observed to be variable under all kinds of circumstances, including complete rest. Physiologically it is known that the HR is determined by the firing rate of the natural cardiac pacemaker, that is, by the sinoatrial nodal (SA) cells, or more precisely, by the rate of depolarization of these cells. This rate is influenced by both sympathetic and parasympathetic (vagal) control. There are a large number of factors underlying this neural control which is part of the so-called integrative neural cardiovascular control system [17,122]. External influences are muscular exercise, digestion, posture, altitude, climate, noise and psychosensory activity. The internal influences stem from autonomous physiological activity. For example, the HR fluctuates synchronously with respiration. This phenomenon is known as respiratory arrhythmia. In this part of work, an attempt has been made to study the relation between the HR and rather well known physiological influences viz. respiration rate, which affects the HR variations. Spectral and non-spectral heart rate variability (HRV) parameters have been used to analyze the heart rate variability. Fluctuations in HR are of more interest than the average heart rate. Therefore, the concept of heart rate variability (HRV) has been introduced by different researchers [68,75,89,95,112,113,143].

The HR information is normally derived from the ECG signal. The HRV can be defined as the quantitative fluctuations in heart rate. The analysis of HRV is a well accepted method, and the evaluation of HR data can yield useful information about the condition of the patients heart as well as the neural cardiovascular system. The HRV often mirrors the effects of the underlying control activities. The fluctuations in the HR are due to imbalance between the sympathetic and parasympathetic autonomic nervous systems and these counteractions give a continuous variation in the heart rate [32,68,142]. The HR series is formed by a sequence of values at different time instances, and at time, it is a function of the previous R-R intervals. This time-series is not evenly sampled since the time occurrence of the heart beat does not follow a perfect regular pattern. It is worth noting that R-R series is not constant but is characterized by oscillations of up to 10% around its mean value. These oscillations are not casual but are the effect of the action of the autonomic nervous system in controlling the heart rate [32,68]. For investigations of normal physiology and disease, the HRV has become a

topic of considerable interest [154]. The effects of respiration on HR are mediated through the parasympathetic (vagal) system [154]. The HRV related to respiration has been quantified by conventional time series techniques such as power spectrum analysis, which separates the power on the basis of the frequency components in the interbeat interval (IBI) signal. Using this method, we can separate the average power associated with respiration (which we call vagal power) from the rest of the signal. The vagal influences on the heart can then be measured by finding vagal power under different conditions. These techniques have been used to understand the role of vagal control of the heart in normal (healthy) and diseased cases [154].

As discussed in the review of the literature in chapter I, the HRV opens number of directions and highlights the importance of HRV analysis. The reduced HRV has been reported as a predictor of mortality in recent MI patients. However, its automated assessment in long-term ECG recordings is complicated by recording noise and beat-recognition errors which necessitate filtering of the computer-established sequence of beat-to-beat intervals, and visual checking and manual editing of the long-term recording, making the whole method operator-dependent and cumbersome [84]. The spectral-domain methods are known to be sensitive to artifacts in automatic recognition of long-term ECG signals. Some of the time-domain methods are believed to be less sensitive and others have only been used together with visual checking and manual editing of the automatic recognition. A perceived need for such a manual intervention discourages the assessment of HRV in routine clinical practice and confines the investigation of HRV to an academic setting. Therefore, there is a practical demand for fully automatic methods of HRV measurements which are robust and which provide clinically useful results for recordings of typical quality [85]. The assessment of HRV by using different commercially available systems has been carried out by Jens Jung et al. [53] and it has been concluded that the results of HRV analysis of the same Holter tape by using different commercially available systems are statistically noncomparable. These findings may be due to different levels of accuracy in removing ectopic beats and artifacts or different algorithms for HRV analysis. This should be kept in mind when projecting and evaluating the clinical trials. They urged to setup standards for proper assessment of HRV to avoid conflicting data due to different methodological approaches. Mainardi et al. [83] studied short-term parameters obtained from HRV analysis and observed decreased R-R interval values and an increased LF power in the five minutes following the AWS maneuver. As neither the HF power nor the RMSSD values increase, it suggests an increased sympathetic activity induced by AWS. These results indirectly confirm the R-R series as a

most sensitive index of altered physiological status. Time-varying HRV analysis applied to ICU monitoring has been found useful to detect the occurrence of physiological deterioration as well as the response to therapy, thus improving knowledge and control of patient status [89,153] have used a wavelet transform to build a simulated model of an HRV signal and to create an algorithm for HRV signal decomposition. D. Hoyer et al. [48] have introduced a concept of nonlinear HR analysis and respiratory dynamics that may improve the understanding of the underlying physiological processes of the autonomic nervous system (ANS), in comparison with the conventional linear analysis. Since HRV and RESP can be measured non-invasively, this concept may also be advantageous in diagnostic investigations of the patients. T. Harel et al. [46] observed that lower the sampling frequency is, greater are the inaccuracies in R-R interval measurements. This seriously reduces the quality of the power spectrum estimates of the HRV signal. They have reported a method to reduce the imprecision in R-R interval measurement caused by the low finite sampling frequency of ECG signals and to investigate the effect of noise on the accuracy of those measurements. They have implemented a robust algorithm to measure the R-R intervals with a high-resolution accuracy despite the finite resolution of the sampled ECG signal. Lund et al. [76] have introduced a method for extraction of beat-to-beat patterns and for noise reduction in the analysis of beat-to-beat variations of the morphology. They have observed that beat-to-beat variations in the QRS morphology are in general cyclic, with a main period of about four cardiac cycles. Narayan and Smith have reported that sudden cardiac death affects over 3,00,000 individuals per annum in the United States alone and is predominantly thought to follow ventricular tachycardia or fibrillation [99].

6.2 IMPORTANCE OF HRV ANALYSIS

From the review, it is clear that the growing interest of researchers in the field of HRV analysis is due to its importance in knowing about the normal and or diseased heart without invasive technique. There are no any golden standards set to follow in the study and analysis of the HRV, but still the following important findings drawn from the previous work can be used as the reference.

- i) Recently, attention has been focussed on spontaneous HRV on Holter monitoring as a non-invasive measure of cardiac autonomic function, Decreased HRV, indicating either increased sympathetic activity or reduced vagal activity, is associated with increased risk of death in coronary artery disease.

- ii) Previous studies have demonstrated a reduction in HRV with increasing age in patients with coronary artery disease.
- iii) HRV is being used in clinical settings such as in survivors of acute myocardial infarction or in patients with congestive heart failure.
- iv) This technique is able to noninvasively quantify the role played by the autonomic nervous system in much pathology, such as diabetes, myocardial infarction and hypertension.
- v) The patients who are prone to suffer from sustained ventricular arrhythmias could have a lesser HR increase and HRV decrease after atrial pacing than patients with a normal heart who are at no special risk of sudden cardiac arrest.
- vi) The impaired cardiac autonomic function, assessed noninvasively by spontaneous HRV on Holter monitoring, is associated with an increased risk of sudden death after MI.
- vii) Patients with LVH had a higher LV mass index and reduced HRV.
- viii) The HRV is significantly reduced in patients with LVH secondary to hypertension or aortic valve disease.
- ix) A continuous inverse relation exists between HRV and LV mass index.
- x) Increased sympathetic activity is associated with a reduced threshold for ventricular fibrillation, and thereby partially increasing mortality. The increase in parasympathetic activity has the opposition effect and increases the threshold for ventricular fibrillation.
- xi) Standard deviation of R-R normal intervals (SDNN) correlates positively with the low frequency component on power spectral density (PSD) analysis and convey important prognostic information.
- xii) The disturbances in cardiac autonomic function may contribute to the mechanism of sudden death in patients with LVH and assessment of HRV may prove important in the risk stratification of such patients.
- xiii) In ICU patients, the decrease in the total power and the lack of sympathetic modulation is associated with increased mortality.
- xiv) The LF component centered around 0.1 Hz, increases in the presence of sympathetic stimuli, while the HF component, synchronous with respiration, is mainly modulated by parasympathetic (vagal) control. Furthermore, their values accurately reflect the state of the sympatho-vagal balance.

It is clear that the HRV analysis is useful in clinical as well as in psycho-physiological studies, but the whole scenario is dependent on the accurate measurements of R-R normal-to-normal (N-N) event series and the spectral and non-spectral HRV indices. In the present work, an accurate measurement of R-R series using wavelet transform is

discussed. This is possible because of multi-resolution signal splitting in different bands of frequency. After accurate detection of N-N R-R series, effect of sympatho-vagal balance on the HRV was studied and relations between spectral and non-spectral indices are discussed.

6.3 AUTONOMIC NERVOUS SYSTEM

Autonomic nervous system (ANS) is involved with emotional responses and controls smooth muscles in various parts of the body and heart muscle. It is composed of two main subsystems namely sympathetic and parasympathetic nervous systems.

Sympathetic nervous system tends to mobilize the body for emergencies. When one or more of the sensory inputs to the brain indicate danger, there is increase in the HR, respiration, red blood cell production and blood pressure. Normal function of the body such as salivation, digestion and sexual function are all inhibited to conserve energy to meet the situation [19].

Parasympathetic nervous system tends to conserve and store bodily resources. It causes dilation of the arteries, inhibition or slowing of the heart rate. The HR is controlled by the frequency, at which, the SA node generates impulses. However, nerves of the sympathetic nervous system and the vagus nerve of the parasympathetic nervous system cause the heart to quicken or slow down, respectively [121,122].

6.4 SA NODE AND RESPIRATION ENTRAINMENT

Physiologically it is known that the HR is determined by the firing rate of SA node under the control of sympathetic and parasympathetic systems. One may distinguish between two types of influencing factors in this neural system, viz. external and internal influences, though a strict separation between these factors is not easily established. The external influences are muscular exercise, digestion, posture, altitude, climate, noise and psychosensory activity. The internal influences stem from the autonomous physiological activity. The HR for instance fluctuates synchronously with respiration. This phenomenon is known as the respiratory arrhythmia. Moreover, the HR often exhibits periodicities of about 10 seconds related to blood pressure oscillations [121,122].

The analysis of HRV is in fact the analysis of alterations in autonomous pacemaker activity. Both sympathetic and vagal pathways are responsible for these alterations causing fluctuations in heart rate. The best approximation to derive SA node activity would be the determination of the onsets of the P waves. This is, however, a difficult task, firstly because of the low rate of change of electrocardiographic potentials in this region and secondly

because of the unfavorable signal-to-noise ratio. Therefore, HR information is usually derived from the QRS complexes from which much more accurate and reliable triggers can be derived. In most circumstances of physiological rest or minor physical load, this procedure is permissible since the fluctuations in the PR interval (mainly due to AV node conduction time) are small in comparison to the accuracy of the QRS complex detection. These fluctuations are less than 5ms.

The HR is typically not constant. It usually increases during inspiration and decreases during expiration. The effects of respiration on HR are mediated through the vagal system. The HRV related to respiration has been quantified by conventional time series techniques such as power spectrum analysis, which separates the power on the basis of the frequency components in the interbeat interval (IBI) signal. Using this method, we can separate the average power associated with respiration (which we call vagal power) from the rest of the signal. The vagal influences on the heart can then be measured by finding vagal power under different conditions. These techniques have been used in an effort to understand the role of vagal control of the heart in normal healthy subjects and in diseased subjects.

The SA node of the heart acts as a self-sustaining oscillator. In the absence of stimuli, the SA node progresses through its cycle, exhibiting its own intrinsic rate. When a volley of vagal stimuli arrive at the SA node, their effect is to reset the cardiac cycle, usually delaying the next beat and slowing heart rate. The vagus is inhibited during inspiration and uninhibited during expiration. Since vagal stimulation follows respiration, we analyze HR changes at different phases of the respiration cycle.

A general observation is that, there is a noticeable decrease of the magnitude of the respiration response curve (RRC) with an increase of the pacing rate Zhang [154]. Therefore, fast vagal modulation by the paced breathing produces less cardiac resetting. This suggests that phase changes of the heartbeat in response to respiratory stimulation is frequency-dependent. It is observed that the entrainment phenomenon occurs strongly during the slow pacing condition and occurs weakly during the fast pacing condition.

6.5 METHODOLOGY

It has been suggested by different researchers that the analysis should take into account only N-N intervals differing less than ± 20 per cent from the previous intervals. But the continuous ECG recording is not perfect and contains noise of both biological and environmental origin. The amplitude and ECG pattern of normal QRS complexes can vary to the extent that even a sophisticated analysis algorithm designed to update the matched

sample may not recognize all normal complexes. The ECG morphology of ectopic cardiac beats of atrial or atrioventricular nodal origin is not distinguishable from normal sinus rhythm beats, and therefore, such complexes are included into the automatically generated normal-normal (N-N) interval sequence and the same is not desirable for accurate HRV analysis.

When the R waves are detected with an accuracy of 2ms (which is not high) for event process analysis, a sample frequency of 500 Hz is needed. However, the bandwidth of a signal describing HRV is restricted to say 0.5 Hz. This is corresponding to the mean HR of 60 BPM and the bandwidth (BW) of chosen HRV signal is always less than 0.5 Hz. The sample frequency necessary for the HRV signal is therefore 1 Hz.

Even after a good amount of work, there is necessity to develop a reliable technique to handle large amount of the ECG data effectively with an efficient data compression technique, and thereafter, use the same for HRV analysis. In the present work, the wavelet transforms (WTs) have been used to compress large amount of ECG data to determine QRS complexes and R-peak locations effectively. The WTs in conjunction with a spectral analysis technique can be conveniently implemented on a dedicated microcomputer based portable system and the signals from the subjects can be collected over an extended period of time without hampering daily schedule of activity. The data acquired from the standard database/subject is firstly scanned by the WT based QRS detection algorithm to detect the R-R time series. The use of WT serves three purposes; firstly it removes the noise and baseline wander, secondly it provides data compression up to 8:1 ratio without losing the R-peak information, and finally the most useful purpose of accurate detection of R-R time series. After detecting R-R time series, the HRV analysis is being carried out by estimating the spectral and non-spectral parameters and the study of HRV related curves. The quantitative estimation of HRV is performed using spectral and non-spectral indices. The power spectral density (PSD) distribution of the HR series has established itself as one of the best indices to read the information about cardiovascular autonomic system.

Some of the HRV indices are normal-to-normal standard deviation (SDNN), beat-to-beat standard deviation (SDBTB), percentage of normal-to-normal prolongation >50 ms (pNN50), heart rate variability index (HRV index), triangular interpolation of the normal-to-normal histogram (TINN), and left ventricular mass index. In addition to spectral and non-spectral indices, the HRV analysis is also being carried out by graphical representations such as power spectral density (PSD) curve, interval tachogram (IT) and distribution density curve (DDC).

The previous studies reveal three different frequency components; the first one a high frequency component (HF) i.e. spectral component around the respiratory frequency (approximately 0.3 Hz) and mainly related to vagal activity, the second one a low frequency component (LF) and generally centered around 0.1 Hz and having power variations related to sympathetic activity, and the third one a very low frequency component (VLF) associated with the slow regulation mechanism such as thermoregulations [53,88,89,121].

The HRV signal (obtained from the R event series) is a slowly varying signal with a bandwidth of 0-0.5 Hz and can be considered to be a fair representation of the integral neural influence on autonomous pacemaker activity. This HRV signal may then be subjected to spectral analysis. There are three regions of interest in the spectrum, indicated by R, B, and T as shown in Fig. 6.1.

R – Respiratory fluctuations: This is in most cases a predominant contribution to HRV (therefore, the terms sinus arrhythmia and respiratory arrhythmia are often used as synonyms). Obviously, the location of this spectral peak is dependent on the rate of respiration.

B – Blood pressure fluctuations: The neural blood pressure control system via the arch and carotid sinus baroreceptors exhibits spontaneous oscillations with a periodicity of about 10 seconds. These oscillations are reflected in heart rate variability.

T – Thermoregulation fluctuations: The thermoregulation control system is subjected to spontaneous oscillations as is the blood pressure control system. These oscillations are also reflected in heart rate variability. The influence is much less than the other two mentioned influences.

The system performance has been evaluated by using the standard MIT/BIH database and the database created by on-line recording from different subjects in the laboratory itself. The second set of database obtained from the subjects in the laboratory characterizes the dynamic response of the heart to the vagus nerve i.e. during slow, comfortable and fast paced respiration (12, 19 and 24 breaths/min).

6.6 DETECTION OF R-R EVENT SERIES

The reported studies also propose patho-physiological background for the prognostic value of HRV, suggesting that decreased HRV may correlate with decreased vagal nervous activity or increased sympathetic activity which may enhance the risk of ventricular

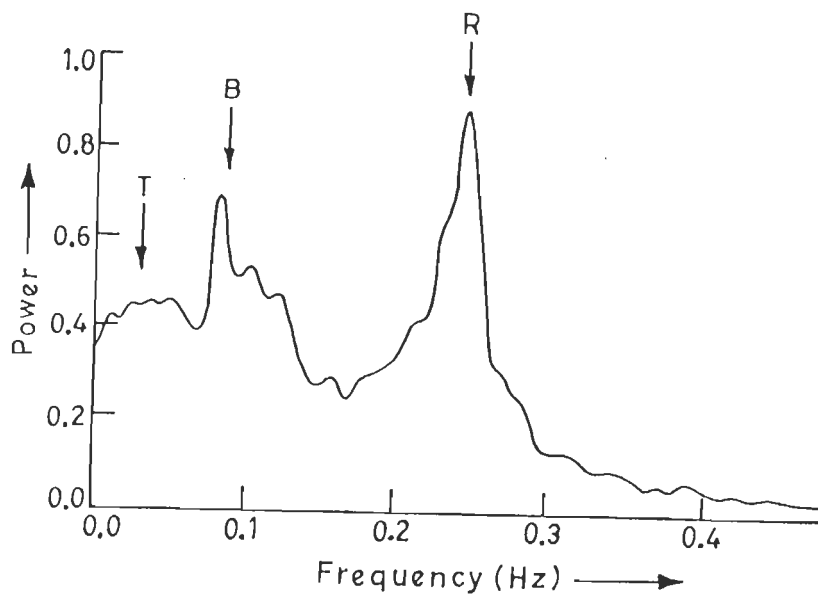


Fig. 6.1 HRV power spectrum. (T -thermoregulation fluctuations, B -blood pressure fluctuations, R -respiratory fluctuations)

[Rompelman O., et al., 1977, (121)]

fibrillation. The correlation between the sympathetic tone and HRV power spectral components is also reported. Therefore, measurement of HRV in post infarction patients is a promising technique, which may prove to be of clinical importance, but standardization of HRV measurement poses severe problem at the data processing level.

Unfortunately, the need for visual checking and manual editing is impractical in the clinical setting and discredits the potential clinical value of the whole method because such a time-consuming and specialized operation is beyond the capabilities of a typical clinical cardiology department. Hence, a fully automatic method of HRV measurement in postmyocardial infarction patients would be of value, yet no attempt have been reported until now to determine the optimal method for filtering the N-N sequence and the optimal formula for the numerical expression of heart rate variability.

The dependability of interpretation and diagnostics by the computer is based on the accuracy of the extraction of the characteristic features of the ECG signal. Currently WT based feature extraction techniques have gained lot of attention of researchers and are being explored as an effective and dependable tools for computer aided diagnostics[38,115,153]. One of the reasons in favour of WTs is that they characterize the local regularity of signals by decomposing the signal into elementary building blocks. These blocks are well localized both in time and frequency and make wavelets robust to eliminate noise [109,115,153]. It is being felt that in future, WTs may be one of the ultimate choice for ECG feature extraction as the standardization of HRV measurement poses severe problems at the data-processing level for other QRS detection techniques. The continuous ECG recording is not perfect and contains noise of both the biological and environmental origin. In addition to this, the amplitude and ECG pattern of normal QRS complexes can vary to the extent that even a sophisticated analysis algorithm designed to update the matched sample may not recognize all normal complexes. Similarly, the ECG morphology of ectopic cardiac beats of atrial or atrioventricular nodal origin is not distinguishable from normal sinus rhythm beats, and therefore, such complexes are included into the automatically generated normal-normal (N-N) interval sequence and the same is not desirable for accurate HRV analysis. It has been suggested that analysis should take into account only N-N intervals differing less than $\pm 20\%$ from the previous intervals [84]. However, in many situations, such filtering is not effective in removing all artefacts from the original N-N sequence. Therefore, reported study also employ a visual check of the recorded ECG and manual editing of the N-N sequence prior to establishing the numerical value of heart rate variability. However, the use of multi-resolution decomposition process to split the signal into one detail and one low resolution

signal to carry out the QRS detection, as given in chapter III, gives solutions to all noise related difficulties in detecting N-N R-R events.

6.7 TEST RESULTS AND DISCUSSIONS

Figures 6.2(a-c) show the flowcharts indicating the ECG signal acquisition, use of the WT for QRS detection and removal of ectopic beats and artifacts, determination of spectral and non-spectral indices and displaying of HRV related plots, namely interval tachogram, PSD and DDC curves. The system performance has been evaluated using the standard MIT/BIH database and the database created by on-line recording from different subjects in the laboratory itself. The MIT/BIH ST-change database has been taken from record numbers 300 to 323 obtained during exercise stress tests. The WT has been used to detect the R-R normal intervals from the ectopic beats and artifacts. This is because of splitting the ECG signal in different bands of frequencies and the use of frequency band containing the QRS complexes. Fig.6.3 shows a long record (3 minutes) which depicts the detection of R peaks. Tables 6.1 and 6.2 show sample results. On the basis of these results, it can be stated that the HRV spectral and non-spectral indices are less prone to fluctuations in heart rate due to autonomic imbalance than the fluctuations due to improper and incorrect detection of a single heartbeat. This is confirmed by the result shown in Table 6.2, which shows the detection of false (abnormal) beats in the records from the MIT/BIH database. This false detection gives substantial rise to the values of HR, SDNN, LFP (low frequency power) and HFP (high frequency power) parameters.

The second set of database obtained from the subjects in the laboratory characterizes the dynamic response of the heart to the vagus nerve i.e. during slow, comfortable and fast paced respiration. At first, the subjects were asked to sit and breathe naturally for 2 min in order to be stable. Then subjects were asked to pace their breathing by inhaling and exhaling in synchrony with a time pointer moving up and down at the desired pacing rate. The inspiration and expiration each should take approximately half of the respiration cycle. Three different breathing rates, 12, 19, and 24 breaths/min were chosen to represent slow, comfortable, and fast pacing rates, respectively. These three pacing rates were chosen to facilitate examination of the dependence on the respiration frequency. Table 6.3 shows quantization of the data in terms of their relative spectral and non-spectral indices for different respiration phases. To illustrate the influence of different respiration phases on the vagal activity, the HRV and corresponding PSD curves have been plotted and are shown in Fig.6.4. For slow respiration (Fig.6.4 a), the HR gradually changes and this change is in the

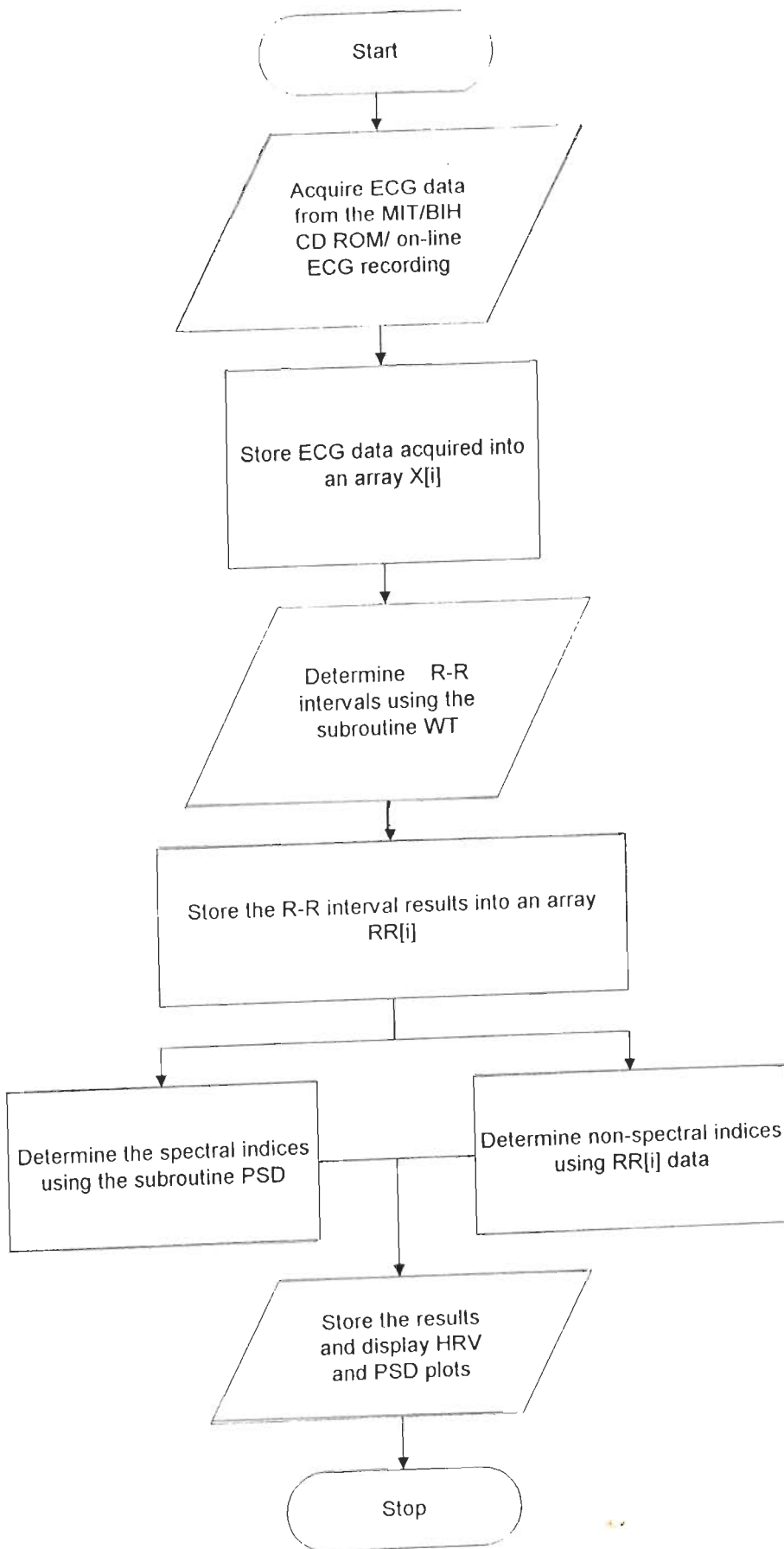


Fig. 6.2(a) Flow chart for HRV analysis

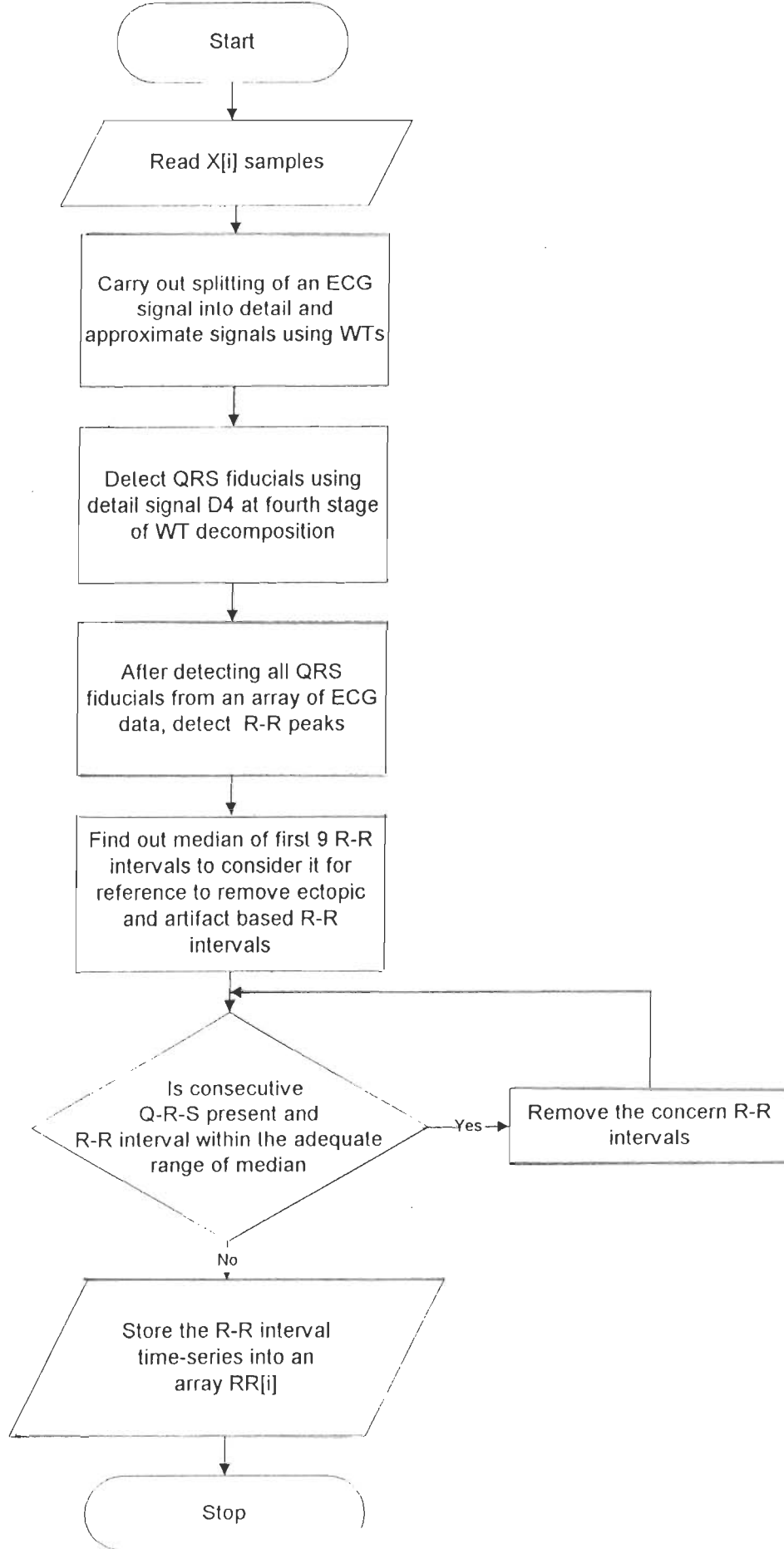


Fig. 6.2(b) WT subroutine

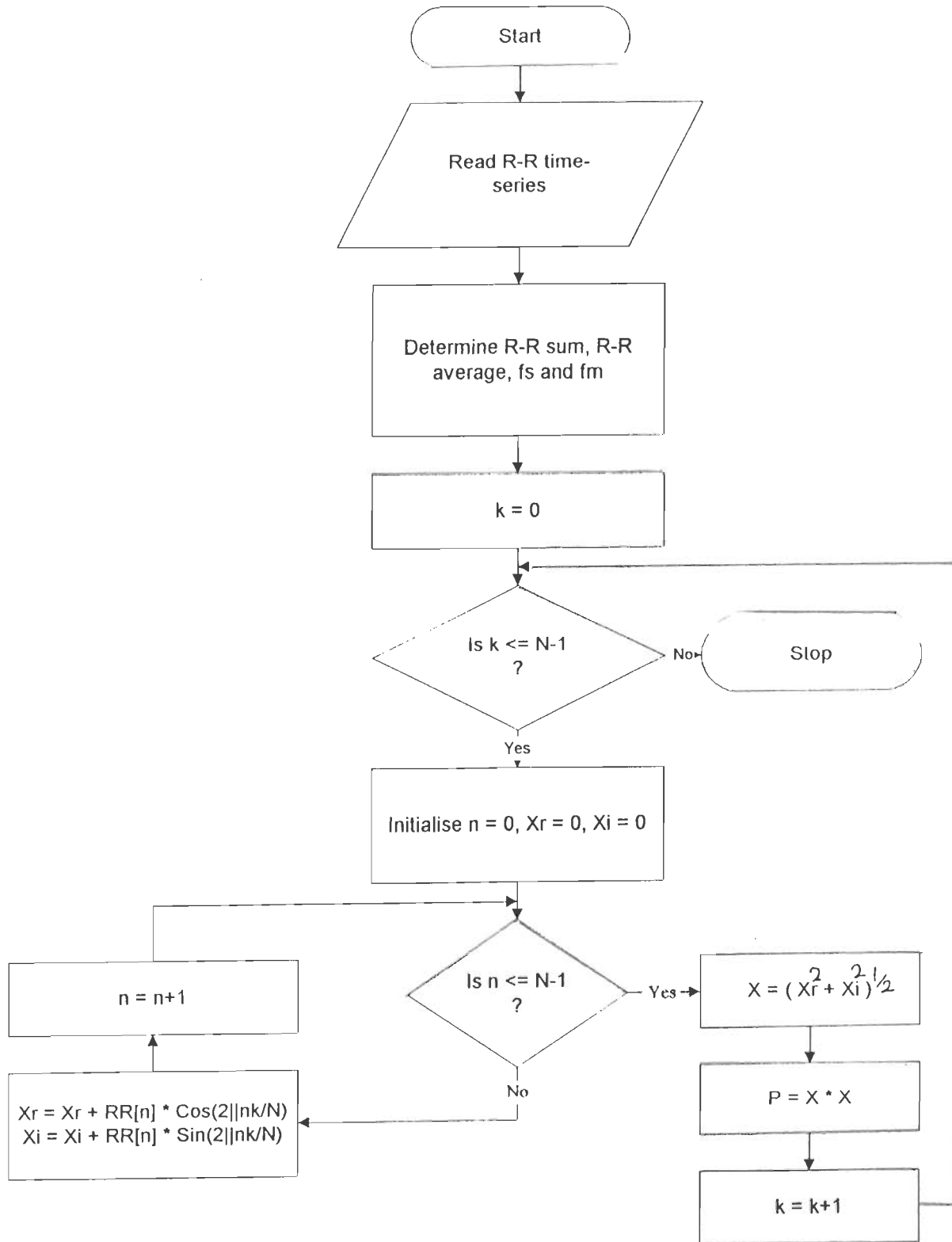


Fig. 6.2(c) PSD subroutine

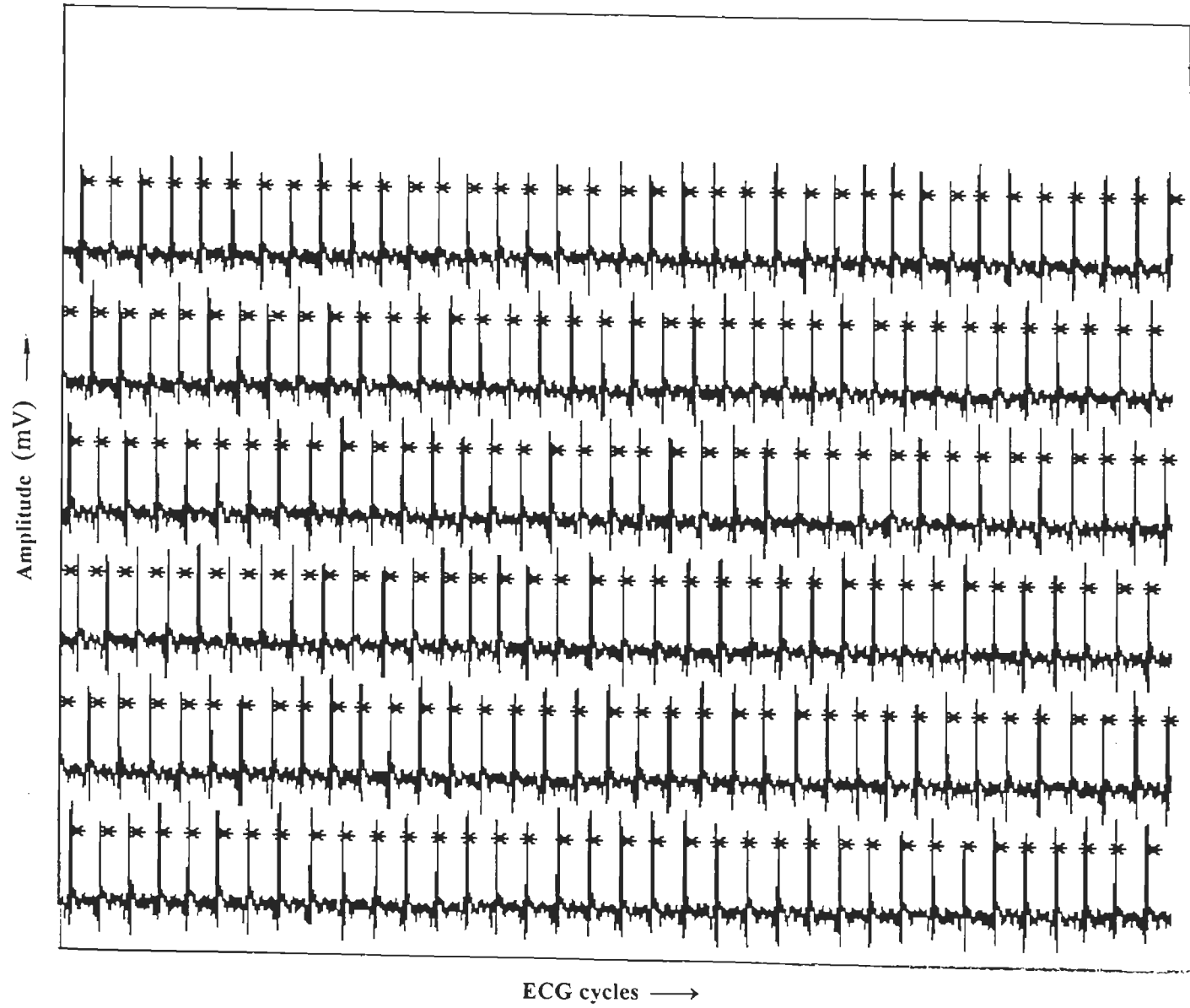


Fig. 6.3 Detection of R peaks using WT in long recording

Table 6.1 Extraction of spectral and non-spectral indices

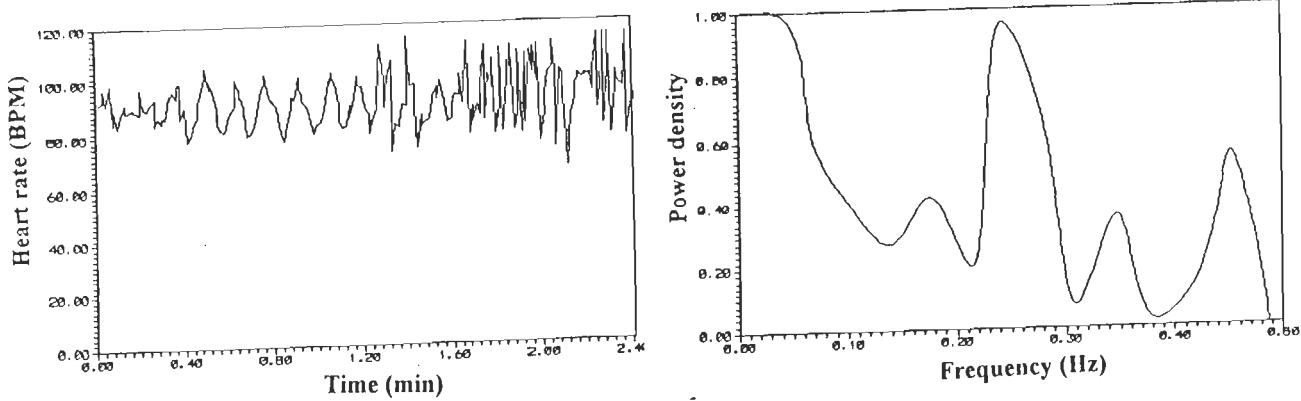
MIT Record no.	Average R-R ms	HR BPM	SDNN ms	LFP ms ²	HFP ms ²	Ratio LFP/HFP
100	814.12	75.82	8.43	0.58	13.75	0.04
200	730.64	84.48	6.56	0.11	1.79	0.06
300	663.51	93.03	3.40	0.01	3.76	0.00
301	1056.68	58.42	10.34	1.36	25.01	0.05
302	977.98	63.12	11.51	0.98	30.08	0.03
303	722.78	85.40	10.04	0.11	33.26	0.00

Table 6.2 Effect of abnormal beat on HRV indices

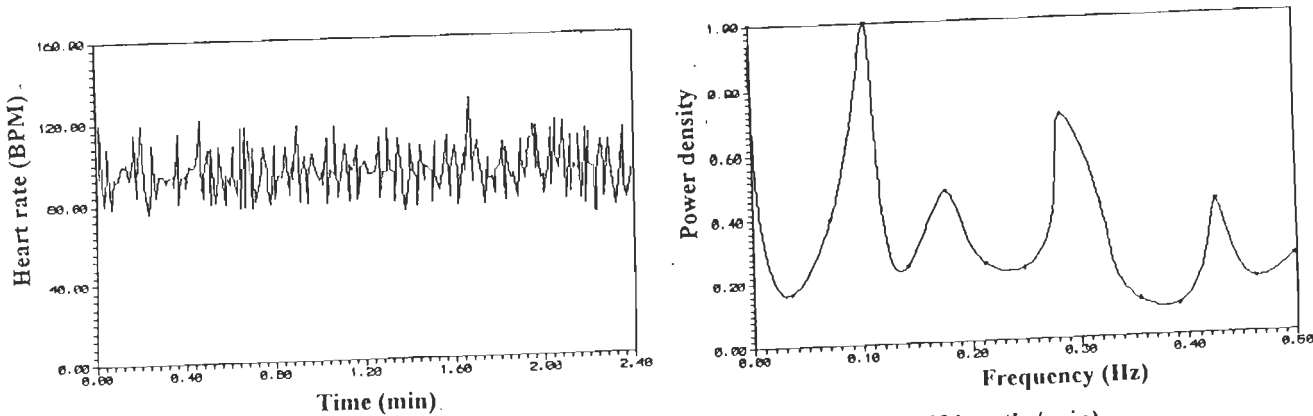
MIT/BIH Record no.	Average R-R ms	HR BPM	SDNN ms	LFP ms ²	HFP ms ²	Ratio LFP/HFP
100 (normal beats)	814.12	75.82	8.43	0.58	13.75	0.04
(with one abnormal beat)	815.63	75.68	24.63	0.46	32.24	0.01
200 (normal beats)	730.64	84.48	6.56	0.11	1.79	0.06
(with one abnormal beat)	651.36	94.77	43.33	1.62	40.58	0.04
300 (normal beats)	663.51	93.03	3.40	0.01	3.76	0.00
(with one abnormal beat)	656.73	93.99	13.80	3.51	23.09	0.15

Table 6.3 Effect of slow, normal and fast respiration rates on HRV indices studied over consecutive four days

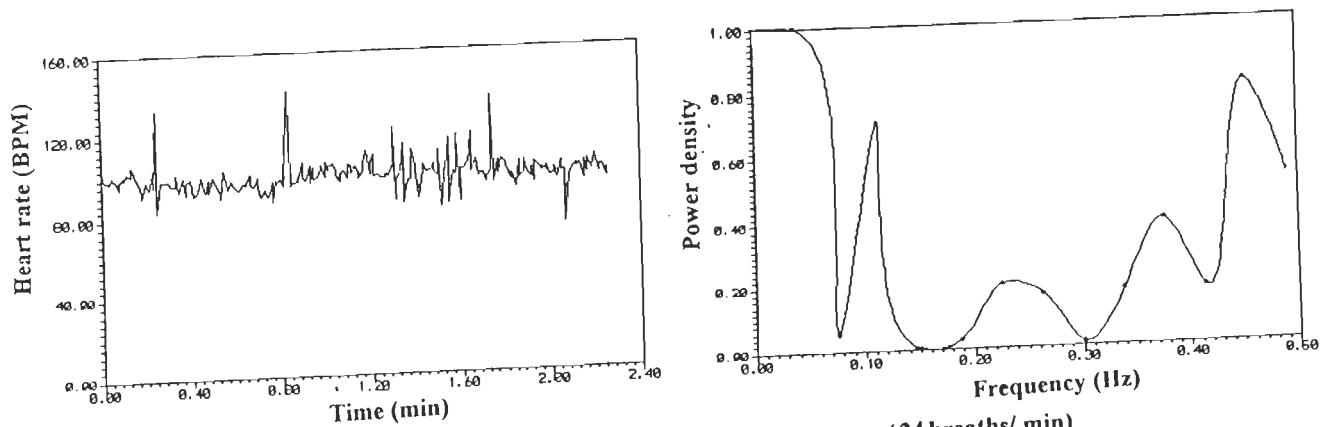
Respiration rate Breaths/ min	Average R-R ms	HR BPM	SDNN ms	LFP ms ²	HFP ms ²	Ratio LFP/HFP
First day						
12(slow breathing)	722	83.09	15.12	4.27	9.92	0.43
19 (normal breath)	682	87.89	11.72	3.68	10.21	0.36
24 (fast breathing)	679	88.28	11.21	13.73	2.26	6.08
Second day						
12	629	95.32	15.00	2.84	10.15	0.28
19	598	100.3	12.62	3.12	4.54	0.69
24	581	103.1	9.87	2.72	4.30	0.63
Third day						
12	659	91.00	15.85	4.70	7.13	0.66
19	645	92.88	15.25	5.21	9.0	0.58
24	609	98.37	8.37	3.98	5.59	0.71
Fourth day						
12	622	96.39	15.29	2.5	10.26	0.24
19	581	103.1	14.83	1.05	5.51	0.19
24	569	105.3	12.24	3.04	4.09	0.74



(a) HRV and PSD curves for slow breathing rate (12 breaths/min)



(b) HRV and PSD curves for normal breathing rate (19 breaths/min)



(c) HRV and PSD curves for fast breathing rate (24 breaths/min)

Fig. 6.4 Comparison of HRV signals in different respiration phases

range of 80 to 100 BPM. So far as normal breathing is concerned (Fig. 6.4 b), the HR change is fast and varies from 80 to 120 BPM. For fast respiration (Fig. 6.4 c), the HR variations are less except few high HR spikes and the change is in the range from 90 to 110 BPM. There is a negative relationship between the respiratory rate and the spectrum measures of parasympathetic activity (vagal power). For slow respiration, high power peak emerges around the frequency of 0.3 Hz. A low power peak emerges in case of fast respiration rate. This indicates the influence of vagal control on heart activity. The test results are consistent and reliable and show high promise for the effective use of this technique for the HRV study and analysis.

6.8 CONCLUSIONS

The following conclusions can be drawn on the basis of study carried out:

- i) The use of wavelets for feature extraction using adaptive window scanning improves the detection sensitivity of the QRS complexes which results into an accurate measurement of R-R time series which is must for proper HRV analysis.
- ii) It can be stated that the HRV spectral and non-spectral indices are less prone to fluctuations in heart rate due to autonomic imbalance than the fluctuations due to improper and incorrect detection of even a single heart beat.
- iii) It has been observed that the incorrect beats in the records from the MIT/BIH database have given substantial rise to the values of HR, SDNN, LFP and HFP parameters.
- iv) In general, there is a negative relationship between respiratory rate and spectrum measures of parasympathetic activity (vagal power). For slow respiration, high power peak emerges at 0.3 Hz. A low power peak emerges in case of fast respiration rate. This indicates the influence of vagal control on the heart activity and the entrainment of respiration on SA node activity is more during the slow breathing phase.
- v) For increased rate of respiration (slow, normal and fast), there is corresponding increase in HR and decrease in SDNN values.
- vi) The strategy of HRV analysis in different respiration phases helps in understanding the role of vagal control of the heart. This simple approach can be used in actual clinical practice to study the status of the heart without using invasive techniques.

ECG DATA COMPRESSION USING NON-REDUNDANT TEMPLATE AND WAVELET TRANSFORM

7.1 INTRODUCTION

Considering the tremendous volume of electrocardiogram (ECG) data being recorded each year, the ability to efficiently manage the storage and retrieval of this data for the purposes of comparison and evaluation mandates the need for compression techniques. The storage and transmission limitations have made ECG data compression an important feature for most of the computerized systems. For example, modern Holter systems call for long term (24 hours) storage of single or multichannel ECG data, transmission of ECG data over telephone lines and mobile radio links, the performance and functionality of ambulatory monitors and recorders, and the implementation of real-time rhythm analysis and automatic diagnostic algorithms[11,13,21,73,55]. In addition, the capability of efficient transmission of the stored data to diagnostic centers is becoming a standard requirement. Such systems invariably require a means of data compression which lead to the conflicting requirements of a high compression ratio (CR) versus good signal fidelity. Another scenario for the use of compression methods is the storage of signal databases from numerous patients with different etiologies. Likewise, signal databases have proved to be very useful for the evaluation of new automated analysis systems and algorithms. Although a good number of compression techniques have been reported in literature, the search for new method continues, with the aim of achieving greater compression ratio (CR) while preserving the clinical information content in the reconstructed signal is continuing. The CR depends on the intended data application and the common way to measure it, is through performance indices like, percent root mean square difference (PRD), signal powers (original signal, reconstructed signal and error signal), diagnostic ECG parameters and visual inspection.

The ECG data compression methods reported in the literature fall mainly into four categories, namely (i) direct data compression (DDC), ii) transformative, iii) hybrid and iv) parameter extraction techniques. These techniques are reviewed in chapter I. As these data-compression algorithms have been tested with different databases for different signal sampling ratio and precision of original data, thus their direct comparison is very difficult and even not logical at times [100,131].

The commonly used direct data compression techniques are Amplitude Zone Time Epoch Coding (AZTEC), modified AZTEC, FAN, Scan Along Polygonal Approximation (SAPA), Coordinate Reduction Time Encoding System (CORTES), Turning Point (TP) and Delta Pulse Code Modulation (DPCM) [50,130]. Some of the commonly used transform techniques are Karhunen-Loeve transform (KLT), Fourier Transform (FT), Cosine Transform (CT), Walsh transform (WT), Haar-transform (HT), optimally warped transform, sub-band coding and the wavelet transform (WT) [26,34,47,52,60,70]. In parameter extraction methods, the techniques covered are peak-picking, cycle-pool-based, linear prediction, and neural network methods. Vector quantization (VQ) has also been used for data compression[55,100]. It is employed in conjunction with any of the previously mentioned methods mainly as a way of quantizing the resulting data after compression. In most of these data compression methods, a complicated procedure is involved to select the line segments, slope segments, segment lengths, amplitude of segment extreme points, setting of error thresholds, and coding schemes. The compressed data is in the form of numerals, or codes and not in the form of signals. Again a procedure is involved to decode the information stored in some coded form to reconstruct the signal. Even with the complex procedure and computations required for compression and decompression, performance-wise no method can be placed in a category which satisfies all the requirements of compression and decompression. Thus there is still a necessity to develop such techniques which can be still ahead in performance compared to existing techniques. In the present work, a simple non-redundant-template direct data compression (NRT-DDC) method is developed which retains 100% information of compressed signal and provides a high compression ratio (8:1). Some work has also been carried out on WT based data compression. NRT-DDC perform the compression by down-sampling the ECG signal in steps by using a non-redundant template. The removed data samples in the process of down-sampling are stored in a data array as non-redundant template. The signal is compressed by a factor of about 8 for the signal sampled at 500 Hz or 16 for the signal sampled at 1000 Hz. It has been noted that 100 percent information w.r.t. the morphology of the original signal is retained in the reconstructed signal. The method is consistent and reliable and can be used for both the online and offline ECG data compression.

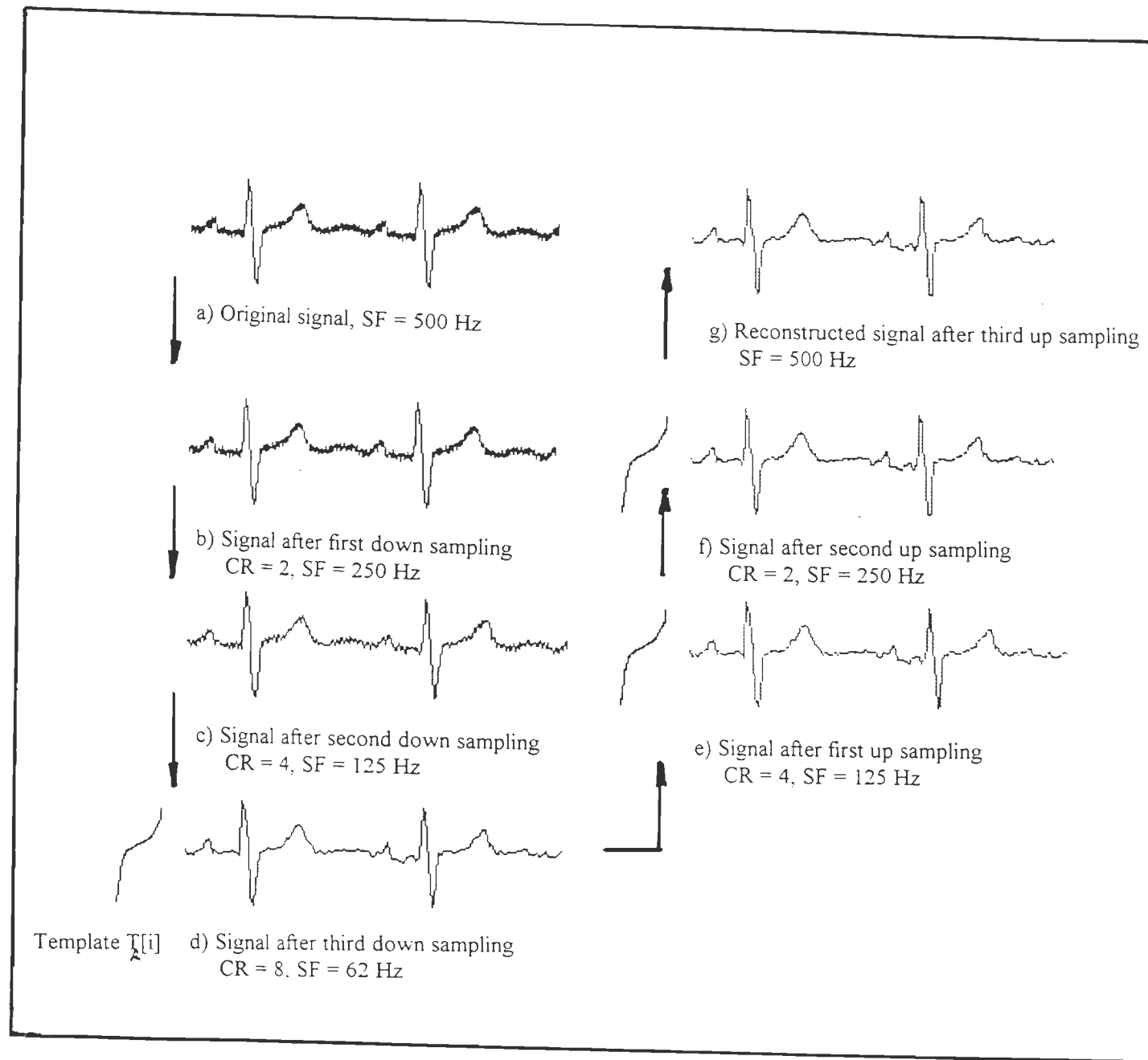


Fig.7.1 Steps of ECG compression and decompression using NRT-DDC

7.2 A NEW NON-REDUNDANT TEMPLATE - DIRECT DATA COMPRESSION TECHNIQUE

The steps used for compression and decompression in this technique are given below:

7.2.1 Compression

(i) Data compression is performed by downsampling the original ECG signal in steps. Downsampling means, picking an alternate samples from the original signal, which reduces original signal into its half data length containing $N/2$ number of samples as that of original signal. The care is taken to retain the peak and valley points.

Consider $X(n)$ as the original signal with N number of samples as shown in Fig.7.1(a). In first downsampling, alternate samples are removed from the array $X(n)$ and stored into another array $T(i)$, called as redundant template.

$$X(n), (n = 0 \text{ to } N) = [X(2k) + X(2k+1)], (k=0 \text{ to } \frac{N}{2} - 1)$$

From these even numbered samples, $X(2k)$ are to be used as compressed data and the odd numbered samples ($X(2k+1)$) are to be used as redundant data samples.

$$\text{Thus, } T_1(i), (i=0 \text{ to } \frac{N}{2} - 1) = X(2k+1), k = 0 \text{ to } \frac{N}{2} - 1$$

(ii) In the second step of compression, again downsampling of the signal is carried out by removing the alternate samples from the series $X^1(k)$ as shown in Fig.7.1(b).

$$X^1(k) = X(2k), k=0 \text{ to } \frac{N}{2} - 1$$

The removed odd numbered samples from the series $X^1(k)$ are stored into redundant array $T_2(i)$ as given below:

$$X^1(k), (k=0 \text{ to } \frac{N}{2}) = [X^1(2l) + X^1(2l+1)], (l=0 \text{ to } \frac{N}{4} - 1)$$

$$\text{Thus, } T_2(i) = X^1(2l+1), l=0 \text{ to } \frac{N}{4} - 1$$

After this step, we get $\frac{N}{4}$ number of samples stored in $X^1(2l)$.

(iii) In the third step, further downsampling of the signal is carried out to remove the odd numbered signal samples.

$$X^{11}(l) = X^1(2l), l=0 \text{ to } \frac{N}{4} - 1$$

The removed samples from the signal $X^{11}(l)$ (as shown in Fig.7.1(c)), are stored in redundant template $T_3(i)$ as given below:

$$X^{11}(l), (l=0 \text{ to } \frac{N}{4}) = [X^{11}(2m) + X^{11}(2m+1)], m=0 \text{ to } \frac{N}{8} - 1$$

$$\text{Thus, } T_3(i) = X^{11}(2m+1), m=0 \text{ to } \frac{N}{8} - 1$$

The retained samples $X^{11}(2m)$, $m=0 \text{ to } \frac{N}{8} - 1$ are the samples of compressed signal as shown in Fig. 7.1(d).

(iv) With this compression procedure, we store first and every 8th sample from the original ECG signal $X(n)$ having N number of samples, therefore, compressed signal $X_c(n)$ contains

$$X_c(n) = X(8m), m=0 \text{ to } N-1$$

$$\text{i.e. } X_c(n) = X^{11}(2m), m=0 \text{ to } \frac{N}{8} - 1$$

and except such $X_c(n)$ samples, other samples are stored in the template $T(i)$.

where,

$$\begin{aligned} T(i) &= T_1(i) + T_2(i) + T_3(i) \\ &= X(2k+1), k=0 \text{ to } \frac{N}{2} - 1 \\ &+ X^1(2l+1), l=0 \text{ to } \frac{N}{4} - 1 \\ &+ X^{11}(2m+1), m=0 \text{ to } \frac{N}{8} - 1 \end{aligned}$$

Finally, $T(i)$ samples are arranged in an ascending order with the removal of redundant samples, retaining unique sample amplitudes in a non-redundant template $T_R(i)$.

The result of these four steps is a compressed signal $X_c(n)$ and a non-redundant template $T_R(i)$, which gives a compression ratio of 8. The sampling of a signal at 500 Hz having N number of samples reduces it to $N/2$ number of samples by first downsampling resulting an effective sampling of 250 Hz. After the first step, a signal as shown in Fig.7.1(b) having $N/2$ number of samples is reduced to $N/4$ number of samples and the effective sampling is 125 Hz. In the third step, the signal as shown in Fig. 7.1(c) with $N/4$ number of samples is reduced to $N/8$ samples and the effective sampling at this stage becomes 62.5 Hz. The removed samples are stored into an array called a redundant arrays which are finally grouped to form a non-redundant array, removing the redundant samples. In particular it is observed

that for a original signal with the data length of 10,000 samples with 30 to 40 cycles, when compressed by this algorithm retains about 1250 samples in the compressed signal and about 150 samples in a template. Hence the $1250+150 = 1400$ samples hold 100% sample amplitude information contained in the original signal of 10,000 samples. The information regarding the position of the removed samples is retained by the compressed signal (Fig.7.1(d)). Hence we need to store or transmit a compressed and a non-redundant template $T_R(i)$, which gives a compression ratio of about 8, for a sampling of 500 Hz and about 16, for a sampling of 1000 Hz. The CR of 8 or 16 is depending on the number of stored samples in the compressed signal as well as in the redundant template array $T_R(i)$, therefore, it has mentioned as about 8 or 16. With this procedure, we get CR of about 8 or 16. As it is difficult to retain all peaks and valleys of the original signal, therefore, it is desirable to retain some major peaks and valleys which are higher in magnitude than the retained first and the 8th samples, i.e., if the sample peak or valley between first and eighth such samples is greater in magnitude than these two samples (first and eighth), then it is retained. Retaining of such peaks and valleys help to maintain the signal morphology and the information of clinical significance. If a peak or a valley falls on the samples $X(0)$ or $X(8)$, then these points by itself hold the information of a peak or a valley. If the peak and valley are the samples among $X(1)$ to $X(7)$, then the first two $X(1)$ and $X(2)$ samples peaks or valleys are replaced to $X(0)$ and $X(6)$, and $X(7)$ peak or valley is replaced to $X(8)$. The peak or valley among the $X(3)$, $X(5)$ samples is replaced in place of $X(4)$, and this $X(4)$ sample is stored by adding a threshold value 'Th' to its amplitude, which helps to recognize this additional peak or valleys being stored between the points $X(0)$ and $X(8)$.

The strategy of retaining the peak or valley of the neighbor sample i.e. $X(1)$, $X(2)$ in place of $X(0)$, and $X(3)$, $X(4)$, $X(5)$, in place of $X(4)$ with a threshold 'Th' and for $X(6)$, $X(7)$, the place of $X(8)$ is used. This procedure adds shifting of sample positions by an amount of one sample displacement in case of $X(1)$, $X(3)$ and $X(7)$ samples and two sample position shifting for $X(2)$ and $X(6)$ samples, and no shifting to $X(0)$, $X(4)$ and $X(8)$ samples. The effect of this maximum displacement equivalent to two sample durations (4ms) in comparison to R-R duration of about 1000 ms, is negligible if sampling frequency is 500 Hz.

7.2.2 Decompression

After looking at different data compression methods, it can be stated that retaining the morphology of original signal in the reconstructed signal puts lot of constraints and scrutiny

check on the compression technique. In the present method, the steps of reconstruction at different stages of procedure are explained below.

(i) In the first step of reconstruction, a compressed signal is traversed by the template to overlap and map the samples of compressed signal with the samples of non-redundant template from the starting of compressed signal to the end for interpolation. To do this, firstly $X(0)$ sample of the original signal (Fig.7.2) is mapped with the same amplitude sample of $T_R(i)$ as $X(t)$ and $X(8)$ is also mapped with the same amplitude sample of $T_R(i)$ as $X(t+m)$. These 'm' number of samples of $T_R(i)$ from $X(t)$ to $X(t+m)$ are considered to select the median numbered sample among the number of samples of $T_R(i)$ to select middle point $X(4)$ of $X(0)$ and $X(8)$. It is observed that the density of samples in the vicinity of baseline (zero crossing region) is more compared to maxima or minima amplitude levels i.e. the region of R and S peaks of the signal. Hence the sample $X(4)$ selected as $X(t+m/2)$ is more near to $X(0)$ than $X(8)$ as shown in Fig.7.2. This procedure of interpolation of such $X(4)$ samples from the $T_R(i)$, throughout the compressed signal, completes the first upsampling. If a peak or a valley sample point is present as can be recognized by the threshold point 'Th', then the $X(0)$ and $X(4)$ samples are considered in place of $X(0)$ and $X(8)$ to fill up the middle point $X(2)$ from the template, by the same upsampling procedure. This step of reconstruction converts a signal with $N/8$ number of samples to high resolution signal having $N/4$ number of samples and an effective sampling of about 125 Hz.

(ii) In the second step, signal is further up-sampled by the same procedure as explained above, to convert the signal having $N/4$ samples into a high resolution signal with $N/2$ number of samples to represent an effective sampling of 250 Hz. This step completes the second up-sampling.

(iii) In the final step, the signal is up-sampled to get resolution equal to the original signal by interpolating the required samples from the template $T_R(i)$.

This three step reconstruction procedure is shown in Fig.7.1. It consists of the output of compression procedure shown by the signals in Fig 7.1(a), (b), (c) and (d). The signals shown in Fig.7.1(e), (f), and g) are the output signals at different stages of reconstruction. The details of reconstruction procedure are shown in Fig.7.2. Considering two consecutive points of a compressed signal 'd' (fig.7.1) as say $X(n)$ and $X(8n)$, $n=0$ to $N/8-1$, wherein, among the first slot of samples from $X(0)$ to $X(8)$, $X(1)$ to $X(7)$ samples are to be interpolated from the template $T_R(i)$, ($i=0$ to m) to bring out the complete reconstruction. When there is no peak or valley point stored between $X(0)$ to $X(8)$ as can be recognized by

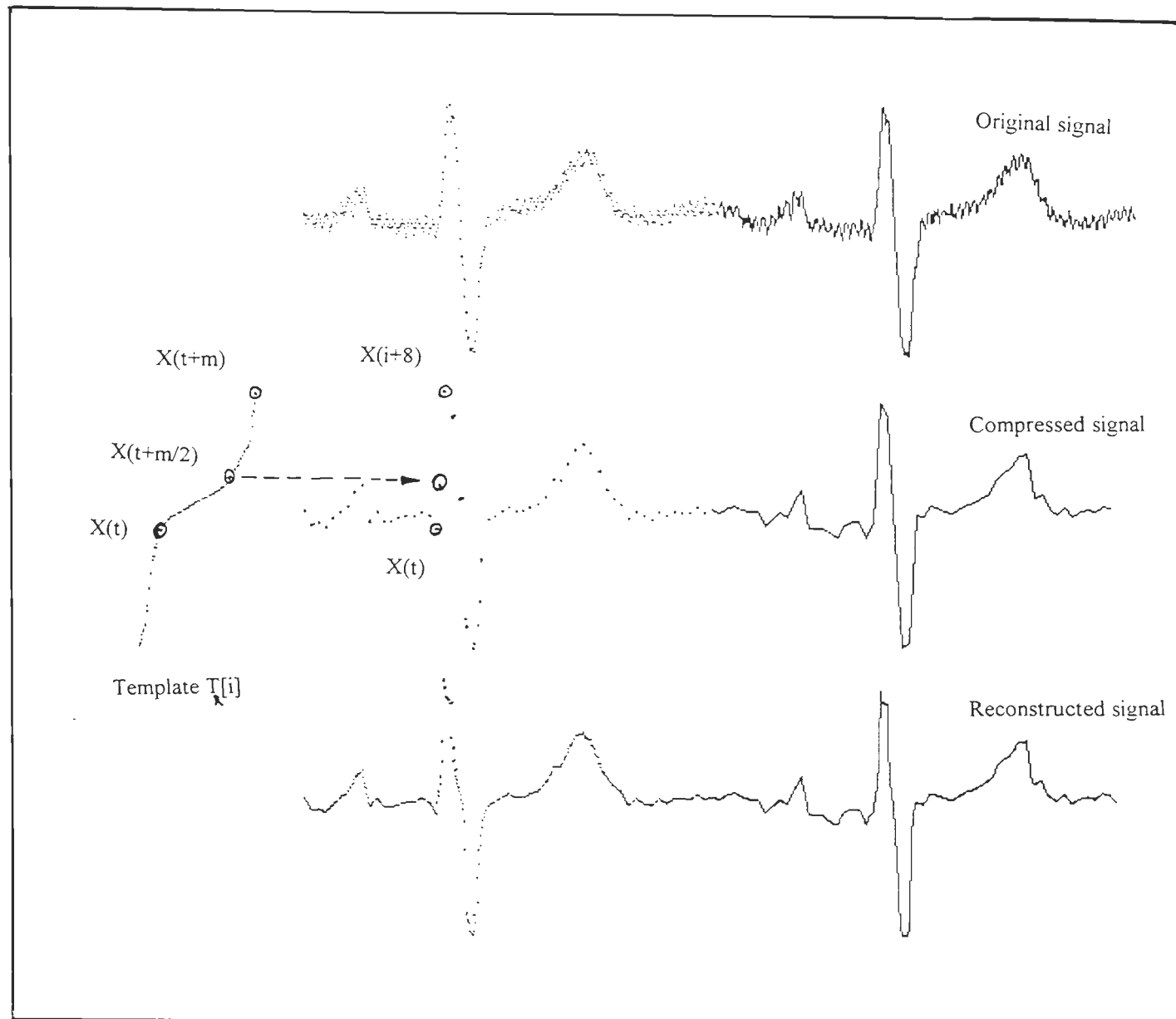


Fig. 7.2 Signal reconstruction by interpolating template samples (NRT-DDC)

knowing the threshold amplitude 'Th'. If there is a peak or valley added in place of X(4), then the points X(1) to X(3) are to be extracted from the TR(i), to feed between X(0) to X(4) and the points X(5) to X(7) are to be added between X(4) to X(8). The procedure, as shown in Fig.7.2, is used to interpolate the samples between X(0) to X(8). Firstly X(0) and X(8) samples of compressed signal are mapped with the TR(i) samples and the number of samples of TR(i) falling in the amplitude level of X(0), X(8) are considered and the median of these samples is considered to feed the sample X(4). The mapping of X(0) and X(4) with TR(i) samples are carried out to feed X(2), mapping of X(0) and X(2) with the same amplitude samples of TR(i) is used to feed the X(1) and the same procedure is repeated to feed all required samples by traversing the template TR(i) over the complete compressed signal, from starting to end of the signal. The signal, shown in Fig.7.1(g), is a completely reconstructed signal having N number of samples with an effective sampling frequency of 500 Hz.

7.3 WAVELET TRANSFORM BASED ECG DATA COMPRESSION

In most cases, DDC methods are superior to transform methods with respect to system complexity and the error control mechanism. However, transform methods usually achieve higher compression ratios and are insensitive to the noise contained in original ECG signals [26]. With regard to other transform-based compression techniques which have been reported in the recent literature [21], only qualitative compressions can be performed due to the use of different ECG databases. The algorithm based on multiresolution wavelet analysis achieves high data compression rates and good quality of retrieved signal. The technique presented here produces compression ratio of the order of 16:1 for reasonable signal quality.

7.3.1 Method

The wavelet transform is a special case of perfect-reconstruction filter banks [139]. The main idea of the transform is to subdivide an arbitrary signal into constant-Q frequency bands using recursive filter banks generated from a small number of prototype filters. The filtering process is equivalent to decomposing the signal using a set of basis functions which are localized in both space and frequency and are scaled and shifted versions of a prototype mother wavelet [7,47]. Figure 7.3 shows three-level analysis and synthesis of one-dimensional data. $H(n)$ and $G(n)$ are low-pass and high-pass filters for analysis. $H(-n)$ and $G(-n)$ are low-pass and high-pass filters for synthesis. The four filters are related in the z-domain as follows:

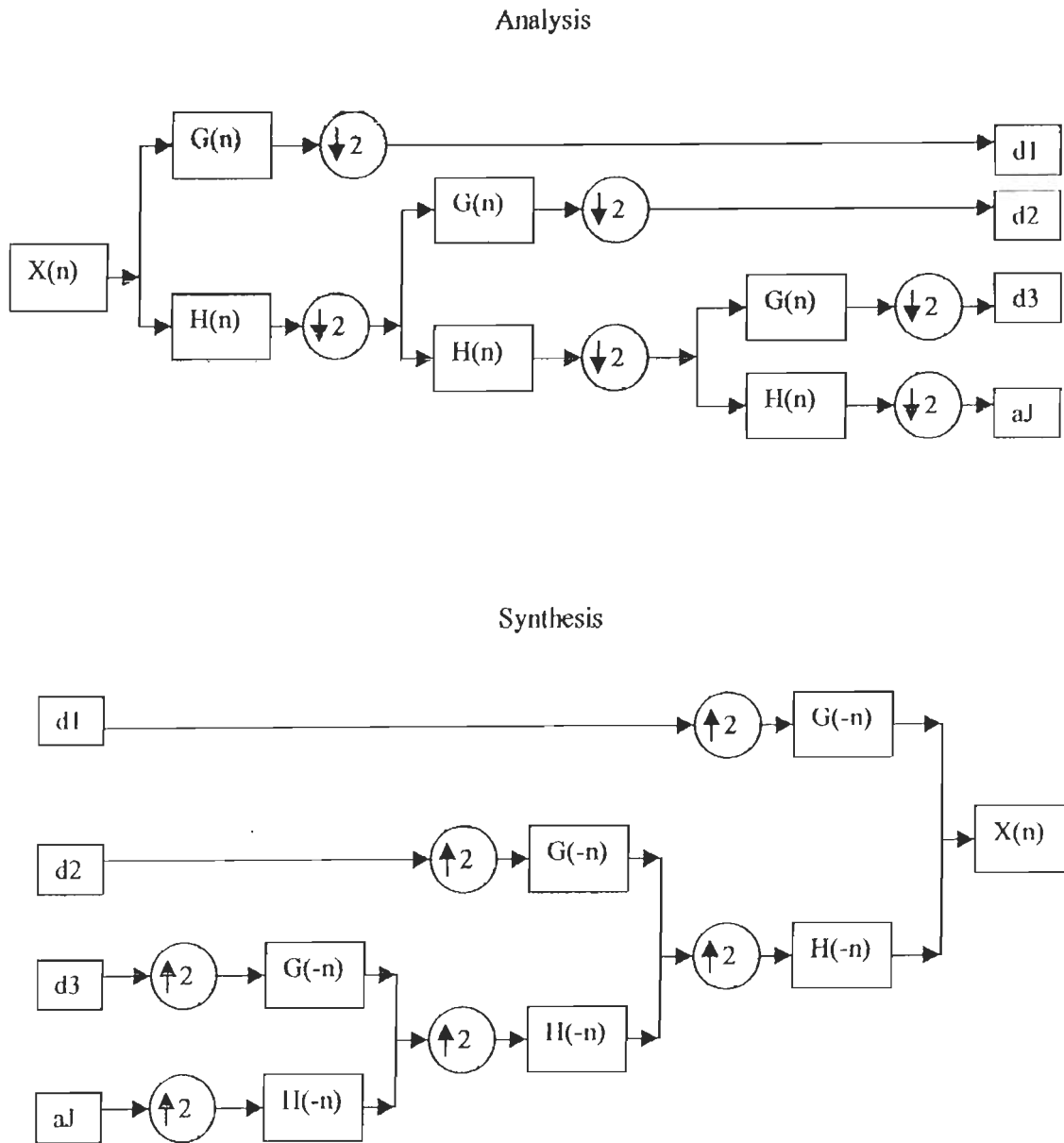


Fig. 7.3 Three stages of analysis and synthesis of a wavelet transform

$$H^{\sim}(z) = G(-z)$$

$$G^{\sim}(z) = -H(-z)$$

$$H(z)G(-z) - G(z)H(-z) = 2$$

Where H and G are WT analysis filter coefficients and H^{\sim} and G^{\sim} are WT synthesis filter coefficients.

The first two conditions eliminate aliasing and the last one condition eliminates phase and amplitude distortion in the reconstructed signal.

A wide variety of functions can be chosen as the mother wavelet $\psi(t)$, provided $\psi(t) \in L^2$ and $\int \psi(t) dt = 0$. This flexibility in the choice of mother wavelet allows $\psi(t)$ to be tailored to the specific application at hand. For signal compression, compact support of $\psi(t)$ can discriminate signal features in both time and scale. If the basis functions generated from $\psi(t)$ are orthogonal or biorthogonal to each other, they minimise the interscale correlation of the decomposed signal.

The choice of wavelet in a compression system is of critical importance, because the wavelet affects reconstruction signal quality and the design of the system as a whole. At this time, there are no theoretical results that can predict which wavelet is suitable for signal compression a priori. A specific wavelet is usually chosen by comparing the actual compression performance of different wavelets [47]. Daubechies's six coefficient is found to be the most suitable wavelet for ECG data compression and retrieval of diagnostic information, hence the same wavelet has been used here.

The wavelet technique developed by Mallat [86] and others is called multiresolution wavelet. It has desirable feature, as the wavelet functions are orthogonal and divided over a dyadic scale. The signal of interest $X(n)$ can be decomposed into its coarse component a^j and detail component d^j at various scales (or resolutions) 2^j . This is also called a pyramidal algorithm. Thus, at scale $j=1$, the signal is decomposed into a coarse component and a remainder detail component. Then, at the next scale $j=2$ and beyond, the procedure is repeated.

The coarse component is obtained by convolving the signal with a scaling function $\phi(t)$, whose Fourier transform appears as a lowpass filter. The coarse component is obtained by modifying the scaling function for each successive scale, and convolution of the signal with the scaled and translated version of the scaling function. The detail component is the remainder after the coarse component is obtained. The detail component is obtained by convolving the signal with a wavelet function $\psi(t)$ whose Fourier transform appears as a

bandpass filter. At each successive scale j , the coarse signal is produced by lowpass filtering and decimation. The discarded detail signal is the same as the signal removed by a bandpass filter. At each compression level, a new bandpass filter is employed to remove the higher frequency components. These functions are orthogonal, and resulting bandpass filters are non-overlapping.

Data reduction is achieved by accepting the signal only upto a certain scale. The detail beyond that scale is discarded. As shown in Fig.7.3, the ECG signal can be divided into coarse and fine components at successive levels. In obtaining the component at the lower scale, alternate samples are discarded, resulting in a 2:1 compression of the data. The scaling level selected depends on the data compression rate desired and the distortion error acceptable. Data compression proceeds in steps of 2:1, 4:1, and so on.

The original signal can be easily resynthesized using inverse wavelet transform (synthesis) as shown in Fig.7.3. Decompression is being carried out by reconstructing the coarse (a^j) and the detail (d^j) components at the higher scales from the coarse and the detail components at the lower scales. The performance of this algorithm is evaluated on CSE data set three and five and the sample results are given in the section on results and discussions.

7.4 PERFORMANCE EVALUATION OF DATA COMPRESSION TECHNIQUES

Some important performances indices used in data compression analysis are:

a) Compression Ratio

The degree of compression is represented in terms of compression ratio (CR) and is defined as:

$$CR = \frac{\text{Number of samples in the original signal (Xorg)}}{\text{Number of samples in the reconstructed signal (Xrec)}}$$

It is generally desired to have high CR by caution against using this parameter as the sole basis of compression among data reduction - algorithm. Factors such as bandwidth, sampling frequency, and precision of the original data generally have considerable influence on the compression ratio. The high CR is meaningful only when the algorithm represents the data with acceptable fidelity.

b) Percent-Root-Mean Square Difference

In biomedical signal compression, we usually determine the clinical acceptability of the reconstructed signal through visual inspection. Many researchers have used the quantitative comparison of the distortion in the reconstructed signal, i.e., the residual which is

the difference between the reconstructed signal and the original signal. Such numerical measure is the percent-root-mean square difference (PRD) and is given as

$$PRD = \sqrt{\frac{\sum_{n=0}^N [X_{org}(n) - X_{rec}(n)]^2}{\sum_{n=0}^N X_{org}^2(n)}} * 100$$

where $X_{org}(n)$ and $X_{rec}(n)$ are the samples of the original and reconstructed data. A lossless data reduction algorithm produces zero residual and the reconstructed signal exactly replicates the original signal. However, clinically acceptable quality is neither guaranteed by a low nonzero residual nor ruled out by a high numerical residual [50].

c) Fidelity

An effective evaluation, however, requires that the signal be reconstructed and compared with the original signal. The comparison can be made either visually or by calculating a suitable index, such as the ratio of error power to signal power or the cross-correlation coefficient (CCC) as given below [26]:

$$CCC = \frac{\frac{1}{N} \sum_{n=1}^N (X_{org}(n) - \bar{X}_{org}(n))(X_{rec}(n) - \bar{X}_{rec}(n))}{\sqrt{\frac{1}{N} \sum_{n=1}^N (X_{org}(n) - \bar{X}_{org}(n))^2} \sqrt{\frac{1}{N} \sum_{n=1}^N (X_{rec}(n) - \bar{X}_{rec}(n))^2}}$$

Some other related terms are,

$$\text{Original signal power } P_{org} = \sum_{n=0}^N x_{org}^2(n)$$

$$\text{Reconstructed signal power } P_{rec} = \sum_{n=0}^N x_{rec}^2(n)$$

$$\text{Error power } P_{err} = \sum_{n=0}^N [x_{org}(n) - x_{rec}(n)]^2$$

where $X_{org}(n)$ and $X_{rec}(n)$ are the samples of the original signal and its reproduced version and $\bar{x}_{org}(n)$ and $\bar{x}_{rec}(n)$ are their average values, respectively.

Fidelity can also be checked graphically by observing the difference of original and reconstructed signals. If the difference signal is approximately a straight line i.e. the signal samples falling in the vicinity of base line, ideally a straight line from starting to end of signal,

then it can be said that the reconstructed signal is perfectly retrieved. In addition to these performance indices, the comparison of diagnostically important parameters like onsets and offsets of ECG waves and their amplitude and duration determined from the Xrec and Xorg signals are being used to decide the extent to which the algorithm is capable of preserving the diagnostic information.

7.5 RESULTS AND DISCUSSIONS

a) NRT-DDC Technique

The performance evaluation of the non-redundant template DDC (NRT-DDC) has been carried out using the CSE data sets 3 and dataset 5. The CSE has given the measurement results of every fifth record of CSE DS-3 and the same have been used to evaluate the accuracy of parameters estimated from the reconstructed signal. To evaluate the performance of the NRT-DDC method, in general, signals with different morphology have been used as shown in Figures 7.1,7.4-7.6. As shown in Fig.7.1, the Xorg signal 'a' has very small spikes overriding the ECG signal. These spikes are reduced in the process of compression as can be seen in the signals 'b', 'c' and 'd'. The signal 'd' is a compressed signal, which seems to be a low resolution signal with the waves slightly wider compared to original signal 'a'. The process of decompression, as shown in the signals Fig.7.1(e), (f) and (g) is performed in three steps by redundant template interpolation. The final signal 'g' has equal resolution as that of the Xorg signal with additional advantage of reduced noise. Different performance indices values used to see the performance of NRT-DDC are given in Table 7.1. For record MA - 001.DCD Lead I, the indices values are as CR=7, PRD=9.05. The high value of PRD is due to displaced reconstructed samples in the region of the QRS complex as shown in Fig.7.4, which is a difference in original and reconstructed signals. In this case, QRS region shows some high amplitude difference because of sample masking or shifting with the neighbor samples to retain the peak or valley falling out of samples X(1) to X(7), as explained in section 7.2. Except the QRS region, the difference signal represents a straight line (Fig.7.4), which indicates the perfect reconstruction in the iso-electric and low amplitude low frequency region (P, T and U waves). The fidelity of the reconstructed signal is checked by observing the difference signal (as shown in Fig.7.4) and the performance indices viz. original signal power $P_{org} = 9.43 \text{ mv}^2$, reconstructed signal power $P_{rec} = 9.035 \text{ mv}^2$, error power $P_{err} = 0.39 \text{ mv}^2$ and cross correlation coefficient CCC= 94.2 %. Looking to the small value of error power (0.39 mv^2)

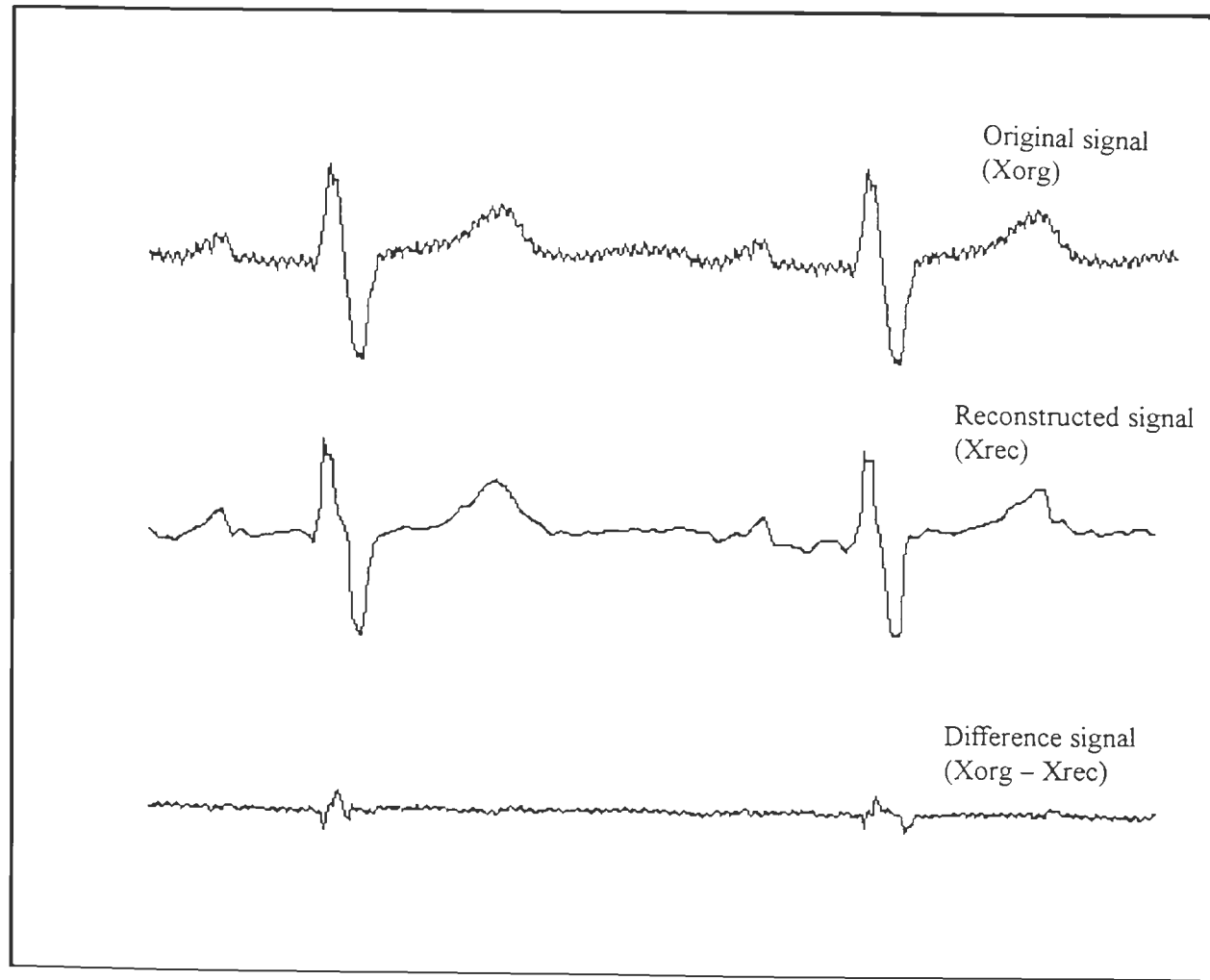


Fig. 7.4 Difference signal extracted from original and reconstructed signals
(NRT-DDC) (Record No. MA-001.DCD, Lead I)

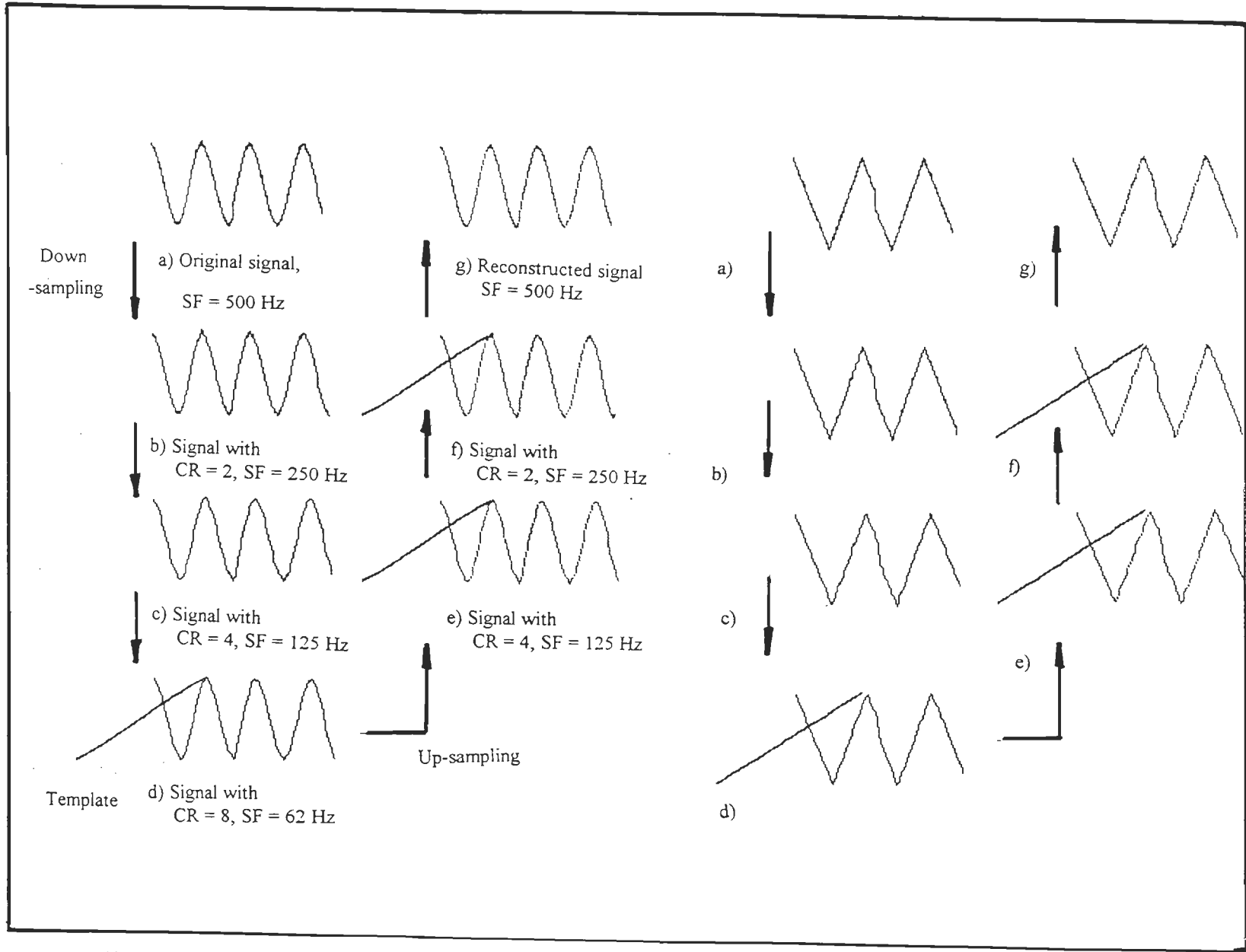


Fig. 7.5 Performance evaluation of the algorithm using standard signals

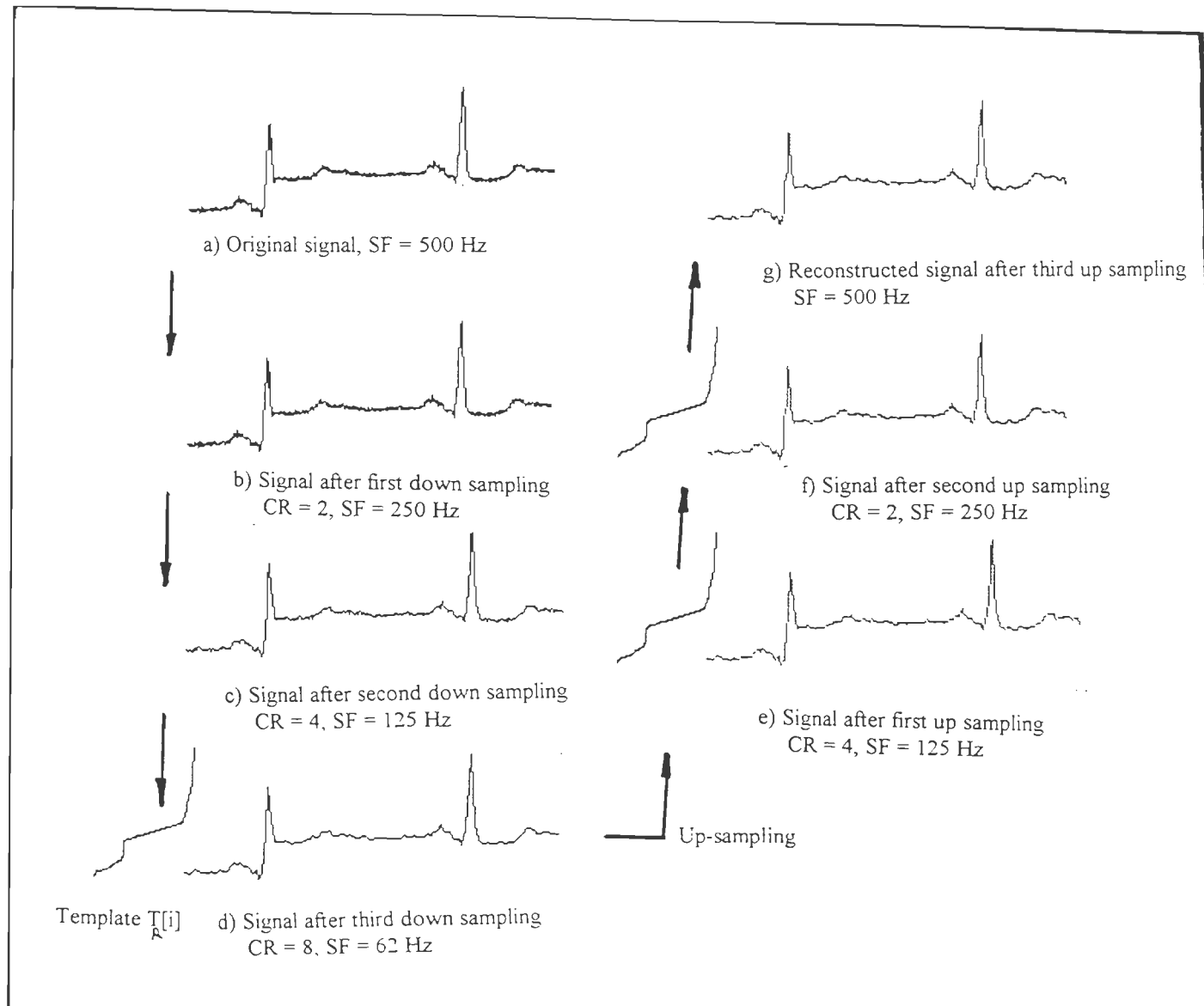


Fig. 7.6 Compression and decompression using an ECG signal with baseline wander (NRT) (Record D-00001.DCD, Lead II)

Table 7.1 Performance indices for NRT-DDC technique

Record No.	P-org mV ²	P-rec mV ²	P-err MV ²	CR	PRD %	CCC %
DS-3						
1L1	9.431	9.035	0.39	7.0	9.05	94.2
1L2	65.76	65.10	0.66	6.0	9.33	97.7
1AF	47.04	46.32	0.72	6.16	13.35	96.1
1V1	114.45	114.17	0.28	7.0	8.17	91.1
1V4	97.26	93.91	3.35	6.32	12.99	95.2
1V6	9.814	9.692	0.12	6.30	11.03	99.2
DS-5						
1L2	334.23	332.76	1.47	4.41	3.27	99.2
1V2	138.82	133.59	5.23	4.0	11.58	99.1

P-org: original signal power;

P-rec: reconstructed signal power

P-err : error power

CR: compression ratio

PRD: percent RMS difference

CCC: cross correlation coefficient

and large values of CCC (94.2 %), it is confirmed that the retrieval of the signal is good to give high fidelity.

The ECGs used in Figs.7.5 and 7.6 have been used to see the performance. As shown in Fig.7.5, the use of sinusoidal and triangular waveforms demonstrate the faithful compression and decompression. As shown in Fig.7.6, a record from DS-5, D-0001.DCD Lead II, has high baseline drift in some region of the signal, even with this quality of the signal. The perfectness of reconstruction can be observed from the values of performance indices given in the Table 7.1, where $P_{err}=1.47 \text{ mv}^2$, $PRD=3.27$. The PRD of about 3 and high CCC, 99.2% indicate accurate reconstruction of the signal even with baseline wander.

A typical high frequency noise signal (record MA-120.DCD, Lead I), shown in Fig.7.7, is used to show the procedure of peak and valley retaining capability of this method and the reconstruction is also good.

The information retained about the peaks and duration in the reconstructed signal is clinically important in classifying certain cardiac diseases, particularly when we use scoring criteria based on ECG parameters. Utility of the present method in this regard is utmost guaranteed as the method is capable of holding 100% sample amplitude levels from the original signal. Also the reconstruction accuracy in the low frequency low amplitude (baseline) region is at the highest level, which helps in accurate detection of onsets and offsets of ECG waves. Hence the reconstructed signal has 100% accuracy in the measurement of ECG wave amplitudes as can be observed from the Table 7.2, almost in all ECG waves, and the original and reconstructed signal amplitude are the same. The onset and offset measurements in original and reconstructed signal given in Table 7.3 are compared and found well within the tolerance limits suggested by the CSE working party. Table 7.4 shows some diagnostically important parameters which are measured from the original and reconstructed signals and are comparable with the measurement results given by the CSE Working Party in the reference manual [147].

To compare the performance of this method with the existing techniques, we have selected the reported data as well as the techniques reported with the performance evaluation based on CR and PRD for data sampled at 500Hz. The details are listed in Table 7.5. In this Table, the CR ranges from 7 to 10 in most of the cases (except in two, having high CR of about 16) and PRD from 3 to 28. It means that only CR or PRD do not give proper scale for comparison. Therefore, the only way is to see whether the clinical information is being retained or can be retrieved or not. This aspect has been considered and the comparison with

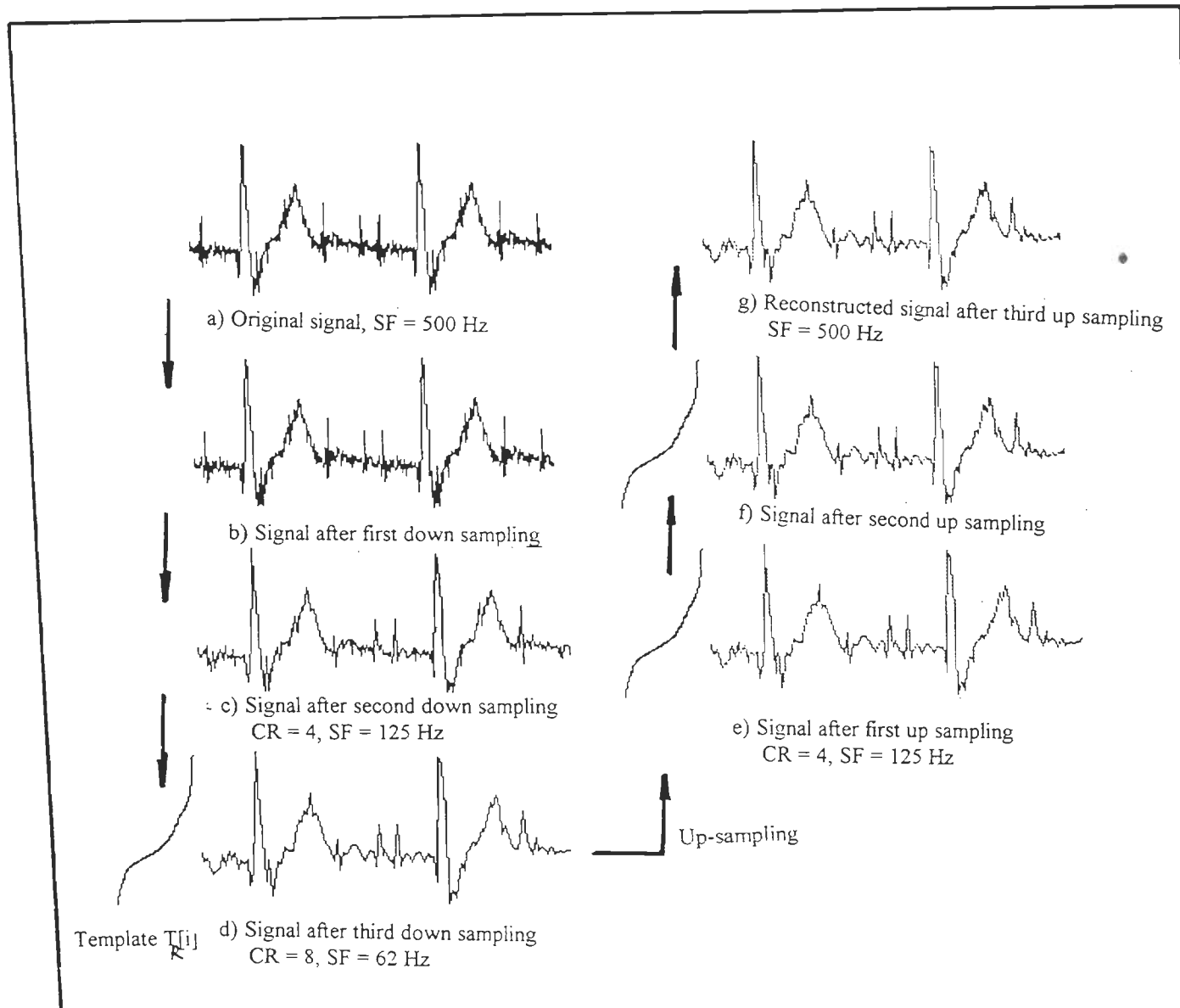


Fig. 7.7 Compression and decompression using a typical ECG signal

(NRT-DDC) (Record No. MA-120.DCD, Lead II)

Table 7.2 Amplitudes measured in original and reconstructed signals for NRT-DDC
(for CR = 8)

Record No.	P (mV)	Q (mV)	R (mV)	S (mV)	T (mV)
MA-001.DCD					
1L1 Original	0.08	-0.01	0.31	-0.33	0.16
Reconstr.	0.08	-0.01	0.28	-0.31	0.14
1L2 Original	0.11	0.00	0.13	-0.49	0.24
Reconstr.	0.11	-0.01	0.13	-0.50	0.24
MA-120.DCD					
1L1 Original	0.06	-0.08	0.56	-0.20	0.35
Reconstr.	0.06	-0.07	0.55	-0.25	0.33

Table 7.3 ECG wave onsets and offset measured in original and reconstructed signals
for NRT-DDC technique (CR 8)

Record No.	P onset	P Offset	QRS Onset	QRS Offset	T End
MA-001 L1 Original sig.	103	151	215	273	443
Reconstructed signal	100	152	212	267	430
MA-001 L2 Original sig.	103	195	223	284	455
Reconstructed signal	99	190	220	279	451
MA-120 L1 Original sig.	93	155	249	297	457
Reconstructed signal	101	160	252	296	464
Accepted limit(samples)	6	6	4	6	15

Table 7.4 Diagnostically important parameters measured in original and reconstructed signals for NRT-DDC technique

Record No.	IIR BPM	P -dur. sec	QRS -dur. sec	PR -inter sec	QT – inter sec	VAT Sec
MA-001						
L1 Org.	63.83	0.10	0.12	0.23	0.46	0.04
Rec.	64.52	0.14	0.11	0.26	0.42	0.05
L2 Org.	63.83	0.18	0.12	0.24	0.46	0.02
Rec.	63.56	0.16	0.12	0.25	0.47	0.03
MA-120						
L1 Org.	61.22	0.10	0.10	0.32	0.42	0.03
Rec.	61.48	0.10	0.09	0.29	0.42	0.02

Table 7.5 Comparison of data compression techniques

Method	Sampl Freq.	CR	PRD	ADC (bits)	Comments
AZTEC [50]	500	10	28	12	Poor P & T fidelity & retrieval of duration related parameters
Peak-Picking (spline) with entropy coding[50]	500	10	14	8	Loss of information contained in low amplitude low freq. Region
DPCM-linear prediction interpretation and entropy coding [55]	500	7.8	3.5	8	Sensitive to SF and quantization
Adaptive Fourier coefficient estimation [55]	500	16	3	-	Truncation of coefficients to reduce the data affect the reconstruction quality.
Sub-band coding with extensive Markov system[55]	500	25	-	12	-
ANN [125]	500	16	7	12	Sensitive to SF and data length
CORTES [64]	500	10	-	12	Poor P & T fidelity
MAZTEC [64]	500	7.6	-	12	Poor P & T fidelity
SAPA [64]	500	10	-	12	Loss of information contained in low amplitude low freq. region.
Wavelet Transform	500	16	-	12	Loss of information due to truncation.
NRT-DDC (present method)	500	8	3-13	12	Retain about 99% information regarding the amplitude and duration.

CSE results of the diagnostically important parameters measured in original and reconstructed signal (Tables 7.2-7.4). This comparison shows that there is faithful information retrieval.

b) Wavelet Transform Technique

Cardiologists suggest that the clinically useful information present in original ECG signals is preserved in general by 8:1 compression and in some case by 16:1 compressed ECG's [47]. Considering this, the data compression has been carried out using WT technique to provide the CR of 8:1 and 16:1. The sample results are given in Table 7.6 and 7.7 and to see the changes in the morphologies of ECG waves, the graphical representation are shown in Figs. 7.8 to 7.13.

The PRD indicates reconstruction fidelity by pointwise comparison with the original signal; but as pointed out by many researchers that it is not by itself, an accurate indicator of the utility of a reconstructed signal [47]. To assess the clinical utility of the wavelet compression algorithm, a comparison of diagnostically important parameters measured from the original and compressed signals is used. The use of CSE results for the CSE DS3 data are used to see that the results measured in compressed signal are in the tolerable limits or not. From the parameters (Table 7.6), it is not so clear that the reconstructed signal is of diagnostic acceptance or not, because of different PRD values for different signals even with same resolution. Looking at the value of P-err and the corresponding nature of the ECG signal, it is observed that there exist no significant relationship hence, as pointed out by many researcher, the performance indices like PRD, P-err give no judgement. Therefore, the use of diagnostic parameters measured from the original and the reconstructed signals are compared to see the performance of WT based data compression for different compression ratios. The comparison given in Table 7.7 makes it clear that the 8:1 compressed signals have the exact reconstruction giving 100% accurate retrieval of diagnostic parameters. For 16:1 compression rate, reconstruction is also satisfactory and is signal dependent, but in some parameters like QRS-interval, QT-interval and VAT, inaccurate retrieval of diagnostic information is observed. For example, QRS-interval in all three signals shown in Table 7.7 is differed by about 0.01 second (i.e. in place of 0.12 second it shows 0.13 second), QT-interval is differed by 0.02 second (i.e. in place of 0.46 it shows 0.48 second) and VAT differed by 0.03 second (shows 0.07 for 0.04 second).

Table 7.6 Performance indices for WT based data compression technique

Record No.	CR	P-org mV ²	P-rec mV ²	P-err mV ²	PRD %
MA-001.DCD Lead 1	8.0	19.98	18.46	1.52	16.30
	16.0	19.98	23.98	-4.00	44.78
MA-120.DCD Lead 3	8.0	18.52	23.40	-4.88	69.24
	16.0	18.52	28.12	-6.46	59.09
D-001.DCD Lead 3	8.0	983.0	960.90	22.10	3.98
	16.0	983.0	1581.0	-57.20	24.10

P-org: original signal power

P-rec: reconstructed signal power

P-err: error power;

CR: compression ratio

PRD: percent RMS difference

Table 7.7 Diagnostically important parameters measured in original and reconstructed signals for WT based compression technique

Recd. No.	CR	IIR BPM	Pamp mV	PRint sec	QRS int sec	QRS _{p-p} mV	QT int sec	VAT sec	Tamp mV
MA-001 Lead 1	Org								
	signal	63.8	0.06	0.23	0.12	0.64	0.46	0.04	0.18
	08	63.5	0.06	0.24	0.11	0.58	0.46	0.04	0.17
	16	63.0	0.06	0.22	0.13	0.53	0.48	0.07	0.20
MA-120 Lead 3	Org								
	signal	61.2	0.03	0.18	0.10	0.85	0.40	0.02	-0.21
	08	61.4	0.05	0.18	0.12	0.87	0.43	0.02	-0.21
	16	61.0	0.02	0.15	0.15	0.84	0.46	0.03	-1.25
D-0001 Lead 2	Org								
	signal	57.0	0.08	0.20	0.07	1.00	0.39	0.04	0.23
	08	57.6	0.05	0.18	0.08	0.85	0.41	0.04	-0.57
	16	58.0	0.04	0.21	0.08	1.32	0.42	0.06	-1.0

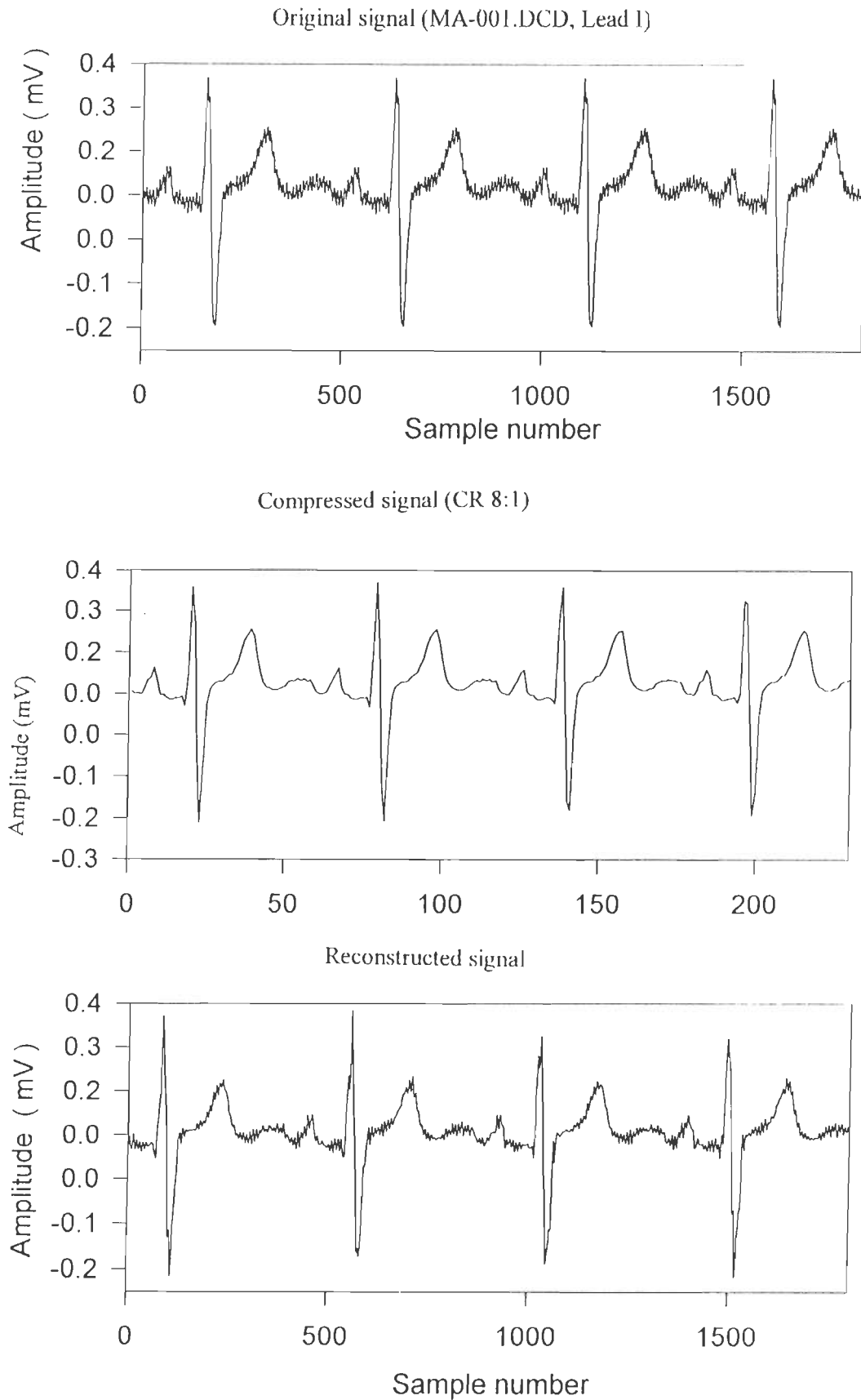


Fig. 7.8 WT based ECG data compression (CR 8:1)
(Record MA-001.DCD, Lead I)

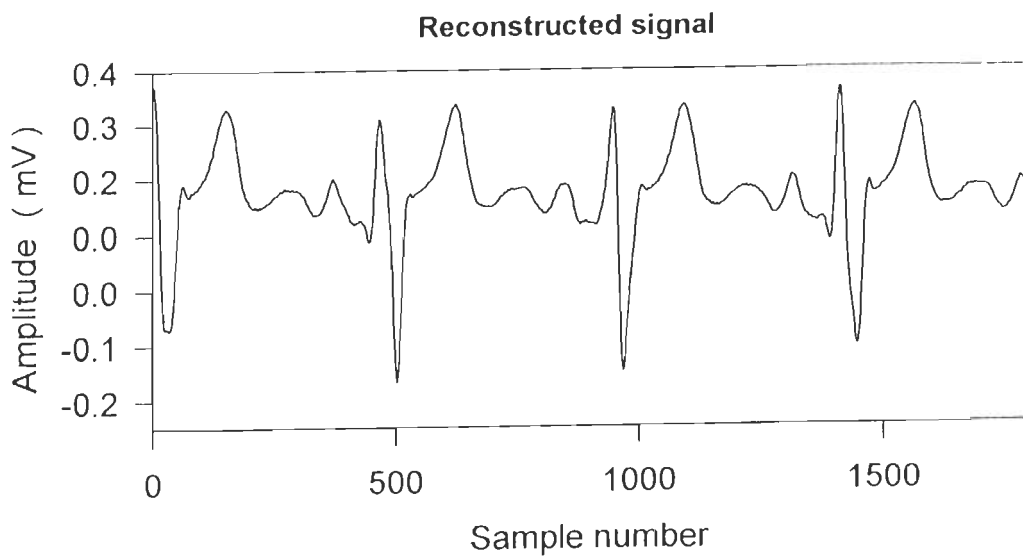
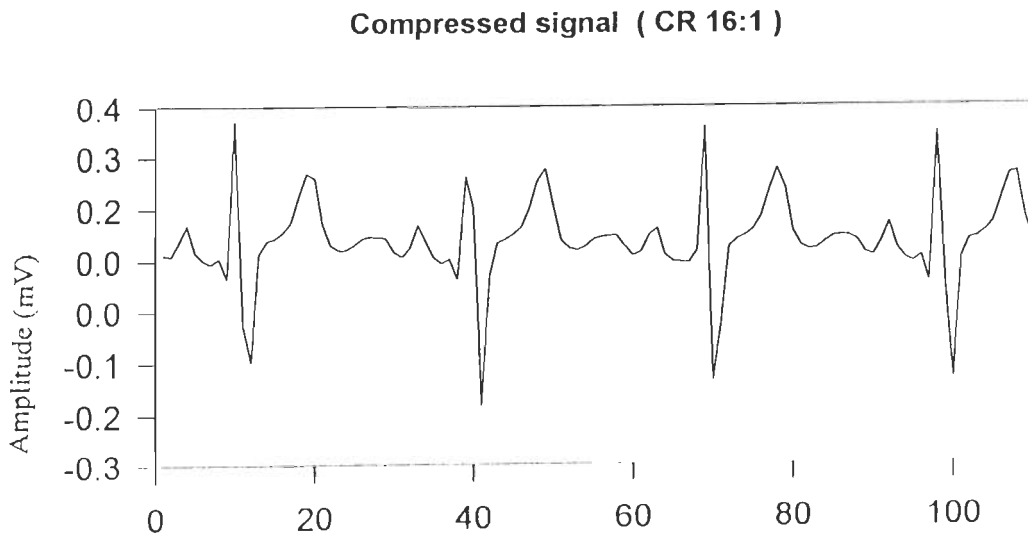
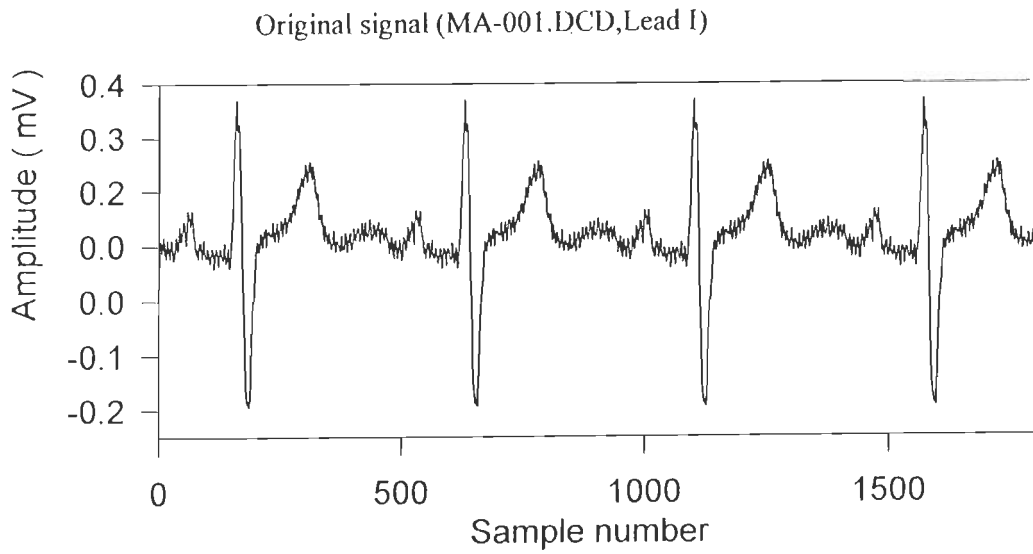


Fig. 7.9 WT based ECG data compression (CR 16:1)
(Record MA-001.DCD, Lead I)

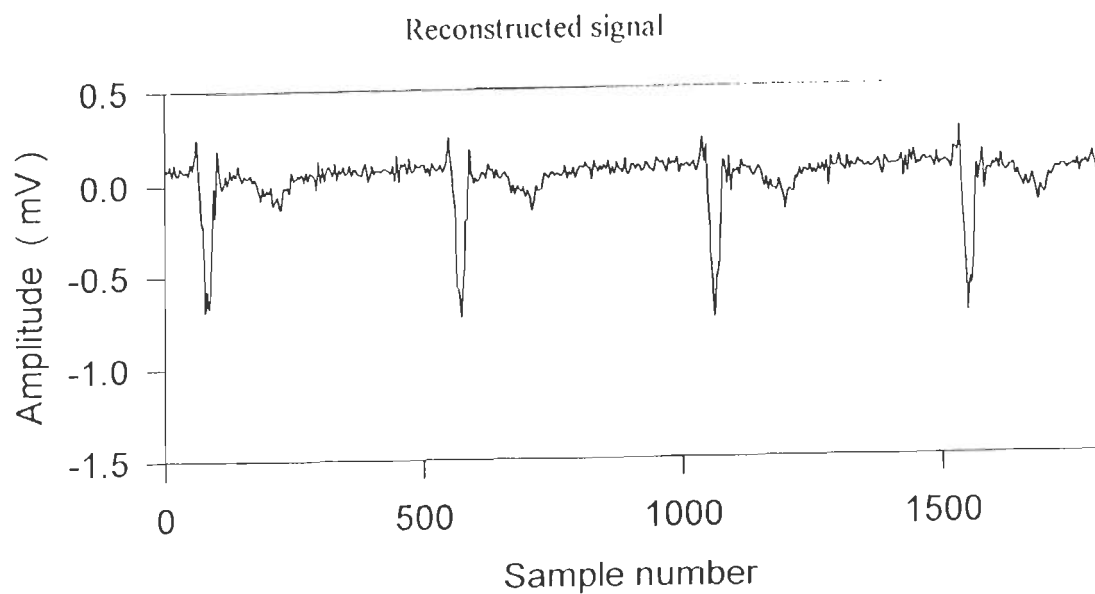
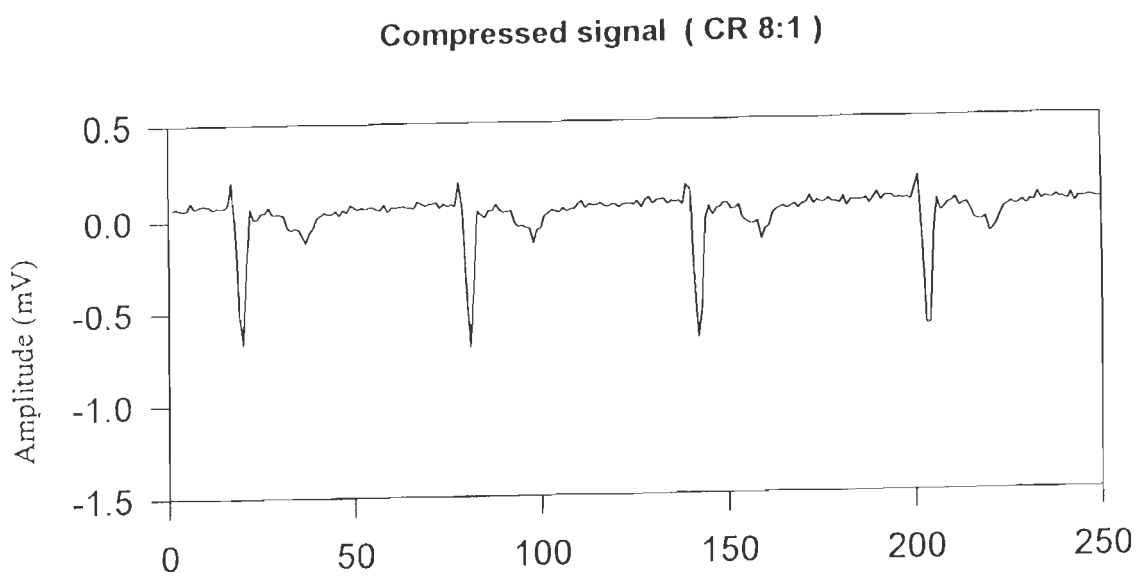
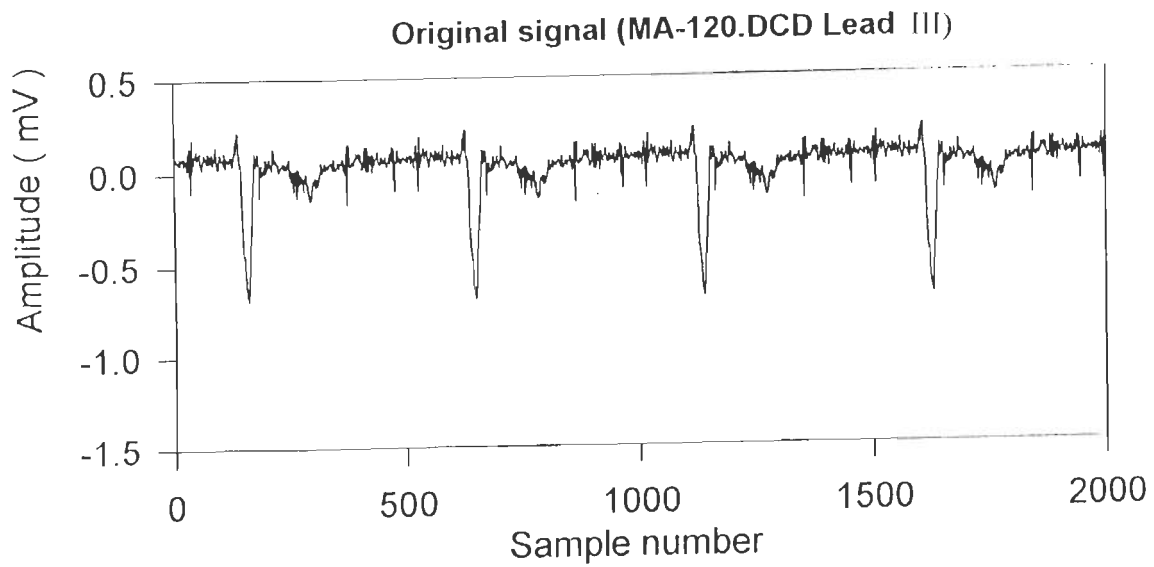


Fig. 7.10 WT based ECG data compression using a signal containing noise (CR 8:1)
(Record MA-120.DCD, Lead III)

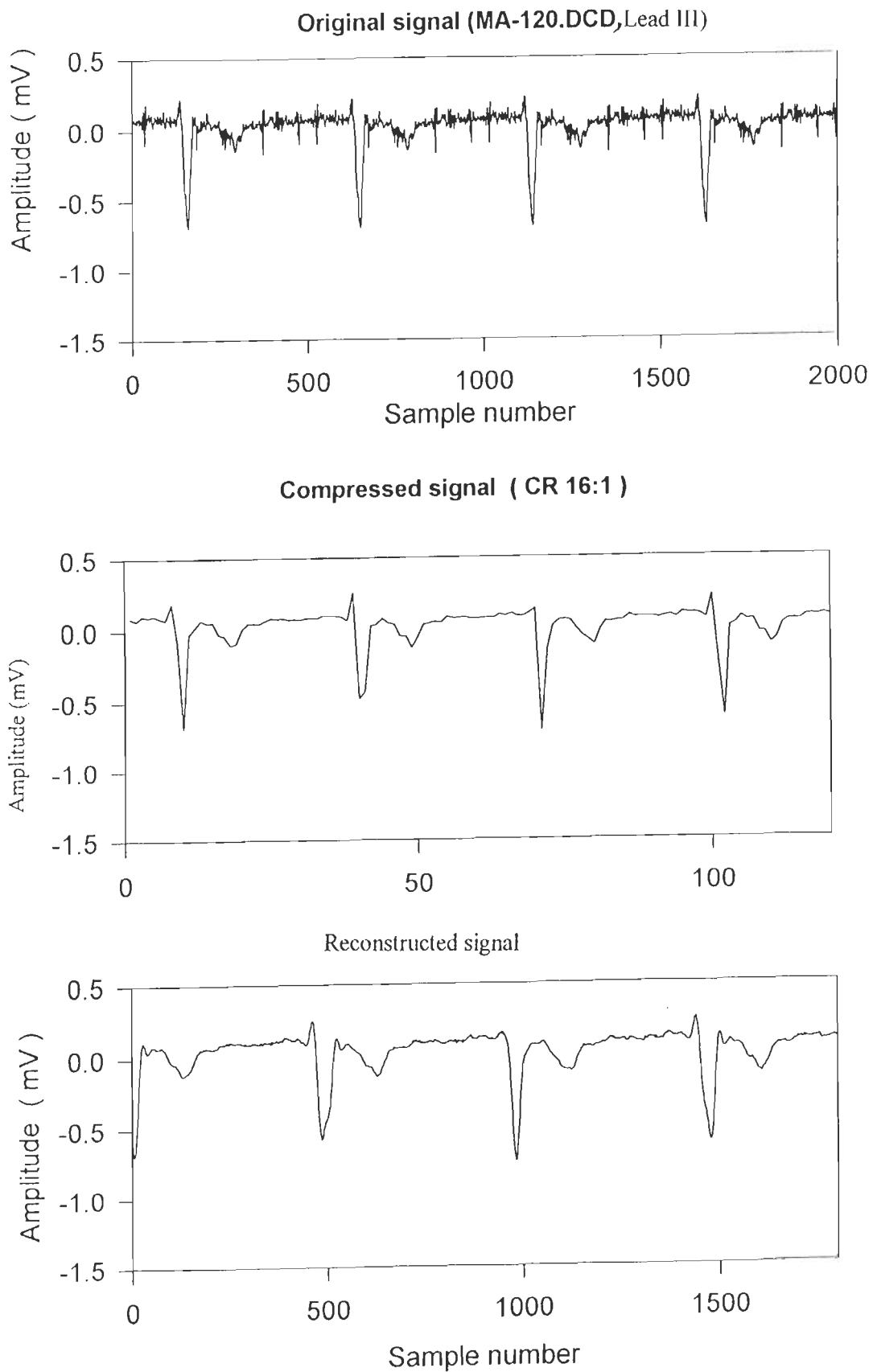


Fig. 7.11 WT based ECG data compression using a signal containing noise (CR 16:1)
(Record MA-120.DCD, Lead III)

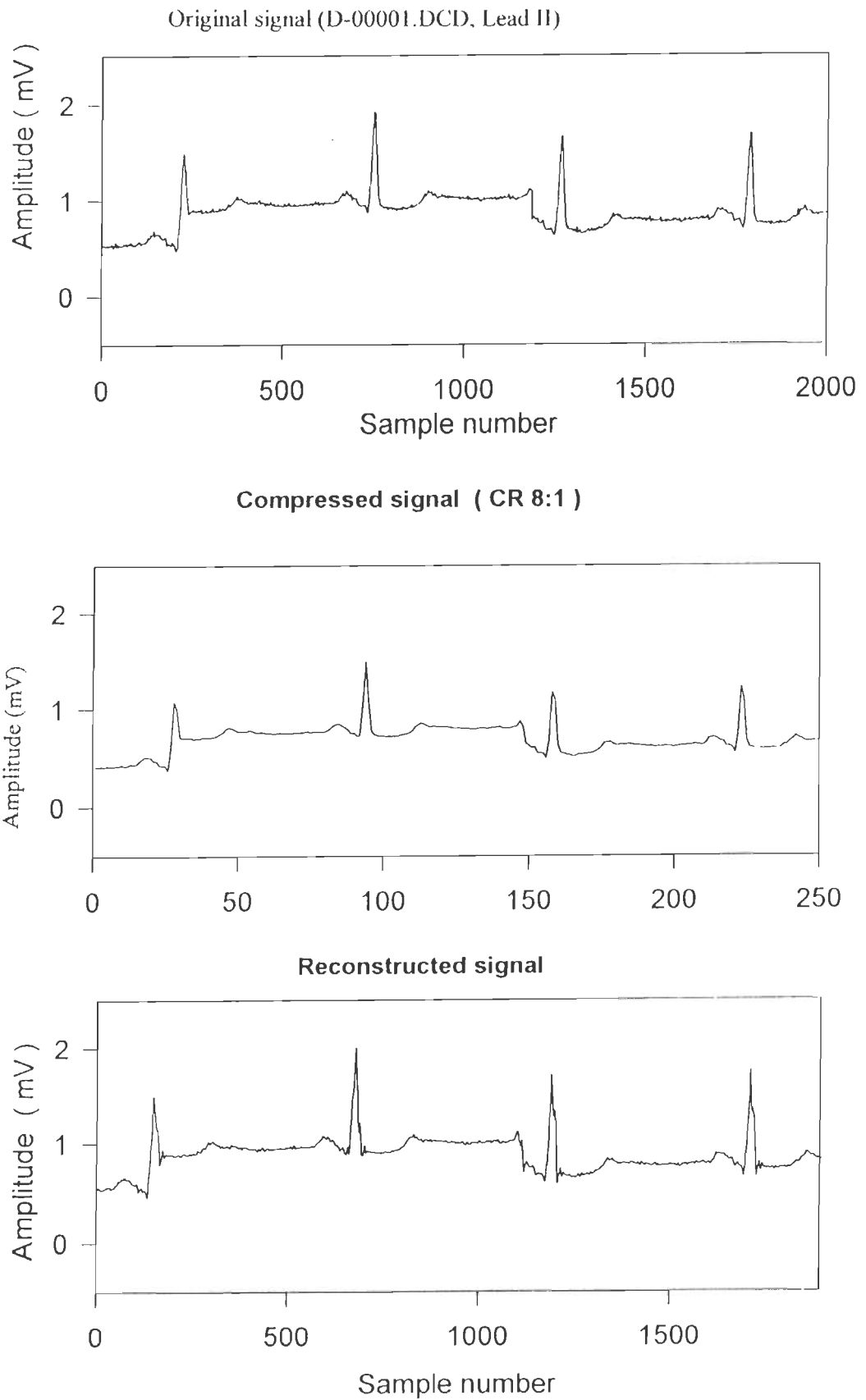


Fig. 7.12 WT based ECG data compression using a signal with baseline wander (CR 8:1)
(Record D-00001.DCD, Lead II)

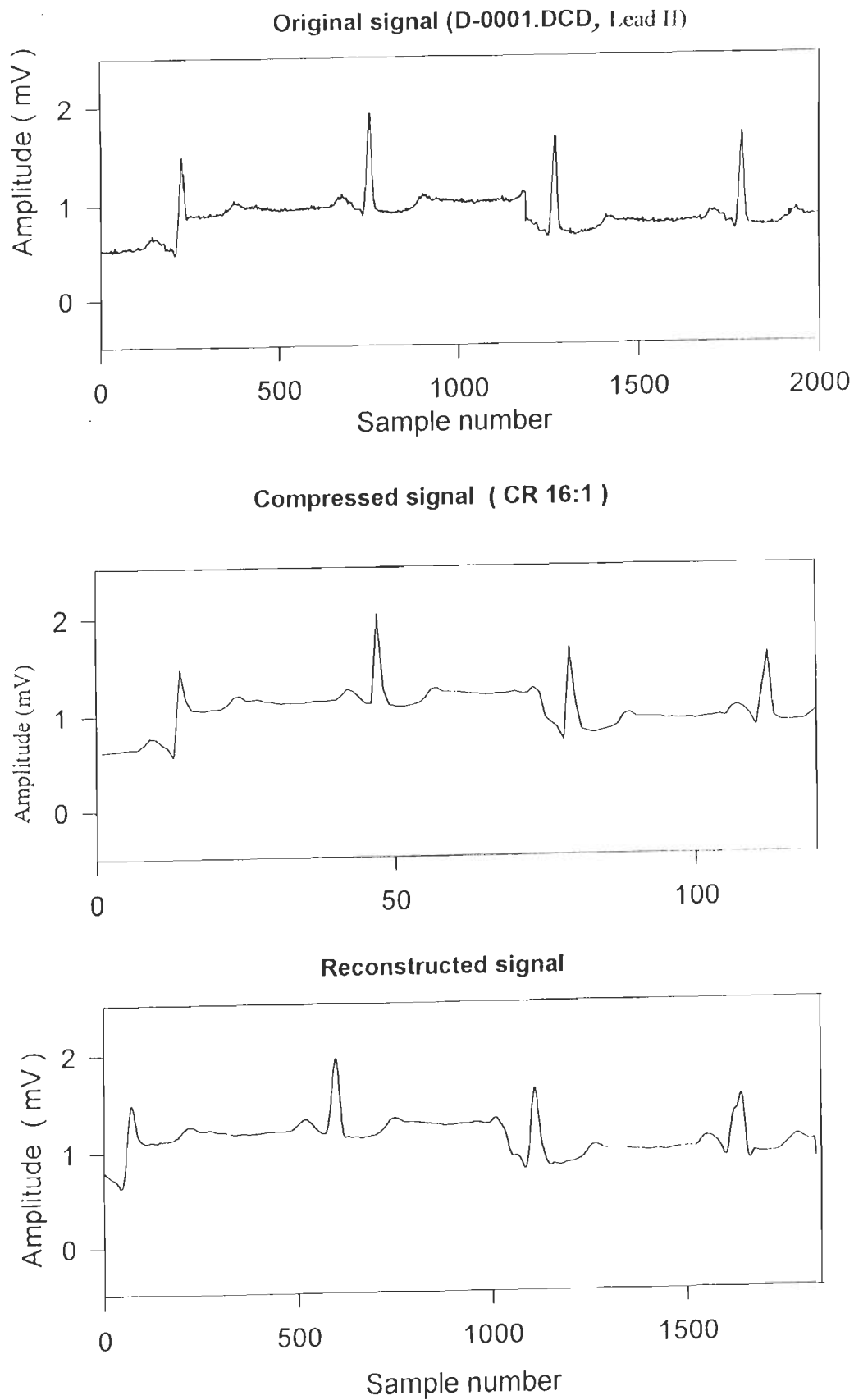


Fig. 7.13 WT based ECG data compression using a signal with baseline wander (CR 16:1)
(Record D-00001.DCD, Lead II)

7.6 CONCLUSIONS

The NRT-DDC and WT methods produce compressions by downsampling technique. Data compression (up to 8:1) and retrieval of information by both the methods is of diagnostically acceptable level. Therefore, the use of NRT-DDC is restricted up to 8:1 but the WT can be used for higher CR if the selective information is of importance, like the use of R-R intervals in the study of HRV analysis.

Some of the important findings about the NRT-DDC method are as follows:

- i) The present method is best suited for online data compression and reconstruction. The CR in this method is dependent on the signal sampling frequency. At 500 Hz sampling rate, it gives CR of about 8 and retains clinical information by preserving 100% amplitude level and the morphological information.
- ii) As the peaks and valleys are being retained by the compressed signal and the interpolation is being carried out by the actual samples (removed samples stored in template while compression) from the template, and the density of samples in the iso-electric region of ECG signal is more and these redundant samples are interpolated accurately by the template. In this case, the accurate measurement of onsets and offsets of the ECG waves is possible.
- iii) In comparison to the other DDC methods, the present method is simple and superior in performance when evaluated using the performance indices like CR, PRD, fidelity, CCC, signal power (original, reconstructed and error signals) and diagnostic parameters.
- iv) By considering these aspects, it can be stated that this method is suitable for on-line data management for Holter recording, ambulatory monitoring and multi-lead diagnostic data systems.

The results of WT based compression are also very much satisfactory as the method is based on retaining of selective components of the signal. In case of ECG sampled at 500 Hz, most of the ECG wave components lie below 30 Hz frequency, hence the compression up to 8:1 retains ECG wave components with frequency less than 30 Hz. It is clear that for high resolution signals, the WT based compression can be the most useful. These are suitable in storing the data of special cases like in heart rate monitor and HRV analysis, where there is a need to store the information regarding the R-R occurrence. As discussed in an earlier chapter on QRS detection, the WT based QRS detection serves two purposes, i.e. accurate detection of R peaks as well as data compression.

The methods of coding and decoding of slopes, plateaus, segment lengths and positions based on approximate thresholding seek error in reconstruction. There is approximations in the sense that the group of samples having close amplitude or slope are considered to be of same value. This assumption is very critical to induce the error in measurement of onsets and offsets of ECG waves. This is due to the low frequency and low amplitude regions (P, T and U segment), wherein, slope and amplitude are small, and therefore, small tolerance limit results into large shifts in onsets and offsets of the ECG waves.

CONCLUSIONS AND SCOPE FOR FUTURE WORK

8.1 CONCLUSIONS

Considering the increased number of cardiac patients and need of sophistication for want of information on pressing a tip of finger, there is no better assisting alternative than the automated ECG analysis and disease diagnosis system to help an expert cardiologist. ECG, a non-stationary signal, can be faithfully analysed through a time-frequency analysis using tools like wavelet transform. The use of wavelet transform is very effective for the analysis of ECG signals. Its extensive use has been made in signal processing, right from the stage of noise reduction to feature extraction and disease interpretation.

After introducing the area in chapter I and wavelet transform in chapter II, the work has been reported regarding the QRS detection using wavelet transform in chapter III of the thesis. The major conclusions drawn in respect of this work are summarised as follows: The developed algorithm works satisfactorily in all typical morphologies of the ECG. Among the wavelets evaluated for the QRS detection, quadratic spline wavelet and the new developed wavelet (WT6) are found to be the best suitable for the QRS detection. The developed algorithm gives the detection rate of 99.806% with the sensitivity of 99.904% when tested on all 48 records of the MIT/BIH Arrhythmia database and rate of QRS detection of 99.866% with the sensitivity of 100% on complete CSE DS-3 dataset. The performance indicates that the wavelet can be considered as one of the most effective techniques for computer aided QRS detection in ECG analysis and interpretation. Even with baseline wander, muscle artifacts, high frequency noise and higher amplitude P and T waves, the detection of the QRS by wavelet transform is very accurate. The wavelet transform emerges different wave components at different frequencies taking care of variations in the ECG.

In the fourth chapter of the work, all the fundamental and diagnostically important features of ECG are measured by using the QRS location as a time reference. The comparison of five wave fiducial points (P-onset and -offset, QRS -onset and -offset and T-end) with the CSE measurement results, shows that the overall accuracy in the measurement is about 91.00 %. Out of total 125 fiducial location estimates in 25 records, 11 estimates deviate from the tolerance. The software has also been tested using the ECGs recorded in the laboratory. After confirmation of the reliability of software using CSE DS-3 and the ECG records of this lab, diagnostic dataset DS-5 has been carried out for the analysis and disease diagnosis. As there are no measurement results published by the CSE for dataset DS-5, statistical analysis

has been used to see the distribution of programme estimates around a mean value. From a record, five regular beats per lead are selected and 29 parameters per beat per lead are extracted. Therefore, the software extracts the parameters from five such beats in 12 standard leads and stores the features. The statistical parameters are used to see measurement performance of the developed software. The statistical parameters, namely, variance and standard deviation (SD), derived from 12 SL measurements show the best performance of wave detection and parameter measurements.

The use of the ECG analysis for the disease diagnostic and the strategy to use five beats from all the standard 12 has been discussed in chapter V. The strategy used to develop modified scoring criteria for three main diseases reduces the complexity of using individual scoring schemes reported by different researchers. The strategy of disease interpretation by decision tree, which gives 80% accuracy in disease diagnostics, can be used in actual clinical practice after an exhaustive training of the system in consultation with the cardiac experts. This accuracy could be obtained because of the reliable feature extraction by WT and also because of the new approach of analyzing the five consecutive beats per lead of a record. The use of modified scoring schemes, which includes required number of criteria, strengthens the reliability of cardiac disease diagnostics. The use of multiple beats (5 beats per lead), helps to assure the disease diagnosis by repeating the procedure of interpretation. Also it is equivalent to seeking the second, third or more. opinions about a cardiac disease from different cardiac experts. There is less chance of incorrect opinion as the final disease diagnosis is dependent on the analysis and confirmation of disease by exiting as well as modified scoring schemes on five beat analysis.

The rhythm analysis and its use in heart rate variability can be used in routine disease diagnosis for monitoring the response of the diseased heart under different conditions and medical treatments. The reliability of HRV analysis is solely on the accurate detection of R-R intervals. The use of different QRS detection methods result into different interpretation, because of inaccurate detection of R-R time series. This difficulty is being reduced by the use of wavelet transform for QRS detection to get dependable information from the HRV analysis as supported by the results given in chapter VI. It is observed that the HRV spectral and non-spectral indices are less prone to the fluctuations in heart rate due to autonomic imbalance than the fluctuations due to improper and incorrect detection of even a single heart beat. The incorrect beat detection gives substantial rise to the values of HR, SDNN, and low frequency power (LFP) and/ or high frequency power (HFP) parameters. In general, there is a inverse the relationship between respiratory rate and the spectrum measures of

parasympathetic activity (vagal power). For slow respiration, high power peak emerges at 0.3 Hz. A low power peak emerges in case of fast respiration rate. This indicates the influence of vagal control on the heart activity and the entrainment of respiration on SA node activity is more during the slow breathing phase. For increased rate of respiration (slow, normal and fast), there is corresponding increase in HR and decrease in SDNN values. The strategy of HRV analysis by different respiration phases helps in understanding the role of vagal control of the heart. This simple approach can be used in actual clinical practice to study the status of the heart without invasive techniques.

To handle a large volume of ECG data without losing the diagnostic information, a simple NRT-DDC technique is given in chapter VII. This technique is capable of holding 100% information about amplitude and duration of the original signal and is found useful in storing the data of 12 standard leads. The wavelet transform based data compression is found very much suitable in holding the information from the specific frequency band of the original signal. The HRV analysis work deals with the use of only R-R intervals from the long single lead records, therefore, the use of wavelet transform based data compression is effective in storing the selective information from the frequency band of QRS complexes. Both the methods, NRT-DDC and wavelet transform based data compression produce compression by the down sampling. Data compression up to 8:1 and retrieval of information by both the methods is of diagnostic acceptance. Therefore, the use of NRT-DDC is restricted up to 8:1 and wavelet transform based data compression is used for both 8:1 and 16:1 compressions. By considering the aspects of retaining of selective components, the method is found very much suitable for on-line data management for Holter recording, ambulatory monitoring, heart rate monitor and HRV analysis systems.

On the basis of the outcome of the present work, it can be stated that the use of combined wavelets in ECG analysis has the advantages in following respects: (i) The WT eliminates baseline wander, muscle artifacts and noise and detects QRS complexes with high sensitivity, (ii) The approach of combined wavelets (i.e. the use of QSWT for QRS detection and DU-6 wavelet for P & T detection) proved very powerful as it gives high sensitivity for QRS, P and T detection compared to other existing methods of detection even with signals corrupted with baseline wander, noise and artifacts, (iii) The use of a quadratic spline wavelet provides fixed correlation between ECG characteristic points and modulus maxima lines, thereby resulting in reliable QRS detection, (iv) The smoothing feature of the DU-6 wavelet makes it more suitable than the QS wavelet to detect P and T wave fiducials and (v) Due to the high accuracy of the R-R interval measurement, this method may find wider use in

arrhythmia and heart rate variability detection and the use of WT will definitely find distinct place in the field of computer aided ECG analysis and interpretation.

8.2 SCOPE FOR FUTURE WORK

Considering the need of automated disease diagnosis system with the increased number of cardiac patients compared to the available number of cardiac specialists, it has become difficult to provide effective cardiac care without the help of computer based expert systems. With the fast developments in the field of information technology, an individual always seeks the use of recent trends, like automated disease diagnosis and telemedicine. Looking to the need of time and the exhaustive literature survey, though there are existing automated ECG analysis and interpretation systems being used in clinical practices, it is recommended by the researchers, that there is still a great need to enhance, modify the programs to cope up with the modern techniques and the information technology, and hence, there is always scope for further development. It is therefore, required to strengthen the reliability of the algorithm by continuous upgrading from the experience and the knowledge gained using such system in the real medical care systems.

There is increased importance of study and analysis of heart rate variability in clinical practice because the time and frequency domain analysis of HRV allows to predict mortality risk after cardiac infarction and congestive heart failure. As there are no any standards to use the HRV, the study and analysis of HRV software can be trailed to monitor the heart to correlate the physical and psychophysical conditions. In addition to HRV analysis, disease diagnosis system can be supported by the study and analysis of late potentials and His signals. The late potentials are a particular case of delayed inhomogeneous depolarization which may occur elsewhere, for example under the QRS or after and under the P wave. The presence of late potentials and more particularly ventricular late potentials increases the probability of sudden death [119]. It is also important to observe the His signal, which occurs between the P and Q waves and reflects the conduction from the auricles to the ventricles. So the proper technique allowing the detection and analysis of ECG features is of precious help for the physicians. Also the evaluation of HRV, ventricular late potentials or His signals is impossible without the use of computerised cardiac analysis.

PANEL OF MEDICAL EXPERTS

The panel of medical experts consulted by the author during research is as follows:

1. Dr. Rajat Mohan, Chief, Department of Non Invasive Cardiology, Sir Ganga Ram Hospital, New Rajinder Nagar, New Delhi.
2. Dr. Ravi Jain, Consulting Physician and Cardiologist, Roorkee.
3. Dr. B. R. Madnurkar, M.D. (Medicine), Ashwini Hospital and Intensive Care Unit, Doctors Lane, Nanded.
4. Dr. D. V. Mandakhalikar, Consulting Physician and Cardiologist, Sri Nagar, Nanded.
5. Dr. R. N. Kagne, Assistant Professor, Department of Forensic Medicine, Government Medical College, Nanded.
6. Dr. Purushotam Dad, Consulting Physician and Cardiologist, Gurudwara Hospital, Nanded.

AUTHOR'S RESEARCH CONTRIBUTIONS

1. "A new Technique for Identification of QRS Complex", Proceedings of National Conference on Bio-Medical Engineering, Manipal Institute of Technology, Manipal, India, pp. 11-25-27, April 9-11, 1998.
2. "Computerized Cardiac Disease Diagnostics Using Wavelet Transforms and Modified Scoring Criteria", Proceedings of the Symposium on Bio-Medical Engineering and Nuclear Medicine, BARC Training School Hostel, Mumbai, India, pp. 210-218, January 27-29, 2000.
3. "Study and Analysis of the Heart Rate Variability using Wavelet Transforms and Power Spectral Density Distribution", National Conference on Bio-Medical Engineering, Department of Electrical Engineering, University of Roorkee, Roorkee, India, pp. 107-118, April 21-22, 2000.
4. "ECG Data Compression Using Non-Redundant Templates", IETE Technical Review, to be published in Vol. 17, No. 5, 2000
5. "Feature Extraction from ECG Signal using Wavelet Transformation for Disease Diagnostics", submitted to International Journal of Systems Science, U.K. (revised and communicated)
6. "QRS Detection Using New Wavelets", Journal of Medical Engineering and Technology, U.K. (Communicated).

REFERENCES

1. Abreu-Lima and Marques de Sa., " Interpretation of short ECGs with a PC: The Porto Program", *Methods of Information in Medicine*, Vol. 29, pp. 410-412, 1990.
2. Acar B., Yi G., Hnatkova K. and Malik M., "Spatial, temporal and wavefront direction characteristics of 12-lead T-wave morphology", *Medical & Bio. Engg. & Computing*, Vol. 37, pp. 574-584, 1999.
3. Afonso V.X., Tompkin W.J., Nguyen N.Q. and Luo S., "ECG beat detection using filter banks", *IEEE Trans. on BME*, Vol. 46(2), pp.192-202, 1999.
4. Ahlstrom M. L. and Tompkins W.J., "Digital filters for real-time ECG signal processing using microprocessors", *IEEE Trans. on BME*, Vol. BME-32(9), pp. 708-713 Sept. 1985.
5. Akay Metin, "Wavelet application in medicine", *IEEE spectrum*, pp. 50-56, May 1997.
6. Almenar V. and Albiol A., "A new adaptive scheme for ECG enhancement", *Signal Proc.*, Vol. 75, pp. 253-263, 1999.
7. Amra Graps, "An introduction to wavelets", *IEEE Journal of Computational Science and Engineering*, Vol.2(2), pp. 1-17, Summer 1995.
8. Antti Ruha, Sallinen S. and Nissila S., "A real-time microprocessor QRS detector system with a 1-ms timing accuracy for the measurement of ambulatory HRV", *IEEE Trans. on BME*, Vol. 44(3), pp. 159-167, March 1997.
9. Arnaud P., Rubel P., Morlet D.E., Fayn and Forlini M.C., "Methods of ECG interpretation in the Lyon program", *Methods of Information in Medicine*, Vol. 29, pp. 393-402, 1990.
10. Badilini F., Maison-Blanche P., Childers R. and Coumel P., "QT interval analysis on ambulatory ECG recordings: a selective beat averaging approach", *Medical & Bio. Engg. & Computing*, Vol. 37, pp. 71-79, 1999.
11. Bai J., Zhang Y., Shen D., Wen L., Ding C., Cui Z., Tian F., Yu B., Dai B. and Zhang J., "A portable ECG and blood pressure telemonitoring system", *IEEE Engg. in Medicine and Biology*, pp. 63-70, July-Aug. 1999.
12. Barlas G.D. and Skordalakis E.S., "A novel family of compression algorithms for ECG and other semiperiodical, one-dimensional, biomedical signals", *IEEE Trans. on BME*, Vol. 47(8), pp. 820-828, 1990.
13. Barro S., Presedo J., Castro D., Fernandez M., Fraga S., Lama M. and Vila J., "Intelligent telemonitoring of critical-care patients", *IEEE Engg. in Medicine and Biology*, pp. 80-88, July-Aug. 1999.

14. Bates R.A., Hilton M.F., Godfrey K.R. and Chappell M.J., "Comparison of methods for harmonic wavelet analysis of heart rate variability", IEE Proc. Sci. Meas. & Tech., Vol. 145(6), Nov. 1998.
15. Bommel van J.H., Kors J.A. and Herpen van G., "Methods of the Modular ECG Analysis System MEANS", Methods of Information in Medicine, Vol. 29, pp. 346-353, 1990.
16. Bommel van J.H., Zywiets Chr. and Kors J.A., "Signal analysis for ECG interpretation", Methods of Information in Medicine, Vol. 29, pp. 317-329, 1990.
17. Bianchi A.M., Luca T.M., Carlo M., Sergio Chierchia. and Sergio Cerutti, "Continuous monitoring of the sympatho-vagal balance through spectral analysis", IEEE Engg. in Medicine and Biology, pp. 64 -73, Sept.-Oct. 1997.
18. Boer R.W.de, Karemaker and Strackee J., "Relationships between short-term blood-pressure fluctuations and HRV in resting subjects I: a spectral analysis approach", Medical & Bio. Engg. & Computing, Vol. 23, pp. 352-358, July 1985.
19. Boer R.W.de, Karemaker and Strackee J., "Relationships between short-term blood-pressure fluctuations and HRV in resting subjects II: a simple model", Medical & Bio. Engg. & Computing, Vol. 23, pp. 359-364, July 1985.
20. Bortolan G., Cavaggion C. and Degani R.T., "A comparative study of measurement precision on QRST and P waves", Computers in Cardiology, pp. 273-276, 1982.
21. Bradie B., "Wavelet packet-based compression of single lead ECG", IEEE Trans. on BME, Vol. 43(5), pp. 493-501, May 1996.
22. Brohet C.R., Derwael C., Robert A. and Fesler R., "Methods of ECG interpretation in the Louvain program", Methods of Information in Medicine, Vol. 29, pp. 403-409, 1990.
23. Bronzino J.D., "The biomedical engineering handbook", CRC Handbook, IEEE press, 1995.
24. Bruce W.S., "Multirate and wavelet signal processing", Academic Press, New York, 1996.
25. Chan B. C. B., Chan F.H.Y., Lam F.K., Lui P-W and Poon W.F., "Fast detection of Venous air embolism in doppler heart sound using the wavelet transform", IEEE Trans. on BME, Vol. 44(4), pp. 237-246, April 1997.
26. Chen J. and Shuichi, "A wavelet transform-based ECG compression method guaranteeing desired signal quality", IEEE Trans. on BME, Vol. 45(12), pp. 1414-1419, Dec. 1998.

27. Cox J. R., Nolle F. M., Fozzard H. A. and Oliver G. C., "AZTEC, a preprocessing program for real-time ECG rhythm analysis", *IEEE Trans. on BME*, pp. 128-129, April 1968.
28. Craelius W., Akay M. and Tangella M., "Heart rate variability as an index autonomic imbalance in patients with recent myocardial infarction", *Medical & Bio. Engg. & Computing*, Vol. 30, pp. 385-388, July 1992.
29. Dandapat S. and Ray G.C., "Spike detection in biomedical signals using midprediction filter", *Medical & Bio. Engg. & Computing*, pp. 354-360, July 1997.
30. Daskalov I. K. and Christov I. I., "Automatic detection of the electrocardiogram T-wave end", *Medical & Bio. Engg. & Computing*, Vol. 37, pp. 348-353, 1999.
31. Degani R. and Bortolan G., "Methods of ECG interpretation in the Padova program", *Methods of Information in Medicine*, Vol. 29, pp. 386-392, 1990.
32. Dekker J.M., Shouten E.G., Klootwijk P., Pool J. and Kromhout D., "ST segment and T wave characteristics as indicators of coronary heart disease risk: the Zutphen study", *Jl. of American College of Cardiology*, Vol. 25(6), pp. 1321-1326, May 1995.
33. Dipersio D. A. and Barr R. C., "Evaluation of the fan method of adaptive sampling on human electrocardiograms", *Medical & Bio. Engg. & Computing*, pp. 401-409, September 1985.
34. Djohan A., Nguyen T.Q. and Tompkins W.J., "ECG compression using discrete symmetric wavelet transform", *EMBC*, 1995.
35. Dokur Z., Olmez T. and Yazgan E., "Comparison of discrete wavelet and Fourier transforms for ECG beat classification", *Electronics Letters*, Vol. 35(18), pp. 1502-1504, Sept. 1999.
36. Escalona O.J., Mitchell R.H., Balderson P.E. and Harron D.W.G., "Fast and reliable QRS alignment technique for high-frequency analysis of signal-averaged ECG", *Medical & Bio. Engg. & Computing*, pp. 137-146, July 1993.
37. Evans F.G., Rogers J.M., Smith W.M. and Ideker R.E., "Automatic detection of conduction block based on time-frequency analysis of unipolar electrograms", *IEEE Trans. on BME*, Vol. 46(9), pp. 1090-1097, Sept. 1999.
38. Figliola A. and Serrano E., "Analysis of physiological time series using wavelet transforms," *IEEE Engg. in Medicine and Biology*, pp.74-79, May/June 1997.
39. Fuenmayor A.J., Rosales J.G. and Fuenmayor A.M., "Heart rate and heart rate variability changes induced by right atrial pacing", *Intl. Jl. of cardiology*, Vol. 54, pp. 21-25, 1996.

40. Gang Li, Wenyu Y., Ling L., Qilian Y. and Xuemin Y., "An artificial-intelligence approach to ECG analysis", *IEEE Engg. in Medicine and Biology*, pp.95-100, March/April 2000.
41. Gary M. F., Thomas C.J., Manal A.J., Stanford L.Y., Stephen R.Q. and H. Troy N., "A comparison of the noise sensitivity of nine QRS detection algorithms", *IEEE Trans. on BME*, Vol.37(1), pp. 85-98, Jan. 1990.
42. Goldman M. J., "Principles of clinical Electrocardiography", Larngce Medical Publications/Los Altos, California, U.S.A., 1986.
43. Gurgen F., "Neural-network-based decision making in diagnostic applications", *IEEE Engg. in Medicine and Biology*, pp. 89-93, July-Aug. 1999.
44. Gustavo B., Renato D. and Franco F., "A contribution to the automatic processing of electrocardiograms using syntactic methods", *IEEE Trans. on BME* Vol. 26(3), pp. 125-136, March 1979.
45. Hamilton P.S. and Tompkins W.J., "Quantitative investigation of QRS detection rules using the MIT/BIH Arrhythmia database", *IEEE Trans. on BME*, Vol. 33(12), pp. 1157-1165, 1986.
46. Harel T., Gath I. and Ben-Haim S., "High-resolution estimation of the HRV signal", *Medical & Bio. Engg. & Computing*, Vol. 35, pp. 61-65, Jan 1997.
47. Hilton M.L., "Wavelet and wavelet packet compression of electrocardiograms", *IEEE Trans. on BME*, Vol. 44(5), pp. 394-402, May 1997.
48. Hoyer D., Schmidt K., Bauer R., Zwiener U., Kohler M., Luthke B. and Eiselt M., "Nonlinear analysis of heart rate and respiratory dynamics", *IEEE Engg. in Medicine and Biology*, pp. 31-39, Jan-Feb 1997.
49. Ivan K.D., Ivan A.D. and Ivailo I. C., "Developments in ECG acquisition, preprocessing, parameter measurement, and recording", *IEEE Engg. in Medical and Biology*, pp. 50-57, March-April 1998.
50. Jalaleddine S.M.S., Chriswell G. Hutchens, Robert D. Strattan and William A. Coberly, "ECG data compression techniques -a unified approach", *IEEE Trans. on BME*, Vol. 37(4), pp. 329-343, April 1990.
51. Jan. L.T., Jan A. K. and Jan H.V. B., "Algorithms for the detection of events in electrocardiograms", *Computer methods and programs in Biomedicine*, pp.149-161, 1986.
52. Jane R., Olmos S., Laguna P. and Chaminal P., "Adaptive hermite models for ECG data compression: performance and evaluation with automatic wave detection", *Computers in Cardiology*, Los Alamitos, CA, USA, IEEE Computer Society Press, pp. 389-392, 1993.

53. Jens J., Heisel A., Fries D. T. R., Schieffer H. and Ozbek C., "Assessment of HRV by using different commercially available systems," *Excerpta Medica*, pp. 118-120, 1996.
54. Jose Garcia, Sornmo L., Olmos S. and Laguna P., "Automatic detection of ST-T complex changes on the ECG using filtered RMS difference series application to ambulatory ischemia monitoring", *IEEE Trans. BME*, Vol. 47(9), pp. 1195-1201, Sep. 2000.
55. Julian L. Cardenas B. and Juan V. L. G., "Mean-shape vector quantizer for ECG signal compression", *IEEE Trans. on BME*, Vol. 46(1), pp. 62-70, January 1999.
56. Kadambe S., Murray R. and Bartels G.F.B., "Wavelet transform based QRS complex detector", *IEEE Trans. on BME*, Vol. 46(7), pp. 838-848, 1999.
57. Kanwaldip A, Farid D and Garry R., "Vector quantization of ECG wavelet coefficients", *IEEE Signal Processing Letters*, Vol. 2(7), pp. 129-131, July 1995.
58. Keele C.A. and Neil E., "Samson Wright's Applied Physiology", The English Language Book Society and Oxford University Press, 1971.
59. Kors J.A and Bommel van J.H., "Classification methods for computerized interpretation of the ECG", *Methods of Information in Medicine*, Vol. 29, pp. 330-336, 1990.
60. Kuklinski W.S., "Fast Walsh transform data-compression algorithm: ECG applications", *Medical & Bio. Engg. & Computing*, Vol. 21, pp. 465-472, July 1983.
61. Kulkarni P.K., "Ambulatory monitoring and analysis of ECG signals", Ph.D. thesis, Dept. of Electrical Engg., University of Roorkee, Roorkee, India, 1997.
62. Kulkarni P.K., Kumar V. and Verma H.K., "ECG data compression using fast Walse transform and its clinical acceptability", *IJSS*, Vol. 28(8), Aug. 1997.
63. Kulkarni P.K., Vinod Kumar and Verma H.K., "Diagnostic acceptability of FFT-based ECG data compression", *Jl. of Medical Engg. and Tech.*, Vol. 25(5), pp. 185-189, Sept-Oct., 1997.
64. Kulkarni P.K., Vinod Kumar and Verma H.K., "Direct data compression techniques for ECG signals: effect of sampling frequency on performance", *IJSS*, Vol. 28(3), pp. 217-228, 1997.
65. Kundu M., Nasipuri M. and Basu D. K., "A knowledge based approach to ECG interpretation using fuzzy logic", *IEEE Trans. on Sys. Man and Cyber.*, Vol. 28(2) pp. 237-243, April 1998.
66. Laguna P., Jane R., Olmos S., Thakor N.V., Rix H. and Caminal P., "Adaptive estimation of QRS complex wave features of ECG signal by the Hermite Model", *Medical & Bio. Engg & Computing*, pp. 58-68, Jan. 1996.

67. Laguna P., Thakor N.V., Pere C. and Raimon J., "Low-pass differentiators for biological signals with known spectra: application to ECG signal processing", *IEEE Trans. on BME*, Vol. 37(4), pp. 420-425, April 1990.
68. Laguna P., Thakor N.V., Caminal P., Jane R. and Yoon H.R., "New algorithm for QT interval analysis in 24-hour Holter ECG: performance and applications", *Medical & Bio. Engg. & Computing*, Vol. 28, pp. 67-73, Jan., 1990.
69. Laguna P., Vigo D., Jane R. and Caminal P., "Automatic wave onset and offset determination in ECG signals: validation with the CSE database", *Computers in Cardiology*, Los Alamitos, CA, USA, IEEE Computer Society Press, pp. 167-170, 1992.
70. Lee H. and Buckley K.V., "ECG data compression using cut and align beats approach and 2-D transforms", *IEEE Trans. on BME*, Vol. 46(5), pp. 556-564, May 1999.
71. Levkov C., Michov G., Ivanov R. and Daskalov I.K., "Subtraction of 50Hz interference from the electrocardiogram", *Medical & Bio. Engg. & Computing*, Vol. 22, pp.371-373, July 1984.
72. Li C., Zheng C. and Tai C., "Detection of ECG characteristic points using wavelet transforms", *IEEE Trans. on BME*, Vol. 42(1), pp. 21-28, Jan. 1995.
73. Lin J.C., "Applying telecommunication technology to health-care delivery", *IEEE Engg. in Medical and Biology* pp. 28-31, July-Aug. 1999.
74. Lipman B. S. and Massie, E., "Clinical Scalar Electrocardiography", Year Book Medical Publishers, 5th Edition,.....
75. Luczak H. and Laurig W., "An analysis of heart rate variability", *Ergonomics*, Vol., 16(1), pp. 85-97, 1973.
76. Lund K., Christiansel E. H., Lund B. and Pedersen A. K., "Recovery of beat-to-beat variations of QRS", *Medical & Bio. Engg. & Computing*, pp. 438-444, July 1998.
77. Lum Zhitao, Kim D. Y. and Pearlonan W. A., "Wavelet compression of ECG signals by the set partitioning in hierarchical trees algorithm", *IEEE Trans. on BME*, Vol. 47(7), pp. 849-856, July 2000.
78. Macfarlane P.W. and Lamarie T.D.V., "Comprehensive electrocardiography: theory & practice in health & disease", Vol. 1 & 2, Pergamon Press, New York, 1989.
79. Macfarlane P.W., "Methods of ECG interpretation in the Glasgow program", *Methods of Information in Medicine*, Vol. 29, pp. 354 -361, 1990.
80. Macfarlane P.W., "A brief history of computer-assisted electrocardiography", *Methods of Information in Medicine*, Vol. 29, pp. 272-281, 1990.

81. Maglaveras N., Stamkopoulos T., Pappas C. and Strintzis M.G., "An adaptive backpropagation for real-time ischemia episodes detection: development and performance analysis using European ST-T database", *IEEE Trans. on BME* Vol. 45(7), pp. 805-813, July 1998.
82. Maheshwari R., Vijaya G., Kumar V. and Verma H.K., "Signal-analysis and a heuro-logic interpretation of multi-lead electrocardiograms", *IJSS*, Vol. 29(3), pp. 323-334, 1998.
83. Mainardi L.T., Yli-hankala A., Korhonen I., Signorini M.G., Bianchi A.M., Takala J., Nieminen K. and Cerutti S., "Monitoring the autonomic nervous system in the ICU through cardiovascular variability signals", *IEEE Engg. in Medicine and Biology*, pp. 64 - 75, Nov-Dec., 1997.
84. Malik M., Cripps T., Farrell T. and Camm A.J., "Prognostic value of HRV after myocardial infarction. A comparison of different data-processing methods," *Medical & Bio. Engg. & Computing*, pp. 603-611, November 1989.
85. Malik M., Xia R, Odemuyiwa O, Staunton A., Poloniecki J. and Camm A.J., "Influence of the recognition artifact in automatic analysis of long-term ECGs on time-domain measurement of HRV", *Medical & Bio. Engg. & Computing*, pp. 539-544, Sept. 1993.
86. Mallat S.G., "A theory for multiresolution signal decomposition: the wavelet representation", *IEEE Trans. on PAMI*, Vol. 11(7), pp. 674-693, July 1989.
87. Mallet Y., Coomans D., Kautsky J. and Olivier D.V., "Classification Using adaptive wavelets for feature extraction", *IEEE Trans. on PAMI*, Vol. 19(10), pp. 1058-1066, Oct 1997.
88. Mandawat M. K., Wallbridge D. R., Pringle S. D., Riyami A., Sornmo L, Macfarlane P. W., Lorimer A. R. and Cobbe S.M., "Heart rate variability in left ventricular hypertrophy", *American Heart Journal*, Vol. 73, pp. 139-144, 1995.
89. Mario C., Bifulco P. and Bracale M., "Evaluating time-varying HRV power spectral density," *IEEE Engg. in Medicine and Biology*, pp.76-79, November/December 1997.
90. Mario Merri, David C.F., Jack G.M. and Edward L.T., "Sampling frequency of the ECG for spectral analysis of the HRV", *IEEE Trans. on BME*, Vol. 37(1), pp. 99-106, Jan 1990.
91. Marriot H. J. L., "Practical electrocardiography ", Sixth edition, The W & W Co. Baltimore, 1978.

92. Masa I., Soon-Bun S., Hostter G.H. and Sklansky J., "Scan-along polygonal approximation for data compression of electrocardiograms", *IEEE Trans. on BME*, Vol. 30(11), pp. 723-729, November 1983.
93. Mehta S.S., Saxena S.C. and Verma H.K., "Computer-aided interpretation of ECG for diagnostics", *IJSS*, Vol. 27(1), pp. 43-58, 1996.
94. Moody G.B., "ECG database application guide", Harvard Univ. MIT, Div. Health Sci. Technol., Cambridge – M.A. 1992.
95. Morlet D, Rubel P. and Willems J.L., "Value of scatter-graph for the assessment of ECG computer measurement results", *Methods of Information in Medicine*, Vol. 29, pp. 413-423, 1990.
96. Murthy I. S. N. and Prasad G. S. D., "Analysis of ECG from Pole-zero models", *IEEE Trans. on BME*, Vol. 39(7), pp. 741-751, 1992.
97. Naima F. M. A. and Saxena S. C., "Analysis of ECG signal using mixed mathematical basis functions," *IEEE MELECON*, Vol. 2, pp. 139-142, 1985.
98. Naima F. M. A. and Saxena S. C., "Computer-aided techniques for the extraction of ECG parameters," *IJSS*, Vol. 20(5), pp.747-757, 1989.
99. Narayan S.M. and Smith J.M., "Spectral analysis of periodic fluctuations in electrocardiographic repolarization", *IEEE Trans. on BME*, Vol. 46 (2), pp. 203-212, February 1999.
100. Nave G. and Cohen A., "ECG compression using long-term prediction", *IEEE Trans. on BME*, Vol. 40(9), pp. 877-885, Sept., 1993.
101. Okada M., "A digital filter for the QRS complex detection", *IEEE Trans on BME*, Vol. BME-26(12), pp. 700-703, Dec. 1979.
102. Okajima M., Okamoto N., Yokoi M., Iwatsuka T. and Ohsawa N., "Methods of ECG interpretation in the Nagoya program", *Methods of Information in Medicine*, Vol. 29, pp. 341-345, 1990.
103. Pahlm O. and Sornmo L., "Software QRS detection in ambulatory monitoring-a review", *Medical & Bio. Engg. & Computing*, pp. 289-297, July 1984.
104. Pan J. and Tompkins W. J., "A real - time QRS detection algorithm", *IEEE Trans. on BME*, Vol. 32(3), pp. 230-236, 1985.
105. Panagiotis T. and Emmanuel S., "Syntactic pattern recognition of the ECG", *IEEE Trans. on PAMI*, Vol. 12(7), pp. 648-657, July 1990.

106. Park K. L., Lee K. J. and Yoon H. R., "Application of a wavelet adaptive filter to minimize distortion of the ST-segment", *Medical & Bio. Engg. & Computing*, Vol. 36, pp. 581-586, Sept. 1998.
107. Park Y.C., Lee K.Y., Youn D.H., Kim N.H., Kim W.K and Park S.H., "On detecting the presence of fetal R-wave using the moving averaged magnitude difference algorithm", *IEEE Trans. on BME*, Vol. 39(8), pp. 868-871, August 1992.
108. Paul J.S., Reddy M.R. and Kumar V.J., "A QRS estimator using linear prediction approach", *Signal Processing*, Vol. 72, pp. 15-22, 1999.
109. Philippe C., Helene L., Christine F. and Catherine M., "Denoising of the uterine EHG by an undecimated wavelet transform", *IEEE Trans. on BME*, Vol. 45(9), pp. 1104-1113, Sept., 1998.
110. Pipberger H.V., McManus C.D. and Pipberger H.A., "Methods of ECG interpretation in the AVA program", *Methods of Information in Medicine*, Vol. 29, pp. 337-341, 1990.
111. Polikar R., "The wavelet tutorial part I-IV", Iowa state University, USA, 1996.
112. Porta A., Baselli G., Caiani E., Malliani A., Lombardi F. and Cerutti S., "Quantifying electrocardiogram RT-RR variability interactions", *Medical & Bio. Engg. & Computing*, Vol. 36, pp. 27-34, Jan 1998.
113. Porta A., Baselli G., Lombardi F., Cerutti S., Antolini R., Del Greco M., Ravelli F. and Nollo G., "Performance assessment of standard algorithms for dynamic R-T interval measurement: comparison between R-T_{apex} and R-T_{end} approach", *Medical & Bio. Engg. & Computing*, pp. 35-42, Jan 1998.
114. Quang M.T and Wageeh W.B., "Wavelet based affine invariant representation: a tool for recognizing planar objects in 3D space", *IEEE Trans. on PAMI*, Vol. 19(8), pp. 846-857, Aug 1997.
115. Rao K. D., "DWT based detection of R-peaks and data compression of ECG signals," *IETE Journal of Research*, Vol. 43(5), pp. 345-349, Sept/Oct 1997.
116. Rautaharju, P.M., MacInnis P.J., Warren J.W., Wolf H.K., Rykers, and Calhoun, "Methodology of ECG interpretation in the Dalhousie program; NOVACODE ECG classification procedures for clinical trials and population health surveys", *Methods of Information in Medicine*, Vol. 29, pp. 362-374, 1990.
117. Reddy B.R.S. and Murthy I.S.N., "ECG data compression using Fourier descriptors", *IEEE Trans. on BME*, Vol. 33(4), pp. 428-433, April 1986.

118. Rioul O. and Vetterli M., "Wavelets and signal processing", IEEE SP Magazine, pp. 14-35 Oct. 1991.
119. Rix H. and Meste O., "Fine structure of ECG signal using wavelet transform", in D'Attellis C.E. and Fernandez-Berdaguer (Eds.), Wavelet theory and harmonic analysis in applied sciences, Birkhauser Publications-Boston, 1997.
120. Roger C. Barr, Susan M. Blanchard and Deborah A. Dipersio, "SAPA-2 Is the Fan", IEEE Trans. on BME, Vol. 32(5), pp. 337-343, May 1985.
121. Rompelman O., Coenen A.J.R.M. and Kitney R.I., "Measurement of heart-rate variability part I-comparative study of heart-rate variability analysis methods", Medical & Bio. Engg. & Computing, Vol. 15, pp. 233-269, May 1977.
122. Rompelman O., Kampen W. and Backer E., "HRV in relation to psychological factors," Ergonomics, Vol. 23(12), pp. 1101-1115, 1980.
123. Sahambi J. S., Tandon S. N. and Bhatt R. K. P., "Using wavelet transforms for ECG characterization - An on-line digital signal processing system", IEEE Engg. in Medicine and Biology, pp. 77-83, Jan/Feb 1997.
124. Sahambi J.S., Tandon S.N. and Bhat R.K.P., "Wavelet based ST-segment analysis", Medical & Bio. Engg. & Computing, Vol. 36, pp. 568-572, Sept. 1998.
125. Saxena S.C., Sharma A. and Chaudhary S.C., "Data compression and feature extraction of ECG signals", IJSS, Vol. 28(5), pp. 483-498, 1997.
126. Senhadji L., Carrault G., Bellanger J. J. and Passariello G., "Comparing wavelet transforms for recognizing cardiac patterns", IEEE Engg. in Medicine and Biology, pp. 167-173, March-April, 1995.
127. Shaw G. R. and Savard P., "On the detection of QRS variations in the ECG", IEEE Trans. on BME, Vol. 42(7), pp.736-741, 1995.
128. Sornmo L., Pahlm O., Mats-Erik N. and Per O. B., "A mathematical approach to QRS detection", IEEE Computers in Cardiology, pp. 205-208, 1980.
129. Tai S.C., "ECG data compression by corner detection", Medical & Bio. Engg. & Computing, Vol. 30, pp. 584-590, Nov. 1992.
130. Tai S.C., "Slope-a real-time ECG data compressor", Medical & Bio. Engg. & Computing, Vol. 29, pp. 175-179, March 1991.
131. Tai S.C., Chang C.W. and Chen C.F., "Designing better adaptive sampling algorithms for ECG Holter systems", IEEE Trans. on BME, Vol. 44(9), pp. 901-903, Sept. 1997.

132. Tartakovsky M.B., Rosenberg N., Ron S., Shabtai I., Elkin S. and Cocos M.,
 "Unsupervised template construction for QRS classification in Holter tape analysis",
 IEEE Computers in Cardiology, pp. 9-14, 1991.
133. Thakor N.V, Webster J.G. and Tompkins W.J, "Estimation of QRS complex power
 spectra for design of a QRS filter", IEEE Trans. on BME, Vol. 31(11), pp. 702-706,
 Nov. 1984.
134. Tompkins W.J., "Biomedical Digital Signal Processing", Prentice Hall of India Private
 Limited, New Delhi, 1999.
135. Trahanias P. and Skordalakis E., "Bottom-up approach to the ECG pattern-recognition
 problem", Medical & Bio. Engg. & Computing, Vol. 27, pp. 221-229, May 1989.
136. Trahanias P.E, "An approach to QRS complex detection using mathematical
 morphology", IEEE Trans. on BME, Vol. 40(2), pp. 201-205, Feb. 1993.
137. Unser M. and Aldroubi A., "A review of wavelets in biomedical applications", Proc. of
 The IEEE, Vol. 84(4), pp. 626-638, April 1996.
138. Urrusti J.L. and Tompkins W.J., "Performance evaluation of an ECG QRS complex
 detection algorithm", Computers in Cardiology (Los Alamitos California, U.S.A, IEEE,
 Computer Society Press), pp. 800 -801, 1993.
139. Vetterli M. and Cormac H., "Wavelet and filter banks: theory and design", IEEE Trans.
 on Signal Processing, Vol. 40(9), pp. 2207-2232, September 1992.
140. Vijaya G., "Artificial neural network based ECG classification", Ph.D. thesis, Dept. of
 Electrical Engg., University of Roorkee, Roorkee, India, 1997.
141. Vijaya G., Kumar V. and Verma H. K., "Artificial neural network based wave complex
 detection in electrocardiograms", IJSS, Vol. 28(2), pp. 125-132, 1997.
142. Vila J., Palacios F., Presedo J., Fernandez-Delgada M., Felix P. and Barro S., "Time-
 frequency analysis of heart-rate variability", IEEE Engg. in Medicine and Biology, pp.
 119-125, Sept.-Oct. 1997.
143. Voulgaris N.C. and Bailas A.A., "Digital beat-to-beat heart-rate meter", Medical & Bio.
 Engg. & Computing, Vol. 22, pp. 181-183, March 1984.
144. Wachowiak M. P., Rash G. S., Quesada and Desoky A. H., "Wavelet-based noise
 removal for biomedical signals : A comparative study", IEEE Trans. on BME, Vol. 47(3),
 pp. 360-368, March, 2000.
145. Webster J. G., "Encyclopedia of medical devices and instrumentation – Vol. 2",
 John Wiley & Sons, 1988.

146. Wiklund U., Akay M. and Niklasson U., "Short-term analysis of heart-rate variability by adopted wavelet transforms", IEEE Engg. in Medicine and Biology, pp. 113-118, Sept.-Oct. 1997.
147. Willems J. L., "The CSE Multilead atlas manual-measurement results dataset-3", Printed in Belgium by ACCO, Brusselsestraat-118a, 3000 Leuven, Belgium, 1988.
148. Willems J.L., "Common standards for quantitative electrocardiography-10th and final progress report," 1990, Leuven, Dec. 1990.
149. Willems J.L., "Recommendations for measurement standards in quantitative electrocardiography", European Heart Jl., Vol. 6, pp. 815-825, 1985.
150. Willems J.L., Abreu-Lima, Arnaud P., Brohet C.R., Denis B., Gehing J., Graham I., Herpen van G., Machado H., Michaelis J. and Mouloupoulos, "Evaluation of ECG interpretation results obtained by computer and cardiologists", Methods of Information in Medicine, Vol. 29, pp. 308-316, 1990.
151. Willems J.L., Arnaud P., Bemmél van J.H., Degani R., Macfarlane P.W., and Zywiets Chr., "Common standards for quantitative electrocardiography: Goals and main results", Methods of Information in Medicine, Vol. 29, pp. 263-271, 1990.
152. Xue Q., Yu Hen Hu, and Tompkins W.J., "Neural network based adaptive matched filtering for QRS detection", IEEE Trans. on BME, Vol. 39 (4), pp. 317-329, April 1992.
153. Yang F. and Lio W., "Modeling and decomposition of HRV signals with wavelet transforms", IEEE Engg. in Medicine and Biology, pp. 17-22, July-Aug. 1997.
154. Zhang P.Z., Tapp W., Reisman S., and Natelson B., "Respiration response curve analysis of HRV," IEEE Trans. on BME, Vol. 44(4), April 1997.
155. Zywiets Chr., Bemmél van J.H. and Degani R., "Evaluation of ECG interpretation systems: signal analysis", Methods of Information in Medicine, Vol. 29, pp. 298-307, 1990.
156. Zywiets Chr., Borovsky D., Gotsch G., and Joseph G., "Methods of ECG interpretation in the Nagoya program", Methods of Information in Medicine, Vol. 29, pp. 375-385, 1990.

